CHAPTER 1

Ozone-Depleting Substances (ODSs) and Related Chemicals

Coordinating Lead Authors:
S.A. Montzka
S. Reimann

Lead Authors:
A. Engel
K. Krüger
S. O'Doherty
W.T. Sturges

Coauthors:
D. Blake
M. Dorf
P. Fraser
L. Froidevaux
K. Jucks
K. Kreher
M.J. Kurylo
A. Mellouki
J. Miller
O.-J. Nielsen
V.L. Orkin
R.G. Prinn
R. Rhew
M.L. Santee
A. Stohl
D. Verdonik

Contributors:
E. Atlas
P. Bernath
T. Blumenstock
J.H. Butler
A. Butz
B. Connor
P. Duchatelet
G. Dutton
F. Hendrick
P.B. Krummel
L.J.M. Kuijpers
E. Mahieu
A. Manning
J. Mühle
K. Pfeilsticker
B. Quack
M. Ross
R.J. Salawitch
S. Schauffler
I.J. Simpson
D. Toohey
M.K. Vollmer
T.J. Wallington
H.J.R. Wang
R.F. Weiss
M. Yamabe
Y. Yokouchi
S. Yvon-Lewis

CHAPTER 1

OZONE-DEPLETING SUBSTANCES (ODSs) AND RELATED CHEMICALS

Contents

SCIENTIFIC SUMMARY

The amended and adjusted Montreal Protocol continues to be successful at reducing emissions and atmospheric abundances of most controlled ozone-depleting substances (ODSs).

Tropospheric Chlorine

- **Total tropospheric chlorine from long-lived chemicals (~3.4 parts per billion (ppb) in 2008) continued to decrease between 2005 and 2008.** Recent decreases in tropospheric chlorine (Cl) have been at a slower rate than in earlier years (decreasing at 14 parts per trillion per year (ppt/yr) during 2007–2008 compared to a decline of 21 ppt/yr during 2003–2004) and were slower than the decline of 23 ppt/yr projected in the A1 (most likely, or baseline) scenario of the 2006 Assessment. The tropospheric Cl decline has recently been slower than projected in the A1 scenario because chlorofluorocarbon-11 (CFC-11) and CFC-12 did not decline as rapidly as projected and because increases in hydrochlorofluorocarbons (HCFCs) were larger than projected.

- **The contributions of specific substances or groups of substances to the decline in tropospheric Cl have changed since the previous Assessment.** Compared to 2004, by 2008 observed declines in Cl from methyl chloroform (CH_3CCl_3) had become smaller, declines in Cl from CFCs had become larger (particularly CFC-12), and increases in Cl from HCFCs had accelerated. Thus, the observed change in total tropospheric Cl of −14 ppt/yr during 2007–2008 arose from:
  - −13.2 ppt Cl/yr from changes observed for CFCs
  - −6.2 ppt Cl/yr from changes observed for methyl chloroform
  - −5.1 ppt Cl/yr from changes observed for carbon tetrachloride
  - −0.1 ppt Cl/yr from changes observed for halon-1211
  - +10.6 ppt Cl/yr from changes observed for HCFCs

- **Chlorofluorocarbons (CFCs), consisting primarily of CFC-11, -12, and -113, accounted for 2.08 ppb (about 62%) of total tropospheric Cl in 2008.** The global atmospheric mixing ratio of CFC-12, which accounts for about one-third of the current atmospheric chlorine loading, decreased for the first time during 2005–2008 and by mid-2008 had declined by 1.3% (7.1 ± 0.2 parts per trillion, ppt) from peak levels observed during 2000–2004.

- **Hydrochlorofluorocarbons (HCFCs), which are substitutes for long-lived ozone-depleting substances, accounted for 251 ppt (7.5%) of total tropospheric Cl in 2008.** HCFC-22, the most abundant of the HCFCs, increased at a rate of about 8 ppt/yr (4.3%/yr) during 2007–2008, more than 50% faster than observed in 2003–2004 but comparable to the 7 ppt/yr projected in the A1 scenario of the 2006 Assessment for 2007–2008. HCFC-142b mixing ratios increased by 1.1 ppt/yr (6%/yr) during 2007–2008, about twice as fast as was observed during 2003–2004 and substantially faster than the 0.2 ppt/yr projected in the 2006 Assessment A1 scenario for 2007–2008. HCFC-141b mixing ratios increased by 0.6 ppt/yr (3%/yr) during 2007–2008, which is a similar rate observed in 2003–2004 and projected in the 2006 Assessment A1 scenario.

- **Methyl chloroform (CH_3CCl_3) accounted for only 32 ppt (1%) of total tropospheric Cl in 2008, down from a mean contribution of about 10% during the 1980s.**

- **Carbon tetrachloride (CCl_4) accounted for 359 ppt (about 11%) of total tropospheric Cl in 2008**. Mixing ratios of CCl_4 declined slightly less than projected in the A1 scenario of the 2006 Assessment during 2005–2008.

Stratospheric Chlorine and Fluorine

- **The stratospheric chlorine burden derived by ground-based total column and space-based measurements of inorganic chlorine continued to decline during 2005–2008.** This burden agrees within ±0.3 ppb (±8%) with the amounts expected from surface data when the delay due to transport is considered. The uncertainty in this burden is large relative to the expected chlorine contributions from shorter-lived source gases and product gases of 80 (40–130)

ppt. Declines since 1996 in total column and stratospheric abundances of inorganic chlorine compounds are reasonably consistent with the observed trends in long-lived source gases over this period.

- **Measured column abundances of hydrogen fluoride increased during 2005–2008 at a smaller rate than in earlier year**s. This is qualitatively consistent with observed changes in tropospheric fluorine (F) from CFCs, HCFCs, hydrofluorocarbons (HFCs), and perfluorocarbons (PFCs) that increased at a mean annual rate of 40 ± 4 ppt/yr (1.6 ± 0.1%/yr) since late 1996, which is reduced from 60–100 ppt/yr observed during the 1980s and early 1990s.

Tropospheric Bromine

- **Total organic bromine from controlled ODSs continued to decrease in the troposphere and by mid-2008 was 15.7 ± 0.2 ppt, approximately 1 ppt below peak levels observed in 1998.** This decrease was close to that expected in the A1 scenario of the 2006 Assessment and was driven by declines observed for methyl bromide (CH_3Br) that more than offset increased bromine (Br) from halons.

- **Bromine from halons stopped increasing during 2005–2008.** Mixing ratios of halon-1211 decreased for the first time during 2005–2008 and by mid-2008 were 0.1 ppt below levels observed in 2004. Halon-1301 continued to increase in the atmosphere during 2005–2008 but at a slower rate than observed during 2003–2004. The mean rate of increase was 0.03–0.04 ppt/yr during 2007–2008. A decrease of 0.01 ppt/yr was observed for halon-2402 in the global troposphere during 2007–2008.

- **Tropospheric methyl bromide (CH_3Br) mixing ratios continued to decline during 2005–2008, and by 2008 had declined by 1.9 ppt (about 20%) from peak levels measured during 1996–1998.** Evidence continues to suggest that this decline is the result of reduced industrial production, consumption, and emission. This industry-derived emission is estimated to have accounted for 25–35% of total global CH_3Br emissions during 1996–1998, before industrial production and consumption were reduced. Uncertainties in the variability of natural emissions and in the magnitude of methyl bromide stockpiles in recent years limit our understanding of this anthropogenic emissions fraction, which is derived by comparing the observed atmospheric changes to emission changes derived from reported production and consumption.

- **By 2008, nearly 50% of total methyl bromide consumption was for uses not controlled by the Montreal Protocol (quarantine and pre-shipment applications).** From peak levels in 1996–1998, industrial consumption in 2008 for controlled and non-controlled uses of CH_3Br had declined by about 70%. Sulfuryl fluoride (SO_2F_2) is used increasingly as a fumigant to replace methyl bromide for controlled uses because it does not directly cause ozone depletion, but it has a calculated direct, 100-year Global Warming Potential (GWP_{100}) of 4740. The SO_2F_2 global background mixing ratio increased during recent decades and had reached about 1.5 ppt by 2008.

Stratospheric Bromine

- **Total bromine in the stratosphere was 22.5 (19.5–24.5) ppt in 2008. It is no longer increasing and by some measures has decreased slightly during recent years.** Multiple measures of stratospheric bromine monoxide (BrO) show changes consistent with tropospheric Br trends derived from observed atmospheric changes in CH_3Br and the halons. Slightly less than half of the stratospheric bromine derived from these BrO observations is from controlled uses of halons and methyl bromide. The remainder comes from natural sources of methyl bromide and other bromocarbons, and from quarantine and pre-shipment uses of methyl bromide not controlled by the Montreal Protocol.

Very Short-Lived Halogenated Substances (VSLS)

VSLS are defined as trace gases whose local lifetimes are comparable to, or shorter than, tropospheric transport timescales and that have non-uniform tropospheric abundances. In practice, VSLS are considered to be those compounds having atmospheric lifetimes of less than 6 months.

- **The amount of halogen from a very short-lived source substance that reaches the stratosphere depends on the location of the VSLS emissions, as well as atmospheric removal and transport processes.** Substantial uncertainties remain in quantifying the full impact of chlorine- and bromine-containing VSLS on stratospheric ozone. Updated results continue to suggest that brominated VSLS contribute to stratospheric ozone depletion, particularly under enhanced aerosol loading. It is unlikely that iodinated gases are important for stratospheric ozone loss in the present-day atmosphere.

- **Based on a limited number of observations, very short-lived source gases account for 55 (38–80) ppt chlorine in the middle of the tropical tropopause layer (TTL).** From observations of hydrogen chloride (HCl) and carbonyl chloride ($COCl_2$) in this region, an additional ~25 (0–50) ppt chlorine is estimated to arise from VSLS degradation. The sum of contributions from source gases and these product gases amounts to ~80 (40–130) ppt chlorine from VSLS that potentially reaches the stratosphere. About 40 ppt of the 55 ppt of chlorine in the TTL from source gases is from anthropogenic VSLS emissions (e.g., methylene chloride, CH_2Cl_2; chloroform, $CHCl_3$; 1,2 dichloroethane, CH_2ClCH_2Cl; perchloroethylene, CCl_2CCl_2), but their contribution to stratospheric chlorine loading is not well quantified.

- **Two independent approaches suggest that VSLS contribute significantly to stratospheric bromine.** Stratospheric bromine derived from observations of BrO implies a contribution of 6 (3–8) ppt of bromine from VSLS. Observed, very short-lived source gases account for 2.7 (1.4–4.6) ppt Br in the middle of the tropical tropopause layer. By including modeled estimates of product gas injection into the stratosphere, the total contribution of VSLS to stratospheric bromine is estimated to be 1–8 ppt.

- **Future climate changes could affect the contribution of VSLS to stratospheric halogen and its influence on stratospheric ozone.** Future potential use of anthropogenic halogenated VSLS may contribute to stratospheric halogen in a similar way as do present-day natural VSLS. Future environmental changes could influence both anthropogenic and natural VSLS contributions to stratospheric halogens.

Equivalent Effective Stratospheric Chlorine (EESC)

EESC is a sum of chlorine and bromine derived from ODS tropospheric abundances weighted to reflect their potential influence on ozone in different parts of the stratosphere. The growth and decline in EESC varies in different regions of the atmosphere because a given tropospheric abundance propagates to the stratosphere with varying time lags associated with transport. Thus the EESC abundance, when it peaks, and how much it has declined from its peak vary in different regions of the atmosphere.

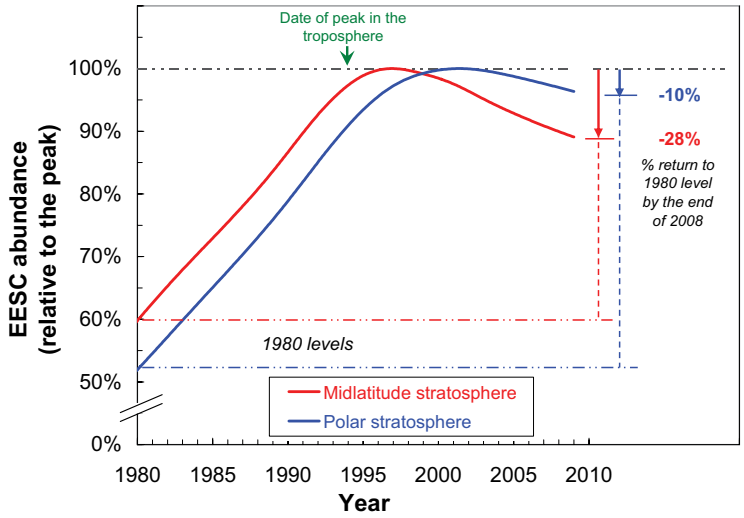

Figure S1-1. Stratospheric EESC derived for the midlatitude and polar stratospheric regions relative to peak abundances, plotted as a function of time. Peak abundances are ~1950 ppt for the midlatitude stratosphere and ~4200 ppt for the polar stratosphere. Percentages shown to the right indicate the observed change in EESC by the end of 2008 relative to the change needed for EESC to return to its 1980 abundance. A significant portion of the 1980 EESC level is from natural emissions.

- **EESC has decreased throughout the stratosphere.**
  - By the end of 2008, midlatitude EESC had decreased by about 11% from its peak value in 1997. This drop is 28% of the decrease required for EESC in midlatitudes (red curve in figure) to return to the 1980 benchmark level.
  - By the end of 2008, polar EESC had decreased by about 5% from its peak value in 2002. This drop is 10% of the decrease required for EESC in polar regions (blue curve in figure) to return to the 1980 benchmark level.

- **During the past four years, no specific substance or group of substances dominated the decline in the total combined abundance of ozone-depleting halogen in the troposphere**. In contrast to earlier years, the long-lived CFCs now contribute similarly to the decline as do the short-lived CH_3CCl_3 and CH_3Br. Other substances contributed less to this decline, and HCFCs added to this halogen burden over this period.

Emission Estimates and Lifetimes

- **While global emissions of CFC-12 derived from atmospheric observations decreased during 2005–2008, those for CFC-11 did not change significantly over this period.** Emissions from banks account for a substantial fraction of current emissions of the CFCs, halons, and HCFCs. Emissions inferred for CFCs from global observed changes did not decline during 2005–2008 as rapidly as projected in the A1 scenario of the 2006 Assessment, most likely because of underestimates of bank emissions.

- **Global emissions of CCl_4 have declined only slowly over the past decade.**
  - These emissions, when inferred from observed global trends, were between 40 and 80 gigagrams per year (Gg/yr) during 2005–2008 given a range for the global CCl_4 lifetime of 33–23 years. By contrast, CCl_4 emissions derived with a number of assumptions from data reported to the United Nations Environment Programme (UNEP) ranged from 0–30 Gg/yr over this same period.
  - In addition, there is a large variability in CCl_4 emissions derived from data reported to UNEP that is not reflected in emissions derived from measured global mixing ratio changes. This additional discrepancy cannot be explained by scaling the lifetime or by uncertainties in the atmospheric trends. If the analysis of data reported to UNEP is correct, unknown anthropogenic sources may be partly responsible for these observed discrepancies.

- **Global emissions of HCFC-22 and HCFC-142b derived from observed atmospheric trends increased during 2005–2008.** HCFC-142b global emissions increased appreciably over this period, compared to a projected emissions decline of 23% from 2004 to 2008. By 2008, emissions for HCFC-142b were two times larger than had been projected in the A1 scenario of the 2006 Assessment. These emission increases were coincident with increasing production of HCFCs in developing countries in general and in East Asia particularly. It is too soon to discern any influence of the 2007 Adjustments to the Montreal Protocol on the abundance and emissions of HCFCs.

- **The sum of CFC emissions (weighted by direct, 100-year GWPs) has decreased on average by 8 ± 1%/yr from 2004 to 2008, and by 2008 amounted to 1.1 ± 0.3 gigatonnes of carbon dioxide–equivalent per year ($GtCO_2$-eq/yr).** The sum of GWP-weighted emissions of HCFCs increased by 5 ± 2%/yr from 2004 to 2008, and by 2008 amounted to 0.74 ± 0.05 $GtCO_2$-eq/yr.

- **Evidence is emerging that lifetimes for some important ODSs (e.g., CFC-11) may be somewhat longer than reported in past assessments**. In the absence of corroborative studies, however, the CFC-11 lifetime reported in this Assessment remains unchanged at 45 years. Revisions in the CFC-11 lifetime would affect estimates of its global emission derived from atmospheric changes and calculated values for Ozone Depletion Potentials (ODPs) and best-estimate lifetimes for some other halocarbons.

Other Trace Gases That Directly Affect Ozone and Climate

- **The methane (CH_4) global growth rate was small, averaging 0.9 ± 3.3 ppb/yr between 1998–2006, but increased to 6.7 ± 0.6 ppb/yr from 2006–2008.** Analysis of atmospheric data suggests that this increase is due to wetland sources in both the high northern latitudes and the tropics. The growth rate variability observed during 2006–2008 is similar in magnitude to that observed over the last two decades.

- **In 2005–2008 the average growth rate of nitrous oxide (N_2O) was 0.8 ppb/yr, with a global average tropospheric mixing ratio of 322 ppb in 2008.** A recent study has suggested that at the present time, Ozone Depletion Potential–weighted anthropogenic emissions of N_2O are the most significant emissions of a substance that depletes ozone.

- **Long-term changes in carbonyl sulfide (COS) measured as total columns above the Jungfraujoch (46.5°N) and from surface flasks sampled in the Northern Hemisphere show that atmospheric mixing ratios have increased slightly during recent years concurrently with increases in "bottom-up" inventory-based emissions of global sulfur.** Results from surface measurements show a mean global surface mixing ratio of 493 ppt in 2008 and a mean rate of increase of 1.8 ppt/yr during 2000–2008. New laboratory, observational, and modeling studies indicate that vegetative uptake of COS is significantly larger than considered in the past.

Other Trace Gases with an Indirect Influence on Ozone

- **The carbon dioxide (CO_2) global average mixing ratio was 385 parts per million (ppm) in 2008 and had increased during 2005–2008 at an average rate of 2.1 ppm/yr.** This rate is higher than the average growth rate during the 1990s of 1.5 ppm/yr and corresponds with increased rates of fossil fuel combustion.

- **Hydrofluorocarbons (HFCs) used as ODS substitutes continued to increase in the global atmosphere.** HFC-134a is the most abundant HFC; its global mixing ratio reached about 48 ppt in 2008 and was increasing at 4.7 ppt/yr. Other HFCs have been identified in the global atmosphere at <10 ppt (e.g., HFC-125, -143a, -32, and -152a) and were increasing at ≤1 ppt/yr in 2008.

- **Emissions of HFC-23, a by-product of HCFC-22 production, have increased over the past decade even as efforts at minimizing these emissions were implemented in both developed and developing countries.** These emission increases are concurrent with rapidly increasing HCFC-22 production in developing countries and are likely due to increasing production of HCFC-22 in facilities not covered by the Kyoto Protocol's Clean Development Mechanism projects. Globally averaged HFC-23 mixing ratios reached 21.8 ppt in 2008, with a yearly increase of 0.8 ppt/yr (3.9%/yr).

- **The sum of emissions (weighted by direct, 100-year GWPs) of HFCs used as ODS replacements has increased by 8–9%/yr from 2004 to 2008, and by 2008 amounted to 0.39 ± 0.03 $GtCO_2$-eq/yr.** Regional studies suggest significant contributions of HFC-134a and -152a emissions during 2005–2006 from Europe, North America, and Asia. Emissions of HFC-23, most of which do not arise from use of this substance as an ODS replacement, added an additional 0.2 Gt CO_2-eq/year, on average, during 2006–2008.

- **Sulfur hexafluoride (SF_6) and nitrogen trifluoride (NF_3):** Global averaged mixing ratios of SF_6 reached 6.4 ppt in 2008, with a yearly increase of 0.2 ppt/yr. NF_3 was detected in the atmosphere for the first time, with a global mean mixing ratio in 2008 of 0.45 ppt and a growth rate of 0.05 ppt/yr, or 11%/yr.

Direct Radiative Forcing

The abundances of ODSs as well as many of their replacements contribute to radiative forcing of the atmosphere. These climate-related forcings have been updated using the current observations of atmospheric abundances and are summarized in Table S1-1. This table also contains the primary Kyoto Protocol gases as reference.

- **Over these 5 years, radiative forcing from the sum of ODSs and HFCs has increased but, by 2008, remained small relative to the forcing changes from CO_2 (see Table S1-1).**

Table S1-1. Direct radiative forcings of ODSs and other gases, and their recent changes.

Specific Substance or Group of Substances	Direct Radiative Forcing (2008), milliWatts per square meter (mW/m^2)	Change in Direct Radiative Forcing (2003.5–2008.5), mW/m^2
CFCs *	262	−6
Other ODSs *	15	−2
HCFCs *	45	8
HFCs #,a	12	5
HFC-23 #	4	0.9
CO_2 #	1740	139
CH_4 #	500	4
N_2O #	170	12
PFCs #	5.4	0.5
SF_6 #	3.4	0.7
Sum of Montreal Protocol gases *	322	0
Sum of Kyoto Protocol gases #	2434	163

* Montreal Protocol Gases refers to CFCs, other ODSs (CCl_4, CH_3CCl_3, halons, CH_3Br), and HCFCs.
# Kyoto Protocol Gases (CO_2, CH_4, N_2O, HFCs, PFCs, and SF_6).
a Only those HFCs for which emissions arise primarily through use as ODS replacements (i.e., not HFC-23).

1.1 SUMMARY OF THE PREVIOUS OZONE ASSESSMENT

The 2006 Assessment report (WMO, 2007) documented the continued success of the Montreal Protocol in reducing the atmospheric abundance of ozone-depleting substances (ODSs). Tropospheric abundances and emissions of most ODSs were decreasing by 2004, and tropospheric chlorine (Cl) and bromine (Br) from ODSs were decreasing as a result. Methyl chloroform contributed more to the decline in tropospheric chlorine than other controlled gases. ODS substitute chemicals containing chlorine, the hydrofluorochlorocarbons (HCFCs), were still increasing during 2000–2004, but at reduced rates compared to earlier years.

A significant mismatch between expected and atmosphere-derived emissions of carbon tetrachloride (CCl_4) was identified. For the first time a decline was observed in the stratospheric burden of inorganic Cl as measured both by ground- and space-based instrumentation. The amount and the trend observed for stratospheric chlorine was consistent with abundances and trends of long-lived ODSs observed in the troposphere, though lag times and mixing complicated direct comparisons.

Tropospheric bromine from methyl bromide and halons was determined in the previous Assessment to be decreasing. Changes derived for stratospheric inorganic bromine (Br_y) from observations of BrO were consistent with tropospheric trends measured from methyl bromide and the halons, but it was too early to detect a decline in stratospheric Br_y. Amounts of stratospheric Br_y were higher than expected from the longer-lived, controlled gases (methyl bromide and halons). This suggested a significant contribution of 5 (3–8) parts per trillion (ppt) of Br potentially from very short-lived substances (VSLS) with predominantly natural sources. Large emissions of very short-lived brominated substances were found in tropical regions, where rapid transport from Earth's surface to the stratosphere is possible. Quantitatively accounting for this extra Br was not straightforward given our understanding at that time of timescales and heterogeneity of VSLS emissions and oxidation product losses as these compounds become transported from Earth's surface to the stratosphere. It was concluded that this additional Br has likely affected stratospheric ozone levels, and the amount of Br from these sources would likely be sensitive to changes in climate that affect ocean conditions, atmospheric loss processes, and atmospheric circulation.

By 2004, equivalent effective chlorine (EECl), a simple metric to express the overall effect of these changes on ozone-depleting halogen abundance, continued to decrease. When based on measured tropospheric changes through 2004, EECl had declined then by an amount that was 20% of what would be needed to return EECl values to those in 1980 (i.e., before the ozone hole was observed).

In the past, the discussion of long-lived and short-lived compounds were presented in separate chapters but are combined in this 2010 Assessment. Terms used to describe measured values throughout Chapter 1 are mixing ratios (for example parts per trillion, ppt, pmol/mol), mole fractions, and concentrations. These terms have been used interchangeably and, as used here, are all considered to be equivalent.

1.2 LONGER-LIVED HALOGENATED SOURCE GASES

1.2.1 Updated Observations, Trends, and Emissions

1.2.1.1 Chlorofluorocarbons (CFCs)

The global surface mean mixing ratios of the three most abundant chlorofluorocarbons (CFCs) declined significantly during 2005–2008 (Figure 1-1 and Table 1-1). After reaching its peak abundance during 2000–2004, the global annual surface mean mixing ratio of CFC-12 (CCl_2F_2) had declined by 7.1 ± 0.2 ppt (1.3%) by mid-2008. Surface means reported for CFC-12 in 2008 by the three independent global sampling networks (532.6–537.4 ppt) agreed to within 5 ppt (0.9%). The consistency for CFC-12 among these networks has improved since the previous Assessment and stems in part from a calibration revision in the National Oceanic and Atmospheric Administration (NOAA) data. The 2008 annual mean mixing ratio of CFC-11 (CCl_3F) from the three global sampling networks (243.4–244.8 ppt) agreed to within 1.4 ppt (0.6%) and decreased at a rate of −2.0 ± 0.6 ppt/yr from 2007 to 2008. Global surface means observed by these networks for CFC-113 (CCl_2FCClF_2) during 2008 were between 76.4 and 78.3 ppt and had decreased from 2007 to 2008 at a rate of −0.7 ppt/yr.

Long-term CFC-11 and CFC-12 data obtained from ground-based infrared solar absorption spectroscopy are available from the Jungfraujoch station (Figure 1-2; an update of Zander et al., 2005). Measured trends in total vertical column abundances during 2001 to 2008 indicate decreases in the atmospheric burdens of these gases that are similar to the declines derived from the global sampling networks over this period. For example, the mean decline in CFC-11 from the Jungfraujoch station column data is −0.83(± 0.06)%/yr during 2001–2009 (relative to 2001), and global and Northern Hemisphere (NH) surface trends range from −0.78 to −0.88%/yr over this same period (range of trends from different networks). For CFC-

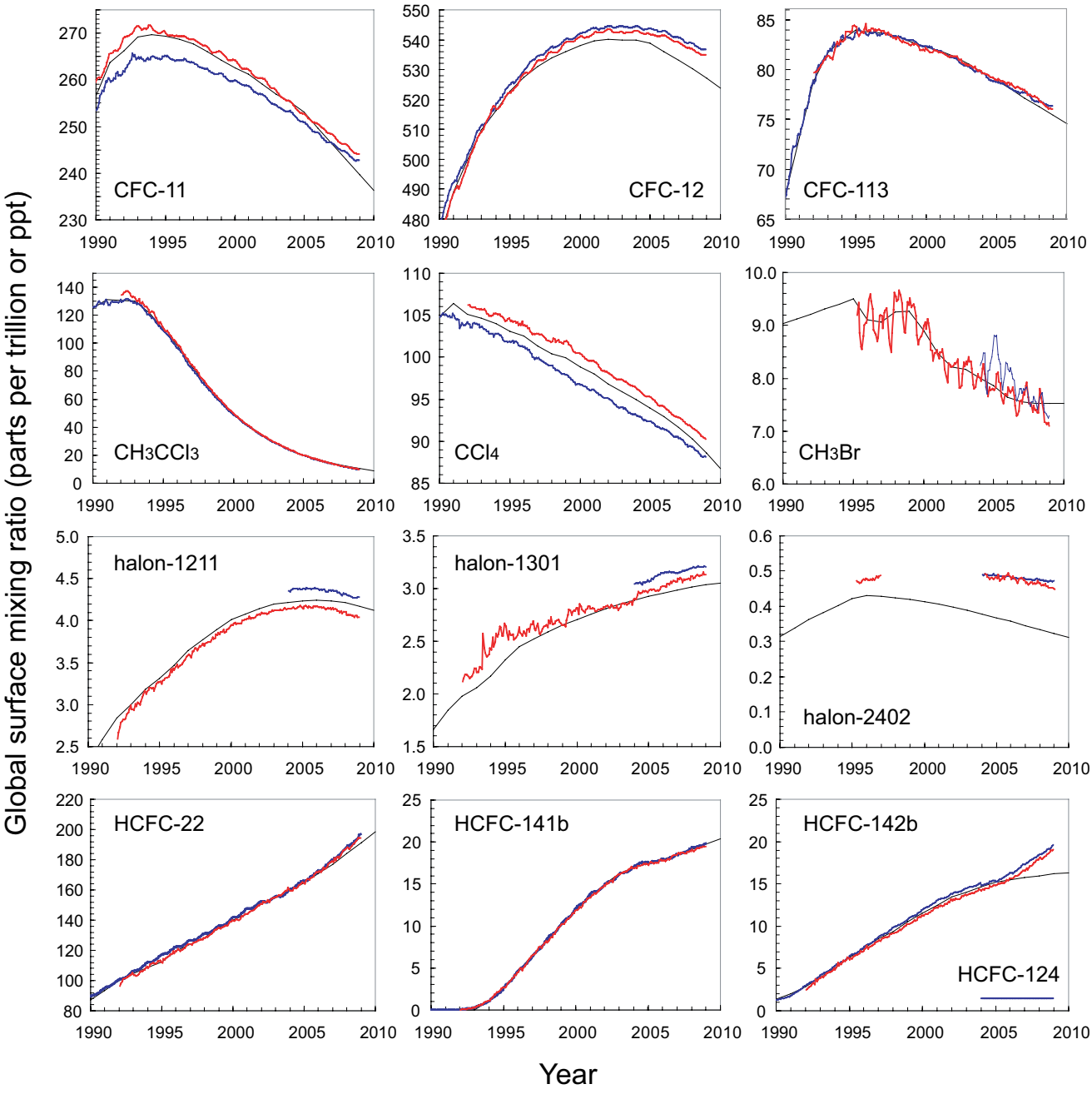

Figure 1-1. Mean global surface mixing ratios (expressed as dry air mole fractions in parts per trillion or ppt) of ozone-depleting substances from independent sampling networks and from scenario A1 of the previous Ozone Assessment (Daniel and Velders et al., 2007) over the past 18 years. Measured global surface monthly means are shown as red lines (NOAA data) and blue lines (AGAGE data). Mixing ratios from scenario A1 from the previous Assessment (black lines) were derived to match observations in years before 2005 as they existed in 2005 (Daniel and Velders et al., 2007). The scenario A1 results shown in years after 2004 are projections made in 2005.

12, the rate of change observed at the Jungfraujoch station was −0.1(± 0.05)% during 2001–2008 (relative to 2001), while observed changes at the surface were slightly larger at −0.2%/yr over this same period.

Additional measurements of CFC-11 in the upper troposphere and stratosphere with near-global coverage have been made from multiple satellite-borne instruments (Kuell et al., 2005; Hoffmann et al., 2008; Fu et al., 2009).

Table 1-1. Measured mole fractions and growth rates of ozone-depleting gases from ground-based sampling.

Chemical Formula	Common or Industrial Name	Annual Mean Mole Fraction (ppt)			Growth (2007–2008)		Network, Method
		2004	2007	2008	(ppt/yr)	(%/yr)	
CFCs							
CCl_2F_2	CFC-12	**543.8**	**539.6**	**537.4**	**−2.2**	**−0.4**	AGAGE, in situ (Global)
		542.3	**537.8**	**535.5**	**−2.3**	**−0.4**	NOAA, flask & in situ (Global)
		539.7	**535.1**	**532.6**	**−2.5**	**−0.5**	UCI, flask (Global)
		541.5	*541.2*	*541.0*	*−0.3*	*−0.05*	NIES, in situ (Japan)
		-	*542.9*	*540.1*	*−2.9*	*−0.5*	SOGE-A, in situ (China)
CCl_3F	CFC-11	**251.8**	**245.4**	**243.4**	**−2.0**	**−0.8**	AGAGE, in situ (Global)
		253.8	**247.0**	**244.8**	**−2.2**	**−0.9**	NOAA, flask & in situ (Global)
		253.7	**246.1**	**244.2**	**−1.9**	**−0.8**	UCI, flask (Global)
		253.6	*247.7*	*247.6*	*−0.1*	*0.0*	NIES, in situ (Japan)
		254.7	*247.4*	*244.9*	*−2.6*	*−1.1*	SOGE, in situ (Europe)
		-	*246.8*	*245.0*	*−1.8*	*−0.7*	SOGE-A, in situ (China)
CCl_2FCClF_2	CFC-113	**79.1**	**77.2**	**76.5**	**−0.6**	**−0.8**	AGAGE, in situ (Global)
		81.1	**78.9**	**78.3**	**−0.6**	**−0.8**	NOAA, in situ (Global)
		79.3	**77.4**	**76.4**	**−1.0**	**−1.3**	NOAA, flask (Global)
		79.1	**77.8**	**77.1**	**−0.7**	**−0.9**	UCI, flask (Global)
		79.7	*78.1*	*78.0*	*−0.1*	*−0.1*	NIES, in situ (Japan)
		-	*77.5*	*76.7*	*−0.8*	*−1.1*	SOGE-A, in situ (China)
$CClF_2CClF_2$	CFC-114	**16.6**	**16.5**	**16.4**	**−0.04**	**−0.2**	AGAGE, in situ (Global)
		16.2	**16.4**	**16.2**	**−0.2**	**−1.3**	UCI, flask (Global)
		16.0	*15.9*	*16.0*	*0.05*	*0.3*	NIES, in situ (Japan)
		-	*16.7*	-	-	-	SOGE, in situ (Europe)
$CClF_2CF_3$	CFC-115	**8.3**	**8.3**	**8.4**	**0.02**	**0.3**	AGAGE, in situ (Global)
		8.6	*8.3*	*8.3*	*0.05*	*0.6*	NIES, in situ (Japan)
		8.3	*8.5*	*8.5*	*0.0*	*0.0*	SOGE, in situ (Europe)
HCFCs							
$CHClF_2$	HCFC-22	**163.4**	**183.6**	**192.1**	**8.6**	**4.6**	AGAGE, in situ (Global)
		162.1	**182.9**	**190.8**	**7.9**	**4.2**	NOAA, flask (Global)
		160.0	**180.7**	**188.3**	**7.6**	**4.2**	UCI, flask (Global)
		-	*190.7*	*200.6*	*9.9*	*5.2*	NIES, in situ (Japan)
		-	*197.3*	*207.3*	*10.0*	*5.0*	SOGE-A, in situ (China)
CH_3CCl_2F	HCFC-141b	**17.5**	**18.8**	**19.5**	**0.7**	**3.6**	AGAGE, in situ (Global)
		17.2	**18.7**	**19.2**	**0.5**	**2.6**	NOAA, flask (Global)
		-	**18.2**	**18.8**	**0.6**	**3.2**	UCI, flask (Global)
		-	*20.2*	*21.2*	*0.9*	*4.6*	NIES, in situ (Japan)
		-	*20.8*	*21.2*	*0.5*	*2.2*	SOGE, in situ (Europe)
CH_3CClF_2	HCFC-142b	**15.1**	**17.9**	**18.9**	**1.1**	**5.9**	AGAGE, in situ (Global)
		14.5	**17.3**	**18.5**	**1.2**	**6.7**	NOAA, flask (Global)
		-	**17.0**	**18.0**	**1.0**	**5.7**	UCI, flask (Global)

Table 1-1, continued.

Chemical Formula	Common or Industrial Name	Annual Mean Mole Fraction (ppt)			Growth (2007–2008)		Network, Method
		2004	2007	2008	(ppt/yr)	(%/yr)	
CH_3CClF_2	HCFC-142b	-	*18.9*	*20.2*	*1.3*	*6.5*	NIES, in situ (Japan)
		-	*19.7*	*21.0*	*1.4*	*6.8*	SOGE, in situ (Europe)
		-	*20.9*	*21.8*	*0.9*	*4.1*	SOGE-A, in situ (China)
$CHClFCF_3$	HCFC-124	**1.43**	**1.48**	**1.47**	**−0.01**	**−0.8**	AGAGE, in situ (Global)
		-	*0.81*	*0.80*	*−0.01*	*−1.2*	NIES, in situ (Japan)
Halons							
CBr_2F_2	halon-1202	*0.038*	*0.029*	*0.027*	*−0.002*	*−7.0*	UEA, flasks (Cape Grim only)
$CBrClF_2$	halon-1211	**4.37**	**4.34**	**4.30**	**−0.04**	**−0.9**	AGAGE, in situ (Global)
		4.15	**4.12**	**4.06**	**−0.06**	**−1.4**	NOAA, flasks (Global)
		4.31	**4.29**	**4.25**	**−0.04**	**−0.8**	NOAA, in situ (Global)
		-	**4.30**	**4.23**	**−0.06**	**−1.4**	UCI, flasks (Global)
		4.62	*4.50*	*4.40*	*−0.1*	*−2.0*	SOGE, in situ (Europe)
		-	*4.40*	*4.31*	*−0.1*	*−2.0*	SOGE-A, in situ (China)
		4.77	*4.82*	*4.80*	*−0.02*	*−0.4*	UEA, flasks (Cape Grim only)
$CBrF_3$	halon-1301	**3.07**	**3.17**	**3.21**	**0.04**	**1.3**	AGAGE, in situ (Global)
		2.95	**3.09**	**3.12**	**0.03**	**1.1**	NOAA, flasks (Global)
		3.16	*3.26*	*3.29*	*0.03*	*1.2*	SOGE, in situ (Europe)
		-	*3.15*	*3.28*	*0.1*	*3.8*	SOGE-A, in situ (China)
		2.45	*2.48*	*2.52*	*0.03*	*1.3*	UEA, flasks (Cape Grim only)
$CBrF_2CBrF_2$	halon-2402	**0.48**	**0.48**	**0.47**	**−0.01**	**−1.2**	AGAGE, in situ (Global)
		0.48	**0.47**	**0.46**	**−0.01**	**−2.0**	NOAA, flasks (Global)
		0.43	*0.41*	*0.40*	*−0.01*	*−1.2*	UEA, flasks (Cape Grim only)
Chlorocarbons							
CH_3Cl	Methyl chloride	**533.7**	**541.7**	**545.0**	**3.3**	**0.6**	AGAGE, in situ (Global)
		545	**550**	**-**	**-**	**-**	NOAA, in situ (Global)
		537	**548**	**547**	**−0.7**	**−0.1**	NOAA, flasks (Global)
		526	*541*	*547*	*5.9*	*1.1*	SOGE, in situ (Europe)
CCl_4	Carbon tetrachloride	**92.7**	**89.8**	**88.7**	**−1.1**	**−1.3**	AGAGE, in situ (Global)
		95.7	**92.3**	**90.9**	**−1.4**	**−1.5**	NOAA, in situ (Global)
		95.1	**92.6**	**91.5**	**−1.1**	**−1.2**	UCI, flask (Global)
		-	*90.2*	*88.9*	*−1.3*	*−1.5*	SOGE-A, in situ (China)
CH_3CCl_3	Methyl chloroform	**21.8**	**12.7**	**10.7**	**−2.0**	**−17.6**	AGAGE, in situ (Global)
		22.5	**13.2**	**11.4**	**−1.9**	**−15.1**	NOAA, in situ (Global)
		22.0	**12.9**	**10.8**	**−2.1**	**−17.8**	NOAA, flasks (Global)
		23.9	**13.7**	**11.5**	**−2.2**	**−17.5**	UCI, flask (Global)
		22.2	*13.1*	*11.0*	*−2.2*	*−18.0*	SOGE, in situ (Europe)
		-	*13.3*	*11.7*	*−1.6*	*−12.8*	SOGE-A, in situ (China)

Table 1-1, continued.

Chemical Formula	Common or Industrial Name	Annual Mean Mole Fraction (ppt)			Growth (2007–2008)		Network, Method
		2004	2007	2008	(ppt/yr)	(%/yr)	
Bromocarbons							
CH_3Br	Methyl bromide	**8.2**	**7.7**	**7.5**	**−0.2**	**−2.7**	AGAGE, in situ (Global)
		7.9	**7.6**	**7.3**	**−0.3**	**−3.6**	NOAA, flasks (Global)
		-	*8.5*	*8.1*	*−0.4*	*−5.2*	SOGE, in situ (Europe)

Notes:

Rates are calculated as the difference in annual means; relative rates are this same difference divided by the average over the two-year period. Results given in bold text and indicated as "Global" are estimates of annual mean global surface mixing ratios. Those indicated with italics are from a single site or subset of sites that do not provide a global surface mean mixing ratio estimate. Measurements of CFC-114 are a combination of CFC-114 and the CFC-114a isomer. The CFC-114a mixing ratio has been independently estimated as being ~10% of the CFC-114 mixing ratio (Oram, 1999) and has been subtracted from the results presented here assuming it has been constant over time.

These observations are updated from the following sources:

Butler et al. (1998), Clerbaux and Cunnold et al. (2007), Fraser et al. (1999), Maione et al. (2004), Makide and Rowland (1981), Montzka et al. (1999; 2000; 2003; 2009), O'Doherty et al. (2004), Oram (1999), Prinn et al. (2000; 2005), Reimann et al. (2008), Rowland et al. (1982), Stohl et al. (2010), Sturrock et al. (2001), Reeves et al. (2005), Simmonds et al. (2004), Simpson et al. (2007), Xiao et al. (2010a ; 2010b), and Yokouchi et al. (2006).

AGAGE, Advanced Global Atmospheric Gases Experiment; NOAA, National Oceanic and Atmospheric Administration; SOGE, System for Observation of halogenated Greenhouse gases in Europe; SOGE-A, System for Observation of halogenated Greenhouse gases in Europe and Asia; NIES, National Institute for Environmental Studies; UEA, University of East Anglia; UCI, University of California-Irvine.

These results uniquely characterize the interhemispheric, interannual, and seasonal variations in the CFC-11 upper-atmosphere distribution, though an analysis of the consistency in trends derived from these platforms and from surface data has not been performed.

The global mixing ratios of the two less abundant CFCs, CFC-114 ($CClF_2CClF_2$) and CFC-115 ($CClF_2CF_3$), have not changed appreciably from 2000 to 2008 (Table 1-1) (Clerbaux and Cunnold et al., 2007). During 2008, global mixing ratios of CFC-114 were between 16.2 and 16.4 ppt based on results from the Advanced Global Atmospheric Gases Experiment (AGAGE) and University of California-Irvine (UCI) networks, and AGAGE measurements show a mean global mixing ratio of 8.4 ppt for CFC-115 (Table 1-1). For these measurements, CFC-114 measurements are actually a combination of CFC-114 and CFC-114a (see notes to Table 1-1).

Observed mixing ratio declines of the three most abundant CFCs during 2005–2008 were slightly slower than projected in scenario A1 (baseline scenario) from the 2006 WMO Ozone Assessment (Daniel and Velders et al., 2007) (Figure 1-1). The observed declines were smaller than projected during 2005–2008 in part because release rates from banks were underestimated in the A1 scenario

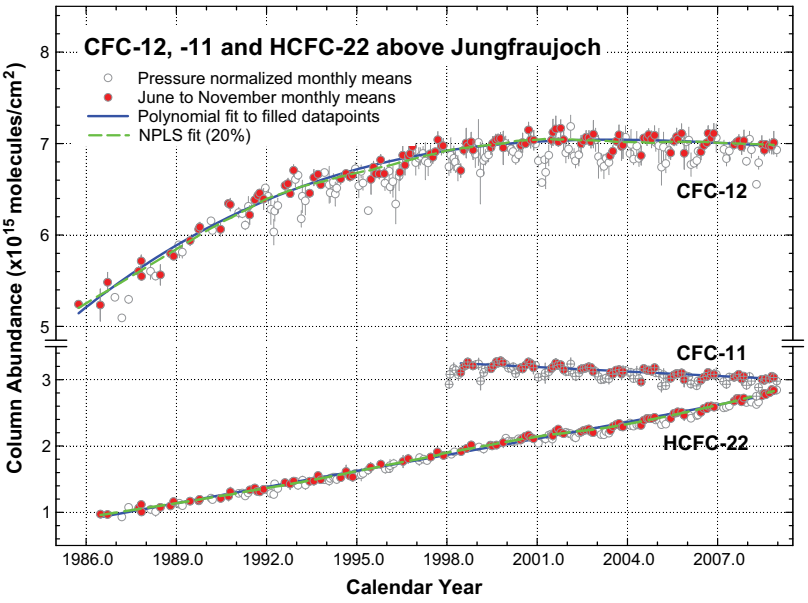

Figure 1-2. The time evolution of the monthly-mean total vertical column abundances (in molecules per square centimeter) of CFC-12, CFC-11, and HCFC-22 above the Jungfraujoch station, Switzerland, through 2008 (update of Zander et al., 2005). Note discontinuity in the vertical scale. Solid blue lines show polynomial fits to the columns measured only in June to November so as to mitigate the influence of variability caused by atmospheric transport and tropopause subsidence during winter and spring (open circles) on derived trends. Dashed green lines show non-parametric least-squares fits (NPLS) to the June to November data.

during this period (Daniel and Velders et al., 2007). For CFC-12, some of the discrepancy is due to revisions to the NOAA calibration scale. In the A1 scenario, CFC-11 and CFC-12 release rates from banks were projected to decrease over time based on anticipated changes in bank sizes from 2002–2015 (IPCC/TEAP 2005). The updated observations of these CFCs, however, are more consistent with emissions from banks having been fairly constant during 2005–2008, or with declines in bank emissions being offset by enhanced emissions from non-bank-related applications. Implications of these findings are further discussed in Chapter 5 of this Assessment.

The slight underestimate of CFC-113 mixing ratios during 2005–2008, however, is not likely the result of inaccuracies related to losses from banks, since banks of CFC-113 are thought to be negligible (Figure 1-1). The measured mean hemispheric difference (North minus South) was ~0.2 ppt during 2005–2008, suggesting the potential presence of only small residual emissions (see Figure 1-4). The mean exponential decay time for CFC-113 over this period is 100–120 years, slightly longer than the steady-state CFC-113 lifetime of 85 years. This observation is consistent with continuing small emissions (≤10 gigagrams (Gg) per year). Small lifetime changes are expected as atmospheric distributions of CFCs respond to emissions becoming negligible, but changes in the atmospheric distribution of CFC-113 relative to loss regions (the stratosphere) suggest that the CFC-113 lifetime should become slightly shorter, not longer, as emissions decline to zero (e.g., Prather, 1997).

CFC Emissions and Banks

Releases from banks account for a large fraction of current emissions for some ODSs and will h.ave an important influence on mixing ratios of many ODSs in the future. Banks of CFCs were 7 to 16 times larger than amounts emitted in 2005 (Montzka et al., 2008). Implications of bank sizes, emissions from them, and their influence on future ODS mixing ratios are discussed further in Chapter 5.

Global, "top-down" emissions of CFCs derived from global surface observations and box models show rapid declines during the early 1990s but only slower changes in more recent years (Figure 1-3) (see Box 1-1 for a description of terms and techniques related to deriving emissions). Emission changes derived for CFC-11, for example, are small enough so that different model approaches (1-box versus 12-box) suggest either slight increases or slight decreases in emissions during 2005–2008. Considering the magnitude of uncertainties on these emissions, changes in CFC-11 emissions are not distinguishable from zero over this four-year period. "Bottom-up" estimates of emissions derived from production and use data have not been updated past 2003 (UNEP/TEAP, 2006), but projections made in 2005 indicated that CFC-11 emissions from banks of ~25 Gg/yr were not expected to decrease substantially from 2002 to 2008 (IPCC/TEAP, 2005) (Figure 1-3).

"Top-down" emissions derived for CFC-11 during 2005–2008 averaged 80 Gg/yr. These emissions are larger than derived from "bottom-up" estimates by an average of 45 (37–60) Gg/yr over this same period. The discrepancy between the atmosphere-derived and "bottom-up" emissions for CFC-11 is not fully understood but could suggest an underestimation of releases from banks or fast-release applications (e.g., solvents, propellants, or open-cell foams). Emissions from such short-term uses were estimated at 15–26 Gg/yr during 2000–2003 (UNEP/TEAP, 2006; Figure 1-3) and these accounted for a substantial fraction of total CFC-11 emissions during those years. The discrepancy may also arise from errors in the CFC-11 lifetime used to derive "top-down" emissions. New results from models that more accurately simulate air transport rates through the stratosphere suggest a steady-state lifetime for CFC-11 of 56–64 years (Douglass et al., 2008), notably longer than 45 years. A relatively longer lifetime for CFC-12 was not suggested in this study. A longer CFC-11 lifetime of 64 years would bring the atmosphere-derived and "bottom-up" emissions into much better agreement (see light blue line in Figure 1-3).

Global emissions of CFC-12 derived from observed atmospheric changes decreased from ~90 to ~65 Gg/yr during 2005–2008 (Figure 1-3). These emissions and their decline from 2002–2008 are well accounted for by leakage from banks as projected in a 2005 report (IPCC/TEAP, 2005). Global emissions of CFC-113 derived from observed global trends and 1-box or 12-box models and a global lifetime of 85 years were small compared to earlier years, and averaged <10 Gg/yr during 2005–2008 (Figure 1-3).

Summed emissions from CFCs have declined during 2005–2008. When weighted by semi-empirical Ozone Depletion Potentials (ODPs) (Chapter 5), the sum of emissions from CFCs totaled 134 ± 30 ODP-Kt in 2008 (where 1 kilotonne (Kt) = 1 Gg = 1×10^9 g). The sum of emissions of CFCs weighted by direct, 100-yr Global Warming Potentials (GWPs) has decreased on average by 8 ± 1%/yr from 2004 to 2008, and by 2008 amounted to 1.1 ± 0.3 gigatonnes of CO_2-equivalents per year (Gt CO_2-eq/yr).

Emission trends and magnitudes can also be inferred from measured hemispheric mixing ratio differences. This approach is valid when emissions are predominantly from the Northern Hemisphere and sink processes are symmetric between the hemispheres. Hemispheric mixing ratio differences for CFC-11 and CFC-12 averaged between 10 and 20 ppt during the 1980s when emissions were large, but since then as emissions declined, hemispheric differences also became smaller. United Nations

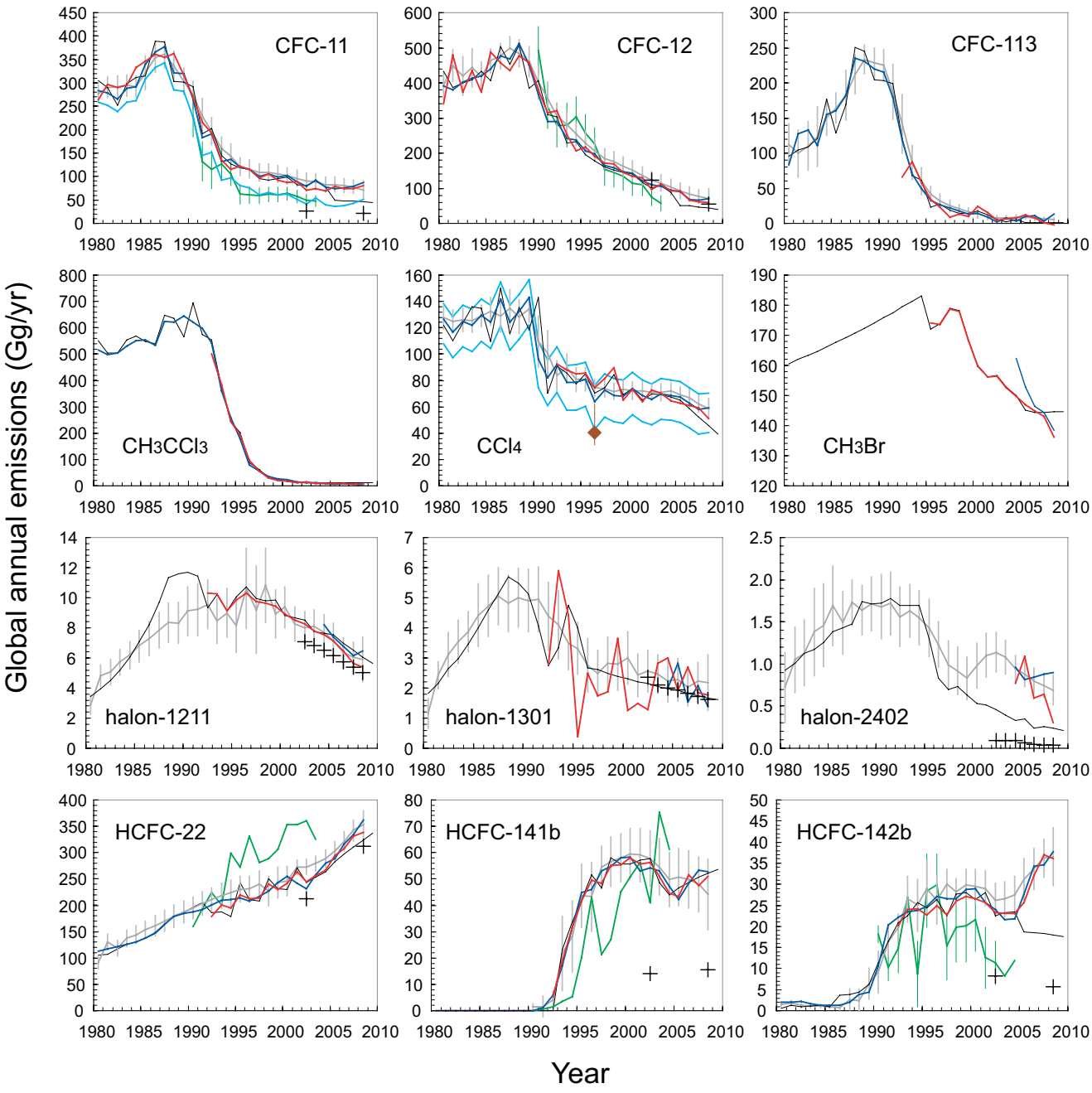

Figure 1-3. "Top-down" and "bottom-up" global emission estimates for ozone-depleting substances (in Gg/yr). "Top-down" emissions are derived with NOAA (red lines) and AGAGE (blue lines) global data and a 1-box model. These emissions are also derived with a 12-box model and AGAGE data (gray lines with uncertainties indicated) (see Box 1-1). Halon and HCFC emissions derived with the 12-box model in years before 2004 are based on an analysis of the Cape Grim Air Archive only (Fraser et al., 1999). A1 scenario emissions from the 2006 Assessment are black lines (Daniel and Velders et al., 2007). "Bottom-up" emissions from banks (refrigeration, air conditioning, foams, and fire protection uses) are given as black plus symbols (IPCC/TEAP, 2005; UNEP, 2007a), and total, "bottom-up" emissions (green lines) including fast-release applications are shown for comparison (UNEP/TEAP, 2006). A previous bottom-up emission estimate for CCl_4 is shown as a brown point for 1996 (UNEP/TEAP, 1998). The influence of a range of lifetimes for CCl_4 (23–33 years) and a lifetime of 64 years for CFC-11 are given as light blue lines.

Box 1-1. Methods for Deriving Trace Gas Emissions

a) Emissions derived from production, sales, and usage (the "bottom-up" method). Global and national emissions of trace gases can be derived from ODS global production and sales magnitudes for different applications and estimates of application-specific leakage rates. For most ODSs in recent years, production is small or insignificant compared to historical levels and most emission is from material in use. Leakage and releases from this "bank" of material (produced but not yet emitted) currently dominate emissions for many ozone-depleting substances (ODSs). Uncertainties in these estimates arise from uncertainty in the amount of material in the bank reservoir and the rate at which material is released or leaks from the bank. Separate estimates of bank magnitudes and loss rates from these banks have been derived from an accounting of devices and appliances in use (IPCC/TEAP, 2005). Emissions from banks alone account for most, if not all, of the "top-down," atmosphere-derived estimates of total global emission for some ODSs (CFC-12, halon-1211, halon-1301, HCFC-22; see Figure 1-3).

b) Global emissions derived from observed global trends (the "top-down" method). Mass balance considerations allow estimates of global emissions for long-lived trace gases based on their global abundance, changes in their global abundance, and their global lifetime. Uncertainties associated with this "top-down" approach stem from measurement calibration uncertainty, imperfect characterization of global burdens and their change from surface observations alone, uncertain lifetimes, and modeling errors. The influence of sampling-related biases and calibration-related biases on derived emissions is small for most ODSs, given the fairly good agreement observed for emissions derived from different measurement networks (Figure 1-3). Hydroxyl radical (OH)-derived lifetimes are believed to have uncertainties on the order of ±20% for hydrochlorofluorocarbons (HCFCs), for example (Clerbaux and Cunnold et al., 2007). Stratospheric lifetimes also have considerable uncertainty despite being based on model calculations (Prinn and Zander et al., 1999) and observational studies (Volk et al., 1997). Recent improvements in model-simulated stratospheric transport suggest that the lifetime of CFC-11, for example, is 56–64 years instead of the current best estimate of 45 years (Douglass et al., 2008).

Global emissions derived for long-lived gases with different models (1-box and 12-box) show small differences in most years (Figure 1-3) (UNEP/TEAP, 2006). Though a simple 1-box approach has been used extensively in past Assessment reports, emissions derived with a 12-box model have also been presented. The 12-box model emissions estimates made here are derived with a Massachusetts Institute of Technology-Advanced Global Atmospheric Gases Experiment (MIT-AGAGE) code that incorporates observed mole fractions and a Kalman filter applying sensitivities of model mole fractions to 12-month semi-hemispheric emission pulses (Chen and Prinn, 2006; Rigby et al., 2008). This code utilizes the information contained in both the global average mole fractions and their latitudinal gradients. Uncertainties computed for these annual emissions enable an assessment of the statistical significance of interannual emission variations.

c) Continental and global-scale emissions derived from measured global distributions. Measured mixing ratios (hourly through monthly averages) can be interpreted using inverse methods with global Eulerian three-dimensional (3-D) chemical transport models (CTMs) to derive source magnitudes for long-lived trace gases such as methane (CH_4), methyl chloride (CH_3Cl), and carbon dioxide (CO_2) on continental scales (e.g., Chen and Prinn, 2006; Xiao, 2008; Xiao et al., 2010a; Peylin et al., 2002; Rödenbeck et al., 2003; Meirink et al., 2008; Peters et al., 2007; Bergamaschi et al., 2009). Although much progress has been made with these techniques in recent years, some important obstacles limit their ability to retrieve unbiased fluxes. The first is the issue that the underdetermined nature of the problem (many fewer observations than unknowns) means that extra information, in the form of predetermined and prior constraints, is typically required to perform an inversion but can potentially impose biases on the retrieved fluxes (Kaminski et al., 2001). Second, all of these methods are only as good as the atmospheric transport models and underpinning meteorology they use. As Stephens et al. (2007) showed for CO_2, biases in large-scale flux optimization can correlate directly with transport biases.

d) Regional-scale emissions derived from high-frequency data at sites near emission regions. High-frequency measurements (e.g., once per hour) near source regions can be used to derive regional-scale (~10^4–10^6 km^2) trace gas emission magnitudes. The method typically involves interpreting measured mixing ratio enhancements above a background as an emissive flux using Lagrangian modeling concepts.

Qualitative indications of emission source regions or "hotspots" are provided by correlating observed mixing ratio enhancements with back trajectories (typically 4- to 10-day) calculated for the sampling time and location (e.g., Maione et al., 2008; Reimann et al., 2004; Reimann et al., 2008).

Quantitative emission magnitudes have been derived with the "ratio-method" (e.g., Dunse et al., 2005; Yokouchi et al., 2006; Millet et al., 2009; Guo et al., 2009). In this straightforward approach, trace-gas emissions are derived from correlations between observed enhancements above background for a trace gas of interest and a second trace gas (e.g., carbon monoxide or radon) whose emissions are independently known. Uncertainties in this approach are reduced when the emissions of the reference substance are well known, co-located, and temporally covarying with the halocarbon of interest, and when the mixing ratio enhancements of both chemicals are well correlated and large relative to uncertainties in the background levels.

More complex and powerful tools combine Lagrangian 3-D models and inverse methods to estimate regional emission fluxes (e.g., Manning et al., 2003; Stohl et al., 2009). As with larger-scale inversions, the challenge with these methods is that the inversion problem is underdetermined and results are dependent on transport accuracy. Furthermore, each station is sensitive to emissions only from a restricted region in its vicinity. To obtain global coverage of emissions from regional measurements, global transport models are used. Stohl et al. (2009) have recently developed a formal analytical method that takes into account a priori information for halocarbon emissions, which allows for regional-scale inversions with a global coverage.

Environment Programme consumption data suggest that CFC emissions continue to be dominated by releases in the Northern Hemisphere (UNEP, 2010). Furthermore, the small (0.2 ppt) hemispheric difference (North minus South) measured for CFC-113 since 2004—when emissions derived from atmospheric trends of this compound were very small (<10 Gg/yr)—indicates at most only a small contribution of loss processes to hemispheric differences for long-lived CFCs (Figure 1-4). By contrast, mean annual hemispheric differences for CFC-11 and CFC-12 have remained between 1.5 and 3 ppt since 2005 and suggest the presence of continued substantial Northern Hemispheric emissions of these chemicals. For CFC-11, the hemispheric difference (North minus South) measured in both global networks has not declined appreciably since 2005 (Figure 1-4), consistent with fairly constant emissions over that period (Figure 1-3).

Polar Firn and Volcano Observations

New CFC observations in firn air collected from the Arctic (two sites) and Antarctic (three sites) show small but detectable CFC-11, -12, and -114 levels increasing after ~1940 and CFC-113 and -115 appearing and increasing after ~1970 (Martinerie et al., 2009). These results add to conclusions from earlier firn-air studies (Butler et al., 1999; Sturrock et al., 2002) indicating that natural sources of CFCs, CCl_4, CH_3CCl_3, halons, and HCFCs, if they exist, must be very small. Such conclusions rely on these compounds being stable in firn. Consistent with this result, studies of fumarole discharges from three Central American volcanoes over two years show that volcanic emissions are not a significant natural source of CFCs (Frische et al., 2006).

1.2.1.2 HALONS

Updated observations show that the annual global surface mean mixing ratio of halon-1301 ($CBrF_3$) increased at a rate of 0.03–0.04 ppt/yr during 2007–2008 and reached 3.1–3.2 ppt in mid-2008 (Figure 1-1; Table 1-1). Revised calibration procedures and reliance on gas chromatography with mass spectrometric detection analyses of flasks within NOAA have improved the consistency (within 5% in 2008) among results from independent laboratories compared to past reports (Clerbaux and Cunnold et al., 2007).

The global surface mean mixing ratio of halon-1211 ($CBrClF_2$) began to decrease during 2004–2005 and changed by -0.05 ± 0.01 ppt/yr during 2007–2008 (Figure 1-1; Table 1-1). The global surface mean in 2008 was only about 0.1 ppt lower than peak levels measured in 2004.

Updated halon-2402 ($CBrF_2CBrF_2$) observations indicate that global surface mixing ratios declined from 0.48 ppt in 2004 to 0.46–0.47 ppt in 2008 at a rate of −0.01 ppt/yr in 2007–2008 (Table 1-1).

Updated halon-1202 (CBr_2F_2) measurements (Fraser et al., 1999; Reeves et al., 2005) show a substantial decrease in mixing ratios of this chemical since 2000. Southern Hemispheric mixing ratios decreased from 0.038 ppt in 2004 to 0.027 ppt in 2008 at a rate of −0.002 ppt/yr in 2007–2008.

The observed changes in halon-1211 mixing ratios during 2005–2008 are similar to those projected in the A1 scenario of the previous Assessment (Daniel and Velders et al., 2007); halon-1301 has increased at a slightly higher rate than projected. Observed surface mixing ratios of halon-2402 are notably higher than scenarios from past

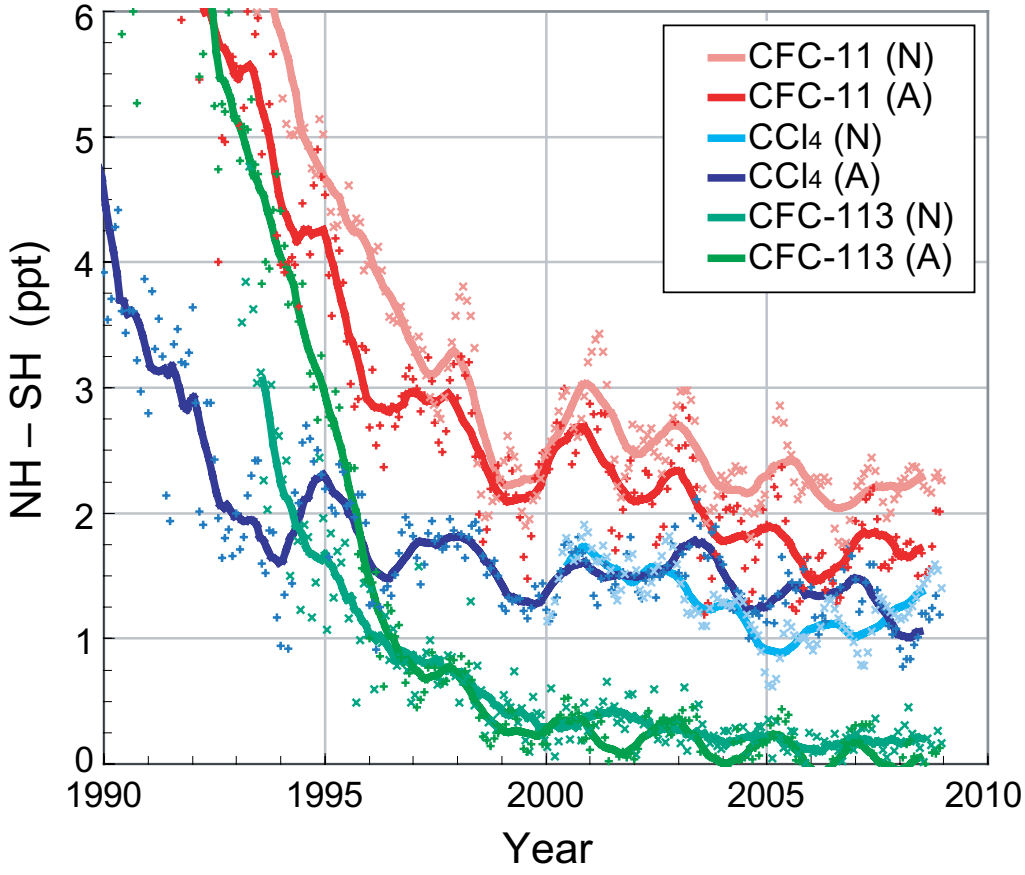

Figure 1-4. Mean hemispheric mixing ratio differences (North minus South, in parts per trillion) measured for some ODSs in recent years from independent sampling networks (AGAGE data (A) as plusses, Prinn et al., 2000; and NOAA data (N) as crosses, Montzka et al., 1999). Points are monthly-mean differences; lines are running 12-month means of the monthly differences.

Assessments because those scenarios were not based on actual measurement data (Figure 1-1).

Halon Emissions, Stockpiles, and Banks

Stockpiles and banks of halons, which are used primarily as fire extinguishing agents, represent a substantial reservoir of these chemicals. The amounts of halons present in stockpiles or banks are not well quantified, but were estimated to be 15–33 times larger than emissions of halon-1211 and halon-1301 in 2008 (UNEP, 2007a). "Bottom-up" estimates of halon emissions derived from production and use data were recently revised based on a reconsideration of historic release rates and the implications of this reanalysis on current bank sizes (UNEP, 2007a). The magnitude and trends in these emission estimates compare well with those derived from global atmospheric data and best-estimate lifetimes for halon-1211 and halon-1301 (Figure 1-3). "Bottom-up" emission estimates of halon-2402 are significantly lower than those derived from global atmospheric trends. Bank-related emissions are thought to account for nearly all halon emissions (plusses in Figure 1-3). Halons are also used in small amounts in non-fire suppressant applications and as chemical feedstocks, but these amounts are not included in the "bottom-up" emissions estimates included in Figure 1-3.

Summed emissions of halons, weighted by semi-empirical ODPs, totaled 90 ± 19 ODP-Kt in 2008. When weighted by 100-yr direct GWPs, summed halon emissions totaled 0.03 Gt CO_2-eq in 2008.

1.2.1.3 Carbon Tetrachloride (CCl_4)

The global mean surface mixing ratio of CCl_4 continued to decrease during 2005–2008 (Figure 1-1). By 2008, the surface mean from the three global surface networks was approximately 90 ± 1.5 ppt and had de-

creased during 2007–2008 at a rate of −1.1 to −1.4 ppt/yr (Table 1-1).

Global CCl_4 Emissions

Though the global surface CCl_4 mixing ratio decreased slightly faster during 2005–2008 than during 2000–2004 (Figure 1-1), the observations imply only a slight decrease in CCl_4 emissions over time (Figure 1-3). The measured global CCl_4 mixing ratio changes suggest "top-down," global emissions between 40 and 80 Gg/yr during 2005–2008 for a lifetime of 33–23 years (see Box 1-2). Similar emission magnitudes and trends are derived for recent years from the independent global sampling networks and with different modeling approaches (Figure 1-3). The decline observed for CCl_4 mixing ratios during 2005–2008 was slightly less rapid than that projected in the A1 scenario of the previous Assessment (Daniel and Velders et al., 2007), which was derived assuming a linear decline in emissions from 65 Gg/yr in 2004 to 0 Gg/yr in 2015 and a 26-year lifetime (Daniel and Velders et al., 2007).

As with other compounds, "top-down" emissions for CCl_4 are sensitive to errors in global lifetimes. A lifetime at the upper (or lower) end of the current uncertainty range yields a smaller (larger) emission than when calculated with the current best-estimate lifetime of 26 years (Figure 1-5). The magnitude of uncertainties that remain in the quantification of CCl_4 sinks (i.e., stratosphere, ocean, and soil), however, do not preclude revisions to the CCl_4 lifetime in the future that could significantly change the magnitude of "top-down" emissions.

Global CCl_4 emission magnitudes and their trends also can be qualitatively assessed from measured hemispheric differences, which are roughly proportional to emissions for long-lived trace gases emitted primarily in the Northern Hemisphere (see Section 1.2.1.1). This difference has remained fairly constant for CCl_4 at 1.25–1.5 ppt over the past decade (Figure 1-4). These differences are independent of measured year-to-year changes in atmospheric mixing ratios and so provide a first-order consistency check on emission magnitudes and trends. Though the hemispheric difference (NH minus SH) expected for CCl_4 in the absence of emissions is not well defined, it is expected to be small because the asymmetry in loss fluxes between the hemispheres due to oceans and soils is likely small (<10 Gg/yr) and offsetting. This analysis suggests, based on the considerations discussed above for CFCs, that the significant and sustained NH minus SH difference observed for CCl_4 mixing ratios arises from substantial NH CCl_4 emissions that have not changed substantially over the past decade (Figure 1-3).

In contrast to the CCl_4 emissions derived from "top-down" methods, those derived with "bottom-up" techniques suggest substantially smaller emissions in most years. In the past two Assessment reports, for example, the "bottom-up" emissions estimate for CCl_4 during 1996 was 41 (31–62) Gg/yr (UNEP/TEAP 1998), or 20–50 Gg/yr lower than the "top-down," atmosphere-derived estimate for that year (Montzka and Fraser et al., 2003; Clerbaux and Cunnold et al., 2007). Because similar estimates have not been made for subsequent years, we derive here "potential emissions" from the difference between CCl_4 production magnitudes in excess of amounts used as feedstock and amounts destroyed that are reported to UNEP (UNEP, 2010) (for the European Union (EU), feedstock magnitudes were determined from numbers reported by the individual EU countries and not from the EU as a whole). An upper limit to these "potential emissions" was also derived from this same data by filling apparent gaps in production and feedstock data reported to UNEP, including a 2% fugitive emissions rate from quantities used as feedstock, and incorporating an efficiency for reported CCl_4 destruction of only 75% (Figure 1-5). This approach yields emissions of 0–30 Gg/yr during 2005–2008. As is apparent from this figure, CCl_4 continues to be produced in substantial quantities (reported production in 2008 was 156 Gg), but the primary use of this production is for feedstocks (e.g., in the production of some hydrofluorocarbons (HFCs), see Table 1-11, and other chemicals) that should yield only small emissions.

This "bottom-up" "potential emission" history derived from reported production, feedstock, and destruction data is inconsistent with the magnitude and variability in the "top-down," atmosphere-derived emissions. Importantly, these differences cannot be reconciled by a simple scaling of the CCl_4 atmospheric lifetime (Figure 1-5). This is particularly true during 2003–2008, when large declines are derived for "bottom-up" "potential emissions" but are not suggested by the atmosphere-derived "top-down" estimates or by the relatively constant NH minus SH difference measured during these years. The discrepancies during 2005–2008 between the "top-down" and "potential emission" estimates are between 30 and 50 Gg/yr. Even when the upper limit to "potential emissions" are compared to the lower range of "top-down" emissions (lifetime = 33 years), a discrepancy during 2005–2008 of 15–30 Gg/yr remains (Figure 1-5). Though the magnitude of this discrepancy is sensitive to the uncertain CCl_4 lifetime (Box 1-2), the different time-dependent changes implied for emissions particularly during 2003–2008 with the different estimation methods are not sensitive to this lifetime.

Regional Studies

Observational studies can potentially provide information about regional source distributions and magnitudes (Box 1-1). Recently, Xiao et al. (2010b) have inversely

Box 1-2. CCl_4 Lifetime Estimates

The loss of carbon tetrachloride (CCl_4) in the global atmosphere is dominated by photolytic destruction in the stratosphere but also occurs by surface ocean uptake and uptake by soils. The atmospheric lifetime due to photolysis is estimated to be 35 years based on older modeling data and measured gradients in the lower stratosphere (Prinn and Zander et al., 1999; Volk et al., 1997). This number is based in part on the atmospheric lifetime of CFC-11. For example, in an analysis of global CCl_4 distributions measured by satellite, Allen et al. (2009) derived a lifetime for CCl_4 of 34 ± 5 years relative to a lifetime for CFC-11 of 45 years. An updated analysis of model-derived lifetimes, however, indicates that current models that more accurately simulate different stratospheric metrics (age of air, for example) calculate a substantially longer stratospheric lifetime for CFC-11 of 56–64 years (Douglass et al., 2008). Although CCl_4 was not explicitly considered in the Douglass et al. study, the results could suggest a longer CCl_4 partial lifetime with respect to stratospheric loss of ~ 44–50 yr. A recent independent analysis provides further evidence that the CCl_4 stratospheric lifetime may be as long as 50 years (Rontu Carlon et al., 2010).

Undersaturations of CCl_4 have been observed in many different regions of the world's ocean waters and are indicative of a CCl_4 sink (Wallace et al., 1994; Lee et al., 1999; Huhn et al., 2001; Yvon-Lewis and Butler, 2002; Tanhua and Olsson, 2005). These undersaturations are larger than can be explained from laboratory-determined hydrolysis rates and the responsible loss mechanism is not known. In the absence of new results, the partial lifetime with respect to oceanic loss of 94 (82–191) years (Yvon-Lewis and Butler, 2002) remains unchanged.

Losses of atmospheric CCl_4 to a subset of terrestrial biomes have been observed in independent studies published since the previous Assessment (Liu, 2006; Rhew et al., 2008). These results confirm that terrestrial biomes can act as a sink for CCl_4, but the magnitude of this loss remains uncertain. Losses to tropical soils account for most of the calculated soil sink (62%), but are based primarily on results from one tropical forest (Happell and Roche, 2003) and have yet to be remeasured. The new flux estimates reported for temperate forest and temperate grassland areas were derived with soil gas gradient methods and, in semi-arid and arid shrublands, with flux chamber methods. In these remeasured biomes, Liu (2006) and Rhew et al. (2008) found a mean sink about half as strong as in the original Happell and Roche (2003) study. When a range of partial lifetimes with respect to soil losses and other losses is considered, a mid-range estimate for CCl_4 lifetime remains at 26 (23–33) years (see Table 1).

Box 1-2 Table 1. Sensitivity of total global CCl_4 lifetime to component sink magnitudes.

Partial Lifetimes (years) with Respect to Loss to:				
Stratosphere	**Ocean**	**Soil**	**Total Lifetime**	**Description and Notes**
35	∞	∞	35	pre-2003 Ozone Assessments
35	94	∞	26	post-2003 Ozone Assessments[1]
35	94	90	20	a
35	94	101	20	b
35	94	195	23	c
44–50	94	∞	30–33	d
44–50	94	195	26–28	c & d
44–50	94	101	23–25	b & d

Notes:

[1] Montzka and Fraser et al. (2003); Clerbaux and Cunnold et al. (2007).

(a) Partial lifetime from loss to soils derived from Happell and Roche (2003) from measurements in seven different biomes.

(b) Rhew et al. (2008) and Liu (2006) estimates of loss to arid land, temperate forest, and temperate grasslands soils used instead of those estimated by Happell and Roche (2003), and Happell and Roche (2003) loss estimates for soils in the other four biomes.

(c) All soil losses in Happell and Roche (2003) were scaled by 0.5 to account for updated results (Rhew et al. (2008) and Liu (2006)) in three of the seven biomes originally studied being only half as large, on average, as originally found.

(d) A longer stratospheric CCl_4 lifetime (of 50 years) is considered based on a CFC-11 lifetime of 56-64 years rather than 45 years (Douglass et al., 2008) (44 yr = 35×56/45; 50 yr = 35×64/45), consistent with the recent work of Rontu Carlon et al. (2010).

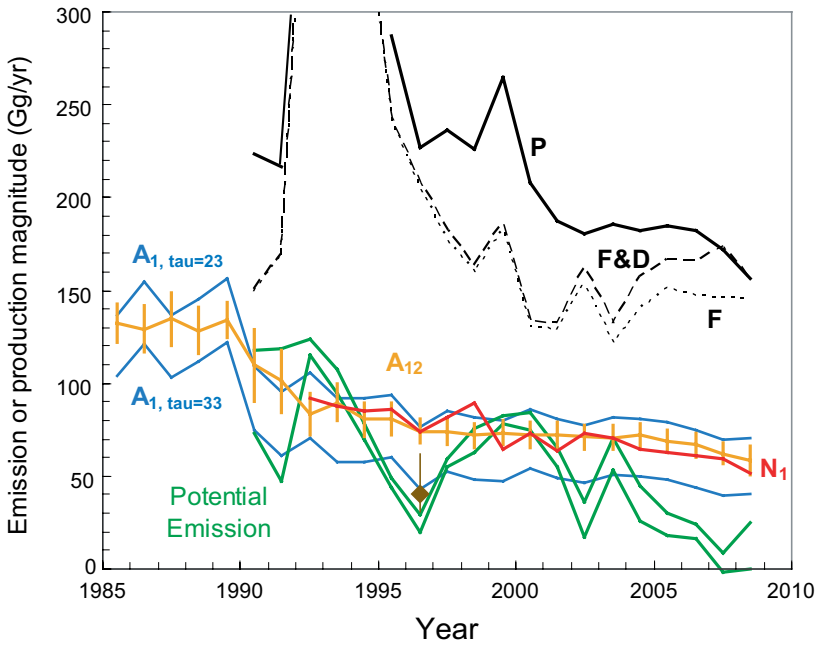

Figure 1-5. Atmospheric ("top-down") global CCl_4 emissions (Gg/yr) derived from observations (blue, red, and orange lines, some of which are shown in Figure 1-3) compared to "potential emissions" derived from UNEP production data (green lines). The lower "potential emissions" green line is derived from the difference between total CCl_4 production (solid black line labeled "P") reported to UNEP and the sum of feedstock and amounts destroyed (dashed line labeled "F&D") (production magnitudes to feedstock alone are indicated with the dotted line labeled "F"). The upper "potential emission" green line was derived similarly as the lower line but was augmented by additional amounts to fill apparent gaps in UNEP reporting, plus an allotment for fugitive emissions of 2% of reported CCl_4 feedstock use, plus an efficiency of only 75% for reported destruction. Top-down emission estimates are derived from a 1-box model of NOAA atmospheric data (red line labeled N_1) and a 12-box analysis of the AGAGE data (orange line labeled A_{12}) with a lifetime of 26 years (see Box 1-1). The influence of lifetimes between 23 and 33 years on emissions derived with the 1-box model from AGAGE data are also indicated (blue lines labeled $A_{1,\,tau=23}$ and $A_{1,\,tau=33}$). The TEAP "bottom-up" emission estimate for 1996 is shown as a brown diamond (UNEP/TEAP, 1998).

estimated regional and global annual CCl_4 emissions and sinks using the three-dimensional Model of Atmospheric Transport and Chemistry (3D-MATCH) model, a monthly applied Kalman filter, a priori industrial emission patterns for 8 regions in the world, and observed monthly-mean mixing ratios from 1996–2004 at multiple, globally distributed AGAGE and NOAA/Earth System Research Laboratory (ESRL) sites. The average 1996–2004 East Asian (including China) emissions accounted for 53.3 ± 3.6% of the global total industrial emissions during this period. The fraction of global emissions inferred from South Asia (including India) were estimated at 22.5 ± 3.0%, those from Africa at 9.0 ± 1.2%, those from North America at 6.6 ± 1.9%, and those from Europe at 4.0 ± 2.2%.

Regional emissions of CCl_4 have also been estimated from measured mixing ratio enhancements in pollution events near source regions. These studies have suggested small or no detectable (ND) emissions from North America during 2003–2006 (Millet et al., 2009: ND; Hurst et al., 2006: <0.6 Gg/yr), Australia (Dunse et al., 2005: none detected in most years during 1995–2000), and Japan (Yokouchi et al., 2005: 1.8 Gg/yr in 2001 decreasing to 0.27 Gg/yr in 2003). Larger emissions have been inferred as coming from China (Vollmer et al., 2009: 15 (10–22) Gg/yr for the period Oct 2006–March 2008). While these studies and those of Xiao et al. (2010b) point to countries in South East Asia (including China) as providing a large fraction of CCl_4 emissions in the past, it is not possible to gauge their consistency relative to one another or relative to "top-down" global emission magnitudes owing to the different time periods included and incomplete geographic coverage addressed by these studies.

1.2.1.4 Methyl Chloroform (CH_3CCl_3)

Surface mixing ratios of methyl chloroform (CH_3CCl_3) continued to decrease at a near-constant exponential rate in the remote global atmosphere during 2005–2008. By mid-2008 the global surface mean mixing ratio had decreased to about 11 ppt (Figure 1-1). This decline represents more than a factor of 10 decrease in global surface mixing ratios of this chemical since the early 1990s. As CH_3CCl_3 mixing ratios have declined in response to reduced emissions, hemispheric differences have also diminished. The mean annual hemispheric difference (NH minus SH) was a few percent of the global mean during 2005–2008, much smaller than during the 1980s when emissions were substantial. Measured abundances and rates of change in 2008 agree to within about

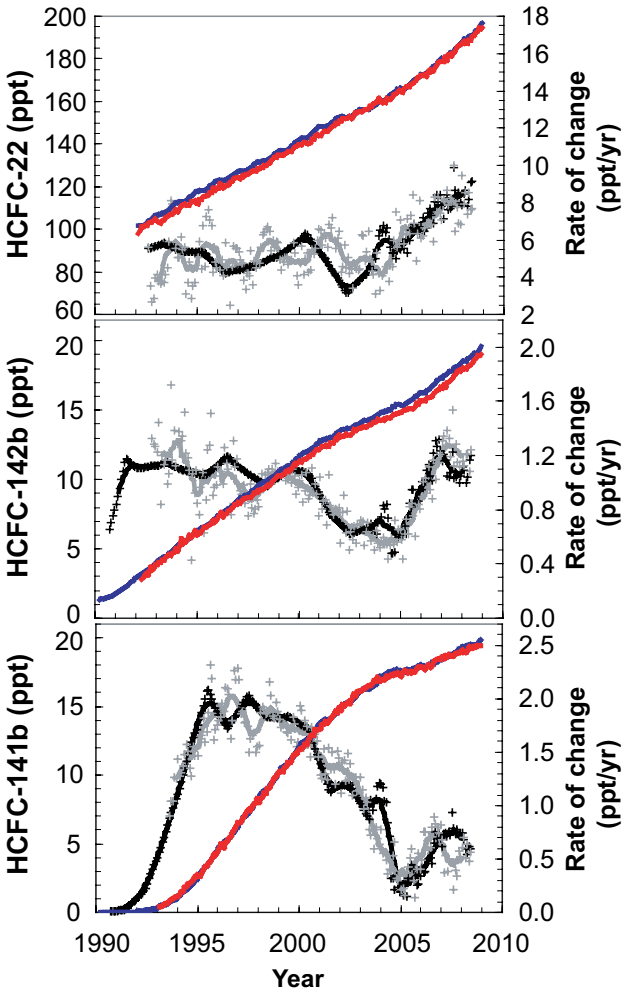

Figure 1-6. Global surface monthly-mean mixing ratios (parts per trillion) measured by NOAA (red) and AGAGE (blue) for the three most abundant HCFCs (left-hand scale) (Montzka et al., 2009; O'Doherty et al., 2004). Growth rates (ppt/yr) estimated as 12-month differences from AGAGE (black points) and NOAA (gray points) are shown relative to the right-hand scale and are plotted relative to the midpoint of the 12-month interval. Growth rates smoothed over 12-month periods appear as black and gray lines. Tic marks correspond to the beginning of each year.

12% among the different ground-based measurement networks (Table 1-1).

Losses of CH_3CCl_3 are dominated by oxidation by the hydroxyl radical (OH). Other processes such as photolysis and oceanic removal also are significant sinks for CH_3CCl_3 (Clerbaux and Cunnold et al., 2007; Yvon-Lewis and Butler, 2002). Accurate quantification of all CH_3CCl_3 loss processes is particularly important because budget analyses of this chemical (e.g., Prinn et al., 2005) provide estimates of global abundance of the hydroxyl radical, an important oxidant for many reduced atmospheric gases.

The potential for significant terrestrial losses of CH_3CCl_3 has been further explored since the previous Assessment. Aerobic soils had been previously identified as a sink for CH_3CCl_3, accounting for 5 ± 4% (26 ± 19 Gg/yr) of global removal rates in 1995 (Happell and Wallace, 1998). This estimate was based on soil gas profiles measured in Long Island, New York. A more recent study using flux chamber methods in southern California salt marshes and shrublands showed average net fluxes for CH_3CCl_3 that were <10% of uptake rates in the Long Island study, suggesting a less significant role for soils as a sink for this compound (Rhew et al., 2008). No new studies related to oceanic losses have been published since 2006; the estimated partial atmospheric lifetime for CH_3CCl_3 with respect to ocean loss remains 94 (81–145) years.

CH_3CCl_3 Emissions and Banks

Emissions of CH_3CCl_3 have declined substantially since the early 1990s. When derived from atmospheric changes and a 5-year lifetime, inferred emissions of CH_3CCl_3 during 2005–2008 are calculated to be less than 10 Gg/yr (Figure 1-3). Banks for CH_3CCl_3 are thought to be negligible owing to its dominant past use in applications resulting in rapid release to the atmosphere.

CH_3CCl_3 emissions arise primarily from industrial production, though some fugitive emissions may arise from its use as a feedstock in the production of HCFC-141b and HCFC-142b. Previous laboratory-based studies of biomass combustion combined with limited field sampling of biomass burning plumes suggested the potential for nonindustrial emissions of 2.5–11.5 Gg/yr CH_3CCl_3 from biomass burning (Rudolph et al., 1995; Rudolph et al., 2000). A recent study of many ambient air samples significantly affected by biomass burning suggests very small or negligible CH_3CCl_3 emissions from this source (<<1 Gg/yr) (Simpson et al., 2007).

1.2.1.5 Hydrochlorofluorocarbons (HCFCs)

HCFCs are regularly measured in three global ground-based networks and at a number of additional sites around the world using grab-sampling techniques (Montzka et al., 2009; O'Doherty et al., 2004; Stemmler et al., 2007; Yokouchi et al., 2006). Results from all three networks indicate that global mean surface mixing ratios of the three most abundant HCFCs (i.e., HCFC-22, -142b, and -141b) continued to increase during 2005–2008 (Figure 1-6). Mixing ratios have also been determined for HCFC-22 and HCFC-142b from Fourier transform infrared (FTIR) instruments onboard the Envisat (the Michelson Interferometer for Passive Atmospheric Sounding, or

MIPAS-E) and Atmospheric Chemistry Experiment (the ACE-Fourier Transform Spectrometer or ACE-FTS instrument) satellites, respectively (Moore and Remedios, 2008; Rinsland et al., 2009).

The global mean surface mixing ratio of HCFC-22 ($CHClF_2$) was 188–192 ppt in 2008, with an averaged annual growth rate of 8.0 ± 0.5 ppt/yr (4.3 ± 0.3%/yr) during 2007–2008 (Table 1-1; Figure 1-6). This increase is approximately 60% larger than the mean rate of change during 1992–2004 or the rate of change reported from global surface sampling networks during 2003–2004 (Clerbaux and Cunnold et al., 2007). Though the rate of HCFC-22 increase from 2007–2008 was comparable to that projected in the A1 scenario of the previous Assessment report (7 ppt/yr; Daniel and Velders et al., 2007), the mixing ratio increase during the entire 2005–2008 period was notably larger than in the scenario projection (Figure 1-1).

Moore and Remedios (2008) report a 2003 global mean HCFC-22 mixing ratio from MIPAS-E at 300 hPa of 177 ± 18 ppt (uncertainty includes 0.5 ppt of random error on the mean and an additional systematic uncertainty); this value is in fairly good agreement with the 2003 global mean surface mixing ratio of 160 ± 2 ppt (Clerbaux and Cunnold et al., 2007). They also deduce an average HCFC-22 growth rate of 3.5 ± 0.4%/yr (5.4 ± 0.7 ppt/yr) in the northern midlatitude (20°N–50°N) lower stratosphere (50–300 hPa) between November 1994 and October 2003 from the Atmospheric Trace Molecule Spectroscopy (ATMOS) (Atmospheric Laboratory for Applications and Science, ATLAS-3) based on measured HCFC-22/nitrous oxide (N_2O) correlations. This rate is similar to the 3.92 ± 2.08%/yr derived using a similar approach with ATMOS and ACE-FTS (from 2004) HCFC-22 data near 30°N (Rinsland et al., 2005). A slightly larger mean growth rate (4.3 ± 0.5%/yr or 6.0 ± 0.7 ppt/yr) is estimated for the lower stratosphere from the MIPAS-E HCFC-22 data at southern high latitudes (60°S–80°S) (Moore and Remedios, 2008). This averaged rate is comparable to global mean HCFC-22 trends at the surface during this period (~5.2 ppt/yr).

Total vertical column abundances of HCFC-22 above the Jungfraujoch station (Figure 1-2, an update of Zander et al., 2005) also indicate an increase of 4.31 ± 0.17%/yr with respect to 2005 values over the 2005–2008 period, which is comparable with NH trends from surface networks (4.2–4.5%/yr calculated similarly). Moreover, Gardiner et al. (2008) applied a bootstrap resampling method to aggregated total and partial column datasets from six European remote sensing sites to quantify long-term trends across the measurement network; they found a mean tropospheric increase for HCFC-22 at these sites of 3.18 ± 0.24%/yr, which is slightly smaller than determined from ground-level grab samples at surface sites in high northern latitudes such as Mace Head, Barrow, or Alert during the analyzed period (1999–2003 rates of 3.7–3.9%/yr).

The global mean surface mixing ratio of HCFC-142b (CH_3CClF_2) increased to 18.0–18.9 ppt in 2008 with an averaged annual growth rate of about 1.0–1.2 ppt/yr (6.1 ± 0.6%/yr) during 2007–2008 (Table 1-1; Figure 1-6). After declining from the late 1990s to 2003, the growth rate of HCFC-142b increased substantially during 2004–2008. During 2007–2008 this rate was approximately two times faster than reported for 2003–2004 (Montzka et al., 2009). This accelerated accumulation of HCFC-142b was not projected in the A1 scenario of the 2006 Assessment (the projected 2007–2008 rate was 0.2 ppt/yr); a substantial divergence occurred between projected and observed mixing ratios after 2004 (Figure 1-1). The mean difference in reported mixing ratios from AGAGE and NOAA of 3.3% (with AGAGE being higher) is primarily related to calibration differences of ~2.9% reported previously (O'Doherty et al., 2004). Global means from UCI are approximately 2% lower than NOAA (Table 1-1).

The first satellite measurements of HCFC-142b have been made from the ACE-FTS instrument (Rinsland et al., 2009). Monthly-mean ACE-FTS HCFC-142b mixing ratios over 13–16 kilometers (km) altitude, with an estimated total (random and systematic) error of ~20%, were used to derive trends at northern (25–35°N) and southern (25–35°S) midlatitudes of 4.94 ± 1.51%/yr and 6.63 ± 1.23%/yr, respectively, over the interval from February 2004 to August 2008. The ACE-FTS trends are consistent with those computed from flask sampling measurements over a similar time period (5.73 ± 0.14%/yr at Niwot Ridge (40°N) and 5.46 ± 0.08%/yr at Cape Grim (40°S) over the interval from July 2003 to July 2008) (Rinsland et al., 2009).

The global mean surface mixing ratio of HCFC-141b (CH_3CCl_2F) continued to increase during 2005–2008. By 2008, mean, global surface mixing ratios were 18.8–19.5 ppt (Table 1-1). The growth rate of HCFC-141b decreased from approximately 2 ppt/yr in the mid-1990s to <0.5 ppt/yr in 2004–2005 (Figure 1-6). Since 2005 the growth rate has varied between 0.2–0.8 ppt/yr, similar to the mean 0.5 ppt/yr increase projected in the A1 scenario over this period (Daniel and Velders et al., 2007). The mean increase during 2007–2008 was 0.6 (±0.1) ppt/yr (or 3.2 ± 0.5%/yr).

The annual global surface mean mixing ratio of HCFC-124 ($CHClFCF_3$) has been updated from AGAGE measurements (Prinn et al., 2000) and has decreased to 1.5 ± 0.1 ppt in 2008, with an averaged annual growth rate of −0.01 ± 0.01 ppt/yr (−0.8 ± 0.8%/yr) for 2007–2008. No updated HCFC-123 ($CHCl_2CF_3$) measurements are available.

Recent changes in atmospheric growth rates of the three most abundant HCFCs can be explained qualitatively with UNEP (2010) production and consumption data (Figure 1-7). Global HCFC production for dispersive uses increased rapidly in developed countries during the

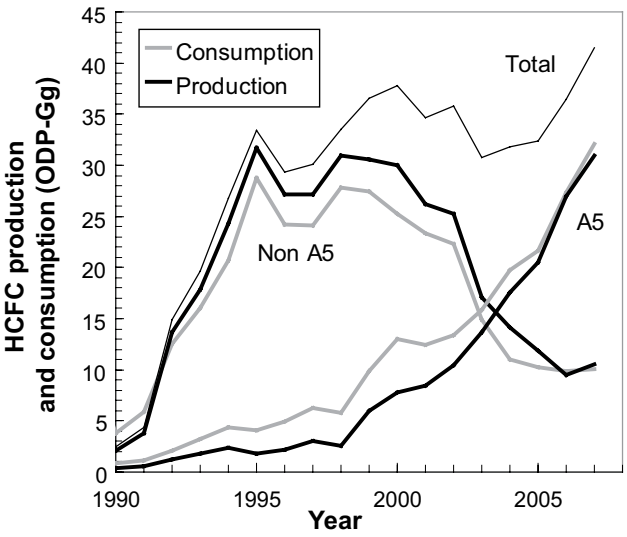

Figure 1-7. Production and consumption (in ODP-Gg) of HCFCs in developed (Non A5) and developing (A5) countries as reported to UNEP for dispersive uses only. Also shown (thin line) is the global total reported production (UNEP, 2010). Note that 1 ODP-Gg = 1 ODP-Kt.

1990s. But as this production was being phased out in developed countries, global totals decreased slightly from 2000–2003. This trend reversed during 2003–2008 as production and consumption grew substantially in developing countries (those operating under Article 5 of the Montreal Protocol, also referred to as A5 countries). In 2008 HCFC data reported to UNEP, developing (A5) countries accounted for 74% and 73% of total, ODP-weighted HCFC consumption and production, respectively (UNEP, 2010).

HCFC Emissions and Banks

Global emissions of HCFC-22 continued to increase during 2005–2008. By 2008, "top-down" emissions inferred from global atmospheric changes totaled 320–380 Gg/yr, up from approximately 280 Gg/yr in 2004. These emissions are reasonably consistent with the emissions derived from banks for 2002 and projected for 2008 in a 2005 study (IPCC/TEAP, 2005) (Figure 1-3). These results suggest that the dominant emission for HCFC-22 is from banks contained in current, in-use applications. Total "bottom-up" emissions derived for past years (UNEP/TEAP, 2006; estimates available through 2003 only) show a similar trend to emissions derived from atmospheric data, but are larger in most years (Figure 1-3).

While atmosphere-derived global emissions for HCFC-141b and HCFC-142b decreased slightly during the 2000–2004 period as production in developed countries was diminishing (Montzka et al., 2009), emissions of both of these HCFCs increased during 2005–2008 (Figure 1-3). The substantial increase in HCFC-142b emissions was not projected in the A1 scenario of the previous Assessment (Daniel and Velders, 2007). In that scenario, a 23% emissions decline was projected during 2004 to 2008 (relative to 2004 levels). Instead, HCFC-142b emissions in 2008 derived from observed global mixing ratio changes (37 ± 7 Gg/yr) were approximately two times larger than had been projected for that year. Changes in HCFC-141b emissions during 2005–2008 were quite consistent with those projected in the A1 scenario (Daniel and Velders, 2007).

"Bottom-up" estimates of HCFC-141b emissions (UNEP/TEAP, 2006) have captured the overall increase in emissions of this compound derived from "top-down" calculations, but with a slightly different time lag. Similar "bottom-up" estimates of HCFC-142b have also captured the rough changes implied from atmospheric data, but in this case, the "bottom-up" estimates are substantially lower than implied from year-to-year atmospheric observations during 2000–2004 (Figure 1-3). For both HCFCs, it is apparent that emissions from banks estimated for 2002 and projected for 2008 (IPCC/TEAP, 2005) account for <50% of total emissions for these compounds. About 10–20% of annual production of HCFC-141b is for solvent uses that result in release to the atmosphere shortly after production (UNEP/TEAP, 2006). Based on production data this would yield emissions of 10–20 Gg/yr and explain some of the difference between atmosphere-derived emissions and bank-related emissions (UNEP/TEAP, 2006). Rapid losses of HCFC-142b during or shortly after production would also provide an explanation for only some of the shortfall in emissions not explained by bank releases. HCFC bank magnitudes have increased in recent years given that reported production in recent years has substantially exceeded emissions (Montzka et al., 2009).

Summed, "top-down" emissions from HCFCs have increased during 2005–2008. When weighted by semi-empirical ODPs (Chapter 5), the sum of emissions from HCFCs totaled 22 ± 2 ODP-Kt in 2008. The sum of emissions of HCFCs weighted by direct, 100-yr GWPs has increased on average by 5 ± 2%/yr from 2004 to 2008, and by 2008 amounted to 0.74 ± 0.05 Gt CO_2-eq/yr.

The 2007 Adjustments to the Montreal Protocol are expected to have a discernable influence on HCFC emissions in the coming decade (see Chapter 5). But because those Adjustments are scheduled to affect HCFC production and consumption only after 2009, it is too soon to discern any influence of these Protocol adjustments in the mixing ratios or emissions derived for 2008 or earlier years reported in this Assessment.

Regional emissions for HCFCs from atmospheric measurements (Box 1-1) have been derived in different studies since the previous Assessment report. Compari-

sons with "bottom-up" estimates provide useful information on the accuracy of individual country accounting of their emissions of ODSs and regional estimates derived from atmospheric measurements. In an analysis of United States (U.S.) HCFC emissions, HCFC-22 mean emissions during 2004–2006 were estimated from aircraft measurements to be 46 (21–69) Gg/yr, or substantially lower than amounts derived from "bottom-up" estimates (Millet et al., 2009). U.S. HCFC-22 emissions estimated with "bottom-up" inventory methods by the U.S. Environmental Protection Agency (EPA) were estimated at between 89 and 97 Gg/yr during 2004–2008 and have been used to derive a U.S. contribution to global HCFC-22 atmospheric mixing ratios of between 21 and 45% during 2006 (Montzka et al., 2008).

Detailed analyses of HCFC emissions have also been reported for China in recent years, concurrent with a substantial increase in reported HCFC production and consumption in this country. Inventory-based, "bottom-up" estimates suggest HCFC-22 emissions increasing from 34 to 69 Gg/yr during 2004–2007 (Wan et al., 2009), or 12–20% of total global emissions during these years. Atmosphere-derived emissions attributed to China based on correlations to carbon monoxide (CO) and inversion modeling of elevated mixing ratios at down-wind sampling locations suggest slightly larger emissions than the inventory approach (52 ± 34 Gg/yr as the average of 2004–2005 from Yokouchi et al., 2006; 60 and 71 Gg/yr for 2005 and 2006 from Stohl et al. (2009); and 165 (140–213) Gg/yr in 2007 from Vollmer et al. (2009), though the Vollmer et al. (2009) estimate may be biased high because of relatively higher per-capita HCFC-22 emissions near Beijing than in other regions of China (Stohl et al., 2009)).

1.2.1.6 Methyl Bromide (CH_3Br)

The global, annual mean surface mixing ratio of methyl bromide (CH_3Br) had reached 7.3 to 7.5 ppt in 2008 (Figure 1-8; Table 1-1), down from the 9.2 ppt measured during the three years (1996–1998) before industrial production declined as a result of the Montreal Protocol (Yvon-Lewis et al., 2009). Global mixing ratios declined during 2005–2008 at a rate of −0.14 ppt/yr, which is slightly slower than the mean decline observed since 1999 when industrial production was first reduced. Since 1999, the annual mean hemispheric difference (NH minus SH) has decreased by nearly 50%: this measured difference was 1.2 ppt in 2008 compared to 2.3 ± 0.1 ppt during 1996–1998 (Figure 1-8).

Declines in the global tropospheric abundance and hemispheric difference of CH_3Br have coincided with decreases in global industrial production and subsequent emission. Reported global methyl bromide consumption in 2008 for all uses including uncontrolled quarantine and pre-shipment (QPS) uses was 73% below peak amounts reported in the late 1990s. An emission history derived from these reported data suggests a reduction in total fumigation-related CH_3Br emissions of 71% by the end of 2008 (see Figure 1-8).

The concurrent decline in the measured hemispheric difference and industrially derived emissions suggests a mean hemispheric mixing ratio difference close to 0 ppt

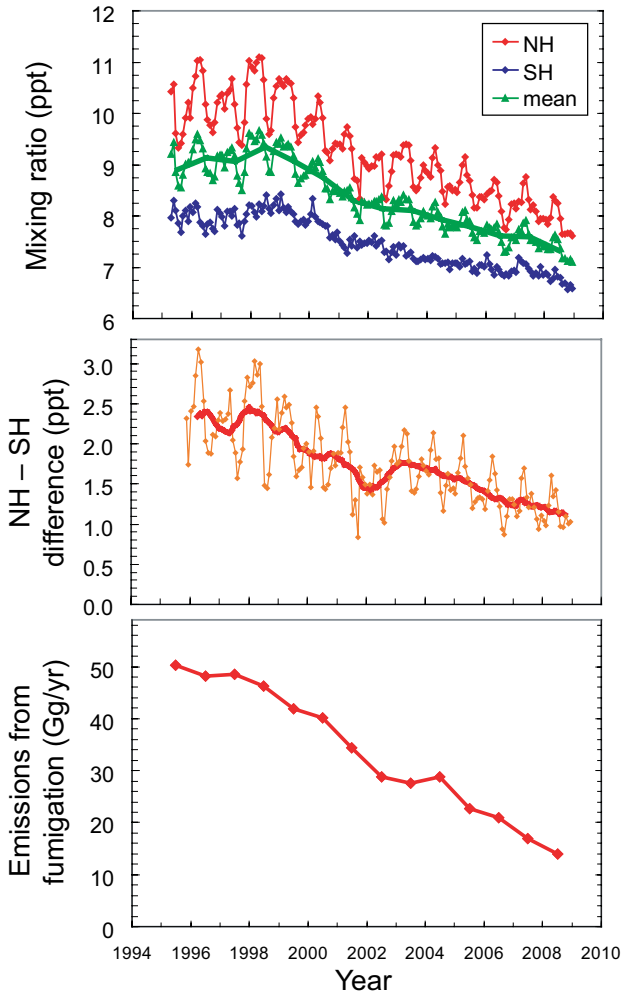

Figure 1-8. Top panel: Monthly hemispheric means for CH_3Br mixing ratios (ppt) (Montzka et al., 2003 updated). Middle panel: NH - SH difference by month (points) and smoothed over 12-month periods (bold red line). Bottom panel: Fumigation-related emissions (Gg/yr) of CH_3Br derived from reported regulated consumption × 0.65 plus reported quarantine and pre-shipment consumption × 0.84 (UNEP 2007b), where 0.65 and 0.84 are the estimated mean fractions of reported production to these different uses that ultimately become emitted to the atmosphere (UNEP 2007b).

Table 1-2. Summary of the estimated source and sink strengths (Gg/yr) of methyl bromide (CH_3Br) for periods 1996–1998 and 2008.

	1996–1998	Range	2008	Range	Reference	Note
SOURCES						
Fumigation- dispersive (soils)	41.5	(28.1 to 55.6)	6.7	(4.6 to 9.0)	1, 2	a
Fumigation- quarantine/ pre-shipment	7.9	(7.4 to 8.5)	7.6	(7.1 to 8.1)	1, 2	b
Ocean	42	(34 to 49)	42	(34 to 49)	3, 4	c
Biomass Burning	29	(10 to 40)	29	(10 to 40)	5, 6	d
Leaded gasoline	5.7	(4.0 to 7.4)	< 5.7		7	e
Temperate peatlands*	0.6	(−0.1 to 1.3)	0.6	(−0.1 to 1.3)	8, 9, 10	f
Rice paddies*	0.7	(0.1 to 1.7)	0.7	(0.1 to 1.7)	11, 12	g
Coastal salt marshes*	7	(0.6 to 14)	7	(0.6 to 14)		h
based on California saltmarshes	14	(7 to 29)	14	(7 to 29)	13, 14	i
based on Scottish saltmarsh	1	(0.5 to 3.0)	1	(0.5 to 3.0)	15	j
based on Tasmania saltmarsh	0.6	(0.2 to 1.0)	0.6	(0.2 to 1.0)	16	k
Mangroves	1.3	(1.2 to 1.3)	1.3	(1.2 to 1.3)	17	l
Shrublands*	0.2	(0 to 1)	0.2	(0 to 1)	18	m
Rapeseed	4.9	(3.8 to 5.8)	5.1	(4.0 to 6.1)	19	n
Fungus (litter decay)	1.7	(0.5 to 5.2)	1.7	(0.5 to 5.2)	20	o
Fungus (leaf-cutter ants)	0.5		0.5		21	p
Potential terrestrial sources						q
Tropical trees	n.q.		n.q.		22, 23	r
Temperate woodlands	n.q.		n.q.		24, 25	s
Tropical ferns	n.q.		n.q.		26	
Abiotic decomposition	n.q.		n.q.		27	t
Subtotal (Sources)	**143**		**111.5**			
SINKS						
Ocean	56	(49 to 64)	49	(45 to 52)	3	u
OH and photolysis	77		63.6		3	v
Soils	40	(23 to 56)	32	(19 to 44)	28,29,30,31	w
Subtotal (Sinks)	**177**		**147.6**			
Total (SOURCES−SINKS)	**−34**		**−36.1**			

* All asterisked items were estimated from measurements of net fluxes and may be influenced by sinks within them, thus they represent minimum gross fluxes. n.q. = not quantified.

Notes:

a. Soil fumigation emission rates estimated as 65% (46–91%) of reported consumption rates (ref 2).

b. QPS emission rates estimated as 84% (78–90%) of reported consumption rates (ref 2).

c. Oceanic production rate calculated based on saturation state of pre-phase-out ocean: production = net oceanic flux − ocean sink, where net flux is −14 (−7 to −22) Gg/yr.

d. Biomass burning estimates unchanged from the previous Assessment (Clerbaux and Cunnold et al., 2007), which is slightly higher than the 18–23 Gg/yr estimate in ref (3).

e. 2006–2008 values are not separately quantified but expected to be lower with the phase-out of leaded gasoline use.

f. Temperate peatlands net flux calculated by updating (ref 7) with 3-year average fluxes at same New Hampshire sites (ref 8). Range includes median estimate of 0.9 Gg/yr from Irish peatland study (ref 10).

Table 1-2, continued (notes).

g. Re-evaluation of global emission rates that were previously estimated as 3.5 Gg/yr in ref (11).
h. Salt marsh net flux estimated as the mid-range of the best estimates provided from four different studies.
i. Estimates were 14 (7–29) Gg/yr from (ref 13) and 8 to 24 Gg/yr (ref 14) depending on whether extrapolation incorporated or excluded mudflats, respectively.
j. Low and high range based on lowest and highest emitting of eight sites in ref (15).
k. Extrapolations calculated using mean fluxes reported in ref (16).
l. Based on study of two mangrove species, with range as results of two different methods of extrapolation.
m. Shrublands range as reported in Montzka and Fraser et al. (2003).
n. Rapeseed flux as reported in ref (19) with year-by-year data from author. 2007–2008 data uses results for 2003, the last year estimated.
o. These emission rates may possibly incorporate emission rates reported for woodlands and forest soils.
p. No range provided.
q. Terrestrial sources are poorly quantified and based on very limited studies so are not included in the tabulated sources.
r. Global extrapolations based on measurements of Malaysian trees (18 Gg/yr in ref 22) exceed the upper limit on net flux estimated in a study of a tropical South American rainforest (17 Gg/yr in ref 23), so no discrete estimate is included here.
s. Range of temperate woodland fluxes of 0.4 to 3.1 Gg/yr can be estimated by extrapolating net fluxes in ref (24) and gross production rates in ref (25) to global area of 13×10^{12} m^2. Eucalyptus forest floor shows no net emissions (ref 16).
t. The largest abiotic production rates, observed from the decomposition of saltwort leaves (ref 27), are roughly 2% of the emission rates from the live saltwort plant (ref 14).
u. Oceanic consumption calculated assuming production rates constant, with a decrease in saturation anomaly because of decreasing atmospheric concentrations, with global average net flux in 2007 predicted to be −6.6 (−3.3 to −10.4) Gg/yr. Range assumes the same net flux error range as 1996–1998 (as percent of flux).
v. A range has not been provided here.
w. Soil sink (refs. 28, 29) scaled to updated background Northern Hemisphere concentrations of 10.3 ppt (1996–1998) and 8.2 ppt (2006–2008), and includes a new tundra sink (refs. 30, 31) and a revised average temperate grasslands flux (refs. 28, 32, 33).

References:
1. UNEP, 2010. 2. UNEP, 2007b. 3. Yvon-Lewis et al., 2009. 4. King et al., 2002. 5. Clerbaux and Cunnold et al., 2007. 6. Andreae and Merlet, 2001. 7. Thomas et al., 1997. 8. Varner et al., 1999a. 9. White et al., 2005. 10. Dimmer et al., 2001. 11. Redeker and Cicerone, 2004. 12. Lee-Taylor and Redeker, 2005. 13. Rhew et al., 2000. 14. Manley et al., 2006. 15. Drewer et al., 2006. 16. Cox et al., 2004. 17. Manley et al., 2007. 18. Rhew et al., 2001. 19. Mead et al., 2008b. 20. Lee-Taylor and Holland, 2000. 21. Mead et al., 2008a. 22. Blei et al., 2010. 23. Gebhardt et al., 2008. 24. Drewer et al., 2008. 25. Rhew et al., 2010. 26. Saito and Yokouchi, 2006. 27. Wishkerman et al., 2008. 28. Shorter et al., 1995. 29. Varner et al., 1999b. 30. Rhew et al., 2007. 31. Hardacre et al., 2009. 32. Rhew and Abel, 2007. 33. Teh et al., 2008.

for CH_3Br in preindustrial times. Accordingly, the pre-1990 global mixing ratio trend used in creating scenario A1 for CH_3Br in Chapter 5 was derived from Southern Hemisphere firn data by including a time-varying hemispheric ratio that increased linearly from 1.0 in 1940 to 1.3 in 1995.

In the past, much research related to methyl bromide focused on refining our understanding of source and sink magnitudes in order to understand the relative contribution of anthropogenic methyl bromide emissions to methyl bromide atmospheric abundance and, therefore, provide more accurate projections of the atmospheric response to reduced industrial production. For example, the global measured decline since 1996–1998 of ~2 ppt in response to a decline in fumigation emissions of 60–70% suggests a total contribution from fumigation-related production before the phase-out (i.e., during 1996–1998) of 2.8–3.2 ppt (provided other sources or loss frequencies did not change appreciably). Considering that peak global mixing ratios were 9.2 ppt during 1996–1998, this suggests that industrially derived emissions accounted for 31–36% of total CH_3Br emissions in the three years before the phase-out began.

A recent modeling analysis of global atmospheric CH_3Br observations provided additional constraints to our understanding (Yvon-Lewis et al., 2009). It suggested that the observed global declines are well explained given our understanding of CH_3Br sources and sinks and the known changes in anthropogenic emissions, though a substantial source (~35 Gg/yr) is still unaccounted for in current budget compilations (Yvon-Lewis et al., 2009) (Table 1-2). The best-estimate budget derived in this work (based on observed global and hemispheric mixing ratio trends and seasonal variations together with time-varying sources and sinks) suggested a pre-phase-out anthropogenic fumigation contribution of ~28%. Though uncertainties in the variability of natural emissions and in the magnitude of methyl bromide stockpiles in recent years add uncertainty to our understanding of this ratio, when these new model result are considered together with the more simple analysis of methyl bromide mixing ratio changes since 1999 (see previous paragraph), a pre-phase-out anthropogenic contribution of 25–35% is estimated.

Our understanding of preindustrial mixing ratios of methyl bromide in the Southern Hemisphere has improved since the 2006 Assessment. A 2000-year record derived for methyl bromide from an ice core collected at South Pole (Saltzman et al., 2008) shows no systematic trend and a mean mixing ratio in samples with mean ages from 160 Before the Common Era (BCE) to 1860 CE of 5.39 ± 0.06

ppt (uncertainty represents 1 standard error here). This preindustrial mixing ratio is similar to the 5.1–5.5 ppt observed in the deepest firn-air samples at South Pole and Law Dome, Antarctica (Butler et al., 1999; Trudinger et al., 2004) and previous ice-core results at a different site in Antarctica in samples dated 1671–1942 CE (5.8 ppt; Saltzman et al., 2004). Based on these preindustrial SH mixing ratio results, the observed decline in SH mixing ratios from their peak (8.0 ppt) through the end of 2008 (6.7 ppt) suggests that SH mixing ratios have declined 50–60% of the way back to preindustrial levels as industrial production declined by a similar magnitude (60–70%).

The concurrence between global atmospheric changes relative to expected emissions declines, the decreased NH–SH differences, and the decline in the mean SH mixing ratio much of the way back to its preindustrial value, all suggest that production restrictions on CH_3Br have been successful at substantially reducing the global atmospheric abundance of CH_3Br. It is worth noting that this benefit was achieved despite substantial emissions from natural sources and an incomplete understanding of the global budget of CH_3Br.

Budget

Significant uncertainties remain in the detailed atmospheric budget of methyl bromide despite additional research since the previous Assessment. As indicated above, known sinks still outweigh best estimates of known sources by about 35 Gg/yr or roughly 20% of the total annual flux. This discrepancy remains even though the tropospheric burden, known sources, and known sinks have quantifiably changed in the last decade.

In light of the changing atmospheric concentrations of CH_3Br, separate budgets are created for pre-phase-out (1996–1998) and the 2008 atmospheres (Table 1-2). Reported consumption of CH_3Br from fumigation (dispersive and quarantine/pre-shipment uses) declined 73% between these periods, from 70.5 Gg/yr to 18.9 Gg/yr (UNEP, 2010). Before phase-out, pre-plant soil fumigation was the major use for CH_3Br, but this use had declined by 84% by 2008. Over the same period, CH_3Br consumption for quarantine and pre-shipment (QPS) applications has ranged between 7.5 and 12.5 Gg/yr, as this particular application is an exempted use (UNEP, 2010). As a result, consumption for QPS use accounted for nearly 50% of total global CH_3Br uses during 2007 and 2008 (UNEP, 2010). These values do not include production for use as a chemical feedstock, which is assumed to be completely consumed and which averaged 3.9 Gg/yr from 1995–1997 and 6.6 Gg/yr from 2003–2005 (the last three years reported in UNEP, 2007b).

Other anthropogenically influenced sources of CH_3Br include leaded gasoline combustion, biomass burning, and growth of certain methyl bromide emitting crops. Our understanding of the amount of methyl bromide emitted from biomass burning remains unchanged from the previous Assessment report as 29 (10 to 40) Gg/yr. Biomass burning emissions, however, vary substantially from year to year and peaked in 1998 during the strong El Niño event and enhanced burning then (van der Werf et al., 2004; Yvon-Lewis et al., 2009). Emissions from biofuel burning in the developing world are included in the above estimate, although they have been derived separately to be 6.1 ± 3.1 Gg/yr (Yvon-Lewis et al., 2009). Crop production levels of rapeseed (canola) and rice, two known crop sources of methyl bromide, have been increasing steadily due to demand for food supply and biofuel (FAO, 2009). A recent extrapolation of rapeseed CH_3Br emissions using crop harvest, growth rate, and global production data suggest a three- to four-fold increase from 1980 to 2003 (Mead et al., 2008a). In this new study, estimated average emission rates ranged from 4.3 to 6.2 Gg/yr between 1996 and 2003 (the final year estimated). These values are slightly less than the previous estimate of 6.6 Gg/yr (Clerbaux and Cunnold et al., 2007; Gan et al., 1998). While cabbage and mustard production also are increasing, total emission from these crops is estimated at <0.1 Gg/yr. A re-evaluation of CH_3Br emission from rice crops using a model incorporating temperature, seasonality, and soil moisture effects yields a lower source estimate (0.5 to 0.9 Gg/yr) than derived previously (3.5 Gg/yr) (Lee-Taylor and Redeker, 2005; Redeker and Cicerone, 2004).

Emission rates from the three known major natural sources (oceans, freshwater wetlands, and coastal salt marshes) have been revised downward since the 2002 Assessment (compare Table 1-2 to Table 1-9 in Montzka and Fraser et al., 2003). Ocean production rates have been revised from 63 (23–119) Gg/yr down to 42 (34–49) Gg/yr (Yvon-Lewis et al., 2009). Freshwater wetlands were previously estimated as a 4.6 (2.3 to 9.2) Gg/yr net source based on a partial season of measurements from two New Hampshire peatlands (Varner et al., 1999a). This source, specified in Table 1-2 as temperate peatlands, has been revised downward to 0.6 (−0.1 to 1.3) Gg/yr based on a 3-year study at the same New Hampshire sites, which showed much lower average net fluxes (White et al., 2005). Coastal salt marshes were previously estimated as a 14 (7–29) Gg/yr source based on a study of two southern California salt marshes (33°N) (Rhew et al., 2000). While a separate, nearby study (34°N) found similar net fluxes, the global extrapolations varied from 8 Gg/yr (assuming salt marsh areas included low-producing mudflats) to 24 Gg/yr (assuming surface areas were entirely vegetated) (Manley et al., 2006). However, much smaller CH_3Br net emission rates were observed from coastal salt marshes in Scotland (56°N) (Drewer et al., 2006) and Tasmania, Aus-

tralia (41°S) (Cox et al., 2004), which suggested global emission rates of 1 (0.5–3.0) Gg/yr and 0.6 (0.2–1.0) Gg/yr, respectively. Because emissions are strongly related to plant species and climatic conditions, the quantification of this source requires a more detailed understanding of salt marsh distributions and vegetation types. The updated value in Table 1-2 (7 Gg/yr) represents the mid-range of globally extrapolated fluxes, with the full range representing the various study mean values.

Since the previous Assessment report, several additional natural CH_3Br sources have been identified (see Table 1-2), although the addition of these sources does not yet resolve the budget imbalance between sources and sinks. Mangroves (Manley et al., 2007) and fungus cultivated by leaf-cutter ants (Mead et al., 2008b) are newly identified sources, although they are estimated to be relatively minor sources globally. Measurements from tropical trees (Blei et al., 2010) and ferns (Saito and Yokouchi, 2006) in SE Asia suggest that these may be large sources, up to 18 Gg/yr if results from these studies are globally representative. Aircraft measurements over a South American rainforest revealed no significant net emissions, however, and suggest an upper limit of 17 Gg/yr for the global tropical forest flux (Gebhardt et al., 2008). Because of this disparity, this source is not included in Table 1-2. In addition to the previously identified mechanism to produce methyl halides abiotically from the degradation of organic matter (Keppler et al., 2000), the abiotic production of methyl bromide in plant material has also been shown (Wishkerman et al., 2008); it is not clear how important these mechanisms are in relation to biotic production rates.

Natural terrestrial ecosystems can be both sources (e.g., from fungi, litter decomposition, certain plant species) and sinks (biological degradation in soils) for CH_3Br. Both emissions and uptake have been observed in temperate grasslands (Cox et al., 2004; Rhew and Abel, 2007; Teh et al., 2008), temperate forest (Dimmer et al., 2001; Varner et al., 2003), temperate shrubland (Rhew et al., 2001), and Arctic tundra (Rhew et al., 2007; Teh et al., 2009). Temperate woodland soils in Scotland are a net source for CH_3Br (Drewer et al., 2008) while oak-savanna woodland soils in California are a net sink (Rhew et al., 2010). To better understand the highly variable net fluxes found in many of these ecosystems, measurements of gross production and consumption rates have been derived by clearing vegetation from some sites (White et al., 2005; Drewer et al., 2006), using a stable isotope tracer method (Rhew and Abel, 2007; Teh et al., 2008; Teh et al., 2009; Rhew et al., 2010), or modeling soil uptake separately (Varner et al., 2003).

Known sinks of CH_3Br (oceans, OH, photolysis, and soil microbial uptake) have uptake rates that scale to tropospheric concentrations and, therefore, have declined in the current decade, as indicated in Table 1-2 (Yvon-Lewis et al., 2009). The partial lifetime of atmospheric CH_3Br with respect to ocean loss has been updated to 2.2–2.4 years based on new model results (Yvon-Lewis et al., 2009). The partial lifetime with respect to loss by oxidation by OH and photolysis remains unchanged at 1.7 years. The partial lifetime with respect to soil loss has increased from 3.1 years to 3.3 to 3.4 years, as described below. The best estimate lifetime for atmospheric CH_3Br has therefore increased slightly from 0.7 years to 0.8 years.

In the last two Assessment reports (Clerbaux and Cunnold et al., 2007; Montzka and Fraser et al., 2003), the soil sink was estimated to be 47 Gg/yr based on earlier studies that assumed Northern Hemisphere tropospheric concentrations of 11 ppt. The soil sink was recalculated for 1996–1998 and 2008 using background Northern Hemisphere concentrations of 10.3 ppt and 8.2 ppt, respectively to yield uptake rates of 44 ± 15 and 35 ± 12 Gg/yr, respectively. The addition of the tundra sink (0.31 ± 0.06 Gg/yr) does not significantly change these results (Rhew et al., 2007; Hardacre et al., 2009). However, recent field studies in temperate grasslands in California (Rhew and Abel, 2007) and Colorado (Teh et al., 2008) show gross uptake rates that are one-fourth and one-eighth of the previous temperate grassland uptake rates. The average growing season uptake rate incorporating these new studies is half of the previously reported flux for temperate grasslands, which implies a 15% reduction of the soil sink to 40 ± 16 Gg/yr for 1996–1998 and 32 ± 13 Gg/yr for 2008. While still within the range of errors, the best estimate for partial atmospheric lifetime for CH_3Br with respect to the soil sink would be increased from 3.0–3.1 years to 3.3–3.4 years. New results from a temperate woodland also suggest lower soil uptake rates (Rhew et al., 2010), but these were not included in the revised soil uptake rate here.

1.2.1.7 Methyl Chloride (CH_3Cl)

Methyl chloride is the most abundant chlorine-containing organic compound in the atmosphere and contributes 16% to the total chlorine from long-lived gases in the troposphere (see, for example, Table 1-12). Although it is not a controlled substance, CH_3Cl has several natural sources and sinks in common with CH_3Br, which is a controlled substance. Thus, atmospheric changes in CH_3Cl and an updated knowledge of its global budgets can provide a context for understanding a large amount of atmospheric Cl that is not controlled by the Montreal Protocol, as well as insights into changes in the natural CH_3Br budget.

Global mixing ratios of CH_3Cl increased by small amounts during 2004–2008 (2.3 to 2.7 ± 1.2 ppt/yr, or 0.4–0.5 ± 0.2%/yr), though these changes follow larger decreases reported for 1998–2001 of −1.5%/yr (Simmonds et al., 2004). Changes observed from 2007 to 2008 are small,

though both increases and decreases are reported by different measurements networks. The cause of these differences is not well documented, but the differences may be insignificant relative to measurement errors, or may reflect regional variations in rates of change for this compound.

Incorporating CH_3Cl observations from global and regional networks (AGAGE, NOAA, System for Observation of halogenated Greenhouse gases in Europe (SOGE), National Institute for Environmental Studies (NIES)) into a 3-D global chemical transport model, Xiao et al. (2010a) estimated global emissions for 2000–2004 to be 4.10 ± 0.47 Tg/yr, which is comparable to emissions reported in the previous Assessment (4.1 to 4.4 Tg/yr, Clerbaux and Cunnold et al., 2007). Model results indicate that about 55%, or 2.3 ± 0.3 Tg/yr, of CH_3Cl comes from tropical terrestrial sources that vary with global temperature changes (Xiao et al., 2010a). This is also comparable to prior model study estimates of 2.4 to 2.9 Tg/yr from tropical ecosystems, as reported in the previous Assessment.

Since the previous Assessment, several studies on South American and Asian rainforests have reinforced the importance of the tropical terrestrial CH_3Cl source. Air samples obtained by aircraft over South American tropical rainforests (Suriname, French Guyana) in 2005 indicated net emissions of CH_3Cl (Gebhardt et al., 2008). A survey of 197 plants from the subtropical island of Iriomote (Japan) found that 18% produced significant amounts of CH_3Cl (Yokouchi et al., 2007), while a survey of 119 tree species from tropical Malaysia found that 21% produced significant amounts of CH_3Cl (Saito et al., 2008). A separate study in Malaysian Borneo showed large emissions from live plants, though much smaller emissions were found from leaf litter (Blei et al., 2010). Global tropical source estimates based on extrapolations of the above studies ranged from 0.9 to 2.5 Tg/yr (Blei et al., 2010; Gebhardt et al., 2008; Saito et al., 2008; Yokouchi et al., 2007). These values are on the lower side of estimates of tropical emission magnitudes provided in the previous Assessment. Additional minor tropical sources of CH_3Cl have been identified, including mangroves (~0.011 Tg/yr) (Manley et al., 2007; Yokouchi et al., 2007) and fungus cultivated by leaf cutter ants (<0.001 Tg/yr) (Mead et al., 2008b).

Emissions of CH_3Cl can originate from biogenic production by vascular plants (Yokouchi et al., 2002), abiotic release from dead or senescent plant material (Hamilton et al., 2003), and emissions from tropical wood-rot fungi (Moore et al., 2005). Mass balance approaches have been used to estimate emission magnitudes from sources that have distinct stable carbon isotope ratios ($\delta^{13}C$). Methyl chloride produced from the abiotic methylation of chloride has an exceptionally depleted $\delta^{13}C$ value (Keppler et al., 2004), and a mass balance approach suggests that this mechanism is a dominant source of atmospheric CH_3Cl in terrestrial tropical and subtropical ecosystems at 1.8 to 2.5 Tg/yr (Keppler et al., 2005). Saito and Yokouchi (2008) also use an isotopic mass balance approach, incorporating more recent isotopic measurements of CH_3Cl from tropical plants, and estimate the total tropical source to be 2.9 to 4.2 Tg/yr, with 1.5 to 3.0 Tg/yr coming from live vegetation and the remainder from abiotic production from senescent leaves.

Biomass burning, oceans, and anthropogenic activities are major sources of atmospheric CH_3Cl. A mechanism to produce CH_3Cl through the photochemical reaction of dissolved organic matter in saline waters has been reported (Moore, 2008). Supersaturations of CH_3Cl have been observed in coastal waters off of the United States (Hu et al., 2010) and China (Lu et al., 2010), and global coastal emissions may increase the global oceanic emission estimate by 0.02 to 0.10 Tg/yr (Hu et al., 2010). The inversion analysis of Xiao et al. (2010a) suggests emissions of 0.43 ± 0.1 Tg/yr from the global ocean, consistent with the estimate of 0.38–0.51 Tg/yr in the previous Assessment. Though there are no updates to the biomass burning and anthropogenic source terms, the Xiao et al. (2010a) inversion analysis suggests global biomass burning emissions of 0.92 ± 0.2 Tg/yr.

Coastal salt marshes were previously estimated to be a large CH_3Cl source, up to 0.17 (0.07 to 0.44) Tg/yr, based on measurements in southern California (Rhew et al., 2000). Recent studies, however, show large geographic variability in this source and high sensitivity to methods of extrapolation. Measurements at a different southern California salt marsh scale up to 0.05 to 0.16 Tg/yr, depending on whether or not the areal averaging incorporates low-producing mudflats along with vegetated areas (Manley et al., 2006). Much smaller emission rates observed at a salt marsh in Tasmania scale to <0.01 Tg/yr (Cox et al., 2004). A salt marsh in China appeared to be a net sink during the growing season, though these results were derived under unusually high ambient concentrations (1–60 parts per billion (ppb)) (Wang et al., 2006).

The major sinks of tropospheric CH_3Cl include oxidation by hydroxyl radicals, loss to the stratosphere, reaction with chlorine radicals, loss to polar ocean waters, and uptake by soils. These sink estimates remain largely unmodified since the previous Assessment so the CH_3Cl lifetime remains unchanged (Table 1-3), although a study using stable isotope ratios suggests that the soil sink may be much larger than previously estimated (Keppler et al., 2005). The Arctic tundra appears to be a net sink for CH_3Cl, with uptake rates increasing under drier conditions (Rhew et al., 2007; Teh et al., 2009). However, measurements at a sub-Arctic wetland show a small net source for CH_3Cl (Hardacre et al., 2009). The causes of such geographic differences are not currently understood, although there are significant temperature, vegetation, and hydrological differences between the two regions.

Table 1-3. Global trace gas lifetimes for selected halocarbons with lifetimes longer than 0.5 years. (See Table 1-4 for estimates of local lifetimes for short-lived gases).

Industrial Designation or Common Name	Chemical Formula	Total Lifetime from Previous Assessments [a] (years)	New Total Lifetime [a] (years)	OH Lifetime [d] (years)	Stratospheric Lifetime (years)	Notes
Halogenated Methanes						
HFC-41	CH_3F	2.4	2.8	2.9	64	2, 5, 6
HFC-32	CH_2F_2	4.9	5.2	5.5	89	1, 4
HFC-23	CHF_3	270	222	245	2347	2, 4
PFC-14 (Carbon tetrafluoride)	CF_4	50,000	> 50,000		> 50,000	7
Methyl chloride	CH_3Cl	1.0	1.0	1.5		1, 8
Carbon tetrachloride	CCl_4	26	26		35	see text and Box 1-2
HCFC-31	CH_2ClF	1.3	1.3	1.3	38	1, 5, 9
HCFC-22	$CHClF_2$	12.0	11.9	12.8	186	1, 4
HCFC-21	$CHCl_2F$	1.7	1.7	1.8	33	1, 5, 6, 9
CFC-11	CCl_3F	45	45		45	8
CFC-12	CCl_2F_2	100	100		100	8
CFC-13	$CClF_3$	640	640		640	7
Methyl bromide	CH_3Br	0.7	0.8	1.9		1, see text
Bromodifluoromethane	$CHBrF_2$	5.8	5.2	6.0	39	1, 5, 9
Halon-1301	$CBrF_3$	65	65		65	8
Halon-1211	$CBrClF_2$	16	16			8, 10
Halon-1202	CBr_2F_2	2.9	2.9			8, 11
Halogenated Ethanes						
HFC-152a	CH_3CHF_2	1.4	1.5	1.6	45.4	2, 4, 6
HFC-143	CH_2FCHF_2	3.5	3.5	3.7	73	1, 5
HFC-143a	CH_3CF_3	52	47.1	55	327	1, 4
HFC-134	CHF_2CHF_2	9.6	9.7	10.5	134	1, 5
HFC-134a	CH_2FCF_3	14.0	13.4	14.3	232	1, 4, 6
HFC-125	CHF_2CF_3	29	28.2	32	246	1, 4, 6
PFC-116 (Perfluoroethane)	CF_3CF_3	10,000	> 10,000		> 10,000	7
Methyl chloroform	CH_3CCl_3	5.0	5.0	6.1 [e]	39	1, 8
HCFC-141b	CH_3CCl_2F	9.3	9.2	10.7	64.9	1, 4, 6
HCFC-142b	CH_3CClF_2	17.9	17.2	19.3	160	1, 4, 6
HCFC-133a	CH_2ClCF_3		4.3	4.5	72	2, 5, 9
HCFC-123	$CHCl_2CF_3$	1.3	1.3	1.4	35.6	1, 4, 6
HCFC-123a	$CHClFCF_2Cl$		4.0	4.3	63	1, 5, 9

Table 1-3, continued.

Industrial Designation or Common Name	Chemical Formula	Total Lifetime from Previous Assessments [a] (years)	New Total Lifetime [a] (years)	OH Lifetime [d] (years)	Stratospheric Lifetime (years)	Notes
HCFC-123b	CHF_2CCl_2F		6.2	~7	52	5, 9, 12
HCFC-124	$CHClFCF_3$	5.8	5.9	6.3	111	1, 4, 6
HCFC-124a	CHF_2CClF_2		9.1	~10	107	5, 9, 12
CFC-113	CCl_2FCClF_2	85	85		85	8
CFC-113a	CCl_3CF_3		~45		~45	13
CFC-114	$CClF_2CClF_2$	300	190		190	34
CFC-114a	CCl_2FCF_3		~100		~100	14
CFC-115	$CClF_2CF_3$	1,700	1020		1020	34
Halon-2311 (Halothane)	$CHBrClCF_3$		1.0	1.1	11	1, 5, 9
Halon-2402	$CBrF_2CBrF_2$	20	20			8, 10
Halogenated Propanes						
HFC-263fb	$CH_3CH_2CF_3$	1.6	1.2	1.2	38	2, 5
HFC-245ca	$CH_2FCF_2CHF_2$	6.2	6.5	6.9	105	1, 5
HFC-245ea	$CHF_2CHFCHF_2$	4.0	3.2	3.4	70	2, 5
HFC-245eb	$CH_2FCHFCF_3$	4.0	3.1	3.3	69	2, 5
HFC-245fa	$CHF_2CH_2CF_3$	7.6	7.7	8.2	116	1, 5
HFC-236cb	$CH_2FCF_2CF_3$	13.6	13.1	14.3	160	2, 5
HFC-236ea	CHF_2CHFCF_3	10.7	11.0	11.9	144	1, 5
HFC-236fa	$CF_3CH_2CF_3$	240	242	253	5676	1, 4
HFC-227ea	CF_3CHFCF_3	34.2	38.9	44.5	310	2, 5
PFC-218 (Perfluoropropane)	$CF_3CF_2CF_3$	2,600	2,600		2,600	8
PFC-c216 (Perfluorocyclopropane)	c-C_3F_6	> 1,000	~3,000		~3,000	15
HCFC-243cc	$CH_3CF_2CCl_2F$	26.4	19.5	27.1	70	1, 5, 9
HCFC-234fb	$CF_3CH_2CCl_2F$		49	117	84	2, 5, 9
HCFC-225ca	$CHCl_2CF_2CF_3$	1.9	1.9	2.0	43.7	1, 4
HCFC-225cb	$CHClFCF_2CClF_2$	5.8	5.9	6.3	101	1, 4
Halogenated Higher Alkanes						
HFC-365mfc	$CH_3CF_2CH_2CF_3$	8.6	8.7	9.3	125	1, 5
HFC-356mcf	$CH_2FCH_2CF_2CF_3$	1.2	1.3	1.3	40	1, 5
HFC-356mff	$CF_3CH_2CH_2CF_3$	8.1	8.3	8.9	122	1, 5
HFC-338pcc	$CHF_2CF_2CF_2CHF_2$	12.3	12.9	14.0	159	1, 5
HFC-329p	$CHF_2CF_2CF_2CF_3$		28.4	32	256	5, 16
PFC-C318 (Perfluorocyclobutane)	c-C_4F_8	3,200	3,200		3,200	7

Table 1-3, continued.

Industrial Designation or Common Name	Chemical Formula	Total Lifetime from Previous Assessments [a] (years)	New Total Lifetime [a] (years)	OH Lifetime [d] (years)	Stratospheric Lifetime (years)	Notes
PFC-31-10 (Perfluorobutane)	C_4F_{10}	2,600	2,600		2,600	7
HFC-43-10mee	$CF_3CHFCHFCF_2CF_3$	15.9	16.1	17.9	157	1, 4
HFC-458mfcf	$CF_3CH_2CF_2CH_2CF_3$	23.2	22.9	25.5	224	1, 5
PFC-41-12 (Perfluoropentane)	C_5F_{12}	4,100	4,100		4,100	7
HFC-55-10mcff	$CF_3CF_2CH_2CH_2CF_2CF_3$	7.7	7.5	8.0	115	1, 5
HFC-52-13p	$CHF_2CF_2CF_2CF_2CF_2CF_3$		32.2	36.4	275	3, 5
PFC-51-14 (Perfluorohexane)	C_6F_{14}	3,200	3,100		3,100	7
PFC-61-16 (Perfluoroheptane)	C_7F_{16}		~3,000		~3,000	17
Perfluorodecalin	$C_{10}F_{18}$	2,000	~2,000		~2,000	18
Fluorinated Alcohols						
1,1,1,3,3,3-hexafluoroisopropanol	$(CF_3)_2CHOH$	2.0	1.9	2.0	51	1, 5
Halogenated Ethers						
HFE-143a	CH_3OCF_3	4.3	4.8	5.1	88	1, 5
HFE-134	CHF_2OCHF_2	26	24.4	28.4	240	1, 5
HFE-125	CHF_2OCF_3	136	119	147	620	1, 5
HFE-227ea	$CF_3OCHFCF_3$	11 [b]	51.6	60	370	2, 5
HCFE-235da2 (Isoflurane)	$CHF_2OCHClCF_3$	2.6	3.5	3.7	65	2, 5, 9
HFE-236ea2 (Desflurane)	$CHF_2OCHFCF_3$	5.8 [b]	10.8	11.7	143	2, 5
HFE-236fa	$CF_3OCH_2CF_3$	3.7 [b]	7.5	~8	115	5, 19
HFE-245fa1	$CF_3OCH_2CHF_2$	2.2 [b]	6.6	~7	106	5, 20
HFE-245fa2	$CHF_2OCH_2CF_3$	4.9	5.5	5.8	95	2, 5
HFE-245cb2	$CH_3OCF_2CF_3$	5.1	4.9	5.2	89	1, 5
HFE-254cb2	$CH_3OCF_2CHF_2$	2.6	2.5	2.6	60	1, 5
HFE-236ca	$CHF_2OCF_2CHF_2$	26.5	20.8	23.1	212	2, 5
HCFE-235ca2 (Enflurane)	CHF_2OCF_2CHFCl		4.3	4.6	62	5, 9, 21
	$CF_3CF_2OCF_2CHF_2$	6.8 [b]	22.5	20–30	222	5, 22
	$CF_3CF_2OCH_2CF_3$	4.3 [b]	7.5	~8	115	5, 23
	$CH_3OCF_2CF_2CF_3$	5.2	5.0	5.3	90	1, 5
	$CF_3CF_2OCH_2CHF_2$	2.8 [b]	6.6	~7	106	5, 24
	$CHF_2OCH_2CF_2CF_3$	5.9	5.7	6.0	97	1, 5

Table 1-3, continued.

Industrial Designation or Common Name	Chemical Formula	Total Lifetime from Previous Assessments [a] (years)	New Total Lifetime [a] (years)	OH Lifetime [d] (years)	Stratospheric Lifetime (years)	Notes
	$CF_3CH_2OCF_2CHF_2$	7.1	6.0	6.4	100	5, 25
	$CH_3OCF_2CHFCF_3$	0.94 [b]	~3	~3	77	5, 26
	$CH_3OCF_2CF_2CHF_2$	0.93 [b]	~3	~3	77	5, 26
	$CHF_2CH_2OCF_2CHF_2$	2.0 [b]	5.7	~6	97	5, 27
	$CHF_2OCH_2CF_2CHF_2$	3.6	3.5	3.7	73	1, 5
HFE-347 isomer (Sevoflurane)	$(CF_3)_2CHOCH_2F$		2.2	2.3	56	5, 28
HFE-338 isomer	$(CF_3)_2CHOCHF_2$	3.1 [b]	21.2	23.5	214	2, 5
	$(CF_3)_2CFOCH_3$	3.4	3.7	3.9	75	2, 5
	$CH_3O(CF_2)_3CF_3$	5	4.7	5.0	87	2, 5
HFE-54-11 isomer	$CF_3CHFCF_2OCH_2CF_2CF_3$	9.1	8.8	9.5	127	5, 29
	$CH_3CH_2O(CF_2)_3CF_3$	0.77	0.8	0.8	30	5, 30
	$CHF_2OCF_2OCHF_2$	12.1 [c]	25.0	28.0	237	2, 5
	$CHF_2OCF_2CF_2OCHF_2$	6.2 [c]	12.9	14.0	159	2, 5
	$CHF_2OCF_2OCF_2CF_2OCHF_2$	6.3 [c]	13.5	14.7	163	2, 5
	$CF_3OC(O)H$	3.6	< 3.5	3.7	73	5, 31, 33
	$C_2F_5OC(O)H$	3.6	< 3.5	3.7	73	5, 32, 33
	n-$C_3F_7OC(O)H$	2.6	< 2.6	2.7	61	5, 32, 33
Other Fluorinated Compounds						
Trifluoromethyl-sulfurpentafluoride	SF_5CF_3	650–950	650–950		650–950	8
Sulfur hexafluoride	SF_6	3,200	3,200		3,200	7
Nitrogen trifluoride	NF_3	740	500		500	34
Sulfuryl fluoride	SO_2F_2		36	> 300	630	35

[a] Includes OH reaction, ocean loss, and stratospheric loss (reactive and photolytic) as appropriate.

[b] Lifetime estimated from theoretically calculated reaction rate constants.

[c] Lifetime estimated using room temperature data.

[d] Lifetime with respect to reaction with tropospheric OH calculated relative to 6.1 years for CH_3CCl_3, assuming an average temperature of 272 K (Spivakovsky et al., 2000; Prather and Ehhalt et al., 2001).

[e] The value of τ_{OH} of 6.1 years for methyl chloroform was derived from its measured overall lifetime of 5.0 years (Clerbaux and Cunnold et al., 2007; Prinn et al., 2005) taking into account an ocean loss of 89 years and stratospheric loss of 39 years.

Notes:

1. OH rate constants taken from JPL 06-2.
2. OH rate constants taken from JPL 10-6. JPL 10-6 is cited here whenever there is a change in a rate constant recommendation or the accompanying note. It does not necessarily mean that a major change was recommended for a rate constant. Nevertheless, updates in JPL 10-6 reflect improved kinetic understanding.

Table 1-3, continued (notes).

3. OH rate constants taken from Atkinson et al. (2008).
4. Stratospheric lifetime taken from Naik et al. (2000).
5. Stratospheric reaction lifetime estimated from an empirical correlation between the tropospheric and stratospheric lifetimes that were reported by Naik et al. (2000) for HFCs for which OH and $O(^1D)$ reaction rate constants were available.
6. Total lifetime includes a very minor contribution for ocean loss derived in Yvon-Lewis and Butler (2002).
7. Total lifetime from Ravishankara et al. (1993). The lifetimes for CF_4, CF_3CF_3, and C_4F_{10} were reported as lower limits.
8. Total lifetime taken from Table 1-4 in Clerbaux and Cunnold et al. (2007).
9. Stratospheric lifetime includes a photolysis lifetime estimated from that of a fully halogenated compound containing equivalent Cl and/or Br groupings.
10. Lifetime is due to a combination of tropospheric and stratospheric photolysis.
11. Lifetime is due primarily to tropospheric photolysis with a smaller contribution associated with the stratospheric photolysis.
12. OH rate constant estimated relative to CHF_2CF_3 using available data on the effects of Cl substitution.
13. Total lifetime assumed to be the same as CFC-11.
14. Total lifetime assumed to be the same as CFC-12.
15. Total lifetime assumed to be comparable to those for perfluoropropane, perfluorobutane, and perfluorocyclobutane.
16. OH rate constants taken from Young et al. (2009).
17. Total lifetime assumed to be the same as perfluorohexane.
18. Total lifetime estimated by Shine et al. (2005).
19. OH lifetime estimated by adjusting the lifetime of $CF_3CH_2OCF_2CHF_2$ for the contribution of $-CF_2CHF_2$.
20. OH lifetime estimated relative to CF_3OCH_3 and $CHF_2CH_2CF_3$.
21. OH rate constants taken from Tokuhashi et al. (1999).
22. OH lifetime estimated as greater than $CHF_2CF_2OCHF_2$ and less than $CHF_2CF_2CF_2CF_3$.
23. OH lifetime assumed to be the same as $CF_3OCH_2CF_3$.
24. OH lifetime assumed to be the same as $CHF_2CH_2OCF_3$.
25. OH rate constants taken from Wilson et al. (2007).
26. OH and total lifetimes estimated as approximately the same as for $CH_3OCF_2CHF_2$.
27. OH lifetime estimated relative to $CF_3CF_2OCF_2CHF_2$ and $CF_3CF_2OCH_2CHF_2$.
28. OH rate constant taken from Langbein et al. (1999) using an estimated temperature dependence.
29. OH rate constants taken from Chen et al. (2005a).
30. OH rate constants taken from Christensen et al. (1998) using an estimated temperature dependence.
31. OH rate constants taken from Chen et al. (2004a).
32. OH rate constants taken from Chen et al. (2004b).
33. Ocean loss for perfluoro esters has been estimated from hydrolysis and solubility data for non-fluorinated and partially fluorinated esters by Kutsuna et al. (2005). These authors suggest that the ocean sink can be comparable to the tropospheric reaction sink for perfluoro ethers, thereby reducing the total lifetimes given in this table by as much as a factor of 2.
34. From Prather and Hsu (2008) with the lifetimes recalculated using the JPL 06-2 recommended rate constants for the $O(^1D)$ reactions corrected for the deactivation channel (see also Section 1.2.2).
35. From Papadimitriou et al. (2008b) and Mühle et al. (2009). The total lifetime is primarily due to ocean uptake.

Box 1-3. Atmospheric Lifetimes and Removal Processes

The total atmospheric lifetime or turnover time (τ_{total}) of a trace gas is the time required to remove or chemically transform approximately 63% (i.e., 1−1/e) of its global atmospheric burden (C_{global}). τ_{total} can be defined as the ratio of the burden to the total removal rate (L_{total}) from the atmosphere:

$$\tau_{total} = C_{global} / L_{total}$$

L_{total} can be broken down into the sum of loss rates associated with various removal processes

$$L_{total} = L_{atm} + L_{soil} + L_{ocean} + \ldots L_X$$

where L_{atm} is the loss rate for processes occurring in the atmosphere, L_{soil} is the loss rate for soil uptake, L_{ocean} is the rate for loss to the oceans, and L_X is the loss rate for any other removal process, X. Each of these loss rates is associated with a characteristic lifetime such that

$$L_i = C_{global} / \tau_i$$

Therefore,

$$L_{total} = C_{global} / \tau_{total} = C_{global} / \tau_{atm} + C_{global} / \tau_{soil} + C_{global} / \tau_{ocean} + \ldots C_{global} / \tau_X$$

and τ_{total} can be expressed as

$$(\tau_{total})^{-1} = (\tau_{atm})^{-1} + (\tau_{soil})^{-1} + (\tau_{ocean})^{-1} + \ldots(\tau_X)^{-1}$$

The atmospheric loss rate is typically broken down into separate loss rates associated with processes occurring in the troposphere and in the stratosphere

$$L_{atm} = L_{trop} + L_{strat} = C_{global} / \tau_{trop} + C_{global} / \tau_{strat}$$

such that

$$(\tau_{atm})^{-1} = (\tau_{trop})^{-1} + (\tau_{strat})^{-1}$$

The tropospheric lifetimes for most trace gases are primarily controlled by reactions with OH, although reactions with ozone (O_3), nitrate radical (NO_3), and chlorine radicals (Cl) can also play limited roles. UV photolysis in the troposphere, designated by the characteristic lifetime τ_J, is the dominant sink for iodine-containing compounds and can also be important for some bromine-containing compounds. Hydrolysis-related removal processes (such as wet deposition, rainout, or washout), characterized collectively by τ_{hydrol}, can also contribute. Thus,

$$(\tau_{trop})^{-1} = (\tau_{OH})^{-1} + (\tau_{O_3})^{-1} + (\tau_{Cl})^{-1} + (\tau_{NO_3})^{-1} + (\tau_{hydrol})^{-1} + (\tau_J)^{-1}$$

Compounds whose tropospheric lifetimes are longer than the characteristic mixing time in the troposphere are designated as “long lived” in this chapter. For such well-mixed compounds, lifetimes due to reaction with tropospheric hydroxyl radicals (OH) can be estimated relative to the corresponding lifetime of methyl chloroform (Spivakovsky et al., 2000)

$$\tau_{OH}^{RH} = \frac{k_{MCF}\ (272\ \mathrm{K})}{k_{RH}\ (272\ \mathrm{K})} \cdot \tau_{OH}^{MCF}$$

where τ_{OH}^{RH} is the partial OH lifetime for the compound of interest (RH), $k_{RH}(272\ \mathrm{K})$ and $k_{MCF}(272\ \mathrm{K})$ are the rate constants for the reactions of OH with RH and with methyl chloroform (MCF) at T = 272 K, and τ_{OH}^{MCF} = 6.1 years (see Table 1-3, footnote “e”).

Stratospheric loss processes, such as reactions with OH, O_3, and excited state oxygen atoms ($O(^1D)$), and UV

photolysis can also play important roles in dictating the lifetime of a long-lived compound. The contribution from photolysis at Lyman-α (121.6 nm), which is important only for very long-lived compounds, can be included here, although it occurs at altitudes above the stratosphere (≥70 km). UV and Lyman-α photolysis are the most important loss processes for nonreactive compounds:

$$(\tau_{strat})^{-1} = (\tau_{OH})^{-1} + (\tau_{O_3})^{-1} + (\tau_{O(^1D)})^{-1} + (\tau_J)^{-1} + (\tau_{Lyman\text{-}\alpha})^{-1}$$

For long-lived compounds, τ_{total} can be considered to be a global lifetime that is representative of the compound's persistence in Earth's atmosphere.

In the context of this chapter, very short-lived substances (VSLS) are compounds with lifetimes less than or equal to 0.5 years (i.e., shorter than the characteristic time of mixing processes in the troposphere) (see Section 1.3). The actual atmospheric lifetimes of VSLS depend on the emission location and season as well as on local atmospheric conditions. Consistent with past Assessments, τ_{OH}^{RH} for VSLS was estimated with hydroxyl radical concentrations [OH] = 1×10^6 molecule/cm^3 and an OH reaction rate constant at T = 275 K:

$$\tau_{OH}^{RH} = 1/(k_{RH}(275\ K) \times [OH])$$

The use of a mean global tropospheric OH concentration in such calculations provides only approximate "local lifetimes." The concept of a single global lifetime, Ozone Depletion Potential (ODP), or Global Warming Potential (GWP) is inappropriate for such short-lived gases (see Section 1.3).

1.2.2 Loss Processes

Halocarbons are removed from the atmosphere by a number of processes including oxidation by hydroxyl radicals, photolysis, uptake by the ocean, and uptake by terrestrial ecosystems. The combined influence of these processes can be expressed as a lifetime (see Box 1-3). Lifetimes for ODSs are generally based on a combination of modeling studies and analysis of observations, particularly stratospheric observations. Updates to our understanding of the persistence, expressed as lifetimes, of halocarbons in the environment are based on the consideration of updated kinetic information (see Table 1-3). Uncertainties associated with these lifetimes stem from uncertain hydroxyl radical concentrations and distributions, and uncertain reaction rate constants. Modeling uncertainties related to absorption cross sections and stratospheric air transport rates also affect the calculation of lifetimes. This is particularly important for CFCs, for example, as this represents their primary sink.

New results from models that more accurately simulate air transport rates through the stratosphere than older models suggest a steady-state lifetime for CFC-11 of 56–64 years (Douglass et al., 2008), notably longer than the 45 years used in recent past Assessments. This finding has the potential to affect lifetimes, ODPs, and emissions derived from global measured trends for some other ODSs. For example, while the CFC-12 lifetime calculated in this same study was not substantially different from its current, best-estimate lifetime of 100 years, the stratospheric lifetime of CCl_4 is calculated as ~50 years in this same model (Rontu Carlon et al., 2010), which is notably longer than the current best estimate of 35 years. A revision to the CFC-11 or CCl_4 lifetime is not recommended in this Assessment, pending a comprehensive analysis by the atmospheric observation and modeling communities.

New modeling calculations by Prather and Hsu (2008) have yielded significantly shorter lifetimes for CFC-114 and CFC-115. The O(^{1}D) (excited-state oxygen atoms) reaction rate coefficients used in their calculation, however, included both the chemical oxidation of the CFCs as well as the nonreactive, physical quenching of O(^{1}D). This resulted in an overestimation of loss for these CFCs from O(^{1}D). When the O(^{1}D) rates for only reactive channels are considered (Sander et al., 2006, hereafter referred to as JPL 06-2), lifetimes of 190 years for CFC-114 and 1020 years for CFC-115 are calculated (Table 1-3; Prather and Hsu, 2010), which are still significantly shorter than considered in past Assessments (300 years for CFC-114 and 1700 years for CFC-115; Clerbaux and Cunnold et al., 2007).

A significantly shorter lifetime for nitrogen trifluoride (NF_3) was also calculated by Prather and Hsu (2008) using an older O(^{1}D) reaction rate constant (Sorokin et al., 1998). The NF_3 lifetime given in this Assessment (500 years compared to 740 years in Clerbaux and Cunnold et al., 2007) is based on the Prather and Hsu (2008) results revised using the O(^{1}D) + NF_3 rate constant recommended in JPL 06-2. A new study of this rate constant has been published by Zhao et al. (2010). Use of the rate constant reported by these authors would reduce the life-

time for NF_3 by about 7% from the 500 years reported in this chapter.

The principal differences between these new (revised) CFC-114 and CFC-115 lifetimes and those recommended in earlier Assessments (based on Ravishankara et al., 1993) are primarily due to improved photolysis models (see Chapter 6 in SPARC CCMVal, 2010) that include updated solar fluxes in the Herzberg continuum (200–220 nanometers (nm)) and in the Schumann-Runge bands (<205 nm). Note that the more rapidly photolyzed CFCs (-11, -12, and -113) are destroyed in the lower stratosphere at wavelengths whose opacities are dominated by the molecular oxygen (O_2) Herzberg continuum, while the much longer-lived gases (CFC-114, -115, and NF_3) are lost primarily between altitudes of 32 to 40 km and in the wavelength region where the opacity is controlled by the O_2 Schumann-Runge bands. This is why the CFC-11, CFC-12, and CFC-113 lifetimes are not appreciably influenced by use of the improved photolysis model.

The Prather and Hsu (2008) model did not include losses above 70 km, where photolysis at Lyman-alpha (121.6 nm) wavelengths occurs. This loss is likely important for some very long-lived chemicals, particularly CFC-115. The lifetime for CFC-13 derived by Ravishankara et al. (1993) remains unchanged here (640 years) despite these considerations because atmospheric loss of this chemical is primarily associated with reactive removal by $O(^1D)$ atoms in the stratosphere. For NF_3, the Prather and Hsu (2008) calculations revise earlier lifetime estimates that were based on a one-dimensional (1-D) photolysis calculation (not including $O(^1D)$ reactions) referenced as a private communication in Molina et al. (1995).

Other considerations also affect the usefulness of the stratospheric lifetimes calculated in Table 1-3. These lifetimes are derived for steady-state conditions, yet global atmospheric mixing ratios of most ODSs are not at steady state. For CFCs and other compounds destroyed primarily by photolysis in the stratosphere, steady-state lifetimes are generally longer than lifetimes in the absence of significant emissions (e.g., Prather, 1997). Finally, many models suggest that future changes in stratospheric circulation expected from enhanced greenhouse gas concentrations will enhance photolytic loss rates for the long-lived halocarbons. This influence is predicted to result in shorter stratospheric lifetimes than those listed in Table 1-3.

Since the previous Assessment, considerably more kinetic data have become available for the reactions of OH with a wide variety of CFC and halon substitutes, especially fluorinated alkenes, ethers, and alcohols for which limited or no data previously existed. A comprehensive analysis of available kinetic data since the last Assessment has revealed a number of compounds for which our understanding of losses has improved.

Most notably, lifetimes of three hydrofluoroethers (HFEs) are now based on experimentally measured OH reaction rate constants (HFE-227ea, HFE-236ea2, and $(CF_3)_2CHOCHF_2$) (Sander et al., 2010; hereafter referred to as JPL 10-6). Previous estimates were based on theoretically calculated OH reaction rate constants that significantly overestimated the loss rates for these gases, leading to unrealistically short lifetimes.

Rate constants for eight other HFEs (HFE-236fa, HFE-245fa1, $CF_3CF_2OCF_2CHF_2$, $CF_3CF_2OCH_2CF_3$, $CF_3CF_2OCH_2CHF_2$, $CH_3OCF_2CHFCF_3$, $CH_3OCF_2CF_2CHF_2$, $CHF_2CH_2OCF_2CHF_2$) that had also been derived from theoretical considerations can now be better estimated from the kinetic data on fluoroethers that are now available (Table 1-3). The revised lifetimes for these HFEs are considerably longer than recommended in the previous Assessment.

Updated lifetimes for three additional HFEs ($CHF_2OCF_2OCF_2CF_2OCHF_2$, $CHF_2OCF_2OCHF_2$, and $CHF_2OCF_2CF_2OCHF_2$) have been derived using the temperature dependencies of the OH reaction rate constants estimated in JPL 10-6 (which are based on existing data for other fluoroethers) and evaluated at 272 K (see Box 1-3). Previously assessed lifetime estimates for these three HFEs were based on rate constants at 298 K (Ramaswamy et al., 2001), which are ~80% faster.

Significant revisions have also been made to the lifetimes of three HFCs:

- The updated total lifetime for HFC-23 (CHF_3) of 222 years is ~20% shorter than the 270 years recommended in the previous Assessment (Clerbaux and Cunnold et al., 2007). This change in total lifetime results from a shorter tropospheric lifetime due to the OH rate constant recommended in JPL 10-6 being ~15% larger than given in JPL 06-2 and a stratospheric lifetime of 2347 years based on the model calculation of Naik et al. (2000).

- The new total lifetime of HFC-227ea (CF_3CHFCF_3) is longer than given in the previous Assessment (38.9 years vs. 34.2 years) primarily because the updated rate constant (JPL 10-6) is smaller than previously recommended due to the inclusion of new temperature-dependent kinetic data (Tokuhashi et al., 2004).

- The revised total lifetime of HFC-41 (CH_3F) is 2.8 years. The revision is based on the current recommendation for the OH reaction rate constant (JPL 10-6) and an estimation of stratospheric loss (64 years derived from Naik et al. (2000); Table 1-3).

1.3 VERY SHORT-LIVED HALOGENATED SUBSTANCES (VSLS)

While the longer-lived ODSs account for the majority of the halogen loading in the present-day stratosphere, there is evidence suggesting that halogenated very short-lived substances (VSLS) with lifetimes of 0.5 years or less and their degradation products contribute to halogen in the stratosphere (Ko and Poulet et al., 2003; Law and Sturges et al., 2007). In Table 1-4, some of the halogenated VSLS considered in this section are listed together with their lifetimes. The abbreviations for chemical and meteorological parameters used in this section are explained in Box 1-4).

While some VSLS originate from anthropogenic sources, others are of partly or wholly natural origins. We include discussions of naturally emitted VSLS here for two reasons. First, much of our current understanding of the mode and rate of delivery of the VSLS—whether natural or anthropogenic—to the stratosphere arises from studies of naturally occurring halocarbons. Second, the emission and the stratospheric injection of natural halocarbons might not be constant in a changing climate.

1.3.1 Emissions, Atmospheric Distributions, and Abundance Trends of Very Short-Lived Source Gases

Since the 2006 Assessment (Law and Sturges et al., 2007) new findings on emissions of anthropogenic and natural VSLS have been made as well as on trends of anthropogenic chlorinated VSLS. New data are also available on very short-lived (VSL) source gases (SGs) in the upper troposphere and the importance of product gases (PGs) is assessed.

1.3.1.1 Chlorine-Containing Very Short-Lived Source Gases

A number of chlorinated VSLS from anthropogenic and natural sources have been measured in the background atmosphere. Industrial sources of these gases are discussed in McCulloch et al. (1999), Simmonds et al. (2006), Worton et al. (2006), and on the web site of the U.S. Environmental Protection Agency (www.epa.gov; Toxic Air Pollutants). Dichloromethane (methylene chloride, CH_2Cl_2) is principally used as a paint remover, and also in foam production and foam blowing applications, as a solvent and degreaser, and in fumigation. Trichloromethane (chloroform, $CHCl_3$) is used almost exclusively in the production of HCFC-22 and fluoropolymers, but is also released as a by-product from chlorine bleaching in the paper and pulp industry, and from water chlorination. Tetrachloroethene (perchloroethylene, CCl_2CCl_2) is used in the textile industry, in dry-cleaning applications, and in vapor degreasing of metals, as is trichloroethene (trichloroethylene, $CHClCCl_2$). 1,2-Dichloroethane (CH_2ClCH_2Cl) is principally used in the production of polymers and rubbers, and is also used as a solvent, as a fumigant, and was historically used widely as an additive to leaded gasoline. Chloroethane (C_2H_5Cl) is mostly used in the manufacture of ethyl cellulose, dyes, and pharmaceuticals and was formerly used in the manufacture of tetraalkyl lead additives for gasoline. Other related compounds include a number of mixed-halogenated compounds, notably the bromochloromethanes. These latter compounds are believed to originate largely from natural sources and are generally present at lower abundances than the aforementioned chlorinated compounds. They are discussed in Section 1.3.1.2 in the context of brominated source gases.

Estimates of total global and industrial emissions of chlorinated VSLS are shown in Table 1-5 for those gases for which such estimates exist. From this table it can be seen that total CCl_2CCl_2 and CH_2Cl_2 emissions derived from a "top-down" analysis of atmospheric observations are similar to independently estimated industrial emissions derived from inventories. Although not all of the estimates coincide in time (e.g., industry inventories are mostly from the early or mid-1990s, whereas the atmospheric measurements used in the emissions models are mostly from several years later), the results suggest that most emissions of CCl_2CCl_2 and CH_2Cl_2 arise from anthropogenic activity. A model analysis of the atmospheric data (Simmonds et al., 2006) also indicates that more than 90% of the emissions for these two compounds emanate from the Northern Hemisphere (NH), further indicative of their predominantly industrial origins. The industrial inventories, however, indicate that only 1% of industrial emissions are in the Southern Hemisphere (SH) (McCulloch et al., 1999), suggesting that other sources such as biomass burning might contribute. An earlier estimate of the biomass burning contribution to global atmospheric CH_2Cl_2 (7% according to Keene et al., 1999) is supported by Xiao (2008), but both are based largely on the same underlying data. These high values have been questioned by Simmonds et al. (2006) on the basis of the lower (by two orders of magnitude) biomass burning emission factors they observed from Australian wild fires.

Industrial emissions of chloroform were estimated to contribute 25 to 29% of total emissions in 2001 by modeling atmospheric measurements (Worton et al., 2006). This is less than that modeled in earlier years due to a rapid decline in emissions attributed to the paper and pulp industry. The absolute emissions estimate from this study for 2001 is, however, higher than an earlier industry inventory figure given by McCulloch et al. (2003) (see

Table 1-4. Lifetimes for very short-lived halogenated source gases.

Compound	Local Lifetime from Previous Assessments (τ_{local}), days	OH Lifetime[1] (τ_{OH}), days	Photolysis Lifetime from Previous Assessments (τ_{local}), days	New Local Lifetime, (τ_{local}), days	Notes
Chlorocarbons					
CH_2Cl_2	140	144	> 15000	144	2, 8
$CHCl_3$	150	149	> 15000	149	2, 8
CH_3CH_2Cl	30	39		39	2
CH_2ClCH_2Cl	70	65		65	4
$CH_3CH_2CH_2Cl$		14		14	5
$CHClCCl_2$		4.9	> 15000	4.9	3, 8
CCl_2CCl_2	99	90		90	3
$CH_3CHClCH_3$		18		18	5
Bromocarbons					
CH_2Br_2	120	123	5000	123	2, 8
$CHBr_3$	26	76	36	24	2, 8
CH_2BrCl	150	137	15000	137	2, 8
$CHBrCl_2$	78	121	222	78	6, 8
$CHBr_2Cl$	69	94	161	59	7, 8
CH_3CH_2Br	34	41		41	2
CH_2BrCH_2Br	55	70		70	4
n-C_3H_7Br	13	12.8	> 1200	12.8	3, 8
Iso-C_3H_7Br		16.7		16.7	3
Iodocarbons					
CH_3I	7	158	7 (4–12)	7	4, 8
CF_3I	4	860	not determined	4	2
CH_2ClI	0.1		0.1	0.1	8
CH_2BrI	0.04		0.04	0.04	8
CH_2I_2	0.003		0.003	0.003	8
CH_3CH_2I	4	17.5	5 (2–8)	4	4, 8
$CH_3CH_2CH_2I$	0.5	7.7	0.6 (0.5–1.5)	0.5	4, 8
CH_3CHICH_3	1.2	9.7	1.4 (1–3)	1.2	4, 8
$CF_3CF_2CF_2I$			< 2	< 2	9

Notes:

1. These local OH lifetimes are calculated using an average tropospheric OH concentration of 1×10^6 molecule/cm^3 and the OH reaction rate constant at T = 275 K. Local lifetimes quoted here are not meant to be estimates of global lifetimes, which for short-lived gases depend on the emission location and season as well as local atmospheric conditions. The concept of a single global lifetime, ODP, or GWP is inappropriate for such short-lived gases.
2. OH reaction rate constant taken from JPL 06-2.
3. OH reaction rate constant taken from JPL 10-6. JPL 10-6 is cited here whenever there is a change in a rate constant recommendation or the accompanying note. It does not necessarily mean that a major change was recommended for a rate constant. Nevertheless, updates in JPL 10-6 reflect improved kinetic understanding.
4. OH reaction rate constant taken from Atkinson et al. (2008).
5. OH reaction rate constant taken from Yujing and Mellouki (2001).
6. Room temperature OH reaction rate constant taken from Bilde et al. (1998). The temperature dependence of the OH reaction rate constant was estimated from the reactivity of $CHCl_3$, $CHCl_2Br$, and $CHBr_3$.
7. OH reaction rate constant estimated from the OH reactivity of $CHCl_3$, $CHCl_2Br$, and $CHBr_3$.
8. Photolysis lifetime taken from Table 2-4 in Ko and Poulet et al. (2003).
9. Photolysis lifetime estimated from comparison of UV spectra and lifetimes for CF_3I and $CF_3CF_2CF_2I$.

Box 1-4. Definition of Acronyms Related to Short-Lived Gases

Chemical Parameters

VSLS	very short-lived substances—organic and inorganic gases with lifetimes of less than 0.5 years
VSL	very short-lived
SG/SGI	source gas / source gas injection—refers to a halogenated organic source gas and its injection into the stratosphere
PG/PGI	product gas / product gas injection—refers to halogenated organic and inorganic degradation products and their injection into the stratosphere
Br_y	total inorganic stratospheric bromine (e.g., HBr, BrO, 2×Br_2) resulting from degradation of bromine-containing organic source gases (halons, methyl bromide, VSLS), and natural inorganic bromine sources (e.g., volcanoes, sea salt, and other aerosols)
Cl_y	total inorganic stratospheric chlorine (e.g., HCl, ClO) resulting from degradation of chlorine-containing source gases (CFCs, HCFCs, organic VSLS), and natural inorganic chlorine sources (e.g., sea salt and other aerosols)
I_y	total inorganic stratospheric iodine (e.g., IO, OIO, HOI) resulting from degradation of iodine-containing source gases (VSLS), and natural inorganic sources (e.g., sea salt and other aerosols)
Br_y^{VSLS}	the component of stratospheric Br_y from the degradation of organic brominated VSL SGs and tropospheric inorganic bromine sources (also called "additional" stratospheric Br_y)

Meteorological Parameters

BDC	Brewer-Dobson circulation
LMS	lowermost stratosphere
TTL	tropical tropopause layer—a layer exhibiting properties of both the stratosphere and troposphere. In this Assessment we follow the definition of the TTL as used in Law and Sturges et al. (2007). The bottom of TTL is taken as the region of maximum convective outflow (about 12 km altitude, or 345K potential temperature) and the upper end is identical to the tropical cold point tropopause (about 17 km or 380 K potential temperature).
z_0	altitude of clear-sky zero radiative heating. As in the previous Assessment (Law and Sturges et al., 2007) we define the level at about 15 km or 360K, where there is a transition from clear-sky radiative cooling to clear-sky radiative heating. In general, air masses above this level are expected to enter the stratosphere.
CPT	cold point tropopause—defined by the minimum atmospheric temperature and gives the position of the tropical tropopause. At this altitude air parcels enter the stratospheric overworld.
Washout	the removal of trace gases from the gas phase, including subsequent falling of rain or ice particles

Table 1-5). Biomass burning is thought to contribute 1% or less to emissions of $CHCl_3$, CCl_2CCl_2, and $CHClCCl_2$ (Table 1-5).

Annual mean mole fractions and trends of some of these chlorinated VSL source gases at Earth's surface during recent years are given in Table 1-6. CH_2Cl_2 has increased significantly in recent years in both hemispheres, having previously fallen from 1995 (when records began) to about 2000 (updated from Simmonds et al., 2006). In the NH, mean surface mixing ratios in 2008 were similar to those previously observed in the mid-1990s. $CHCl_3$ concentrations have remained approximately constant since 2000 suggesting little change in the fraction arising from industrial emissions. CCl_2CCl_2 has decreased almost monotonically since the late 1980s (updated from Simpson et al., 2004). Data in Table 1-6 indicate that this trend may have reversed in the most recently reported year, but this may be within the scatter of the interannual variability of the measurements. Global long-term measurements are available for $CHClCCl_2$ for the first time (Table 1-6). The large standard deviation reflects the very large seasonal cycle of this very reactive gas. The short record and large annual variability do not yet allow a trend to be established for this compound.

There are very few reported lower tropospheric measurements of the other chlorinated VSLS since the last Assessment, and likewise no industrial emission estimates are available for these species. In the last Assessment (Law and Sturges et al., 2007) one citation (Low et al., 2003) gave mean NH and SH C_2H_5Cl mixing ratios of 2.6 and 1.6 ppt, respectively, which, given the short lifetime of this gas (39 days; Table 1-4), requires a significant, presumably nonindustrial, source to sustain the observed SH abundances. Higher values were noted in the tropical

Table 1-5. Annual emissions of chlorinated VSLS.

Compound	Fraction of Global Emissions in the NH (%)	"Top-Down" Average Annual Global Emissions (Gg/yr)	Estimated Industrial Emissions (Gg/yr)	Estimated Biomass Burning Emissions (Gg/yr)	Origin
CH_2Cl_2	93	515 ± 22	519 ± 32	59	1
	-	629 ± 44	430 ± 12	75 ± 18	2
$CHCl_3$	-	-	-	2	1
	62	370 ± 120	-	2 ± 2	2
	-	315–373	79–108	-	3
	-	-	66 ± 23	-	4
CCl_2CCl_2	94	250–205	278 ± 20	0	1
$CHClCCl_2$	-	-	246 ± 13	0	1

Notes:
1. Simmonds et al. (2006) global and hemispheric emissions 1999–2003; McCulloch et al. (1999) industrial emission estimates (using the factors given in McCulloch et al. (1999) to estimate values appropriate for 1995); Keene et al. (1999) biomass burning emissions.
2. Xiao (2008) (values shown are for 2000–2004).
3. Worton et al. (2006) (values shown are for 2001).
4. McCulloch et al. (2003) (reference year not given).

marine boundary layer, also indicative of a natural origin. The mixing ratios given in the last two Assessments for CH_2ClCH_2Cl (20–40 ppt in the NH and 5–7 ppt in the SH) appear to have been incorrectly cited from an original paper (Class and Ballschmiter, 1987). The values given in this latter paper are <1 to 24 ppt for the NH and <1 ppt for the SH. We do not know of any globally distributed or long-term measurements of this species since this date, however, the large interhemispheric ratio suggests predominantly anthropogenic uses at that time. There are no emission estimates or inventories for this compound, making it a significant uncertainty in the chlorinated VSLS budget.

It is likely that significant calibration differences exist between measurements of chlorinated VSLS by different laboratories. This is particularly evident in the case of CCl_2CCl_2 (Table 1-6) but is equally true for all of the chlorocarbons discussed here (e.g., Simmonds et al., 2006; Butler et al., 2010). Simmonds et al. (2006) mention a 10% difference between NOAA and AGAGE measurements for CCl_2CCl_2, but no intercomparison exercises

Table 1-6. Measured mole fractions and growth rates of chlorinated very short-lived source gases.

Chemical Formula	Common or Industrial Name	Annual Mean Mole Fraction (ppt)			Growth (2007–2008)		Laboratory [a]
		2004	2007	2008	(ppt/yr)	(%/yr)	
CH_2Cl_2	dichloromethane	17.3 ± 5.7	20.3 ± 6.7	22.1 ± 6.7	1.8 ± 0.5	8.1 ± 2.3	AGAGE, in situ (Global)
$CHCl_3$	chloroform	6.8 ± 1.2	7.0 ± 1.5	7.0 ± 1.5	−0.02 ± 0.09	−0.3 ± 1.3	AGAGE, in situ (Global)
CCl_2CCl_2	tetrachloroethene	1.9 ± 0.9	1.7 ± 0.7	1.7 ± 0.7	0.01 ± 0.00	0.6 ± 0.1	AGAGE, in situ (Global)
		3.0	2.5	2.7	0.2	7	UCI, flask (Global)
$CHClCCl_2$ [b]	trichloroethene	-	0.19 ± 0.19	0.28 ± 0.28	-	-	AGAGE, in situ (Global)

[a] AGAGE global mixing ratios updated from Simmonds et al. (2006). UCI global mixing ratios updated from Simpson et al. (2004).
[b] Because of the short lifetime (4.9 days) the global mole fraction of $CHClCCl_2$ should be seen rather as an approximation than a defined global value.

have yet been published for CCl_2CCl_2 or any other chlorinated VSLS.

The anthropogenic contribution to the tropospheric abundances of chlorine from VSLS can be estimated by assuming that the anthropogenic fraction (industrial plus biomass burning) of individual gases is 90% for CH_2Cl_2 (average of 100% and 80% from modeled global emissions from Table 1-5); 100% for CCl_2CCl_2, $CHClCCl_2$, and CH_2ClCH_2Cl; and 25% for $CHCl_3$. All other chlorinated gases are assumed to be of solely natural origin. Taking the averaged 2008 molar ratios in Table 1-6 and an average value of approximately 6 ± 6 ppt for CH_2ClCH_2Cl (see above), yields a global average surface abundance of Cl from anthropogenic VSLS in 2008 of 67 ± 30 ppt.

In Table 1-7, observations of a range of various VSLS in the marine boundary layer, the upper troposphere, and the tropical tropopause layer are compiled from a number of measurement campaigns (see also Section 1.3.3.1). These measurement campaigns cover a range of dates and locations and, therefore, are not directly comparable with one another or the surface values in Table 1-6. Nevertheless, mixing ratios in the upper troposphere are on average less than those measured in the marine boundary layer, as would be expected for measurements of VSLS at some distance from their sources.

Updated mixing ratios of organic chlorine from VSLS of 59 (36–70) ppt in the tropical upper troposphere (10–12 km) (Table 1-7) are similar to the value of 55 (52–60) ppt at 10 km reported in the last Assessment, although with a wider spread. The main contributors to organic chlorine from VSLS at this altitude are CH_2Cl_2 and $CHCl_3$.

Abundances at about 15 km in the tropics can be considered to represent the lower limit of source gas injection into the stratosphere (see Section 1.3.3.1). Taking this observed total of 55 (38–80) ppt Cl from all chlorinated VSLS at this height and the same anthropogenic fractions as discussed above, a minimum stratospheric injection of 39 (27–59) ppt Cl from anthropogenic VSLS is estimated (Table 1-7).

These anthropogenic totals do not include the product gases hydrogen chloride (HCl) and phosgene ($COCl_2$), which can be formed during atmospheric decomposition from both VSL SGs (primarily $CHCl_3$ and CCl_2CCl_2) and long-lived SGs (e.g., CCl_4 and CH_3CCl_3) and together could contribute an additional 0–50 ppt Cl to the stratosphere (see Section 1.3.3.3).

1.3.1.2 Bromine-Containing Very Short-Lived Source Gases

In contrast to chlorinated VSLS, anthropogenic sources of brominated VSLS are small in comparison to natural sources. The most notable anthropogenic brominated VSLS are 1-bromopropane (n-propyl bromide, C_3H_7Br), which is used as a substitute for CFC-113 and CH_3CCl_3 in metal and electronic part cleaning; and 1,2-dibromoethane (ethylene dibromide, CH_2BrCH_2Br), which is used as a fumigant and chemical intermediate and was formerly widely used as an additive to leaded gasoline (U.S. EPA web site at www.epa.gov; Toxic Air Pollutants). Small emissions of trihalomethanes, notably $CHBr_3$, occur from chlorination of drinking water and power plant cooling water (Worton et al., 2006). There have been very few studies of long-term trends in atmospheric abundances of brominated VSLS. In the last Assessment one study was reported indicating small increases in brominated trihalomethanes since the early 20th century from Arctic firn air, but no significant trends in dibromomethane (CH_2Br_2) and bromochloromethane (CH_2BrCl) (Worton et al., 2006), which leads to the conclusion that the latter are of entirely natural origin. Atmospheric concentrations of brominated VSLS are highly variable due to the heterogeneous distribution and time-varying nature of sources; notably natural sources. Natural sources include marine phytoplankton, coastal macrophytes (seaweeds), and possibly terrestrial vegetation such as rice (Law and Sturges et al., 2007). Surface mixing ratios (predominantly from the marine boundary layer) reported in the last Assessment are summarized in Table 1-7. Mixing ratios of other bromocarbons tend to be lower than any of the aforementioned substances.

Most progress since the last Assessment has been with regard to estimating natural oceanic emissions of bromocarbons (see Table 1-8), notably bromoform ($CHBr_3$) and CH_2Br_2. These range from 430–1400 Gg Br/yr for $CHBr_3$, and 57–280 Gg Br/yr for CH_2Br_2 and are mostly larger than the estimates given in the previous Assessment report (Table 2-3 in Law and Sturges et al., 2007). There are large uncertainties associated with these estimates, notably due to the large variability in emissions from coastal zones (Butler et al., 2007). Some of the studies included in Table 1-8 emphasize the potential importance of coastal oceans (e.g., Butler et al., 2007; Carpenter et al., 2009; Liang et al., 2010). In contrast, Palmer and Reason (2009) considered tropical coastal sources to be unimportant based on a supposition that seaweeds are largely absent from the tropics. Yokouchi et al. (2005), however, reported very high mixing ratios of $CHBr_3$, dibromochloromethane ($CHBr_2Cl$), and CH_2Br_2 associated with algal-colonized tropical shores. While numerous studies have identified coastal macroalgae as sources of halocarbons, and $CHBr_3$ in particular (Law and Sturges et al., 2007), there have been relatively few studies in the tropics compared to the extratropics. Furthermore, it has not been unequivocally proven that macroalgae account for all such coastal emissions. Close to shore in Cape Verde in the tropical Atlantic, O'Brien et al. (2009) detected elevated mixing ratios of $CHBr_3$ and CH_2Br_2 without evidence of

Table 1-7. Summary of available observations of VSLS source gases from the marine boundary layer (MBL) to the tropical tropopause layer (TTL). Abundances measured in the MBL are taken from the last Assessment (Law and Sturges et al., 2007). Data in and above the upper troposphere have been compiled from observations during the PEM-West A and B, TC4, Pre-AVE, and CR-AVE aircraft campaigns (see Schauffler et al., 1999) and from Teresina balloon observations (Laube et al., 2008 and updates). All table entries are mixing ratios, with units of parts per trillion (ppt).

	Marine Boundary Layer (MBL) [a]		Upper Troposphere (UT) [b]		Lower TTL [c]		LZRH (z_0) [c,d]		Upper TTL [c]		Tropical Tropopause [c]	
Height Range			**10–12 km**		**12–14 km**		**14.5–15.5 km**		**15.5–16.5 km**		**16.5–17 km**	
Potential Temperature Range					**340–355 K**		**355–365 K**		**365–375 K**		**375–385 K**	
	Median (ppt)	Range [e] (ppt)	Mean (ppt)	Range [e] (ppt)	Mean (ppt)	Range [e] (ppt)	Mean (ppt)	Range [e] (ppt)	Mean (ppt)	Range [e] (ppt)	Mean (ppt)	Range [e] (ppt)
CH_2Cl_2	17.5	9-39	13.9	*8.6–20.9*	14.9	*11.7–18.4*	14.3	*10.8–20.6*	13.2	*9.8–21.2*	12.6	*7.2–22.5*
$CHCl_3$	7.8	5.2–13.1	5.8	*3.9–7.5*	7.1	*5.9–9.2*	5.7	*3.5–7.9*	4.8	*3.5–6.6*	4.9	*3.3–6.4*
CH_2ClCH_2Cl	3.7	0.7–14.5	3.7 [f]	*1.9–5.4*	2.9 [g]	*1.9–4.1*	2.7 [g]	*1.6–4.9*	2.2 [g]	*1.2–4.0*	2.0	*0.6–4.3*
$CHClCCl_2$	0.5	0.05–2	0.36 [f]	*0–2.02*	0.05 [g]	*0.00–0.16*	0.03 [g]	*0.00–0.17*	0.02 [g]	*0.00–0.05*	0.03	*0.00–0.17*
CCl_2CCl_2	1.8	1.2–3.8	1.3	*0.7–1.8*	1.1	*0.8–1.5*	0.9	*0.4–1.3*	0.6	*0.3–0.9*	0.5	*0.1–1.0*
CH_2Br_2	1.1	0.7–1.5	0.86	*0.63–1.21*	0.92	*0.77–1.15*	0.74	*0.59–0.99*	0.66	*0.43–0.83*	0.51	*0.3–0.86*
$CHBr_3$	1.6	0.5–2.4	0.50	*0.12–1.21*	0.61	*0.3–1.11*	0.22	*0.00–0.63*	0.14	*0.01–0.29*	0.09	*0.00–0.31*
CH_2BrCl	0.5	0.4–0.6	0.09 [h]	*0.03–0.16*	0.14 [i]	*0.13–0.16*	0.10 [i]	*0.08–0.13*	0.11 [i]	*0.1–0.12*	0.08	*0.05–0.11*
$CHBr_2Cl$	0.3	0.1–0.8	0.11	*0.01–0.36*	0.10 [i]	*0.06–0.15*	0.06 [i]	*0.03–0.11*	0.05 [i]	*0.01–0.11*	0.03	*0.00–0.14*
$CHBrCl_2$	0.3	0.1–0.9	0.11	*0.02–0.28*	0.20	*0.18–0.22*	0.10	*0.12–0.18*	0.12	*0.11–0.14*	0.06	*0.03–0.12*
Other brominated SG [j]							< 0.2 [j]		< 0.2 [j]		< 0.2 [j]	
CH_3I	0.80	0.3–1.9	0.13	0.03–0.42	0.12 [k]	0.00–0.23	0.04 [k]	0.00–0.10	0.00 [k]	0.00–0.01	0.01	0.00–0.06
Total Cl	76	41–171	59	*36–70*	62	*48–78*	55	*38–80*	48	*38–74*	46	*26–77*
Anthrop. Cl [l]	55	27–136	43	*26–51*	43	*32–55*	39	*27–59*	34	*25–55*	32	*17–58*
Total Br	8.40	3.6–13.3	3.5	*1.7–7.4*	4.3	*2.8–6.5*	2.7	*1.4–4.6*	2.0	*1.1–3.2*	1.5	*0.7–3.4*
Total I	0.80	0.3–1.9	0.13	0.03–0.42	0.12	0.00–0.23	0.04	0.00–0.10	0.00	0.00–0.01	0.01	0.00–0.06

PEM-West = Pacific Exploratory Mission-West; TC4 = Tropical Composition, Cloud, and Climate Coupling mission; Pre-AVE = Pre-Aura Validation Experiment; CR-AVE = Costa Rica Aura Validation Experiment.

Notes:

[a] Marine boundary layer mixing ratios are identical to those in Table 2-2 of the previous Assessment (Law and Sturges et al., 2007).

[b] UT data are from DC-8 aircraft observations during PEM-West A, PEM-West B, and TC4.

[c] TTL and tropopause data are from WB-57 aircraft observations during TC4, Pre-AVE, and CR-AVE (see Aschmann et al., 2009, Hossaini et al., 2010 and Liang et al., 2010) and balloon observations from Teresina, Brazil, in June 2005 (Laube et al.2008) and June 2008 (update of Laube et al., 2008).

[d] LZRH(z_0) corresponds to the level of zero clear-sky radiative heating (z_0) (see Box 1-4). As in the previous assessment (Law and Sturges et al., 2007), we define this level at about 15 km or 360K, where there is a transition from clear-sky radiative cooling to clear-sky radiative heating. In general, air masses above this level are expected to enter the stratosphere.

[e] The stated observed range represents the smallest mean minus 1 standard deviation and the largest mean plus 1 standard deviation

Table 1-7, continued (notes).

among all measurement campaigns.

[f] CH_2ClCH_2Cl (dichloroethane) and $CHClCCl_2$ (trichloroethene) in the UT only from TC4.

[g] CH_2ClCH_2Cl and $CHClCCl_2$ in the TTL, including the LZRH, only from TC4, Pre-AVE, and CRAVE.

[h] CH_2BrCl in the UT only from PEM-West B.

[i] CH_2BrCl and $CHBrCl_2$ in the TTL, including the LZRH, only from TC4 and Teresina balloon measurements.

[j] Estimated maximum contribution from species like C_2H_5Br, $C_2H_4Br_2$, C_3H_7Br.

[k] CH_3I in the TTL, including the LZRH, only from TC4 and Pre-AVE.

[l] The anthropogenic fraction of chlorinated VSLS (Anthrop. Cl) has been calculated by adding 90% of CH_2Cl_2, 25% of $CHCl_3$, and 100% of CCl_2CCl_2, $CHClCCl_2$, and CH_2ClCH_2Cl (see also Section 1.3.1.1).

significant macroalgae on the local shore. Peak concentrations were observed at solar noon (2–44 ppt $CHBr_3$ and 1–9 ppt CH_2Br_2), rather than low tide as would be expected for emissions from intertidal macroalgae.

In a case study off the West coast of Africa, Quack et al. (2007) suggest that CH_2Br_2 might originate partly from biologically mediated reductive hydrogenolysis of $CHBr_3$. Some studies (e.g., Palmer and Reason, 2009; Kerkweg et al., 2008) suggest significant regional "hotspots" in the tropics and subtropics especially in the west Pacific Ocean near Indonesia, but with large seasonal and temporal variations. This point is also in accord with Butler et al. (2007), who estimated that 64% of bromoform emissions originated from the Pacific (47% from the tropical Pacific, and 70% in total from the tropics), compared with just 3% from the Atlantic. For CH_2Br_2 the corresponding figures were 40% (24%, 40%) and 20%, respectively. In the last Assessment (Law and Sturges et al., 2007) it was proposed that regions of oceanic upwelling could be important sources of bromocarbon emissions. Since then Quack et al. (2007) and Carpenter et al. (2009) have shown, based on measurements in the Mauritanian upwelling, that such regions may be collectively relatively minor contributors to global emissions (e.g., around 1% of $CHBr_3$ and CH_2Br_2 global emissions).

It should also be noted that discrepancies between observation-based studies arise from the "snapshot" picture they supply of a highly heterogeneous and variable system, as well as possible substantial differences between calibration scales (Butler et al., 2010) and methods of estimating fluxes and extrapolating them to larger areas (e.g., Carpenter et al., 2009 and O'Brien et al., 2009). The picture of global bromocarbon emissions is therefore highly complex with substantial uncertainties. Understanding the regional and seasonal variability of emissions is, however,

Table 1-8. Fluxes of bromine from bromoform ($CHBr_3$) and dibromomethane (CH_2Br_2) in Gg Br/yr, and iodine from methyl iodide (CH_3I) in Gg I/yr.

Reference	$CHBr_3$ Flux (Gg Br/yr)			CH_2Br_2 Flux (Gg Br/yr)			CH_3I Flux (Gg I/yr)		
	Global	Open Ocean	Coastal	Global	Open Ocean	Coastal	Global	Open Ocean	Coastal
Butler et al. (2007)	800	150	650	280	50	230	550	270	280
Carpenter et al. (2009)			200						
Liang et al. (2010) [e]	430	260	170	57	34	23			
O'Brien et al. (2009)	820 [a] 1400 [b]								
Palmer and Reason (2009)		120 [c]							
Yokouchi et al. (2005)	820 [a]								
Warwick et al. (2006)	560 [d]	280 [d]	280 [d]	100					

[a] Scaled to CH_2Br_2 emissions from Ko and Poulet et al. (2003), based on global loss rates and an estimated global burden.

[b] Scaled to CH_2Br_2 emissions from Warwick et al. (2006).

[c] Tropical ocean only.

[d] Modeling study: "Scenario 5": 70% of emissions in the tropics; August/September.

[e] Emissions from Liang et al. (2010) are from modeling of airborne measurements in the Pacific and North American troposphere and lower stratosphere.

vital in assessing their likely impact on the stratosphere, since it is the coincidence in both space and time of VSL SG emissions with surface to tropical tropopause layer (TTL) transport that will largely dictate the efficiency with which these emissions reach the stratosphere.

Updated mixing ratios of organic bromine from VSLS of 3.5 (1.7–7.4) ppt in the tropical upper troposphere (10–12 km) (Table 1-7) confirm reported figures from the last Assessment of 3.5 (3.1–4.0) ppt at 10 km. This organic bromine from VSLS consists mostly of CH_2Br_2 and $CHBr_3$ with smaller amounts of bromochloromethanes and is discussed further in Section 1.3.3.1.

1.3.1.3 Iodine-Containing Very Short-Lived Source Gases

The occurrence and chemistry of iodinated compounds, all of which are VSLS, were discussed extensively in previous Assessments due to their potentially very high ODPs should they reach the stratosphere (the "alpha" factor for iodine in the stratosphere is higher than bromine). Iodinated gases are predominantly of natural origin, but have been considered for use as fire suppressants as a halon replacement on aircraft (e.g., CF_3I) or to reduce flammability in refrigerant mixtures. CH_3I is also currently being licensed in the U.S. and Japan as a replacement for CH_3Br as a fumigant (UNEP/TEAP, 2010). Domestic biomass burning in Africa reportedly contributes a small flux of CH_3I to the atmosphere (Mead et al., 2008c).

The dominant source of iodinated VSLS is from the ocean. Butler et al. (2007) estimated approximately equal global fluxes of CH_3I from the open ocean and coastal regions (Table 1-8) and a higher total flux than given in the previous Assessment by about a factor of two. Yokouchi et al. (2008) observed an increase in CH_3I with sea surface temperature at midlatitudes, which might be of significance in a warming climate, and a corresponding seasonality with higher concentrations in summer. An intriguing observation is that of Williams et al. (2007), who presented evidence for enhanced emissions of CH_3I from the ocean, apparently from an abiotic chemical mechanism stimulated by dust deposition. A corollary of this is that a similar mechanism might operate in atmospheric aerosols. Sive et al. (2007) conclude that terrestrial biomes contribute a small but significant flux to the atmosphere.

Several recent studies have measured a range of iodinated species in the marine boundary layer (MBL) and considered the active iodine-mediated chemistry therein. It is unlikely, however, that either the shortest-lived iodinated species (those with lifetimes of minutes or hours), or inorganic iodinated gases (e.g., I_2, IO, and OIO; Read et al., 2008), would escape the MBL in appreciable quantities (see also Section 1.4.3).

1.3.1.4 Halogen-Containing Aerosols

In addition to organic VSLS, inorganic sources, notably halogen-containing aerosols, may be precursors of reactive halogens in the atmosphere. Although aerosols are subject to gravitational and wet depositional processes, they can have significant atmospheric residence times under the dry conditions prevalent in the free troposphere (e.g., several days for sea salt aerosol; Yang et al., 2005). Yang et al. (2005) suggested that 0.1–1.0 ppt of bromine monoxide (BrO) in the troposphere arises from a combination of Br release from sea salt and decomposition of bromomethanes. Support for such a mechanism comes from the model described by O'Brien et al. (2009) where additional release of halogens from halide-containing aerosol (over and above that from degradation of bromocarbons) was required to explain BrO abundances measured within the tropical marine boundary layer (Read et al., 2008). Pyle et al. (2007) note that sea salt production rates are highly uncertain and that using two separate formulations results in a factor of two difference in sea salt aerosol production rates. Bromine and iodine have been detected in aerosols of tropospheric origin in the stratosphere several kilometers above the local tropopause height (Murphy et al., 2007). The influence of these aerosols on lower stratospheric halogen abundances is likely small but is poorly quantified. We conclude that the contribution from sea salt aerosol to stratospheric Br_y is likely to be substantially less than 1 ppt.

1.3.2 Transport of Very Short-Lived Substances into the Stratosphere

The efficiency of VSLS transport into the stratosphere results from the competition between fast vertical transport and chemical destruction or removal via washout of the source gases (SGs) and product gases (PGs). Conversion of SG to PG reduces the efficiency of halogen transport to the stratosphere if the PG is taken up by aerosols and becomes washed out before reaching the stratosphere. The probability of washout decreases with increasing height within the troposphere and becomes small in the TTL. In general, SG and PG reach the "tropical stratosphere" above the cold point tropopause (CPT), which is climatologically located at 380 K (~17 km altitude). Therefore, timescales for transport through the TTL are especially important for determining the efficiency of VSLS transport through this layer. For a detailed TTL schematic see Figure 1-9 (adapted from Fueglistaler et al. (2009a) and modified to provide definitions of the TTL consistent with past Assessments).

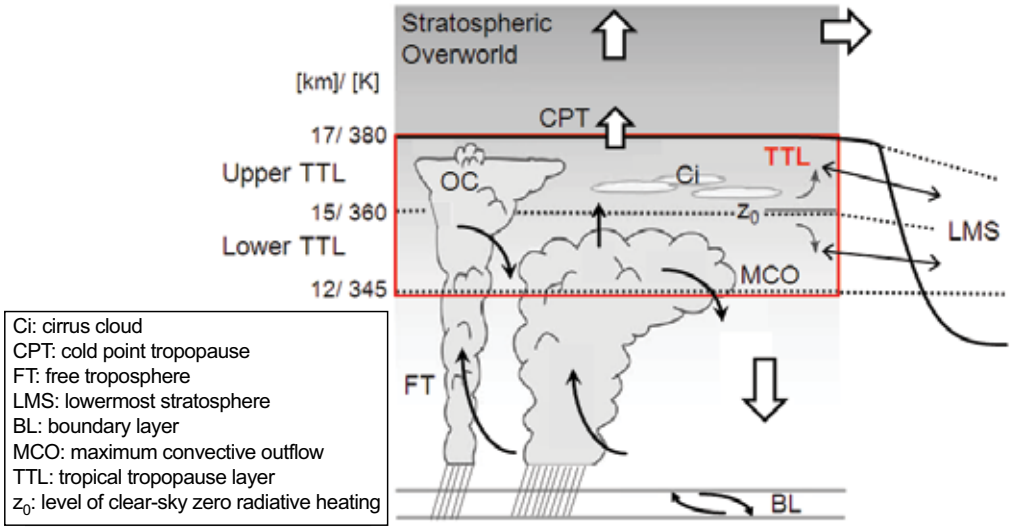

Figure 1-9. Schematic showing principal dynamical pathways in the tropics transporting VSL source gases (SG) and product gases (PGs) into the stratosphere (modified from Fueglistaler, 2009a). The position of the tropopause is designated by the bold black line.

1.3.2.1 VSLS Transport from the Surface in the Tropics to the Tropical Tropopause Layer (TTL)

While shorter-lived VSLS with lifetimes of only hours to days are unlikely to reach the TTL unless emitted directly into the active cell of tropical deep convection, VSLS with lifetimes of weeks to months can reach the TTL via a range of transport pathways described in Figure 1-9.

Additional evidence has become available since the previous Assessment supporting the tropical Western Pacific as a region where VSLS emissions can be efficiently transported to the TTL (Aschmann et al., 2009) (Figure 1-10). New results also suggest that the efficiency of this TTL transport varies with season. Higher VSLS concentrations in the TTL are predicted in NH winter compared to the rest of the year (Aschmann et al., 2009; Gettelman et al., 2009) due to a combination of higher convective cloud tops reaching the TTL and higher vertical velocities within the TTL (Gettelman et al., 2009).

In NH summer, air masses can cross the TTL and enter the stratosphere, but with a reduced and more zonally uniform distributed flux compared to NH winter (Fueg-

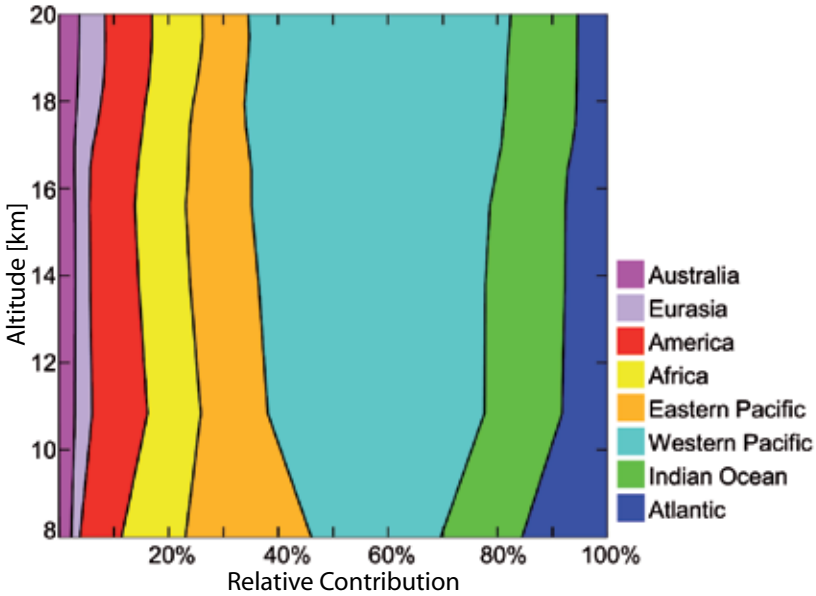

Figure 1-10. The relative contribution (%) of individual source regions to the total amount of an idealized $CHBr_3$ tracer (with a 20-day lifetime) between 8 and 20 km in the tropics, averaged over 2000–2005. Australia includes Maritime Continent and Africa includes Arabian Peninsula. The relative contribution from the Mediterranean region was also diagnosed but is too small to be visible in this figure (modified from Aschmann et al., 2009).

listaler et al., 2005). However, the northward shift of the deepest convection with the Indian summer monsoon linked with the anticyclonic circulation in the upper troposphere/lower stratosphere could lead to more efficient transport of surface emissions in certain regions of the world (e.g., Bay of Bengal and Sea of China) to the TTL and potentially to the stratospheric overworld (e.g., James et al., 2008; Randel et al., 2010). For instance, Stohl et al. (2002) have estimated that in NH summer, Asian surface emissions can be transported into the TTL with average timescales of a week or less instead of three weeks in NH winter. Consistent with these findings, Donner et al. (2007) simulate enhanced methyl iodide (CH_3I) concentrations over the Tibetan plateau and the Himalaya during NH summer in the free troposphere and above the cold-point tropopause due to overshooting convection. Thus tropical overshooting convection can directly inject surface air into the upper TTL and to the stratosphere as is observed (e.g., Ricaud et al., 2007) and simulated by different models (Donner et al., 2007; James et al., 2008). Due to the very rare and localized occurrence of such events (Liu and Zipser, 2005; Liu et al., 2007), the amount of VSLS halogen reaching the stratosphere via these events is expected to be small on a global basis, as has been discussed analogously for the stratospheric water vapor budget (Fueglistaler et al., 2009b; Schiller et al., 2009; Homan et al., 2010). Besides, Hossaini et al. (2010) suggest that especially for longer-lived VSLS (e.g., CH_2Br_2), large-scale transport and mixing of planetary boundary layer (PBL) air to the TTL could also be important transport processes in addition to overshooting convection.

Because observational evidence for direct VSLS transport from the surface to the TTL and to the stratosphere is scarce, the relative roles of boundary layer mixing, convection, and overshooting convection are still a matter of debate. In addition to the uncertainties in convective parameterizations in models discussed in the last Assessment (Law and Sturges et al., 2007), washout of VSLS influences the amount of VSLS actually reaching the stratosphere (Section 1.3.3).

1.3.2.2 VSLS Transport from the TTL to the Stratosphere

Transport through the upper TTL primarily takes place as large-scale horizontal and slow vertical motions (weeks to ascend through this region of the TTL) accompanied by infrequent localized and rapid (hours) overshooting convection into the stratosphere (Law and Sturges et al., 2007; Fueglistaler et al., 2009a; Figure 1-9). Furthermore, the transport of VSLS through the TTL is also dependent on the region and season of VSLS emissions and varies interannually (Aschmann et al., 2009; Gettelman et al., 2009; Krüger et al., 2009).

In the last Assessment a large uncertainty was reported for the residence time in the TTL, with a range of 20 to 80 days in the upper TTL. The understanding of residence times in the TTL has since improved to some extent. In particular, the residence time depends strongly on vertical velocities, on the particular layer being considered within the TTL, and on the temporal and horizontal variability used for calculating the transport. New approaches and improved data assimilation have become available. This has led to a reduced uncertainty range of 25 to 45 days for transport through the upper TTL (Krüger et al., 2009; Ploeger et al., 2010).

Of particular relevance for the VSLS fraction reaching the stratosphere is the slow, radiatively driven transport through the upper TTL (from the level of clear-sky zero radiative heating (z_0) at 360 K to the CPT at 380 K) (see Figure 1-9). The annual cycle of air mass transport from the TTL to the stratosphere peaks over the tropical Western Pacific during NH winter and over the Indian monsoon regions during NH summer (Fueglistaler et al., 2005; Law and Sturges et al., 2007). In addition, the TTL residence time close to the CPT is lower by 25% in NH winter compared to NH summer (Kremser et al., 2009; Ploeger et al., 2009) and this also influences the efficiency of VSLS transport to the stratosphere.

At the CPT and above, large-scale vertical motion dominates the air mass transport (Krüger et al., 2008; Fueglistaler et al., 2009a; Gettelman et al., 2009) and readily brings air to regions of the stratosphere where ozone is depleted. Above the tropical Western Pacific, Krüger et al. (2009) found that most air parcels are transported in less than 25 days through the 360 K to 380 K layers during NH winters 1962–2001, which is at the lower end of the averaged residence time of 25–45 days stated above. They derived a long-term interannual variability of the averaged residence time for air parcels in the upper TTL during NH winter of up to 20% (±2 sigma); with shorter residence times being significantly correlated with periods of enhanced extratropical and subtropical wave driving. General changes in tropical upwelling rates and of the Brewer-Dobson circulation (BDC) are discussed in more detail in later Chapters (Sections 3.2.4 and 4.2.2). These considerations lead to a higher potential of halogens from VSLS entering the stratosphere within these regions and seasons during periods of enhanced wave driving and/or convective overshoot.

1.3.2.3 VSLS Transport from the Surface to the Extratropical Stratosphere

The extratropical lowermost stratosphere (LMS) is the region between the extratropical tropopause and approximately the 380 K isentropic surface (see Figure 1-9). While the contribution of VSLS to halogen in the extra-

tropical stratosphere is mainly controlled by upwelling into the tropical stratosphere and quasi-horizontal isentropic transport into the extratropics, it has been perceived in recent years that vertical transport by convection into the extratropical stratosphere can also be of importance (Section 2.4.2 of Law and Sturges et al., 2007). Furthermore, new evidence suggests that a larger fraction of tropical air masses in the TTL are transported into the extratropical stratosphere than into the stratospheric overworld, as detailed below.

Levine et al. (2008) simulate that up to 5 times more air mass is transported from the bottom of the TTL into the LMS than from the bottom of the TTL into the tropical stratospheric overworld throughout the year. However, the amount of transport into the extratropical LMS is largest toward the SH and shows, for both transport pathways, a seasonal dependence with a maximum during NH winter and a minimum during NH summer.

In contrast, the studies by Bönisch et al. (2009) and Berthet et al. (2007), which concentrated on the NH only, analyzed a stronger transport from the tropical troposphere to the extratropical LMS during NH summer. Bönisch et al. (2009) estimate a strong seasonality of the origin of tropical air masses in the LMS of the NH, with a maximum tropospheric influence during October. The authors conclude that the seasonality is influenced by the transit times from the tropical troposphere into the LMS, which are shortest (<0.3 years) during summer and longest (>0.8 years) during late spring. From this it can be concluded that the strength of the subtropical jet and the lower branch of the BDC strongly influence the transport of VSLS in the LMS (i.e., the subtropical jet is weaker from summer to mid-autumn, and the residual transport time-scales within the lower branch of the BDC are shorter in summer than in winter and dominate the tropospheric influence in the LMS). Berthet et al. (2007) also find that during NH summer, the extratropical LMS layer between 370 K and 410 K is well ventilated with tropospheric air from the tropics compared to the layer below 340 K, which is mainly influenced by extratropical air. During NH winter this distinction holds but with weaker tropical troposphere-to-stratosphere transport (TST) due to a more impermeable barrier.

Convective overshooting of air across the tropopause into the LMS is quite frequent in the extratropics. These injections, together with transport from the TTL, form a mixed layer extending about 25 K above the tropopause (Hoor et al., 2004). Sometimes, injections even deeper into the stratosphere can occur and influence the chemical composition of the lower stratosphere (Hegglin et al., 2004). The deepest injections are produced by the high instability and breaking of gravity waves excited by strong convection inside super-cell thunderstorms (Wang, 2007; Wang et al., 2009). While water vapor enrichments have been documented by this mechanism, no studies related to VSLS transport via this mechanism have been published. Another possibility for surface air to be injected directly into the extratropical stratosphere (even into the stratospheric overworld) is by pyro-convection associated with strong forest fires. Single pyro-convection events can double the zonally averaged aerosol optical depth in the LMS and these aerosol layers can persist in the stratosphere for months (Fromm et al., 2008). While this process is not captured by global models, special high-resolution models have recently shown skill in simulating pyro-convection (Trentmann et al., 2006; Luderer et al., 2007). So far, no observations of halogenated VSLS in pyro-convective outflows have been reported.

1.3.3 VSLS and Inorganic Halogen Input to the Stratosphere

In the previous Assessment (Law and Sturges et al., 2007) the contribution of VSLS species to the stratospheric halogen loading was discussed in detail. Since this last Assessment new observations of VSLS SGs in the tropical upper troposphere and TTL have become available, as well as modeling studies of the possible input of product gases (PG) from these VSLS. However, for brominated PGs still no observations are available from the upper tropical troposphere and from the TTL that would enable us to identify the contribution of PGs to stratospheric bromine loading.

1.3.3.1 Source Gas Injection (SGI)

Source gases deliver halogen into the stratosphere in the same form as they are emitted at the surface. Some recent modeling studies (Donner et al., 2007; Aschmann et al., 2009; Liang et al., 2010; Hossaini et al., 2010) have used observational data of the most important bromine- and iodine-containing VSLS species (CH_2Br_2, $CHBr_3$, and CH_3I) to compare with their modeling results. These new observational data on VSLS species in the TTL have become available from the Aura Validation Experiment (AVE; http://espoarchive.nasa.gov/archive/arcs/pre_ave/ and http://www.espo.nasa.gov/ave-costarica2/) and TC4 (Tropical Composition, Cloud and Climate Coupling, http://www.espo.nasa.gov/tc4/) missions, and from balloonborne observations (Laube et al., 2008). In addition, available data from the Pacific Exploratory Mission (PEM) West A and B campaigns have been used. New balloonborne observations of chlorinated VSLS and of additional brominated VSLS have also been reported by Laube et al. (2008). The averages and the ranges of these observations are compiled in Table 1-7 for the upper tropical troposphere (10 km altitude range), the bottom of the TTL (340–355 K), z_0 (taken as about 355–365 K), the upper

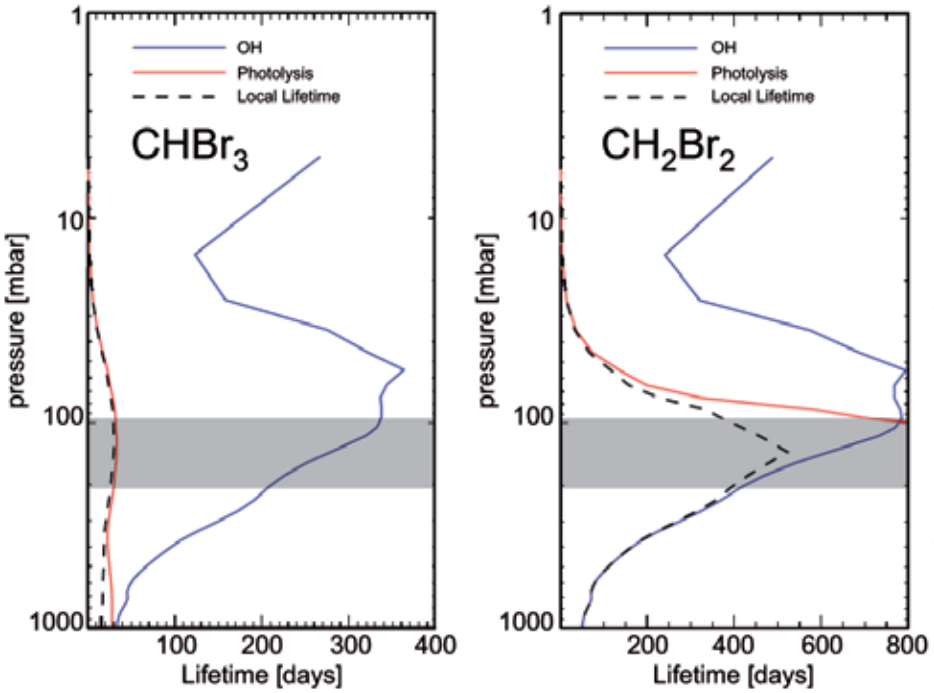

Figure 1-11. The modeled vertical distribution of the annual mean lifetime (days) of $CHBr_3$ and CH_2Br_2 in the tropics (±20° latitude) with respect to the two main loss processes: photolysis (solid red line) and reaction with OH (solid blue line), as well as the overall lifetime (dashed black line). The region between the base of the TTL and of the cold-point tropopause (CPT) is indicated as the gray bar. Modified from Hossaini et al. (2010).

TTL (365–375 K), and the tropical cold point tropopause (375–385 K) (Figure 1-9). In the following discussion of uncertainties, we do not take into account uncertainties in absolute calibrations (e.g., Butler et al., 2010). Rather we use data from different sources and take the ranges of the reported mixing ratios. Uncertainties in the absolute calibrations will thus be reflected in the range of uncertainties due to the use of data from different sources. Furthermore, the data coverage is still sparse (e.g., not all possible input areas and seasons have been sampled) and it is unclear how far the available observations reflect the complete range of possible input values.

SGI from Chlorinated VSLS

Law and Sturges et al. (2007) concluded that the chlorine content from VSL SGs in the tropical upper troposphere was about 50 ppt on the basis of multiple airborne campaigns, representing about 1 to 2% of the inorganic stratospheric chlorine (Cl_y) input from long-lived source gases. Recent airborne and balloonborne observations in the tropics have confirmed and refined these conclusions (Laube et al., 2008) (see Table 1-7). The major loss process for most chlorine-containing VSLS is the reaction with OH. As the rate constants for these reactions decrease at the low temperatures in the upper tropical troposphere and TTL, vertical mixing ratio gradients are rather small. The total chlorine contained in VSLS source gases decreases from about 60 ppt in the upper tropical troposphere and lower TTL to about 50 ppt near the tropical tropopause. C_2H_5Cl was not quantified, but was estimated to be on the order of 1.5 ppt in the upper tropical troposphere (Law and Sturges et al., 2007).

Our best estimate of chlorine injected as SG from VSLS into the stratosphere is 55 (38–80) ppt and largely confirms the estimate of 50 (±10) ppt given in the previous Assessment (Law and Sturges et al., 2007).

SGI from Brominated VSLS

The two main brominated VSLS ($CHBr_3$ and CH_2Br_2) show different vertical gradients in the transition region between the troposphere and the stratosphere (see Table 1-7). Whereas mixing ratios of CH_2Br_2 decrease from about 0.9 ppt in the upper tropical troposphere and the lower TTL to about 0.5 ppt near the tropical tropopause, mixing ratios of $CHBr_3$ decrease more substantially in this region, declining from 0.5 ppt in the upper troposphere and lower TTL to 0.1 ppt near the tropical tropopause.

These observed differences are explained by the different local lifetimes of these gases within the TTL. While photolysis dominates the destruction of $CHBr_3$ and leads to a modeled local lifetime that is similar to transport times for air through the TTL, the lifetime of CH_2Br_2 (set mainly by [OH]) is much longer than transport timescales (Figure 1-11).

Lifetime differences are also noted in the troposphere for these gases, and this influences the efficiency of surface emissions reaching the upper troposphere. The tropospheric local lifetime of 23 days for $CHBr_3$ is mainly determined by photolysis (36-day partial lifetime) and to a lesser degree by its reaction with the OH radical (76-day

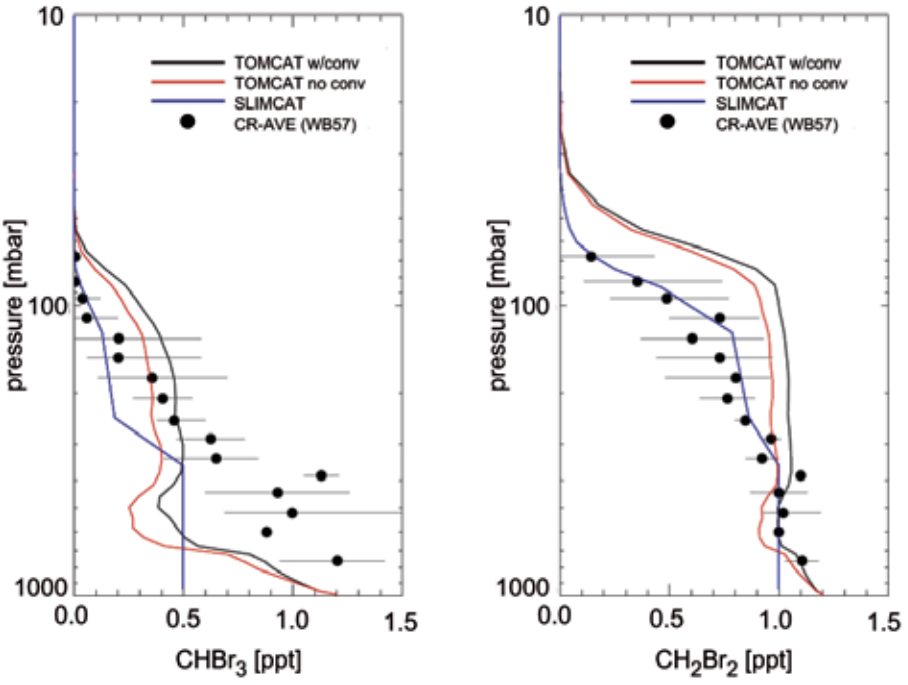

Figure 1-12. A comparison between observed and modeled vertical distributions of $CHBr_3$ (left panel) and CH_2Br_2 (right panel) mixing ratios (ppt) at tropical latitudes (Hossaini et al., 2010). The red and black lines are from TOMCAT model runs using ECMWF vertical velocities, without and with parameterized convection, respectively, while the SLIMCAT model run (blue lines) is based on calculated diabatic heating rates. Black dots are measurements from the CR-AVE campaign. Modified from Hossaini et al. (2010).

partial lifetime). In contrast, the considerably longer tropospheric local lifetime of CH_2Br_2 of 123 days is nearly completely governed by its reaction with the OH radical (Table 1-4 and Figure 1-11).

As a result of these influences, a 1-D model calculation suggests that 70% and 28% of the specified surface concentrations of CH_2Br_2 and $CHBr_3$, respectively, reach 18 km altitude (top of the TTL), when operational European Centre for Medium-Range Weather Forecasts (ECMWF) velocity fields, a convective source, and a VSLS sink are taken into account (Gettelman et al., 2009). Hossaini et al. (2010) also discuss the breakdown of CH_2Br_2 and $CHBr_3$ in the atmosphere and compare their three-dimensional (3-D) model results with observational data (Figure 1-12). In the upper tropical troposphere and the TTL, Hossaini et al. (2010) achieved an overall better agreement of simulated and observed CH_2Br_2 and $CHBr_3$ profiles when using the slower (climatological) diabatic heating rates in the Single Layer Isentropic Model of Chemistry and Transport (SLIMCAT) model compared to using the faster analyzed vertical velocities in the Toulouse Off-line Model of Chemistry and Transport (TOMCAT)-chemical transport model. Assuming uniform mixing ratios of 1.2 ppt of CH_2Br_2 and $CHBr_3$ in the tropical lower troposphere, they derive a SGI of about 2 ppt Br into the stratosphere. Additionally, the sum of CH_2BrCl, $CHBr_2Cl$, and $CHBrCl_2$ contributes about 0.5 ppt of bromine to the upper troposphere and lower TTL. Near the tropical tropopause the total contribution of these source gases declines to about 0.2 ppt. Additional bromine from species not quantified, like C_2H_5Br and n-propylbromide (C_3H_7Br), is expected to be presently less than 0.2 ppt in the TTL. In summary, we estimate VSLS bromine source gases, including unmeasured species, to account for about 2.7 (1.4–4.6) ppt of bromine at about 15 km altitude in the tropics and about 1.5 (0.7–3.4) ppt at the tropical CPT at around 17 km altitude.

SGI from Iodinated VSLS

Newly available data for CH_3I in the TTL from the Pre-AVE and TC4 experiments (see Table 1-7) (Aschmann et al., 2009) as well as data from Bell et al. (2002), which are compared to modeling results in Donner et al. (2007), indicate that the mixing ratios of this most important iodine source gas in the TTL at 15 km altitude are generally below 0.1 ppt and drop below 0.05 ppt at the cold point tropopause. This is consistent with the estimate of 0.08 ppt from the previous Assessment for CH_3I in the upper tropical troposphere (Law and Sturges et al., 2007). Three recent studies have also investigated the transport of methyl iodide into the TTL (Donner et al., 2007; Gettelman et al., 2009; Aschmann et al., 2009). These studies confirm that due to its short lifetime, only a very small fraction of CH_3I from the boundary layer reaches the TTL and the stratosphere.

1.3.3.2 Product Gas Injection (PGI)

In addition to the input of halogen from VSLS source gases, their chemical degradation products (so called product gases or PGs) are also likely to contribute halogens to the stratosphere. Due to their solubility in wa-

ter and the significant uptake coefficients on ice of many of these PGs (see Law and Sturges et al., 2007, for a detailed discussion) their fate is less clear than that of source gases and depends critically on the physical and chemical conditions in the area where they are formed. This leads to a strong coupling between chemistry, removal processes, and atmospheric transport processes relevant for VSLS species. While observations of source gases discussed in Section 1.3.3.1 have become available, observations of PGs are sparse for chlorine and no observations of PGs above detection limits of the respective instruments have been reported for bromine and iodine in the upper tropical troposphere and the TTL. An assessment of plausible values of PGI for these two halogens therefore relies largely on modeling results that are not currently constrained by observations.

PGI from Chlorinated VSLS

In the previous Assessment there were large uncertainties regarding the contribution of chlorinated PGs, notably $COCl_2$ (phosgene) and HCl, arising from degradation of chlorinated VSLS (and longer-lived SGs) to Cl_y. The picture is complicated due to possible "double counting" of chlorinated PGs recirculated from the stratosphere and thus already taken into account in the budget of source gases entering the stratosphere. Fu et al. (2007) reported satellite measurements of $COCl_2$, albeit with large uncertainty limits, between February 2004 and May 2006. Chlorine from $COCl_2$ between 15 and 20°N was 43 ± 27 ppt Cl at 8.5 km (upper troposphere), 31 ± 22 ppt Cl at 14.5 km, and 36 ± 26 ppt Cl at 17.5 km, i.e., approximately 32 ± 22 ppt of chlorine at z_0 (~15 km). These values are at the lower end of the range (40 – 50 ppt Cl) estimated in the previous Assessment (Law and Sturges et al., 2007). As it is unclear how much of the chlorine in $COCl_2$ is already included in the budgets from the SGs, we follow the same approach as in the previous Assessment by considering a range of values, or 0–32 ppt of additional chlorine. A best estimate of 16 ppt results as possible additional chlorine input to the stratosphere in the form of $COCl_2$, which is not accounted for in the very short-lived source gas budgets.

Marcy et al. (2007) reported HCl to be below their detection limit of 5 ppt in upper tropospheric air over the tropical east Pacific. In the lower TTL over the east Pacific in January 2004, however, Marcy et al. (2007) reported HCl to be mostly non-zero with values ranging to almost 40 ppt around 15 km altitude, and increasing to about 20–80 ppt in the upper TTL, with the increase being mainly attributed to in-mixing of lowermost extratropical stratospheric air. Mébarki et al. (2010), using a less sensitive long-path instrument, placed an upper limit of 30 and 20 ppt HCl in the upper TTL (~15–17 km) from two flights over Brazil in June 2005 and June 2008, respectively. Marcy et al. (2007) estimated that at most only 3–8 ppt of the HCl that they observed in the TTL could have originated from in situ degradation of CH_3Cl. Park et al. (2008) report that profiles of HCl concentration reached minimum values of about 10 to 30 ppt at around 13 km above the Asian continent, consistent with the measurements reported by Marcy et al. (2007). In summary, we conclude that HCl values in the TTL are typically on the order of 20 (0–40) ppt. As it is unclear how much of this chlorine will eventually reach the stratosphere or has already been accounted for by source gases, we estimate that somewhere between 0 and 100% of this HCl (i.e., 0–20 ppt of chlorine) could represent an additional source of chlorine from VSLS to the stratosphere, with a best estimate value being the midpoint (10 ppt).

PGI from Brominated VSLS

The only bromine PG that has been measured in the TTL is bromine monoxide (BrO) (Dorf et al., 2008; see also Section 1.4). The observed values were reported to be below detection (i.e., below 1 ppt BrO) in the TTL, though a value of 2 ± 1.5 ppt BrO was derived around the local tropopause at about 17 km. Because this sparse observational information does not tightly constrain the average input of brominated PG into the stratosphere, a range of plausible values is derived here based on modeling studies.

Most modeling studies rely on the assumption that bromine from photo-oxidized VSLS is immediately transformed to inorganic bromine (mainly as hydrogen bromide (HBr), hypobromous acid (HOBr), and BrO). This is supported by Hossaini et al. (2010), who concluded that all intermediate organic products of the oxidation of bromocarbons are short lived, with CBr_2O being the longest-lived organic intermediate with an atmospheric lifetime of 7 days.

The assumption that the degradation of organic bromine-containing VSLS yields inorganic bromine is thus fairly well established. The subsequent fate, however, of this inorganic bromine (Br_y) is less clear. Most inorganic bromine gases, especially HOBr and HBr are highly soluble in water and have high uptake coefficients on ice (see Section 2.3.4 of Law and Sturges et al., 2007). The removal of Br_y from the gas phase and the subsequent washout is parameterized in models. This parameterization has a strong influence on the fraction of product gases reaching the stratosphere. Furthermore, as already emphasized in the last Assessment, heterogeneous reactions of HOBr and HBr with sulfuric acid producing photolabile dibromine monoxide (Br_2O) and molecular bromine (Br_2) further complicate the modeling of this process.

Model studies presented in the previous Assessment used prescribed removal timescales for Br_y in the TTL (e.g., Warwick et al., 2006; Sinnhuber and Folkins,

2006), i.e., the removal processes (wet deposition, uptake on ice, and dehydration) have not been calculated explicitly. Hossaini et al. (2010) follow a similar approach and test the sensitivity of the amount of bromine reaching the stratosphere on different washout times for Br_y, ranging from 10 days to infinity. Depending on the assumed time constants for washout times, the PGI bromine from CH_2Br_2 and $CHBr_3$ varies between 0.4 ppt (10 days washout) and 1.7 ppt (40 days washout time) and can be as high as 3.9 ppt of bromine if an infinite washout time is assumed. This range of values is consistent with the ranges presented in the previous Assessment (Law and Sturges et al., 2007). Two other recent studies (Aschmann et al., 2009; Liang et al., 2010) have attempted to explicitly calculate the removal processes, based on dehydration processes in the model. Aschmann et al. (2009) used an idealized tracer that has properties similar to $CHBr_3$. The inorganic bromine is either completely removed if dehydration occurs in a grid box or it is not removed at all. They derive a bromine input from this tracer that is between 1.6 and 3 ppt, of which 0.3 ppt is in the form of the SGs. The range in PGI from bromoform is thus between 1.3 and 2.7 ppt. Therefore, even with the assumption of complete solubility and instantaneous washout, only about 50% of the PGs are removed in the TTL in this study. Using the Goddard Earth Observing System (GEOS) chemistry-climate model (version 2) with a detailed wet deposition scheme, Liang et al. (2010) suggest that washout is mainly effective below 500 hectoPascals (hPa) and that virtually all inorganic bromine that is released from the SGs above that level reaches the stratosphere.

These large differences in the effect of washout predicted by models show the high degree of uncertainty in the physical understanding of the removal of inorganic bromine during the transport into the tropical stratosphere. Due to this high level of uncertainty and due to the lack of observations of bromine PG in the TTL, it is not possible to derive a best estimate of the amount of bromine entering the stratosphere in the form of PG. Based on the studies presented above and in previous Assessments, the range of PGI from $CHBr_3$ and CH_2Br_2 is estimated to be between 0.4 and 3.9 ppt. Based on the vertical profiles of other minor bromine source gases, an additional product gases injection from these could range between 0 and 0.3 ppt. Total PGI could thus be somewhere in the range between 0.4 and 4.2 ppt Br.

PGI from Iodinated VSLS

Consistent with the observations presented in the previous Assessment (Law and Sturges et al., 2007), balloonborne measurements using the Differential Optical Absorption Spectroscopy (DOAS) technique have revealed no measurable amount of iodine monoxide (IO) or iodine dioxide (OIO) in the TTL above detection limits of 0.1 ppt (Butz et al., 2009).

1.3.3.3 Total Halogen Input into the Stratosphere from VSLS and Their Degradation Products

As discussed above, both PGI and SGI can contribute halogen to the stratosphere. Here we consider only amounts transported into the stratosphere above the CPT as estimated from the mixing ratios of SGs and PGs at that level and at 15 km (z_0). Since the previous Assessment, additional observations of bromine VSL SGs in the TTL have become available. The halogen contribution from PGs, however, remains much more uncertain. We summarize the available estimates of SGI and PGI for the individual halogens (chlorine, bromine, iodine) in Table 1-9. PG observations are available for chlorine but not for bromine. Therefore, a best estimate of total chlorine input to the stratosphere is derived, based on SG values observed at z_0 and typical values of chlorine PG observed in the TTL. In contrast only a range of possible values is derived for bromine, based on observations at the CPT and modeled PGI. Only upper limits are available for iodine from observations.

Total Input from Chlorinated VSLS

Adding up the entire range of SG and PG observations discussed in Sections 1.3.3.1 and 1.3.3.2 yields a range between 25 and 170 ppt of chlorine from VSLS. For a best estimate of chlorine input into the stratosphere from this range, we use SG observations in the middle of the TTL (at z_0), where VSLS chlorine is 55 (38–80) ppt. It is difficult to assess if chlorine from the PGs HCl and $COCl_2$ represents an additional source or is already taken into account in the source gas budgets. The best estimate is 16 (0–32) ppt of chlorine from $COCl_2$ and 10 (0–20) ppt of HCl (see Section 1.3.3.2). The best estimate values for total VSLS chlorine is thus 80 (40–130) ppt, largely in agreement with the estimate given in the previous Assessment of about 50 ppt of chlorine from SGs and about 40 to 50 ppt chlorine from PGs (taken then to include $COCl_2$ only).

Total Input from Brominated VSLS

In order to avoid double counting, two approaches are used to derive total bromine input from VSLS: (i) the range of possible values of VSLS bromine entering the stratosphere is derived from the range of SG observations at the CPT and the range of modeled PG injections, and (ii) a probable input is derived based on SG observations at z_0, and assuming that PGs produced above that level

Table 1-9. Summary of source gas (SG) and product gas (PG) observations and modeling results to constrain input of halogens from VSLS into the stratosphere. Note that only observations of chlorine-containing PGs exist; estimates of PG amounts for bromine are based solely on modeling studies and only upper limits of iodine-containing PGs are available. For bromine and iodine only ranges can be estimated from this. Details on the way that these numbers have been derived can be found in the Sections 1.3.3.1 (SG), 1.3.3.2 (PG) and 1.3.3.3 (total). All values are given in ppt.

Halogen or Compound	Measured TTL to CPT Abundance (ppt Cl, Br, or I)	"Best Estimate" TTL Abundance (ppt Cl, Br, or I)	"Best Estimate" Contribution from VSLS (ppt Cl, Br, or I)
Chlorine			
VSL SGs	26–80 [a, b]	55 (38–80) [c]	55 (38–80)
HCl PG	0–40 [d]	20 (0–40)	10 (0–20)
$COCl_2$ PG	31 ± 22 to 36 ± 26 [e]	32 (± 22)	16 (0–32)
Total chlorine	25–170 [f]		80 (40–130) [f]
Bromine			
VSL SGs	0.7–6.5 [a, b]	2.7 (1.4–4.6) [a, c]	0.7–3.4 [a, g]
PG sum			0.4–4.2 [h]
Total bromine			1–8 [i, f]
Iodine			
CH_3I SG	< 0.05 [a]	< 0.05 [a]	< 0.05 [a]
IO, OIO PG	< 0.1 [j]	< 0.1 [j]	< 0.1 [j]
Total iodine			< 0.15 [k]

[a] Based on observations compiled in Table 1-7.
[b] Entire range of values observed in TTL and at the CPT, based on Table 1-7.
[c] Value and range at the level of zero clear-sky heating (z_0).
[d] Range of observed values from Marcy et al. (2007), Mebarki et al. (2010), Park et al. (2008).
[e] Fu et al. (2007).
[f] Rounded from the range of sums of PG and SG.
[g] For the best estimate of bromine, only the SG range at the CPT has been used, as modeled PGI would include contributions from all SG broken down at lower altitudes.
[h] Based on modeling work of Hossaini et al. (2010), Aschmann et al. (2009), and Liang et al. (2010); see Section 1.3.3.2.
[i] Calculated from the range of SG observations at the tropical tropopause and the PG modeling range.
[j] Upper limits reported by Butz et al. (2009) for IO and OIO, respectively.
[k] Rounded from Butz et al. (2009), based on observed upper limits of IO and OIO in the lower stratosphere and photochemical modeling.

are transported into the stratosphere, while PGs produced lower in the TTL and upper tropical troposphere have been washed out. Following the first approach, we estimate that a lower limit of 1.1 (0.7 SG and 0.4 PG) ppt of bromine from VSLS is transported into the stratosphere, while our upper limit estimate is 7.6 (3.4 ppt SG and 4.2 ppt PG). Based on the SG observations at z_0 (15 km) (the second method of estimation), it is probable that 2.7 (1.4–4.6) ppt reaches the stratosphere. In summary, by taking into account PGI and SGI the total contribution is estimated to be between 1 and 8 ppt (values rounded). This estimated range is slightly lower than given in the previous Assessment (Law and Sturges et al., 2007), where a contribution of 5 ppt (range 3 to 8 ppt) was estimated, but is well within the respective ranges of uncertainty.

Total Input from Iodinated VSLS

Both SG and PG observations suggest that no significant amount of iodine enters the stratosphere. Butz et

al. (2009) derived an upper limit of 0.09–0.16 ppt of total iodine in the stratosphere from photochemical modeling and the upper limits of IO and OIO from their observations in the tropical lower stratosphere. The total amount of inorganic stratospheric iodine (I_y) is thus estimated to be below 0.15 ppt (Table 1-9).

1.3.4 Potential Influence of VSLS on Ozone

In the previous Assessment (Law and Sturges et al., 2007) a modeling study (Salawitch et al., 2005) was discussed that suggested that 4 to 8 ppt of "additional" stratospheric bromine from VSLS caused enhanced ozone depletion primarily during periods of elevated aerosol loading. Halogens are released efficiently from VSL SGs in the lowermost stratosphere, leading to ozone loss at these altitudes by BrO + ClO catalytic cycles. This process is enhanced in the presence of co-located high aerosol loading of volcanic origin. Law and Sturges et al. (2007) also indicated that iodine-mediated ozone loss due to 0.1 ppt of I_y could only account for at most a few percent of ozone loss and only below about 17 km, depending on the efficiency of catalytic cycles. The associated chemistry remains a matter of significant uncertainty.

More recently Feng et al. (2007) and Sinnhuber et al. (2009) have reported qualitative agreement with the above studies in the sense that additional bromine from VSLS decreased modeled column ozone, but only by a small amount, except during volcanic aerosol events. The two studies, however, produced divergent quantitative column ozone amounts that do not fit all features of the trends at all times, nor do they reproduce absolute column ozone amounts simultaneously in both hemispheres. A detailed discussion of possible reasons for these discrepancies in terms of the respective model setups is beyond the scope of this Assessment, but serves to highlight the uncertainties of such modeling studies.

Sinnhuber et al. (2009) showed better agreement between their modeled trends in column ozone and satellite observations (1980–2005) in the midlatitude SH than in the NH using a two-dimensional (2-D) transport, chemistry, and radiation model. Without additional Br from VSLS, the model follows the larger features of the ozone trend in NH midlatitudes but generally underpredicts the observed declines in column ozone, particularly between 1991 and 1998, which includes a period of high aerosol loading from the 1991 eruption of Mt. Pinatubo. Modeled and measured midlatitude NH ozone depletion for this period of time are, however, in closer agreement when an additional 4 ppt of stratospheric bromine from VSLS are included in the calculations. The addition of 4 ppt of bromine from VSLS enhances modeled ozone loss above that due to all other ODSs by as much as 40% at altitudes below 20 km during the period of peak aerosol loading following the eruption of Mt. Pinatubo (see Figure 1-13). The effect of Br_y from VSLS (Br_y^{VSLS}) on calculated ozone during times of background aerosol loading is quite small, in agreement with the results of Salawitch et al. (2005).

Sinnhuber et al. (2009) also discussed altitudinal profiles of the modeled ozone changes. Figure 1-13 compares calculated ozone abundances during NH spring during a year with high stratospheric aerosol (1993 with 1980 as a reference year). The significant modeled impact of bromine from VSLS is evident and is confined between the tropopause and about 20 km, which is in qualitative agreement with the calculations by Salawitch et al. (2005).

We conclude from these various studies that the addition of 4–6 ppt of inorganic bromine to the stratosphere (i.e., 240–360 ppt of equivalent chlorine using $\alpha = 60$) from VSLS results in a considerable increase in midlatitude column ozone loss during times of elevated aerosol

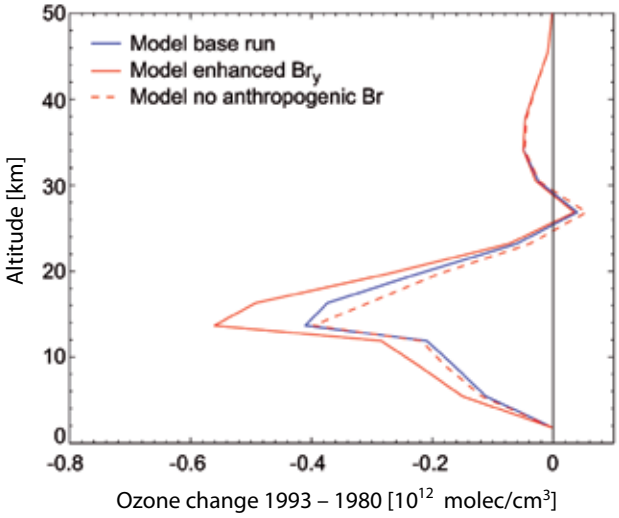

Figure 1-13. Modeled differences between annual mean ozone concentration (molecules per cubic centimeter) calculated for March 1980 and March 1993 at 47°N, illustrating the effect of additional bromine from very short-lived source gases during a period of enhanced stratospheric aerosol (i.e., influenced by the eruption of Mt. Pinatubo in 1991) (Sinnhuber et al., 2009). The base model run (blue line) includes contributions to stratospheric Br_y from CH_3Br, halon-1301, and halon-1211; the solid red model line includes 4 ppt of additional bromine from CH_2Br_2 and $CHBr_3$; and the dashed red line results from the same model run as shown by the solid red line, but with total bromine loading fixed at 1959 levels. Modified from Sinnhuber et al. (2009).

loading, with the largest effect in the lowermost stratosphere (altitudes below ~20 km). To date no analogous study has been undertaken to quantify the effects on ozone of additional chlorine from VSLS, which may amplify the effect on ozone of bromine from VSLS.

1.3.5 The Potential for Changes in Stratospheric Halogen from Naturally Emitted VSLS

As discussed in Section 1.3.4, the current emissions of natural halogenated VSLS have a small but non-negligible impact on the halogen loading in the stratosphere. This situation could change in the future, resulting in a larger role for VSLS in response to factors connected to climate change.

Natural oceanic emissions of VSLS might change in the future in response to changes in climate, as might the efficiency with which VSLS either as SGs or as PGs are transported to the stratosphere. Future oceanic emissions of VSLS will potentially be influenced by changes in seawater temperature, pH, wind speed, mixed layer depth, light penetration, nutrient supply, and depth of biotic production/degradation of trace gases in a potentially more stratified ocean (e.g., Kloster et al., 2007; Schmittner et al., 2008). Hense and Quack (2009) modeled higher $CHBr_3$ emissions in NH winter for the tropical Atlantic Ocean concurrent with a deepening of the mixed layer depth (MLD), enhancing the connection between the zone of subsurface net production and ocean-air transition. For nutrients, diverging effects have been found for different bromocarbons around the Mauritanian Upwelling of West Africa (Quack et al., 2007). Measurements in this region showed that while CH_2Br_2 concentrations were enhanced in colder, nitrogen-enriched and deeper waters, $CHBr_3$ productivity was higher in warmer nutrient-poor waters, with little relationship to chlorophyll *a* abundance. Palmer and Reason (2009), however, found a correlation of elevated $CHBr_3$ concentrations with chlorophyll *a* from the tropical oceans and more surface $CHBr_3$ from waters with a larger MLD. Zhou et al. (2008) found a linear relationship between bromocarbon emissions and wind speeds above 4 meters per second over the ocean, and strong enhancements in air masses recently affected by a tropical storm. Taken together, seasonal MLD deepening and greater wind-driven surface evasion may account for an order of magnitude higher emissions of $CHBr_3$ in winter than summer in tropical oceans (Hense and Quack, 2009; Palmer and Reason, 2009). This leads to the conclusion that if climate change would result in greater amplitudes of MLDs and stronger average wind velocities above the oceans, then future emissions of CH_2Br_2 and $CHBr_3$ could possibly be enhanced, although other factors could either mitigate or enhance such effects (such as deepening of the subsurface production zone).

When assessing the fate of naturally emitted halocarbons in a future atmosphere, two concurring effects have been discussed to be relevant (i.e., changes in transport and in atmospheric degradation). Pyle et al. (2007) and Dessens et al. (2009) modeled higher Br_y in the tropical troposphere and stratosphere by 2100 due to enhanced convection resulting from increased greenhouse gases and sea surface temperatures. This effect, which is mainly attributed to CH_2Br_2 (>90%), and secondarily to $CHBr_3$ was, however, only obtained if VSLS were allowed to be emitted in the tropics (20°N–20°S). Placing the emissions outside the tropics resulted in no enhancement of stratospheric Br_y, as the VSLS species were largely oxidized before injection into the stratosphere. This underlines the crucial influence of the geographic location of sources of VSLS on their impact on the stratosphere.

These projections for atmospheric transport in a warmer climate are, however, still under discussion, as other models simulate a weakening of the tropospheric circulation and convective updrafts in the tropics in the future (e.g., Vecchi and Soden, 2007). Furthermore, Zeng et al. (2008) indicate OH increases in a simulation of 2100 conditions, with the largest increases of 20–30% in the tropics between 3 and 8 km (although some decreases occurred in the boundary layer and upper troposphere due to decreased ozone in these regions). This would likely affect those VSLS species with predominantly OH-oxidation sinks (including CH_2Br_2) but would have little effect on those with predominantly photolysis-limited lifetimes (i.e., $CHBr_3$).

1.3.6 Environmental Impacts of Anthropogenic VSLS, Substitutes for Long-Lived ODSs, and HFCs

Anthropogenic emissions of VSLS can either occur by intensifying natural processes (e.g., agriculture, biomass burning) or by release after industrial production of VSLS. This section covers the potential future influence of both types of emissions. Furthermore, environmental impacts of non-ozone depleting VSLS being considered as substitutes for long-lived HFCs are also discussed in this section.

1.3.6.1 Evaluation of the Impact of Intensified Natural Processes on Stratospheric Ozone

There are a number of ways in which human activity might intensify emissions of otherwise naturally

occurring VSLS. An area of high potential impact is changes in agriculture practices. It is noted in Section 1.2.1.5 that some crops are capable of producing methyl halides. For VSLS, anticipated increases of future rice production in the tropics (Bhatia et al., 2010) could be important, as rice cultivation is known to emit considerable amounts of CH_3I (e.g., Lee-Taylor and Redeker, 2005). Furthermore, Gan et al. (1998) and Rhew et al. (2003) reported that emissions of methyl halides from halogen-methylating plants are strongly linked to the halide content of the growth substrate. With increasing salinization of soils through irrigation, coastal inundation, or deliberate cultivation of poorer soils, emissions might increase in the future. This issue is emphasized by the finding of Sive et al. (2007) that fluxes of CH_3I from terrestrial biomes over the eastern U.S. are presently comparable with oceanic sources over the Atlantic. Another possible impact from future agriculture would be the aquaculture of marine algae for food, chemicals, biofuel, and for sequestering atmospheric carbon (Packer, 2009; Aizawa et al., 2007). Furthermore, water chlorination, both of drinking water and domestic wastewater, and also seawater coolant in coastal power plants may contribute small amounts of halogen to the stratosphere and this contribution could change in the future, but no new information has become available since the previous Assessment concerning these potential contributions.

1.3.6.2 Very Short-Lived New ODSs and Their Potential Influence on Stratospheric Halogen

Chlorocarbons such as CCl_2CCl_2 (perchloroethene) and $CHClCCl_2$ (trichloroethene) have been used for many decades in large quantities as industrial solvents. Additionally, new very short-lived chlorocarbons, bromocarbons, and iodocarbons (with lifetimes <0.5 years) have recently been introduced or are proposed as potential substitutes for long-lived ODSs. The pathways and reactions by which halogens from these anthropogenic VSLS reach the stratosphere are similar to those of natural compounds, such as CH_2Br_2 and $CHBr_3$, as discussed in Sections 1.3.2-1.3.3. These anthropogenic VSLS are considered separately from the long-lived ODS, as the traditional concept of a single, geographical independent Ozone Depletion Potential (ODP) does not apply and their impact depends on the location and season of emissions.

The issue of ODPs for short-lived ODSs has already been discussed for n-propyl bromide and CF_3I in the previous two Assessments (Ko and Poulet et al., 2003; Law and Sturges et al., 2007). For $CHCl_3$, CCl_2CCl_2, and $CHClCCl_2$, Kindler et al. (1995) have derived mean, semi-empirical ODPs of 0.008–0.01, 0.006–0.007, and 0.0005–0.0007, respectively, based on a 2-D modeling analysis and source gas atmospheric distributions that are similar to those observed. Furthermore, in Law and Sturges et al. (2007) it was estimated that 1% of uniformly distributed land mass emissions of a theoretical VSLS with a tropospheric lifetime of 25 days would reach the stratosphere. Consequently the ODP of such a compound with one chlorine atom and similar molecular weight to CFC-11 has been calculated as being about 0.003. This approach, however, neglects the issue of the ODP being sensitive to the location and seasonality of emission.

Wuebbles et al. (2009) updated an earlier 2-D model approach of Li et al. (2006) to calculate the ODPs for CF_3I by using a 3-D global chemical transport model (CTM). An ODP of 0.016 and 0.008 is calculated for CF_3I surface emissions in the tropics and in the midlatitudes, respectively, which compares well with the earlier ODP-values from Li et al. (2006) of 0.018 and 0.011 for CF_3I released in the tropics and in the midlatitudes, respectively. These new figures confirm the higher probability of VSLS released in the tropics reaching the stratosphere, which results in higher ODPs for VSLS released near the equator. In the last Assessment (Law and Sturges et al., 2007) it was also noted that ODPs are dependent upon the altitude of emission, which would be relevant if CF_3I were used on aircraft as a replacement for halons. However, no update on this is available.

1.3.6.3 Evaluation of Potential and In-Use Substitutes for Long-Lived ODSs

A wide range of chemicals with zero or near-zero ODPs and low GWPs are currently being considered as substitutes for ODSs and long-lived HFCs. In Table 1-10, atmospheric lifetimes of substitutes that are already in use or potentially could be used in applications such as refrigeration, foam blowing, fire control, propellants, and solvents are listed. The list is not restricted to VSLS because many longer-lived HFCs are in use or are being considered as ODS replacements.

In Table 1-11, substitutes that are already in use or have been identified as most likely to be used in the near future are listed together with their applications, potential feedstocks and atmospheric lifetime. Furthermore, metrics of environmental effects such as GWP, Photochemical Ozone Creation Potential (POCP), and trifluoroacetic acid (TFA) formation are specified. For reasons of completeness and to link with the issue of global warming and climate change, fluorinated substances are also listed that are not ODS substitutes in the strictest sense (i.e., NF_3, hexafluorobutadiene, COF_2).

Hydrocarbons receive use as ODS substitutes in refrigeration and foam blowing applications. They do not deplete stratospheric ozone and they have very small GWPs. However, the oxidation of hydrocarbons

Table 1-10. Local and partial lifetimes of in-use and potential replacement compounds for long-lived ODSs (long-lived substitutes in italics).

Compound	Local Lifetime from Previous Assessment (days)	OH Lifetime (days)	Photolysis Lifetime (days)	New Local Lifetime (days)	Notes
Hydrocarbons					
CH_2=$CHCH_3$ (propene)	0.37	0.35		0.35	1, 5
$(CH_3)_2C$=CH_2 (isobutene)		0.20		0.20	1, 5
$CH_3CH_2CH_3$ (propane, R-600)		12.5		12.5	1, 3
$(CH_3)_2CHCH_3$ (isobutane, R-600a)		6.0		6.0	1, 5
$CH_3CH_2CH_2CH_2CH_3$ (n-pentane)	3.7	3.4		3.4	1, 6
c-$CH_2CH_2CH_2CH_2CH_2$ (cyclopentane)	2.9	2.7		2.7	1, 6
$(CH_3)_2CHCH_2CH_3$ isopentane	3.7	3.4		3.4	1, 6
CH_3OCHO (methyl formate)	58	72		72	1, 7
$(CH_3)_2CHOH$ (isopropanol)	4.8	2.0		2.0	1, 3
$CH_3OCH_2OCH_3$ (methylal)		2.2		2.2	1, 8
Hydrofluorocarbons					
CH_3CH_2F (HFC-161)	77	66		66	1, 3
CH_2FCH_2F (HFC-152)	219	146		146	1, 4
CH_3CHFCH_3 (HFC-281ea)	22	23		23	1, 3
$CHF_2CH_2CF_3$ (HFC-245fa)	*7.6 years*	*8.2 years*	*116 years*	*7.7 years*	*2, 3, 9*
$CH_3CF_2CH_2CF_3$ (HFC-365mfc)	*8.6 years*	*9.3 years*	*125 years*	*8.7 years*	*2, 3, 9*
CHF_2CHF_2 (HFC-134)	*9.6 years*	*10.5 years*	*134 years*	*9.7 years*	*2, 3, 9*
CF_3CHFCF_3 (HFC-227ea)	*34.2 years*	*44.5 years*	*310 years*	*38.9 years*	*2, 4, 9*
$CF_3CH_2CF_3$ (HFC-236fa)	*240 years*	*253 years*	*5676 years*	*242 years*	*2, 3, 9*
Unsaturated Fluorocarbons					
CH_2=CHF		2.1		2.1	1, 4
CH_2=CF_2		4.0		4.0	1, 4
CF_2=CF_2		1.1		1.1	1, 4
CH_2=$CHCH_2F$		0.7		0.7	1, 4
CH_2=$CHCF_3$		7.6		7.6	1, 4
CH_2=$CFCF_3$		10.5		10.5	1, 4
E-CF_3CH=CHF		16.4		16.4	1, 4
E-CF_3CF=CHF		4.9		4.9	1, 4
Z-CF_3CF=CHF		8.5		8.5	1, 4
CF_2=$CFCF_3$		4.9		4.9	1, 4
CH_2=$CHCF_2CF_3$		7.9		7.9	1, 4
CF_2=$CFCF$=CF_2		1.1		1.1	1, 10
Unsaturated Chlorocarbons					
E-CF_3CH=$CHCl$		26		26	1, 11
CH_2=$CHCl$		1.5		1.5	1, 4

Table 1-10, continued.

Compound	Local Lifetime from Previous Assessment (days)	OH Lifetime (days)	Photolysis Lifetime (days)	New Local Lifetime (days)	Notes
$CH_2=CCl_2$		0.9		0.9	1, 4
$CHCl=CCl_2$	4.6	4.9	> 15000	4.9	1, 4, 21
$CCl_2=CCl_2$	99	90		90	1, 4
$CF_2=CFCl$		1.4		1.4	1, 12
$CF_2=CFCF_2Cl$		~ 5		~ 5	1, 13
$CF_2=CFCF_2CFCl_2$		~ 5		~ 5	1, 13
Unsaturated Bromocarbons					
$CFBr=CF_2$		1.4		1.4	1, 14
$CHBr=CF_2$		2.3		2.3	1, 14
$CH_2=CBrCF_3$		2.7		2.7	1, 14
$CH_2=CBrCF_2CF_3$		3.1		3.1	1, 14
$CH_2=CHCF_2CF_2Br$		6.5		6.5	1, 14
Fluorinated Ethers, HFE					
$CH_3OCH_2CF_3$ (HFE-263fb2)	37	23		23	1, 15, 17
$CH_3OCHFCF_3$ (HFE-254eb2)		88		88	1, 4
$CH_3OCH_2CF_2CF_3$	40	21		21	1, 16, 17
$CH_3CH_2OCF_2CHF_2$	1826 (error)	64		64	1, 4
$CF_3CH_2OCH_2CF_3$	146	105		105	1, 4
$CH_3OCH(CF_3)_2$		61		61	1, 18
Fluorinated Ketones					
$CF_3CF_2C(O)CF(CF_3)_2$ (FK-5-1-12)	< 14	> 63 years	7–14	7–14	19
Fluorinated Alcohols					
CH_2FCH_2OH	15	12.9		12.9	1, 4
CHF_2CH_2OH		51		51	1, 4
CF_3CH_2OH	150	142		142	1, 4
$C_2F_5CH_2OH$	142	143		143	1, 4
$C_4F_9CH_2OH$	164	142		142	1, 4
$CF_3CHFCF_2CH_2OH$	124	112		112	1, 5
Special Compounds					
$CF_3CF_2CF_2I$ (1-iodo-heptafluoropropane)			< 2	< 2	20
CH_3I (methyl iodide)	7	158	7 (4–12)	7	1, 5, 21, 22
COF_2 (carbonyl fluoride)				5–10	27
PBr_3	< 0.01	0.14		< 0.01	22, 23
NH_3	Few days	93		Few days	1, 3, 24
SO_2F_2 (sulfuryl fluoride)		*> 300 years*	*630 years*	*36 years*	*9, 25*
NF_3	*740 years*			*500 years*	*26*
CH_3CH_2Br (bromoethane)	34	41		41	1, 3

Table 1-10, continued (notes).

Notes:

1. These local OH lifetimes are calculated using an average tropospheric OH concentration of 1×10^6 molecule/cm^3 and the OH reaction rate constant at T = 275 K. Local lifetimes quoted here are not meant to be estimates of global lifetimes, which, for short-lived gases depend on the emission location and season as well as local atmospheric conditions. The concept of a single global lifetime, ODP, or GWP is inappropriate for such short-lived gases.
2. Lifetimes for long-lived compounds with respect to reaction with tropospheric OH calculated relative to 6.1 years for CH_3CCl_3, assuming an average temperature of 272 K (Spivakovsky et al., 2000; Prather and Ehhalt et al., 2001).
3. OH reaction rate constant taken from JPL 06-2.
4. OH reaction rate constant taken from JPL 10-6. JPL 10-6 is cited here whenever there is a change in a rate constant recommendation or the accompanying note. It does not necessarily mean that a major change was recommended for a rate constant. Nevertheless, updates in JPL 10-6 reflect improved kinetic understanding.
5. OH reaction rate constant taken from Atkinson et al. (2008).
6. OH reaction rate constant taken from Calvert et al. (2008).
7. OH reaction rate constant taken from Le Calvé et al. (1997).
8. OH reaction rate constant taken from Porter et al. (1997).
9. Lifetime shown in "Photolysis Lifetime" column corresponds to the overall stratospheric lifetime. See Table 1-3.
10. OH reaction rate constant taken from Acerboni et al. (2001).
11. OH reaction rate constant taken from Sulbaek Andersen et al. (2008).
12. OH reaction rate constant taken from Abbatt and Anderson (1991).
13. Local lifetime estimated as similar to that of $CF_3CF=CF_2$.
14. OH reaction rate constant taken from Orkin et al. (2002).
15. OH reaction rate constant taken from Oyaro et al. (2005).
16. OH reaction rate constant taken from Oyaro et al. (2004).
17. Room temperature data only; OH reaction lifetime calculated assuming a temperature dependence (E/R) of 500 K.
18. OH reaction rate constant from Chen et al. (2005b).
19. Lifetimes taken from Taniguchi et al. (2003).
20. Photolysis lifetime estimated from comparison of UV spectra and lifetimes for CF_3I and $CF_3CF_2CF_2I$.
21. Photolysis lifetime taken from Table 2-4 in Ko and Poulet et al. (2003).
22. Local lifetime taken from Table 2-1 in Law and Sturges et al. (2007).
23. OH reaction rate constant taken from Jourdain et al. (1982). Local lifetime is probably dictated by photolysis.
24. Local lifetime taken from IPCC/TEAP (2005); it is dictated by washout rates (see Box 1-4).
25. From Papadimitriou et al. (2008b) and Mühle et al. (2009). The total lifetime is primarily due to ocean uptake.
26. From Prather and Hsu (2008) with the lifetimes recalculated using the JPL 06-2 recommended rate constants for the $O(^1D)$ reactions corrected for the deactivation channel (see also Section 1.2.2).
27. Local lifetime taken from Wallington et al. (1994).

Table 1-11. Applications, feedstocks, and environmental impact of in-use and likely potential future ODS-substitutes (long-lived substitutes in italics).

Compound	Application	Feedstock	Lifetime [1]	POCP [2,3,4]	GWP_{100} [5]	TFA molar yield
Hydrocarbons						
propene, $CH_3CH=CH_2$ (HC1270)	refrigerant	petroleum	0.35 d	117 [2]	5 [6,7]	0%
isopentane, $(CH_3)_2CHCH_2CH_3$	foams (replacing CFC-11 and HCFC-141b)	petroleum/ natural gas	3.4 d	34 [2]		0%
cyclopentane, c-$CH_2CH_2C_2CH_2CH_2$	foams (replacing CFC-11 and HCFC-141b)	natural gas	2.7 d	51 [3]		0%
n-pentane, $CH_3CH_2CH_2CH_2CH_3$	foams (replacing CFC-11 and HCFC-141b)	petroleum/ natural gas	3.4 d	40 [2]		0%
isobutene, $(CH_3)_2C=CH_2$	foams (replacing CFC-12)	petroleum	0.2 d	75 [2]		0%
methylal, $CH_3OCH_2OCH_3$	foams (replacing CFC-11 and HCFC-141b)	methanol	2.2 d	32 [3]		0%
methyl formate, CH_3OCHO	foams (replacing HCFCs)	methanol/ formic acid	72 d	3 [2]		0%
Hydrofluorocarbons						
HFC-245fa, $CHF_2CH_2CF_3$	*foams (replacing HCFCs)*	*$HF + CCl_4 + CH_2=CHCl$*	*7.7 y*	*0.1* [3]	*1050*	*< 10%* [8,9]
HFC-365mfc, $CH_3CF_2CH_2CF_3$	*foams (replacing HCFCs)*	*$HF + CCl_4 + CH_2=CClCH_3$*	*8.7 y*	*0.1* [3]	*842*	*< 10%* [9,10]
HFC-227ea, CF_3CHFCF_3	*propellant for CFC-12 and firefighting for halon-1301*	*$HF + CHCl_3 \rightarrow CHClF_2 \rightarrow CF_3CF=CF_2$*	*39 y*	*< 0.1* [3]	*3580*	*100%* [11]
HFC-236fa, $CF_3CH_2CF_3$	*firefighting for halon-1211/1301 (civil aviation); refrigerant*	*$HF + CCl_4 + CH_2=CCl_2$*	*242 y*	*< 0.1* [3]	*9820*	*< 10%* [12]
Unsaturated Fluorocarbons						
trans-HFC-1234ze, trans-$CF_3CH=CHF$	foams (for CFC-12)	a) $CHCl_3 + HF \rightarrow CHClF_2 \rightarrow CF_3CF=CF_2 \rightarrow CF_3CHFCH_2F$ or b) HFC-245fa	16.4 d	6.4 [4]	7 [6,13]	< 10% [14,9]
HFC-1234yf, $CF_3CF=CH_2$	refrigerant potentially for replacing HFC-134a	$CHCl_3 + HF \rightarrow CHClF_2 \rightarrow CF_3CF=CF_2 \rightarrow CF_3CHFCH_2F$	10.5 d	7.0 [4]	4 [6,15]	100% [16,17]
Fluorinated Ketones						
FK-5-1-12, $CF_3CF_2C(O)CF(CF_3)_2$	halon-1301 replacement	C_3F_6 C_2F_5COF	7-14 d			< 10% [18]

Table 1-11, continued.

Compound	Application	Feedstock	Lifetime [1]	POCP [2,3,4]	GWP_{100} [5]	TFA molar yield
Special Compounds						
ammonia, NH_3	CFC replacement in refrigeration	$N_2 + H_2$	few days	NA		0%
1-iodo-heptafluoropropane, $CF_3CF_2CF_2I$	halon replacement (in Russia: -2402 and/or -1301)	$CF_3I + C_2F_4$	< 2 d	NA		< 10% [18]
bromoethane, CH_3CH_2Br	solvent and part of halon-2402 blend	a) $HBr + C_2H_4$ or b) $HBr + CH_3CH_2OH$	41 d	4.2 [3]		0%
2-bromo-3,3,3-trifluoroprop-1-ene, $CH_2=CBrCF_3$	halon-1211 replacement	$CH_2=CHCF_3$	2.7 d	9.3 [3]		< 10% [19, 9]
methyl iodide, CH_3I	CH_3Br replacement	CH_3OH / I_2	7 d	1.0 [3]		0%
sulfuryl fluoride, SO_2F_2	*CH_3Br replacement*	*$KF + SO_2F_2$*	*36 y* [20]	*NA*	*4740* [21]	*0%*
NF_3	*etchant to replace C_2F_6*	*a) $NH_3 + F_2$ or b) $(NH_4)HF_2$*	*500 y* [22]	*NA*	*17,500*	*0%*
hexafluorobutadiene	etchant		1.1 d	10 [3]		0%
carbonyl fluoride, COF_2	etchant	a) $CO_2 + F_2$ or b) Oxidation of C_2F_4	5–10 d	NA		0%

Notes:

1. See Table 1-10 for notes on lifetime derivations.
2. Derwent et al. (2007).
3. No value for the POCP (Photochemical Ozone Creation Potential) of this substance has been published by full trajectory analyses. This value was calculated based on information from Derwent et al. (1998) and Jenkin (1998), using the method that Wallington et al. (2010) used for unsaturated HFCs. The derived POCP is an approximation and is related to the molecular structure of the compound and its OH-reactivity. The calculations were only conducted for species lost mainly through OH-radical reactions, others are declared as NA (not available). .
4. Wallington et al. (2010).
5. GWPs from Chapter 5 Appendix (Table 5A.1) if not specified differently.
6. GWPs are generally calculated assuming a uniform global distribution of the trace gas. Hence, such methods are in principal not accurate for short-lived gases (i.e., gases with atmospheric lifetime shorter than about 0.5 years) because the atmospheric distribution of short-lived gases will likely be non-uniform and will also depend upon the location and season of emission. Thus, GWPs calculated in this way for short-lived gases provide only a very rough measure of the time-integrated radiative effect of these gases.
7. This value represents an indirect GWP (100-year), derived with a global three-dimensional Lagrangian model (Collins et al., 2002) and an emission distribution related to fossil-fuel use. The indirect GWP includes influences on the abundance of methane (through changes in OH), tropospheric ozone, and on CO_2.
8. The oxidation of HFC-245fa gives CF_3CHO as a major product (Chen et al., 1997).
9. Photolysis is the main fate of CF_3CHO (lifetime of approximately 19 hours in lower troposphere for overhead Sun; Calvert et al., 2008) and this does not give TFA. Reactions with water (Sulbaek Andersen et al., 2006) or OH radicals are minor losses of CF_3CHO and can lead to TFA (Hurley et al., 2006). The yield of TFA is estimated to be <10%.
10. The oxidation of HFC-365mfc gives CF_3CHO and COF_2 as major products (Inoue et al., 2008).
11. Zellner et al. (1994).
12. The oxidation of HFC-236fa gives $CF_3C(O)CF_3$ (Møgelberg et al., 1995). Photolysis is the main fate of $CF_3C(O)CF_3$ (lifetime of approximately 6.2 days in lower troposphere for overhead Sun; Calvert et al., 2008). The photolysis of $CF_3C(O)CF_3$ will give CF_3CO radicals, a small fraction of which

Table 1-11, continued.

can react further to give TFA (Hurley et al., 2006). The molar yield of TFA from the atmospheric oxidation of HFC-236fa is estimated to be <10%.
13. This direct GWP (Orkin et al., 2010) was calculated using a semi-empirical approach with the revised lifetime of 16.4 days given in Table 1-10 but without accounting for inhomogeneous emission and atmospheric mixing ratio distributions.
14. Søndergaard et al. (2007); Javadi et al. (2008).
15. This direct GWP is from Papadimitriou et al. (2008a) and Orkin et al. (2010) and was calculated with the revised lifetime of 10.5 days given in Table 1-10 but without accounting for inhomogeneous emission and atmospheric mixing ratio distributions.
16. Nielsen et al., 2007.
17. Hurley et al., 2008.
18. Photolysis will lead to the formation of C_2F_5 radicals. Approximately 1-10% of C_xF_{2x+1} radicals are converted in the atmosphere into $C_{x-1}F_{2x-1}C(O)F$ (Wallington et al., 2006). The sole atmospheric fate of the 1-10% $CF_3C(O)F$ produced is hydrolysis to give TFA.
19. The atmospheric oxidation of $CF_3CBr{=}CH_2$ is believed to give $CF_3C(OH){=}CH_2$ and/or $CF_3C(O)CH_2OH$ (Orkin et al., 2002; Sulbaek Andersen et al., 2009a). Further oxidation will likely give CF_3CHO.
20. Mühle et al. (2009).
21. Derived from Papadimitriou et al. (2008b) with a radiative efficiency rounded to two decimal places (0.22 W/m^{2}ppb versus 0.222 W/m^{2}ppb) used in Papadimitriou et al. (2008b) (see Chapter 5).
22. See Table 1-10, footnote 26.

in the presence of elevated nitrogen oxides (NO_x) leads to the formation of carbon dioxide (CO_2) (e.g., Collins et al., 2002) and can contribute to the production of tropospheric ozone, which indirectly affects atmospheric levels of methane (CH_4). POCPs are used to assess the relative efficiency of hydrocarbon species for forming tropospheric ozone. POCPs, expressed relatively to ethene (POCP = 100), are shown in Table 1-11 and have either been taken from Derwent et al. (2007) or Wallington et al. (2010) or have been calculated using the method of Derwent et al. (1998) and Jenkin (1998) (specified for unsaturated HFCs by Wallington et al., 2010). While this methodology provides a rough estimate of POCPs for trace gases that are predominately destroyed by atmospheric oxidation, its application to species for which photolysis and hydrolysis are dominant loss processes is not valid.

POCPs are lower for saturated hydrocarbons, typically used as refrigerants and for foam blowing (i.e., propane, isobutane, pentanes), but higher for the alkenes (propene, isobutene). Although releases associated with refrigeration are minor in comparison to hydrocarbon emissions from traffic and solvent usage, the combined impact of these hydrocarbons could be non-negligible, especially in already polluted regions. For the HFCs and other compounds discussed as substitutes in Table 1-11, the POCP values are generally smaller than 10 and hence their relevance for the formation of tropospheric ozone will be very small.

The unsaturated halocarbons (halogenated alkenes) contain a C=C double bond that makes them readily susceptible to degradation by OH (and ozone (O_3)). As a result, their atmospheric lifetimes are typically days to weeks. This group of compounds can be further divided into unsaturated HFCs (sometimes referred to as hydrofluoro-olefins, HFOs) and chloro- and bromoalkenes. Unsaturated HFCs are being considered as potential replacements for ODSs and HFCs in mobile air conditioners and for foam blowing, as they typically have smaller GWPs than saturated (long-lived) HFCs. These smaller GWPs are partially offset for these unsaturated compounds by the production of tropospheric ozone, a strong greenhouse gas.

Chlorinated and brominated alkenes also have short lifetimes but still can have non-negligible ODPs (e.g., Kindler et al., 1995). Chlorinated alkenes such as CCl_2CCl_2 (perchloroethene) and $CHClCCl_2$ (trichloroethene) have been used in large quantities for decades as industrial solvents and a certain amount of this chlorine reaches the stratosphere as a result of use of these gases (see Section 1.3.3.1).

Oxygenated fluorocarbons are another group of ODS replacement compounds with lifetimes typically spanning days to months (Table 1-10 and Table 1-11). In fact a number of fluorinated ethers (e.g., HFE-7100, HFE-7200) have been already used as first-generation ODS substitutes in niche applications such as refrigerants, as solvents, and as heat transfer fluids, but no information about their atmospheric abundance is available.

The atmospheric degradation of (saturated and unsaturated) HFCs and oxygenated fluorocarbons is initiated by their reaction with OH radicals or O_3, (important only for unsaturated HFCs). The oxygenated products from these reactions are removed from the atmosphere via deposition and washout processes and may accumulate in oceans, lakes, and other reservoirs. A potential toxic by-product of the atmospheric degradation of fluorocarbons with CF_3 groups is trifluoroacetic acid (TFA; $CF_3C(O)OH$). Yields of TFA from the degradation of different HFCs are included in Table 1-11. TFA is removed from the atmosphere by wet deposition but is known to accumulate in certain ecosystems. However, much uncertainty remains

in understanding the processes involved in maintaining measured abundances of TFA in the today's aquatic environments. Whereas average TFA concentrations of 200 nanograms per liter in deep ocean waters suggest natural sources in the ocean (Frank et al., 2002), TFA levels were below detection in old ice core and groundwater samples (Nielsen et al., 2001).

At present HFC-134a (CF_3CH_2F) is the HFC that contributes the most TFA to the environment among ODS replacement gases. With global emissions of 149±27 Gg/yr in 2008 (Section 1.5) and a TFA yield of 7–20% (Figure 1-14; Wallington, 1996), a current yearly global input of 9–35 Gg/yr of TFA can be derived from HFC-134a. The unsaturated HFC-1234yf ($CF_3CF=CH_2$) is being considered as a replacement for HFC-134a in mobile air conditioners (Hurley et al., 2008). The TFA production yield of the atmospheric degradation of HFC-1234yf is 100% (Hurley et al., 2008; Figure 1-14; Table 1-11). The use of HFC-1234yf has the potential to influence TFA concentrations near the source regions to a greater extent than HFC-134a, owing to its shorter lifetime and its higher efficiency to produce TFA. A recent modeling study has shown that deposition of TFA could average 0.16–0.24 kg/km^2 by 2017 in the continental U.S. from the full adoption of HFC-1234yf in mobile air conditioners, and that concentrations of TFA in Eastern U.S. rainfall would more than double as a result in comparison to today's values (Luecken et al., 2010).

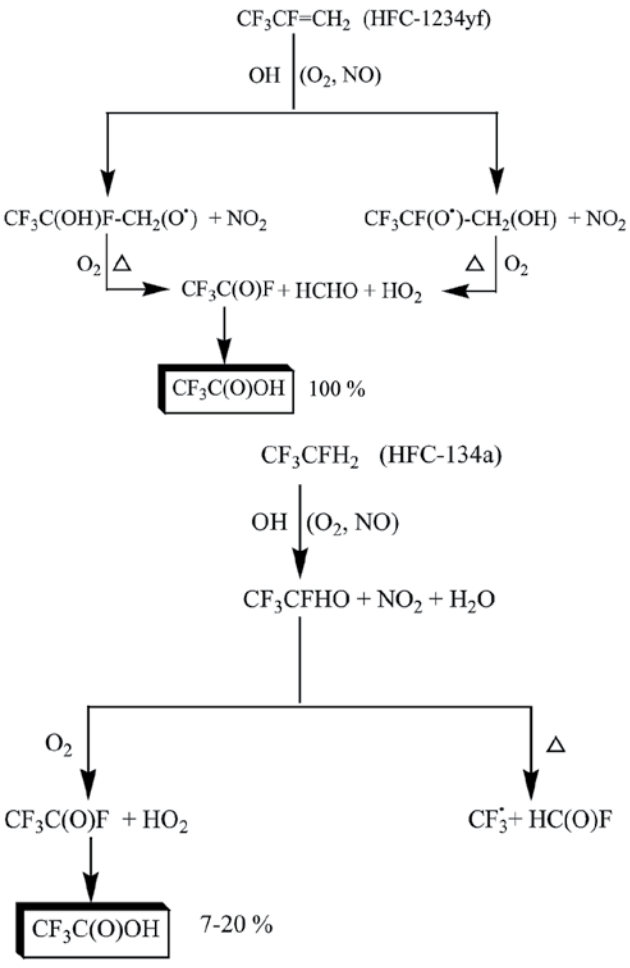

Figure 1-14. Degradation scheme of HFC-1234yf (yielding 100% TFA; $CF_3C(O)OH$) and of HFC-134a (yielding 7–20% TFA) (Wallington et al., 1996; Hurley et al., 2008).

Apart from TFA, monofluoroacetic acid (MFA) and difluoroacetic acid (DFA) could potentially be produced in the degradation of HFCs. MFA and DFA have been measured in the atmosphere and their environmental occurrence has been discussed, for example by Römpp et al. (2001) and Martin et al. (2003).

Replacements for halons (firefighting) and CH_3Br (agriculture) are also being sought. Whereas for halons various substitutes are being considered for different applications, SO_2F_2 is specifically considered as an important replacement for CH_3Br (see also Section 1.5.2.2). This compound is, however, toxic to humans and has a longer atmospheric lifetime (36 years) than CH_3Br (Papadimitriou et al., 2008b).

Ammonia (NH_3) used as a replacement in refrigeration could potentially influence the tropospheric particle loading via its reaction with nitric acid (HNO_3) to form ammonium nitrate (NH_4NO_3). However, emissions from in-use systems are negligible compared to NH_3 emitted from agriculture and natural sources.

Nitrogen trifluoride (NF_3), hexafluorobutadiene, and carbonyl fluoride (COF_2) can be used as substitutes for the extremely long-lived perfluorocarbons (PFC) as etchants in the electronics industry. In fact, NF_3 has already become an important chemical for silicon etching, e.g., in the production of flat computer and television screens (see also Section 1.5), though it has a long lifetime of 500 years and a high GWP_{100} of 17,500 (Chapter 5).

Finally, information on feedstock for the production of many substitutes is provided in Table 1-11. As different production methods exist for specific molecules, this list is not exhaustive, but it is meant to serve as a starting point for a discussion of emission that could potentially arise during production of substitute chemicals. Although emissions to the atmosphere during production are believed to be generally small, a possible pathway of ODSs to the atmosphere could be the production of HFCs, which can include the reaction of carbon tetrachloride (CCl_4) with chlorinated alkenes and subsequent replacement of the Cl-atoms with fluorine (see also the discussion on CCl_4 in Section 1.2.1.3).

1.4 CHANGES IN ATMOSPHERIC HALOGEN

1.4.1 Chlorine in the Troposphere and Stratosphere

1.4.1.1 Tropospheric Chlorine Changes

Total organic chlorine from long-lived gases reached its peak in the troposphere at 3660 ± 23 ppt between 1992 and 1994 and has since declined. While this peak value includes 80 ppt from VSLS, the quoted error encompasses only the difference in total Cl determined from two different sampling networks and not uncertainties related to the contribution of Cl from VSLS (see Section 1.3). By mid-2008, tropospheric organic Cl from long-lived gases had declined by 8.4% from its peak to a value of 3352 ± 4 ppt (Table 1-12 and Figure 1-15). The main drivers behind this decline have changed over time. Methyl chloroform (CH_3CCl_3) now contributes much less to the decline in total Cl than it did in the mid-1990s and early 2000s. This is because the global tropospheric mixing ratio of CH_3CCl_3 has declined substantially: by 2008 it accounted for 32 ± 1 ppt of Cl, or only 1%, of tropospheric Cl (Table 1-12). As a result, declines in Cl from CH_3CCl_3 have become less important to total Cl changes and this influence will continue to diminish in the future.

As the influence of CH_3CCl_3 on tropospheric Cl changes has diminished, declines in tropospheric Cl have slowed. Tropospheric chlorine from long-lived gases changed at a rate of −14 ppt Cl/yr (−0.42%/yr) during 2007–2008, compared to −21 ppt/yr during 2003–2004, and was slower than the change of −23 ppt/yr projected for 2007–2008 in the A1 (most likely, or baseline) scenario of the previous Assessment. The decline observed during 2007–2008 was also about half as rapid as measured in 1995–1996 (−28 ppt Cl/yr or −0.8%/yr; Clerbaux and Cunnold et al., 2007) (Table 1-12). For reference, the mean annual rate of change in tropospheric Cl from long-lived gases averaged over 1996–2008 was −0.6(± 0.05)%/yr in data from the NOAA or AGAGE global sampling networks.

The decline in tropospheric Cl has also slowed recently because of increases observed in the accumulation rate of hydrochlorofluorocarbons (HCFCs) since 2004 (Table 1-12). By 2008, Cl from HCFCs was increasing at a faster rate (10.6 ppt Cl/yr) than had been observed in 2000 and 2004 and Cl from HCFCs accounted for 251 ± 3 ppt Cl, or 7.5% of total tropospheric chlorine.

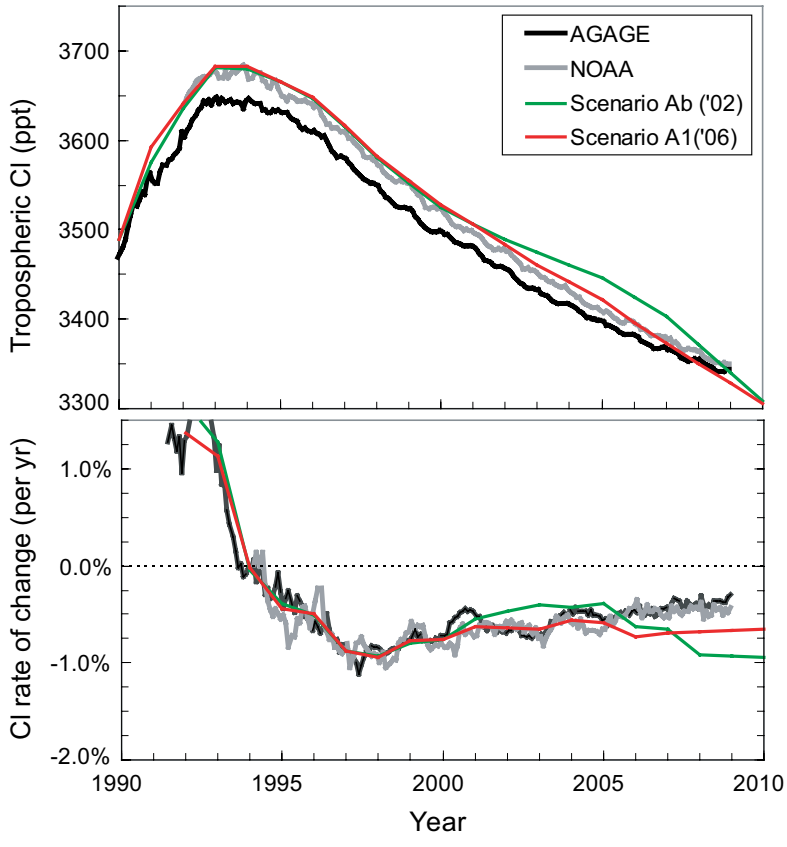

Figure 1-15. Top panel: The tropospheric abundance (ppt) of organic chlorine (CCl_y) from the NOAA (gray) and AGAGE (black) global measurement networks (updates of Montzka et al., 2003, and O'Doherty et al., 2004). Quantities are based upon independently measured mixing ratios of CFC-11, CFC-12, CFC-113, HCFC-22, HCFC-141b, HCFC-142b, methyl chloroform, carbon tetrachloride, and halon-1211. Results for CFC-114 and CFC-115 from Prinn et al. (2000) are used in both aggregations. An additional constant 550 ppt was added for CH_3Cl and 80 ppt was added for short-lived gases such as CH_2Cl_2, $CHCl_3$, CCl_2CCl_2, and $COCl_2$ (consistent with 40–130 ppt discussed in Section 1.3). Bottom panel: Annual rates of change (% per year) determined from 12-month differences. In both panels, observations are compared with the baseline scenario (Ab) from WMO 2002 (green line; Montzka and Fraser et al., 2003) and the baseline scenario A1 from WMO 2006 (red line; Daniel and Velders et al., 2007).

Table 1-12. Contributions of halocarbons to total chlorine in the troposphere.

	Total Cl * (ppt Cl)			Contribution to Total Cl (%)			Rate of Change in Total Cl ** (ppt Cl / yr)		
	Mid-2000	Mid-2004	Mid-2008	Mid-2000	Mid-2004	Mid-2008	2000	2004	2008
All CFCs	2154	2123	2076 (3)	61%	62%	62%	−1.9 (1.9)	−9.4 (2.0)	−13.2 (0.8)
CCl_4	392	377	359 (6)	11.2%	11.0%	10.7%	−4.0 (0.7)	−4.0 (0.6)	−5.1 (0.7)
HCFCs	182	214	251 (3)	5.2%	6.3%	7.5%	9.2 (0.8)	6.0 (1.3)	10.6 (0.5)
CH_3CCl_3	136	66	32 (1)	3.9%	1.9%	1.0%	−26.8 (1.0)	−13.4 (2.1)	−6.2 (0.3)
Halon-1211	4.02	4.26	4.17 (0.1)	0.1%	0.1%	0.1%	0.1 (0.00)	0.0 (0.08)	−0.1 (0.01)
Total Cl	3499	3414	3352 (4)				−23 (2.4)	−21 (3.2)	−14 (1.2)
							−0.67%	−0.61%	−0.42%

* An average of AGAGE and NOAA/ESRL global means was used to derive these mid-year mixing ratios. Uncertainties are given in parentheses and represent 1 standard deviation of the results reported by different global networks. They do not include an additional amount for potential systematic calibration errors, errors associated with deriving tropospheric means from surface measurements, or uncertainties in Cl contributed from VSLS.

** Total Cl changes and relative rates of change are calculated assuming a constant 550 ppt Cl from CH_3Cl and a constant 80 ppt from VSLS (see Section 1.3). Rates of change were calculated as the difference between the indicated year and the previous year and relative rates were normalized by the mean mixing ratio over these two-year periods. Numbers for past years differ slightly from previous Assessments because of updated calibration information (see text).

But while increases in Cl from HCFCs have accelerated, declines in Cl from CFCs have become more rapid. The 2004–2008 period was the first time that declines derived for tropospheric Cl from long-lived CFCs as a class were larger than the decline from CH_3CCl_3 (Table 1-12). CFCs accounted for 2076 ± 3 ppt Cl during 2008. Chlorine from CFCs (as a class) declined by just over 13 ppt (0.6%) from 2007–2008 and this Cl decrease was comparable to the summed influence of other decreasing compounds (CCl_4, CH_3CCl_3, and halon-1211). The fraction of total organic chlorine attributable to CFCs has remained fairly constant at about 62% over the past decade even as Cl from CFCs has decreased by 4% from its 1998 peak.

As mentioned above, the decline in tropospheric Cl since 2004 was slower than anticipated in scenario A1 of the 2006 Ozone Assessment (Daniel and Velders et al., 2007) (Figure 1-15). Measured tropospheric Cl from long-lived gases in 2008 was ~40 ppt higher than projected in the A1 scenario. This slower decline in tropospheric Cl resulted mostly from CFC-11 and CFC-12. Although global mixing ratios of CFC-11 and CFC-12 declined more rapidly during 2005–2008 than in earlier years, Cl from these CFCs in 2008 was ~28 ppt Cl higher than had been projected. HCFCs also played a role in the slower than anticipated Cl decline. By 2008, mixing ratios observed for HCFC-22 and HCFC-142b contributed ~8 ppt more Cl than had been projected (see Figure 1-1). Some of the discrepancy for CFC abundances arises because the calibration of CFC-12 measurements by the NOAA group has been revised with improved standards since the last Assessment. Observed changes for other Cl-containing compounds during 2005–2008 were similar to those projected in the A1 scenario.

1.4.1.2 Stratospheric Chlorine Changes

As discussed in previous Assessments, the stratospheric burden of chlorine is controlled by input from the troposphere and by transport and mixing processes. Timescales for air to be transported to higher altitudes in the midlatitude and polar stratosphere after crossing the tropopause range from 3 to 6 years. As a result, changes in stratospheric chlorine and bromine abundances lag behind tropospheric changes and, furthermore, are smoothed and flattened because of mixing (Waugh and Hall, 2002). Changes in total stratospheric Cl calculated from tropospheric observations allow this lag to be visualized for the midlatitude stratosphere (Figure 1-16) (update of Engel et al., 2002). They also show how the magnitude of the decline in stratospheric Cl is expected to be altitude dependent.

Most chlorine enters the stratosphere chemically bound to carbon (organic Cl) in long-lived source gases and undergoes photochemical oxidation to inorganic forms as air is transported to higher altitudes within the stratosphere. Long-term changes in stratospheric inorganic Cl abundances are derived from ground-based and satellite-based instruments measuring total column abundances or

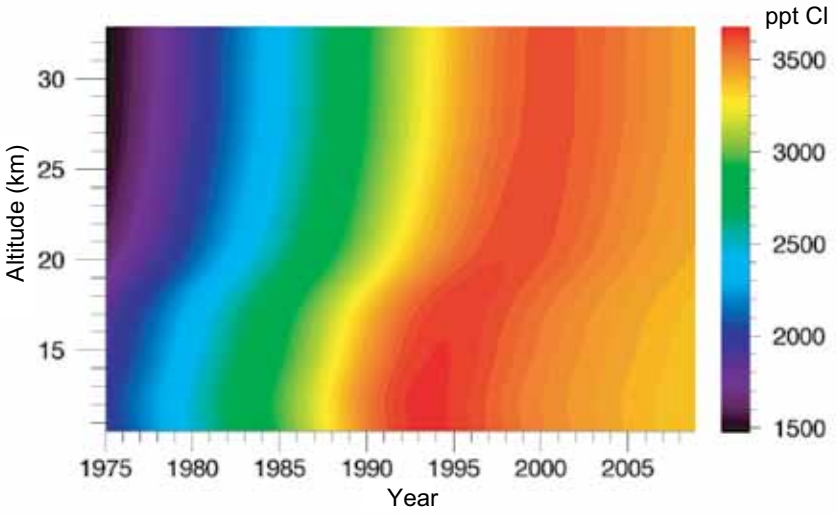

Figure 1-16. The evolution of total chlorine abundance (ppt) in the stratosphere, calculated based on the tropospheric chlorine time series shown in Figure 1-15, and including a constant contribution of 80 ppt of chlorine from VSLS species (consistent with 40–130 ppt estimated in Section 1.3). Typical profiles of mean age in the stratosphere (derived from observations of SF_6 and CO_2) and a parameterization of the age spectrum are used for the calculation of the effects of mixing and transport in the stratosphere (updated from Engel et al., 2002).

mixing ratio profiles of hydrogen chloride (HCl) and chlorine nitrate ($ClONO_2$), the two main inorganic reservoir chemicals for Cl in the stratosphere. Total column measurements from ground-based Fourier transform infrared (FTIR) instrumentation above the Jungfraujoch and Lauder show changes in inorganic Cl compound abundances that are fairly consistent with the amounts and changes in Cl being delivered to the stratosphere from long-lived source gases (Figure 1-17, Table 1-13) (update to Mahieu et al., 2004 and Rinsland et al., 2003). These findings are consistent with only a fairly small contribution of VSLS to stratospheric Cl. The mean fraction of stratospheric Cl attributable to VSLS, 80 (40–130) ppt (see Section 1.3), is approximately 1.5–3%. The relative contribution of VSLS to reactive Cl, however, can be substantially higher in the lower stratosphere for VSLS that have local lifetimes shorter than the longer-lived ODSs.

Average rates of change observed by ground-based FTIR measurements of total stratospheric chlorine (HCl + $ClONO_2$) since 1996 were −0.9 ± 0.2%/yr to −1.5 ± 0.2%/yr (Table 1-13). The faster declines are apparent in the column measurements above Kiruna, but this may reflect greater meteorological variability at polar sites than above lower latitude sites. Comparable or slightly slower rates of change (−0.6 ± 0.1 to −0.9 ± 0.2%/yr) have been measured since 2004 for upper stratospheric HCl measured over much of the globe from ACE-FTS and the Aura Microwave Limb Sounder (MLS) instruments (see Figure 1-18 and Table 1-13). These observed trends are reasonably consistent with the observed changes in total tropospheric Cl since 1996, though uncertainties related to chemical partitioning, mixing processes, and time lags associated with transport make a direct comparison between these different measures difficult.

Satellite data for upper stratospheric and lower mesospheric HCl from two different instruments (MLS and the ACE-FTS) agree to within ~0.15 ppb in recent years. This small difference is not significant given the systematic uncertainties on the ACE-FTS and MLS HCl measurements of 0.15 to 0.3 ppb (Figure 1-18) (Froidevaux et al., 2008; Mahieu et al., 2008). These satellite results agree to within ± 0.3 ppb (± 8%) with total Cl amounts derived from long-lived chlorinated source gases, once mixing and lag times associated with transport are considered (Figure 1-18). The uncertainty in this measured stratospheric Cl burden is large relative to the expected chlorine contributions from shorter-lived source gases and product gases (80, 40–130 ppt), and so these stratospheric data do not provide additional constraints to Cl contributions from chlorinated VSLS gases. HCl is estimated to account for >95% of total stratospheric Cl at altitudes above ~50 km.

Though the Cl contained in HCl and $ClONO_2$ is not directly involved in the chemical reactions depleting stratospheric ozone, their summed abundance in the upper stratosphere is approximately proportional to the amount of reactive Cl present in the stratosphere. Chlorine monoxide (ClO), however, is directly involved in reactions that deplete stratospheric ozone. Updated measurements of upper stratospheric ClO (near 4 hPa) show an overall trend that is consistent with the declines observed for HCl and $ClONO_2$ (Figure 1-19) (update of Solomon et al., 2006). Short-term variability is observed, however, suggesting that other factors influence the proportion of stratospheric Cl present in reactive (e.g., ClO) versus unreactive (e.g., HCl and $ClONO_2$) forms, as discussed previously (e.g., Siskind et al., 1998; Froidevaux et al., 2000). Such influences also imply that measured ClO trends are not directly comparable to changes in total stratospheric chlorine.

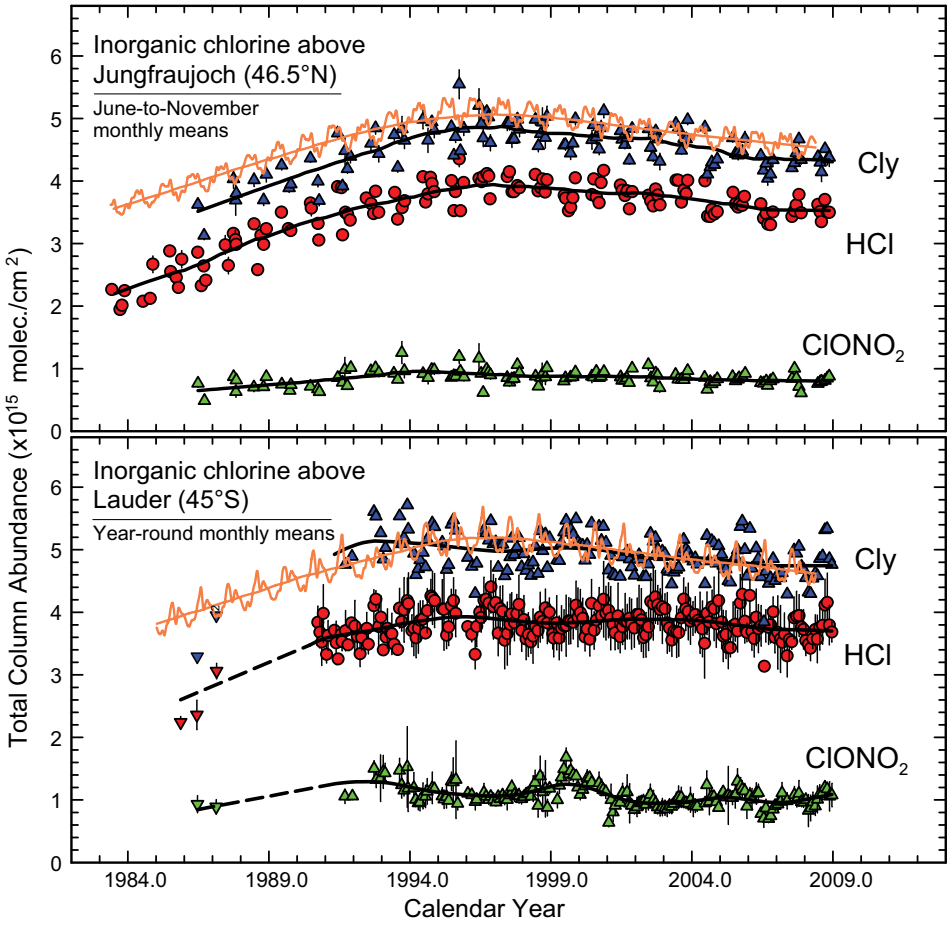

Figure 1-17. Time series of monthly-mean total column HCl (red circles) and $ClONO_2$ (green triangles) abundance (molecules per square centimeter), as measured above the Jungfraujoch (46.5°N) and Lauder (45°S) (updated from Mahieu et al., 2004 and Rinsland et al., 2003). Cl_y column estimates (blue triangles) are the sum of HCl and $ClONO_2$ columns. Jungfraujoch data are shown only for June to November of each year; results from all months are displayed for Lauder. Fits to the datasets are given by the black curves. The orange curves and corresponding fits represent Cl_y (HCl + $ClONO_2$) from the University of Leeds 2-D model, as in the previous Assessment report (Clerbaux and Cunnold et al., 2007).

Given observed changes in methane, a compound that affects this proportion, the measured decline of −0.9 ± 0.2%/yr in ClO for 1995–2007 (Table 1-13) is consistent with a somewhat slower rate of change in total chlorine (about −0.7%/yr) (see Solomon et al., 2006).

New observations of chlorofluorocarbonyl (COFCl) have been reported for the TTL and in the stratosphere (Fu et al., 2009; Rinsland et al., 2007). The contribution of this compound to total Cl above 35 km is expected to be small (<10 ppt) and accounts for only a small portion of total inorganic Cl in the upper stratosphere. Furthermore, COFCl is believed to result almost entirely from degradation of long-lived compounds containing Cl and F in the stratosphere, and so its abundance is not included as an additional term in sums of total organic Cl from long- and short-lived source gases.

1.4.2 Bromine in the Troposphere and Stratosphere

1.4.2.1 Tropospheric Bromine Changes

Bromine in the troposphere from halons and methyl bromide continued to decline during 2005–2008. By 2008, 15.7 ± 0.2 ppt of tropospheric Br was measured at Earth's surface from these long-lived chemicals by two independent networks (annual mean). These results indicate that total Br from these substances has declined by about 1 ppt in the troposphere from peak levels measured in 1998 (Figure 1-20) (Montzka et al., 2003), similar to that expected in the A1 scenario of the last Assessment (Daniel and Velders et al., 2007). This decline has been

Table 1-13. Measured chlorine-related changes in the upper atmosphere.

Instrumentation Technique / Location	Species and Altitude Region	Time Period	Rate of Change (percent/yr) (2-sigma error)
ground-based microwave [1] Hawaii	ClO upper stratosphere	1995–2007	−0.9 (0.2)
spaceborne ACE-FTS [2] IR solar occultation	HCl upper stratosphere	Jan. 2004–Sep. 2009	−0.9 (0.2)
spaceborne Aura MLS [3] Microwave emission	HCl upper stratosphere	Aug. 2004–Jan. 2010	−0.6 (0.1)
ground-based FTIR	HCl column		
Jungfraujoch [4]		1996–2009	−0.9 (0.1)
Kirunawwq [5]		1996–2009	−0.8 (0.2)
ground-based FTIR	$ClONO_2$ column		
Jungfraujoch [4]		1996–2009	−0.9 (0.3)
Kiruna [5]		1996–2009	−2.9 (0.4)
ground-based FTIR	HCl + $ClONO_2$ column		
Jungfraujoch [4]		1996–2009	−0.9 (0.2)
Kiruna [5]		1996–2009	−1.5 (0.2)

1. *Ground-based microwave ClO data (Hawaii, 20°N):* Updated data and results following Solomon et al. (2006). Rate of change (%/yr) is referenced to 1995 (January). See Figure 1-19.
2. *ACE-FTS HCl data (60°S–60°N average):* Updated data and results following Froidevaux et al. (2006). Rate of change (%/yr) is referenced to the average abundance during the data time period. See Figure 1-18.
3. *Aura MLS HCl data (60°S–60°N average):* Updated data and results following Froidevaux et al. (2006). Rate of change (%/yr) is referenced to the average abundance during the data time period. See Figure 1-18.
4. *Ground-based FTIR column data (Jungfraujoch, 46.5°N):* Updated data and results following Mahieu et al. (2004) and Clerbaux and Cunnold et al. (2007). Rates of change (%/yr) are referenced to 1996. See Figure 1-17.
5. *Ground-based FTIR column data (Kiruna, 67.8°N):* Updated data and results following Mikuteit (2008). Rates of change (%/yr) are referenced to 1996.

primarily a result of decreasing mixing ratios of CH_3Br in response to reduced industrial production and emission after 1998. Though Br from halons increased throughout most of the 1998–2008 period, during 2005–2008 Br from halons peaked in air at Earth's surface at 8.2–8.5 ppt and was no longer increasing (see Table 1-1). Surface-based data suggest that global surface Br from halons may have decreased slightly from 2007 to 2008 (at –0.3 to –0.5%/yr).

1.4.2.2 Stratospheric Bromine Changes

New results from ongoing ground-based DOAS (Differential Optical Absorption Spectroscopy) measurements of stratospheric BrO at both Lauder (45°S) and Harestua (60°N) show changes over time in inorganic bromine (Br_y) that are highly consistent with the observed tropospheric Br changes measured for halons and CH_3Br (Hendrick et al., 2008) (Figure 1-21). Updated stratospheric balloon measurements (Dorf et al., 2006) (Figure 1-21) do not provide as tight a constraint on Br_y changes since 2000, but the available results are consistent with the tropospheric trends measured for Br from long-lived gases and the UV-visible measurements of Hendrick et al. (2008). Despite the significant contribution of non-controlled, very short-lived Br source gases to inorganic Br_y in the stratosphere (Section 1.3.3), temporal changes in stratospheric inorganic Br abundance appear to follow the measured changes in tropospheric Br from controlled substances (i.e., CH_3Br and the halons) (Figure 1-21).

Table 1-14 is an update from the previous Assessment (Table 2-8 in Law and Sturges et al., 2007) and lists estimates of Br_y from VSLS (Br_y^{VSLS}) and their uncertainty ranges for 12 studies. The contribution of VSLS to Br_y is derived in these studies by calculating Br_y from measured BrO using a photochemical model and then subtracting the contribution of long-lived gases (halons and CH_3Br). Seven of these studies were discussed previously, though one preliminary study in the previous Assessment is no longer considered. The estimate based on an analysis of MLS measurements of BrO by Livesey et al. (2006) shown in the previous Assessment has been updated with a newer study of the same dataset by Kovalenko et al. (2007) who infer a VSLS contribution of 6.5 ± 5.5 ppt to stratospheric

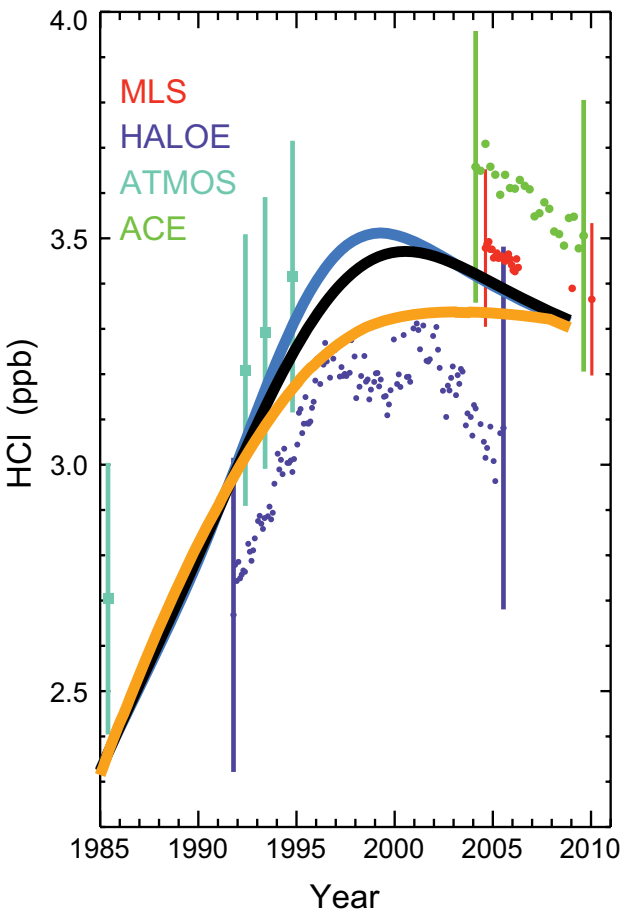

Figure 1-18. Time series of near-global HCl abundances (ppb) at about 53 km (near 0.5 hPa) (updated from Froidevaux et al. (2006) and the previous Assessment report (Clerbaux and Cunnold et al., 2007)). The satellite datasets have been updated for ACE-FTS (version 2.2 data, quarterly averages for 60°S–60°N, green dots) and for Aura MLS (version 2.2 monthly averages for same latitude range, red dots); both these datasets are for averages over 0.46 and 0.68 hPa (about 50 to 54 km). The solid curves are expectations for HCl (total Cl × 0.96) near 55 km based on the ground-based total tropospheric chlorine, and include a range of air-age spectrum widths (blue, black, and orange curves are for widths of 0, 2, and 4 years). The MLS data are interrupted after early 2006, because of a lifetime issue that affects the main HCl band's retrievals so it has been turned on only sparingly since; the MLS points in early 2009 and 2010 represent averages from 3–4 days in early January of each year. The Halogen Occultation Experiment (HALOE) dataset (monthly averages, purple) ended in November 2005 and no updated results are available from the Atmospheric Trace Molecule Spectroscopy (ATMOS) instrument. Error bars (2-sigma estimates of systematic uncertainties) are given for the various time series and are shown typically only for the first and last points in the series (for clarity).

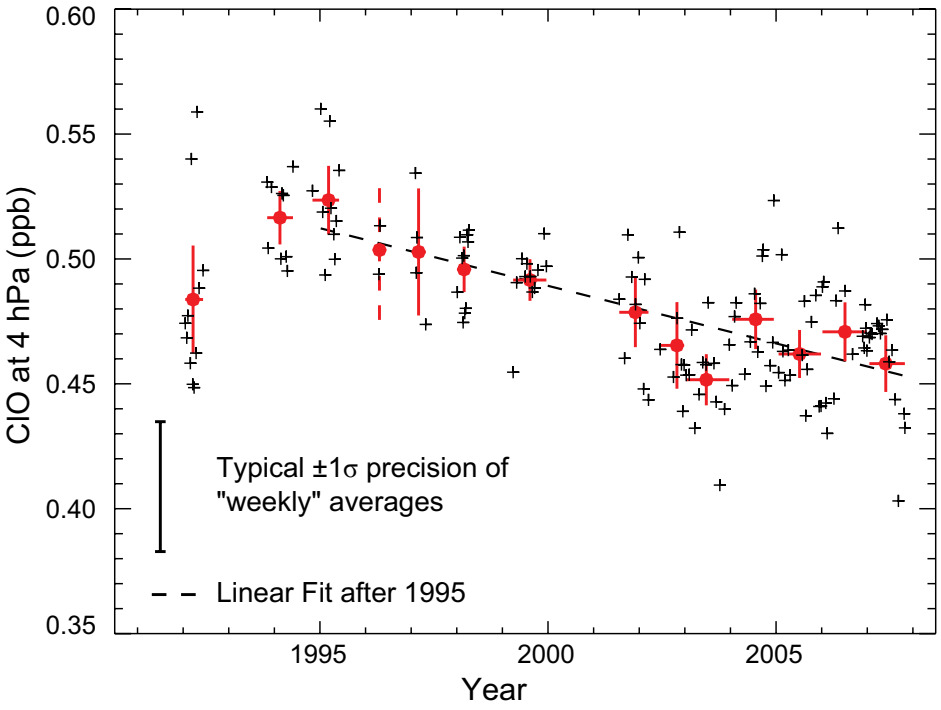

Figure 1-19. Time series of ClO abundances (ppb) above Hawaii (at 35–39 km or about 4 hPa) derived from ground-based millimeter-wave measurements since 1992 (update of Solomon et al., 2006). Black and red symbols are "weekly" and "yearly" averages of deseasonalized data, and error bars typically show two standard deviations about the means (see above reference). Dashed line gives a linear fit to the observations after 1995 (see also Table 1-13).

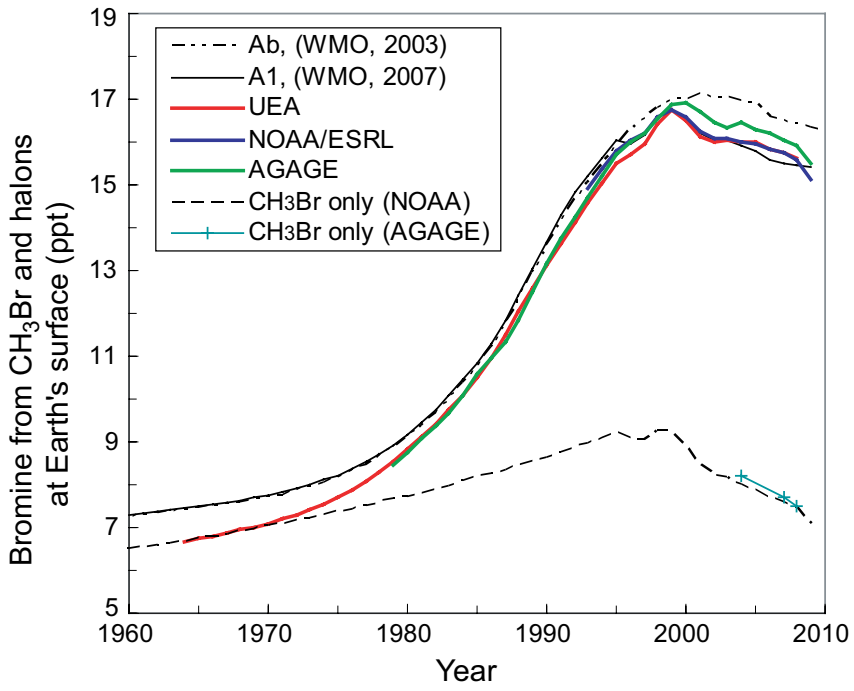

Figure 1-20. Tropospheric Br (ppt) from CH_3Br and halons over time. Halons measured by AGAGE (green line; Prinn et al., 2000; Sturrock et al., 2002), UEA (red line; Reeves et al., 2005), and NOAA (blue line) are added to CH_3Br data from NOAA (dashed black line; Montzka et al., 2003) or AGAGE (plus symbols; Simmonds et al., 2004). Ab (dot-dot-dashed line indicated as WMO, 2003 (Montzka and Fraser et al., 2003)) and A1 (solid black line indicated as WMO, 2007 (Clerbaux and Cunnold et al., 2007)) baseline scenarios are shown for comparison. Updated considerations of preindustrial mixing ratios in the current Assessment cause the differences in earlier years (see Section 1.2.1.6 and Chapter 5).

bromine. Two of the other four new estimates introduced in Table 1-14 are based on ground-based DOAS BrO measurements (Theys et al., 2007 and Hendrick et al., 2008) and suggest that a contribution of 7 ± 4 ppt and 6 ± 4 ppt of bromine, respectively, is needed from VSLS to account for the total measured bromine loading. McLinden et al. (2010) calculate a contribution from VSLS of 5 ± 5 ppt based on stratospheric BrO profiles measured by OSIRIS (Optical Spectrograph and InfraRed Imager System) during 2001–2008. Salawitch et al. (2010) inferred a value for Br_y^{VSLS} of 7 (5 to 10) ppt from OMI (Ozone Monitoring Instrument) measurements of total column BrO and tropospheric partial column BrO calculated from aircraft profiles (Neuman et al., 2010) obtained during Arctic spring.

These new results support the conclusion, made in the last Assessment (Law and Sturges et al., 2007), that substantially more Br_y is measured in the stratosphere than can be accounted for by CH_3Br and the halons alone; the new "ensemble" value reported in Table 1-14 is 1 ppt higher than the 5 ppt previously derived, while the range has stayed the same with 3 to 8 ppt. In other words, the majority of studies available to date continue to suggest a non-zero, positive value for Br_y^{VSLS} of 6 (3–8) ppt, which is large enough to affect ozone photochemistry in the lower middle stratosphere (see Section 1.3.4). Only 2 out of the 12 studies reported in Table 1-14 include a zero contribution from Br_y^{VSLS} in their uncertainty range. Taking this ensemble value for Br_y^{VSLS} of 6 (3–8) ppt derived from consideration of all available stratospheric Br_y estimates, and adding tropospheric Br from CH_3Br and the halons from 2003–2004 in order to account for lags due to transport, a 2008 total stratospheric bromine mixing ratio of 22.5 (19.5–24.5) ppt can be derived. This result is comparable, given the range in results reported by different techniques, to the Br_y abundance derived from stratospheric measurements of BrO made in 2008. Annual mean Br_y derived from the NH Harestua site (60°N) during 2008 averaged 22.5 ± 4 ppt (an update of Hendrick et al., 2008), and 19.5 ± 2.5 ppt Br_y was derived from a single balloon profile made on 27 June 2008 in the tropics (5°S, 43°W; update of Dorf et al., 2006) (Figure 1-21).

These results imply that slightly less than half (40–45%) of the 2008 stratospheric Br_y burden is derived from controlled uses of halons (~8.3 ppt Br) and methyl bromide (0.4–0.9 ppt Br). As a result, more than half of the 2008 stratospheric Br_y burden is accounted for by natural sources of methyl bromide and other bromocarbons, and from quarantine and pre-shipment uses of methyl bromide not controlled by the Montreal Protocol. The total contribution of VSLS to stratospheric Br is estimated to be 1–8 ppt Br from measurements of VSLS source gases and modeling of their chemistry and transport (Table 1-9; Section 1.3.3.3). This magnitude is derived from the observed abundances of brominated source gases (SG) at the tropopause plus the modeled contributions of product gases (PG) in this region of the atmosphere (Hossaini et al., 2010; Aschmann et al., 2009; Liang et al., 2010).

The potential difference between Br_y from SGs and Br_y from BrO is also influenced by uncertainties in

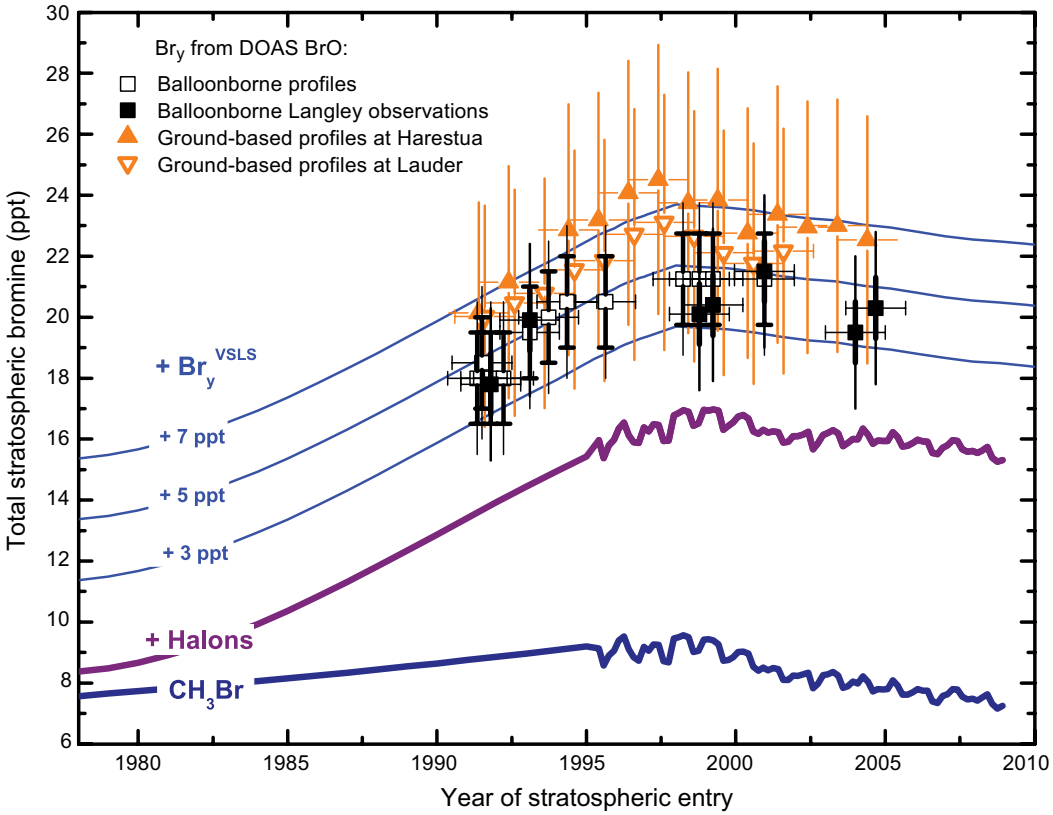

Figure 1-21. Changes in total stratospheric Br_y (ppt) derived from balloonborne BrO observations (squares) (update of Dorf et al., 2006) and annual mean mixing ratios calculated from ground-based UV-visible measurements of stratospheric BrO made at Harestua (60°N) and Lauder (45°S) (filled and open orange triangles, respectively) (adapted from Hendrick et al., 2008). These stratospheric trends are compared to trends in measured bromine (ppt) at Earth's surface with additional constant amounts of Br_y added (thin lines). Lines show global tropospheric bromine from methyl bromide as measured in ambient air and firn air with no correction for tropospheric CH_3Br loss (dark blue line; Butler et al. (1999) through 1998 including a changing interhemispheric gradient—see Chapter 5; Montzka et al. (2003) thereafter); global tropospheric bromine from the sum of methyl bromide plus halons (purple line; Butler et al. (1999) and Fraser et al. (1999) through 1995; Montzka et al. (2003) thereafter); and bromine from CH_3Br, halons, plus additional constant amounts of 3, 5, and 7 ppt Br (thin blue lines). Squares show total inorganic bromine derived from stratospheric measurements of BrO and photochemical modeling that accounts for BrO/Br_y partitioning from slopes of Langley BrO observations above balloon float altitude (filled squares) and lowermost stratospheric BrO measurements (open squares). For the balloonborne observations, bold/faint error bars correspond to the precision/accuracy of the estimates, respectively. For the ground-based measurements (triangles), the error bars correspond to the total uncertainties in the Br_y estimates. For stratospheric data, the date corresponds to the time when the air was last in the troposphere, i.e., sampling date minus estimated mean age of the stratospheric air parcel. For tropospheric data, the date corresponds to the sampling time, i.e., no corrections are applied for the time required to transport air from Earth's surface to the tropopause. Preindustrial levels were 5.8 ± 0.3 ppt for CH_3Br (Saltzman et al., 2004) and 0 ppt for the halons (Reeves et al., 2005). This figure is an update to Figure 2-3 from the previous Assessment (Law and Sturges et al., 2007).

Table 1-14. Estimates of inorganic bromine from very short-lived substances (Br_y^{VSLS}) contribution to stratospheric bromine derived from BrO measurements. Update of Table 2-8 from the previous Assessment (Law and Sturges et al., 2007), extended with new results.

Data Source	Br_y^{VSLS} Central Value (ppt)	Br_y^{VSLS} Range (ppt)	Reference
Ground-based BrO 11 sites, 78°S–79°N	5	1–9 [a]	Sinnhuber et al. (2002)
Ground-based BrO Lauder, New Zealand, 45°S	6	3–9	Schofield et al. (2004)
Ground-based BrO Arrival Heights, Antarctica, 78°S	6	3–9	Schofield et al. (2006)
DOAS balloon BrO profiles 5°S–68°N, 0–35 km	4.1	1.6–6.6	Dorf et al. (2006)
Aircraft & balloon BrO profiles, 22°S–35°N, 17–32 km and GOME satellite column BrO, 60°S–60°N	7	4–10 [a]	Salawitch et al. (2005)
SCIAMACHY satellite BrO profiles 80°S–80°N, 15–28 km	8.4	6.4–10.4	Sioris et al. (2006)
SCIAMACHY satellite BrO profiles 80°S–80°N, 15–28 km	3	0–6	Sinnhuber et al. (2005)
Ground-based BrO Harestua (60°N) and Lauder (45°S)	6	2–10	Hendrick et al. (2008)
Ground-based BrO Reunion Island (21°S, 56°E)	7	3–11 [b]	Theys et al. (2007)
MLS satellite BrO profiles 55°S–55°N, 10–4.6 hPa	6.5	1–12	Kovalenko et al. (2007)
OSIRIS satellite BrO profiles 80°S–80°N, 20–34 km	5	0–10	McLinden et al. (2010)
OMI total column BrO and aircraft tropospheric BrO profiles, Arctic spring	7 [c]	5–10	Salawitch et al. (2010)
Ensemble	**6 (3–8)** [d]		

DOAS, Differential Optical Absorption Spectroscopy; GOME, Global Ozone Monitoring Experiment; SCIAMACHY, Scanning Imaging Absorption Spectrometer for Atmospheric Cartography; MLS, Microwave Limb Sounder; OSIRIS, Optical Spectrograph and InfraRed Imager System; OMI, Ozone Monitoring Instrument.

[a] Range estimated by previous Assessment (Law and Sturges et al., 2007), based on the uncertainty in stratospheric Br_y inferred from BrO that was stated in the reference.

[b] Range estimated based on the Hendrick et al. (2008) study that uses the same method.

[c] Salawitch et al. (2010) has a different treatment of CH_2Br_2 than the other studies listed here. Their estimate for Br_y^{VSLS} would be slightly higher (~ ≤1 ppt) if CH_2Br_2 were treated in the same manner as in the other studies.

[d] Average and range of the central values of the 12 estimates of Br_y^{VSLS}.

absolute calibration scales for measurements of brominated organic SGs (Butler et al., 2010) and product gases. Furthermore, concentrations of VSLS sampled by a whole-air sampler represent only local influences for a small region over a short time in the tropical tropopause layer. In contrast, Br_y from BrO is measured in an air parcel in which the Br content represents a weighted average of Br in air parcels with a distribution of mean ages and that has been influenced by stratospheric mixing processes.

In addition to observations of BrO, measurements of stratospheric bromine nitrate ($BrONO_2$) have been analyzed from the Michelson Interferometer for Passive Atmospheric Sounding (MIPAS-E) instrument onboard the Envisat satellite for September 2002 and September 2003 (Höpfner et al., 2009). The authors report that the maximum values of $BrONO_2$ observed during night are always in the range of 20–25 ppt (with an uncertainty of 20–25% depending upon altitude). Large uncertainties remain, however, in the absorption cross section and its temperature dependence, so reliable estimates of Br_y from these measurements are not currently possible.

The contribution of tropospheric BrO to ground- and satellite-based measurements of stratospheric Br_y has been discussed in recent years. As in the last Ozone Assessment (Law and Sturges et al., 2007), it remains unclear whether BrO is distributed throughout the global troposphere with a background abundance of up to 3 ppt. Such a BrO background is supported by several studies (e.g., Richter et al., 2002; Van Roozendael et al., 2002; Theys et al., 2007), where comparisons of Global Ozone Monitoring Experiment (GOME) BrO vertical columns with model results, balloonborne observations, and ground-based measurements have led to the conclusion that a significant background of several ppt BrO is present in the free troposphere. However, other observations support much lower values that include a contribution of zero ppt Br (e.g., Schofield et al., 2004; Dorf et al., 2008). Tropospheric BrO levels of less than 1 ppt imply larger stratospheric BrO columns than can be accounted for by CH_3Br and halons alone, and, as a result, an important contribution of VSLS to stratospheric Br_y is necessary to explain the total column observations (e.g., Salawitch et al., 2005).

Similarly, two independent studies (also discussed in detail in the previous Assessment) show BrO profiles retrieved from Scanning Imaging Absorption Spectrometer for Atmospheric Cartography (SCIAMACHY) radiances that lead to different results. While Sioris et al. (2006) derive large BrO abundances in the tropical tropopause layer and lowermost stratosphere (LMS), consistent with Br_y^{VSLS} of 8.4 ± 2 ppt, Sinnhuber et al. (2005) imply a much smaller value for Br_y^{VSLS} of 3 ± 3 ppt. One cause for this discrepancy is that Sinnhuber et al. (2005) suggest the presence of 1 ± 0.5 ppt of tropospheric BrO while Sioris et al. (2006) suggest a much smaller level of global tropospheric BrO. Balloonborne DOAS observations of a BrO profile made in the tropics in 2005 found that BrO in the lower and middle troposphere is <1 ppt and compatible with zero within the uncertainties (Dorf et al., 2008). The authors derive a total contribution of 5.2 ± 2.5 ppt from brominated VSL SGs and inorganic PGs to stratospheric Br_y and so suggest a Br_y^{VSLS} magnitude in between the earlier results derived from SCIAMACHY.

The recent ARCTAS (Arctic Research of the Composition of the Troposphere from Aircraft and Satellites) and ARCPAC (Aerosol, Radiation, and Cloud Processes affecting Arctic Climate) campaigns included airborne in situ measurements of BrO and O_3 (Neuman et al., 2010), placed in the footprint of satellite observations, to quantify the relative contribution of tropospheric and stratospheric partial columns to total column BrO and the relation between BrO hotspots (regions where column BrO is enhanced by 2 to 3 × 10^{13} radicals cm^{-2} relative to the zonal mean) and surface ozone depletion events. Salawitch et al. (2010) reported that aircraft in situ measurements of BrO and O_3 near the surface often bear little relation to OMI BrO "hotspots." The geographic location of numerous BrO hotspots was shown to be consistent with the location of high total column ozone and a low-altitude (~5 km) tropopause, suggesting a stratospheric origin to the BrO enhancements that implied, on average, Br_y^{VSLS} equal to 7 (5–10) ppt. It has been noted that the largest source of uncertainty in deriving Br_y from measurements of total column BrO is the rate constant of $BrO + NO_2 + M \rightarrow BrNO_3 + M$ (Sioris et al., 2006; Hendrick et al., 2008; Salawitch et al., 2010). Salawitch et al. (2010) suggest that the preponderance of prior observations of elevated BrO over Hudson Bay during spring may be related to a synoptic weather pattern known as the Hudson Bay low that is responsible for the very low-altitude tropopause (e.g., Liu and Moore, 2004). They stress that proper understanding of BrO "hotspots" requires accurate treatment of perturbations originating from both the stratosphere and troposphere, which generally has not been the focus of prior studies (i.e., many prior studies erroneously treat the stratospheric signal as spatially constant, ascribing all contributions to BrO hotspots as originating from below the tropopause).

In addition to the previously reported observations of BrO in the midlatitude marine boundary layer (Leser et al., 2003; Saiz-Lopez et al., 2004), BrO has now also been observed directly in the tropical and subtropical marine boundary layer. Mean daytime maxima of 2.5 ± 1.1 ppt were reported for observations made from November 2006 until June 2007 at Cape Verde (Read et al., 2008) and peak mixing ratios of 10.2 ± 3.7 ppt were measured during a ship cruise along the African coast during February 2007 (Martin et al., 2009). It is not clear to what extent this BrO influences Br abundances above the marine boundary layer.

1.4.3 Iodine in the Upper Troposphere and Stratosphere

Updated results since the last Assessment continue to suggest that gaseous iodine-bearing compounds contribute very little iodine to the current lower stratosphere. Balloonborne solar occultation spectra of IO and OIO in the tropical upper troposphere/lower stratosphere (UT/LS) obtained during balloon flights in 2005 and 2008 confirm the low values of IO and OIO for the tropical upper troposphere and lower stratosphere (Butz et al., 2009). A photochemical model of these results yields corresponding upper limits for the total gaseous inorganic iodine burden (I_y) of 0.17 to 0.35 (+0.20/−0.08) ppt in the tropical upper troposphere (13.5 km to 16.5 km) and 0.09 to 0.16 (+0.10/−0.04) ppt in the tropical lower stratosphere (16.5 km to 21.0 km).

These observations do not preclude iodine reaching the lower stratosphere in chemical forms other than commonly considered in photochemical models, or in particulate matter. There is evidence that iodine that may have originated in the lower troposphere can be found in lower stratospheric aerosol (Murphy et al., 2007). But if present in the TTL or stratosphere in forms other than IO and OIO, the extent to which this iodine might become available for ozone-depleting reactions in other parts of the stratosphere is not known.

The inferred upper limits for IO and OIO concentrations in the lower stratosphere suggest that catalytic cycles involving iodine have only a minor contribution to total ozone loss, but it remains unclear whether reactive iodine contributes—possibly through coupling with chlorine or bromine—to the observed trend of declining ozone in the lower stratosphere (e.g., Butz et al., 2009).

1.4.4 Equivalent Effective Chlorine (EECl) and Equivalent Effective Stratospheric Chlorine (EESC)

Changes in the stratospheric burden of total inorganic halogen (Cl and Br) are estimated from measured tropospheric changes in ODS abundances with a number of different metrics such as equivalent effective stratospheric chlorine (EESC), EESC-Antarctica, and EESC-Midlatitudes; changes in total tropospheric halogen (Cl and Br) are addressed with the equivalent effective chlorine (EECl), and equivalent chlorine (ECl) metrics (Clerbaux and Cunnold et al., 2007). By accounting for transport times, the efficiency for different halogens to deplete ozone, mixing processes, and age-of-air-dependent ODS decomposition rates (i.e., fractional release values), inorganic halogen abundances and changes can be estimated with EESC for different regions of the stratosphere from tropospheric ODS measurements. As discussed in the last report and in recent publications, new approaches have been explored that enhance the usefulness of EESC for more accurately estimating halogen abundances and changes in specific stratospheric regions by considering that the extent of degradation of an ODS in the stratosphere is fairly well described by the mean stratospheric age of an air parcel (Newman et al., 2007). This new approach incorporates revised fractional release values for some compounds that are based primarily on observations (Schauffler et al., 2003) but that are also consistent with models (Douglass et al., 2008; Daniel and Velders et al., 2007). New fractional releases have not been considered for HCFC-142b and HCFC-141b owing to large discrepancies between the values derived by observations (e.g., Schauffler et al., 2003) and those based on model calculations that have been used in past ozone Assessments.

New methods have been devised to more readily convey the magnitude of decline in EESC over time by referencing the changes in EESC to peak levels observed in the mid-1990s and amounts inferred for 1980 (Hofmann and Montzka, 2009). Though ozone depletion was likely non-negligible in 1980 (see Chapter 2 and Chapter 5), the EESC value in 1980 is still used in this report as an important benchmark for ozone recovery as in past reports.

Stratospheric air parcels in midlatitudes having a mean age of 3 years have substantially less inorganic halogen as EESC than an air parcel with a mean age of 5.5 years typical of the Antarctic spring vortex (Figure 1-22, top panel) (Newman et al., 2007). Older air has larger EESC values because as air ages in the stratosphere, ODSs photochemically decompose so that a higher fraction of available halogen is present in inorganic forms.

As discussed in the last Assessment report (Daniel and Velders et al., 2007), calculating EESC in this way also demonstrates that EESC peaks at different times in different regions of the stratosphere. With the shorter transit times and higher relative contribution of rapidly declining short-lived ODSs in midlatitudes (e.g., CH_3CCl_3), EESC peaks earlier in midlatitudes than in polar regions (Figure 1-22, lower panel).

The date when the second derivative in EESC reaches a minimum also varies with stratospheric region. This date has been proposed as the time when a significant reduction in the rate of ozone decline might be expected, i.e., the "first stage" of ozone recovery (Yang et al., 2008). The second derivative in EESC reaches a minimum in early 1996 in midlatitudes (mean age = 3 years and age-of-air spectrum width = 1.5 years) and in late 1997 in the Antarctic stratosphere (mean age = 5.5 years and age-of-air spectrum width = 2.75 years) (Figure 1-22).

The similarity between global surface means derived for ODSs from independent surface sampling

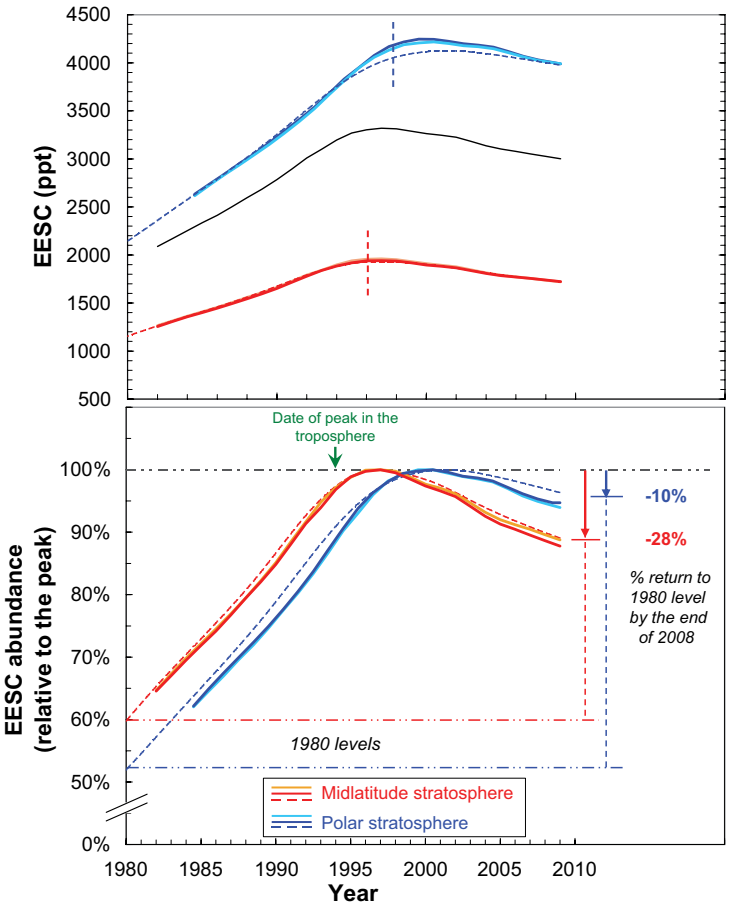

Figure 1-22. Top panel: Equivalent effective stratospheric chlorine (EESC) (ppt) calculated for the midlatitude stratosphere from surface measurements (see Figure 1-1) and absolute fractional release values from Clerbaux and Cunnold et al. (2007) (black line) or with age-of-air-dependent fractional release values for the midlatitude stratosphere (red lines; mean age = 3 years) and the Antarctic springtime stratosphere (blue lines; mean age = 5.5 years). EESC calculated with stratospheric mixing processes included are shown as dashed colored lines for the different stratospheric regions (i.e., an air-age spectrum width equal to one-half the mean age; Newman et al., 2007). Different shades of the same colors represent EESC calculated with tropospheric halocarbon data from the different surface networks (NOAA and AGAGE, not always distinguishable from one another) without consideration of air-age spectra. Vertical dashed lines represent the date when the second derivative of EESC reaches a minimum (see text). Bottom panel: EESC derived for the midlatitude and polar stratospheric regions as a function of time plotted relative to peak abundances of 1950 ppt for the midlatitude stratosphere and 4150 ppt for the polar stratosphere. Percentages shown on right of this panel indicate the observed change in EESC relative to the change needed for EESC to return to its 1980 abundance (note that a significant portion of the 1980 EESC level is from natural emissions of CH_3Cl and CH_3Br). Colors and line styles represent the same quantities as in the top panel.

networks (Table 1-1) suggests only small uncertainties in our estimate of EESC abundance and trend in recent years related to measurement errors. Larger uncertainties are associated with using tropospheric data to derive actual inorganic halogen abundances in different regions of the stratosphere. These additional uncertainties stem from an imperfect understanding of ODS decomposition rates in the stratosphere (fractional release factors), stratospheric mixing processes, and stratospheric air-age spectra (Newman et al., 2007).

Results from all three global surface sampling networks indicate that EESC and tropospheric EECl continued to decline during 2005–2008. By 2008, tropospheric EECl (weighted with fractional release factors appropriate for the midlatitude stratosphere) had dropped 14% from its peak value measured in 1993–1994. Note that the magnitude of this decline is somewhat sensitive to the fractional release factors used. While a 14% drop is calculated with the updated fractional release factors discussed above, a drop in EECl of only 11% would be calculated with the fractional release factors used in the previous Assessment report.

Changes in stratospheric inorganic halogen abundance (EESC) through 2008 can also be estimated from tropospheric measurements of ODSs. By 2008, midlatitude EESC had decreased by about 11% from its peak value in 1997. This stratospheric decline is smaller than derived for tropospheric EECl because of the time lag associated with transporting air from the troposphere to the stratosphere. When referenced to EESC in 1980, this drop is 28% of the decrease required for EESC in midlatitudes to return to that benchmark level (Figure 1-22, bottom panel). These EESC declines calculated for midlatitudes are similar whether or not mixing processes are accounted for with an air-age spectrum.

An even smaller decline is derived for the inorganic halogen abundance in the Antarctic polar vortex. By 2008, polar EESC had decreased by about 5% from its peak value in 2002. The much smaller decline over Antarctica stems from less time having elapsed since peak

abundances were observed in this older air and the dampening of changes by mixing air with a wider age spectrum across the maximum in EESC. This drop is approximately 10% of the decrease required for EESC in polar regions to return to the 1980 benchmark level (Figure 1-22, bottom panel). The EESC declines calculated for polar regions are more sensitive to mixing processes than in midlatitudes (see Figure). Slightly smaller declines are calculated for polar regions when an air-age-spectrum width of 2.75 years (one-half of the mean age of 5.5 years) is considered (a total decline of ~4% compared to 5% when mixing processes are not included in the EESC calculation).

In previous Assessment reports, it was noted that declines in the shorter-lived gases CH_3CCl_3 and CH_3Br were the main reason for the observed declines in EECl and EESC. During the past four years, however, no single chemical class has dominated the decline in the total combined abundance of ozone-depleting halogen in the troposphere. From 2005 through 2008, the long-lived CFCs (−17 ppt EESC) contributed similarly to the EESC decline as did the short-lived CH_3CCl_3 (−20 ppt EESC) and CH_3Br (−24 ppt EESC). Other compounds and compound classes contributed less to this decline (CCl_4: −10 ppt EESC; halons: −4 ppt EESC), and HCFCs (+6 ppt EESC) added to this halogen burden over this period.

1.4.5 Fluorine in the Troposphere and Stratosphere

In contrast to the declines observed for tropospheric Cl and Br in recent years, the tropospheric abundance of fluorine (F) increased at a mean annual rate of 1.6 ± 0.1%/yr (40 ± 4 ppt/yr) since 1996 (fluorine from CFCs -11, -12, -113, -114, -115; HCFCs -22, -141b, -142b, -124; halons -1211, -1301, -2402; HFCs -23, -152a, -134a, -143a, -125; PFCs -14, -116, -218; and SF_6). This rate is substantially less than the annual increases of 60–100 ppt/yr (annually 5.9 ± 0.3%/yr) observed for tropospheric F during the 1980s as CFC abundances were rapidly increasing. Many replacement compounds (HCFCs, HFCs, and PFCs) and other gases contributing F to the atmosphere degrade very slowly in the stratosphere and, therefore, do not affect stratospheric hydrogen fluoride (HF) changes as much as shorter-lived gases. Tropospheric F from compounds having stratospheric lifetimes <100 yrs (CFCs, halons, HCFC-141b, and HFC-152a; see Table 1-3) peaked in 2001 and was decreasing slowly during 2005–2008 (trend of −0.4 ± 0.1%/yr). Stratospheric changes in HF are likely to be between these two ranges (−0.4%/yr to +1.6%/yr).

Stratospheric column FTIR measurements of HF, carbonyl fluoride (COF_2), and F_y^* (where F_y^* = HF + 2×COF_2) also suggest a decrease in accumulation rate for atmospheric F beginning in 1999 (Figure 1-23). During 2005–2008 the rate of increase was 0.4%/yr, which is smaller than observed during the late 1980s–early 1990s. This change in rate is consistent with tropospheric changes in F-containing gases propagating to the stratosphere and a lag associated with transport. While the abundance and rates of change observed for stratospheric F_y^* are fairly well calculated with a 2-D model (Chipperfield et al., 1997) in which tropospheric changes for a subset of F-containing gases were considered, the calculated F abundance is likely a lower limit for F as some less abundant fluorine source gases were not included in the model. Data from other FTIR sites have also reported continued increases in HF column abundances. The measurements from Kiruna, Sweden, for example, indicate that an average increase in HF column of 1%/yr (± 0.3%/yr) occurred during 1996–2008 (relative to 2000; updates to Mikuteit (2008)). The rates of increase in stratospheric HF columns derived from these ground-based observations are within the expected range derived from surface observations (−0.4%/yr to +1.6%/yr).

1.5 CHANGES IN OTHER TRACE GASES THAT INFLUENCE OZONE AND CLIMATE

In addition to the Cl- and Br-containing ODSs, other trace substances can affect stratospheric ozone. The most important substances in this group are the greenhouse gases. As greenhouse gases have been recently assessed by the Working Group I of the IPCC Fourth Assessment Report (AR4) (Forster et al., 2007; Denman et al., 2007) only updates on recent trends of mole fractions (Table 1-15), and information on sources and sinks are provided. Furthermore, in Figure 1-24 the development of the radiative forcing of the greenhouse gases discussed in this section is shown. In Section 1.5.1, CH_4, N_2O, and sulfur compounds are discussed, which, apart from their direct influence on the abundance of the stratospheric ozone, also have an effect on the radiative forcing. A special focus in this section is the renewed increase of atmospheric CH_4 mixing ratios (Rigby et al., 2008; Dlugokencky et al., 2009) and the re-evaluated influence of N_2O on stratospheric ozone (Ravishankara et al., 2009). Sulfur trace gases and SO_2 as their main degradation product can potentially reach the stratosphere and can influence stratospheric ozone by enhancing its degradation through heterogeneous reactions. In Section 1.5.2, fluorinated greenhouse gases, which only indirectly influence stratospheric ozone via the greenhouse effect, are discussed.

The influence of rockets on stratospheric ozone will be discussed in Section 1.5.3, as their emissions could be highly relevant because they are emitted either in or near the stratospheric ozone layer.

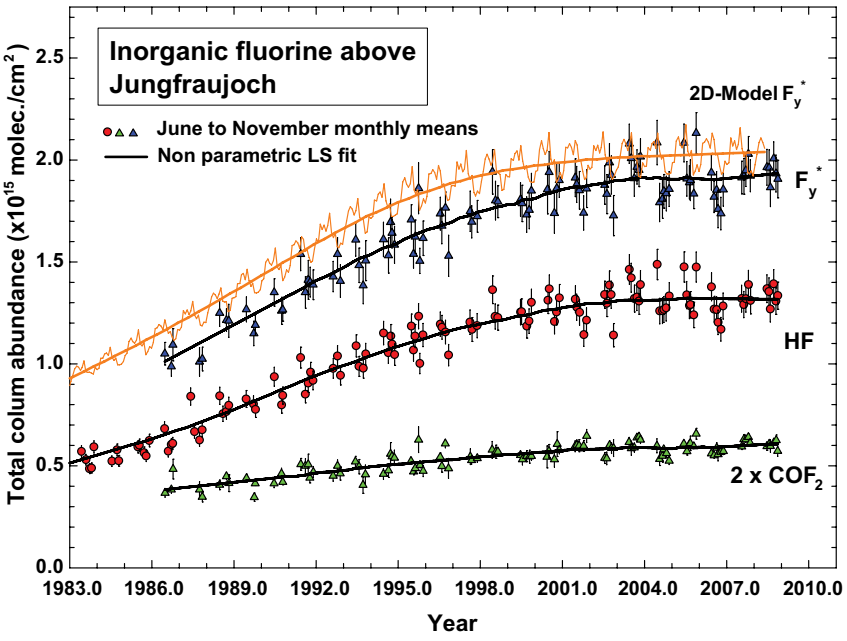

Figure 1-23. Time series of monthly-mean total column HF (red circles) and COF_2 (green triangles) (molecules per square centimeter), as derived from the Jungfraujoch (46.5°N) database, updated from the previous Assessment (Clerbaux and Cunnold et al., 2007). Duchatelet et al. (2009) have provided an updated analysis for the COF_2 results shown here, using a multispectral, multi-window approach. Data values are limited to June to November months to reduce variability. Fits to the data sets are given by the black curves. F_y^* estimates (blue triangles) are calculated from HF + 2×COF_2. Also shown are column F_y^* estimates from a 2-D model (based on Chipperfield et al., 1997) shown by the orange curve, with corresponding fit, that are derived from surface observations of CFC-11, CFC-12, CFC-113, and HCFC-22.

1.5.1 Changes in Radiatively Active Trace Gases that Directly Influence Ozone

In this section substances that are not controlled by the Montreal Protocol but that nevertheless have an influence on stratospheric ozone are discussed.

1.5.1.1 Methane (CH_4)

Apart from its well-established influence on radiative forcing, methane (CH_4) is both a sink of reactive chlorine and a source of water vapor in the stratosphere and, therefore, influences the availability of inorganic halogen for depleting stratospheric ozone (see Section 1.4.1). Furthermore, CH_4 is a significant sink of tropospheric OH radicals and, hence, changes in its abundance can lead to changes in the lifetimes of ozone-depleting substances removed by OH (e.g., CH_3CCl_3, HCFCs, VSLS).

A detailed description of the global methane budget and its uncertainties through 2005 is given in the IPCC AR4 (Forster et al., 2007). They reported that the global average CH_4 mole fraction in 2005 was 1774 ppb, which far exceeds the natural range during the last 650,000 years, and that the observed increase since preindustrial times is very likely due to anthropogenic activities (agriculture, fossil fuel use, etc.). Here we focus on important results published afterwards and any similarities and differences between these recent and earlier studies.

For the IPCC A2 scenario, Portmann and Solomon (2007) compute methane-induced ozone increases over the 21st century of 2–12% below 20 km, and 0–4% between 20 and 40 km. On the other hand, they compute ozone decreases of 0–12% between 40 and 60 km. By 2008, the radiative forcing of CH_4 arising from mixing ratio changes since 1750 had reached about 0.5 W/m^2, second only to CO_2. Indirect effects of atmospheric methane related to changes in stratospheric H_2O and tropospheric ozone suggest that the present-day net radiative forcing of CH_4 could be as large as 0.7 W/m^2 (Forster et al., 2007).

After eight years of minimal net change, the mole fractions of CH_4 began to increase in 2007 in both hemispheres (Rigby et al., 2008; Dluogokencky et al., 2009). The growth rate was about 0.9 ± 3.3 ppb/yr from 1998–2006, while the global growth rate for 2007–2008 averaged 5.9 ppb/yr (NOAA) or 8.4 ppb/yr (AGAGE) (Table 1-15). The growth rate anomalies during 2006–2008 have been similar in magnitude to those observed in some years since 1990. The inverse analysis of Rigby et al. (2008) suggests that the renewed increase in growth rate was attributable either to increasing tropical and high latitude emissions or to a smaller high latitude emissions increase along with a few percent low latitude OH decrease (or to some combination of the two). A second analysis of spatial gradients

Table 1-15. Mole fractions of CO_2, CH_4, N_2O, SF_6, SO_2F_2, COS, and selected HFCs and PFCs.

	Mole Fraction				Annual Change in Mole Fraction		
	2005	**2006**	**2007**	**2008**	**2005/06**	**2006/07**	**2007/08**
CO_2 [ppm] N	378.8	381.0	382.7	384.8	2.2	1.7	2.1
CH_4 [ppb] N	1774.7	1775.4	1781.7	1787.6	0.7	6.3	5.9
CH_4 [ppb] A	1774.2	1774.6	1780.8	1789.2	0.4	6.2	8.4
N_2O [ppb] N	319.0	319.8	320.5	321.5	0.8	0.7	1.0
N_2O [ppb] A	319.2	319.9	320.6	321.6	0.7	0.7	1.0
SF_6 [ppt] N	5.6	5.9	6.2	6.4	0.3	0.3	0.2
SF_6 [ppt] A	5.6	5.9	6.2	6.4	0.3	0.3	0.2
HFC-134a [ppt] N	34.4	38.8	43.2	47.6	4.4	4.4	4.4
HFC-134a [ppt] A	34.6	38.9	43.3	48.2	4.3	4.4	4.9
HFC-23 [ppt] A *	19.0	20.0	21.0	21.8	1.1	1.0	0.8
HFC-152a [ppt] A	4.1	4.5	5.3	5.9	0.4	0.8	0.6
HFC-143a [ppt] A	5.8	6.6	7.5	8.5	0.8	0.9	1.0
HFC-32 [ppt] A	1.3	1.6	2.1	2.7	0.3	0.5	0.6
HFC-125 [ppt] A	3.9	4.5	5.2	6.1	0.6	0.7	0.9
HFC-365mfc [ppt] A	0.1	0.3	0.4	0.4	0.2	0.1	0.1
HFC-245fa [ppt] **	0.4	0.6	0.7	1.0	0.2	0.1	0.4
PFC-14 [ppt] A	75.1	75.7	76.4	77.1	0.6	0.7	0.7
PFC-116 [ppt] A	3.7	3.8	3.8	3.9	0.1	0.0	0.1
PFC-218 [ppt] A	0.4	0.4	0.5	0.5	0.0	0.1	0.0
SO_2F_2 [ppt] A	1.35	1.42	1.47	1.51	0.07	0.05	0.04
COS [ppt] N	488	491	494	491	2.2	2.9	−2.1

Data are global surface means.

These observations are updated from the following sources: Conway et al. (1994), Dlugokencky et al. (2009), Geller et al. (1997), Greally et al. (2005; 2007), Hall et al. (2007), Miller et al. (2010), Montzka et al. (1996; 2007), Mühle et al. (2009; 2010), O'Doherty et al. (2004; 2009), Prinn et al. (2000), Rigby et al. (2008), Stemmler et al. (2007), and Vollmer et al. (2006).

Annual changes in mole fraction are drived from the difference between year *x* and *x*-1.

N denotes data from NOAA.

A denotes data from AGAGE.

* Global averaged mixing ratios for HFC-23 before 2007 have been modeled using archived air data from the SH (Miller et al., 2010)

** Data are an average of measurements from the Jungfraujoch, Switzerland (47°N) and Cape Grim, Australia (40°S) (updated from Vollmer et al., 2006).

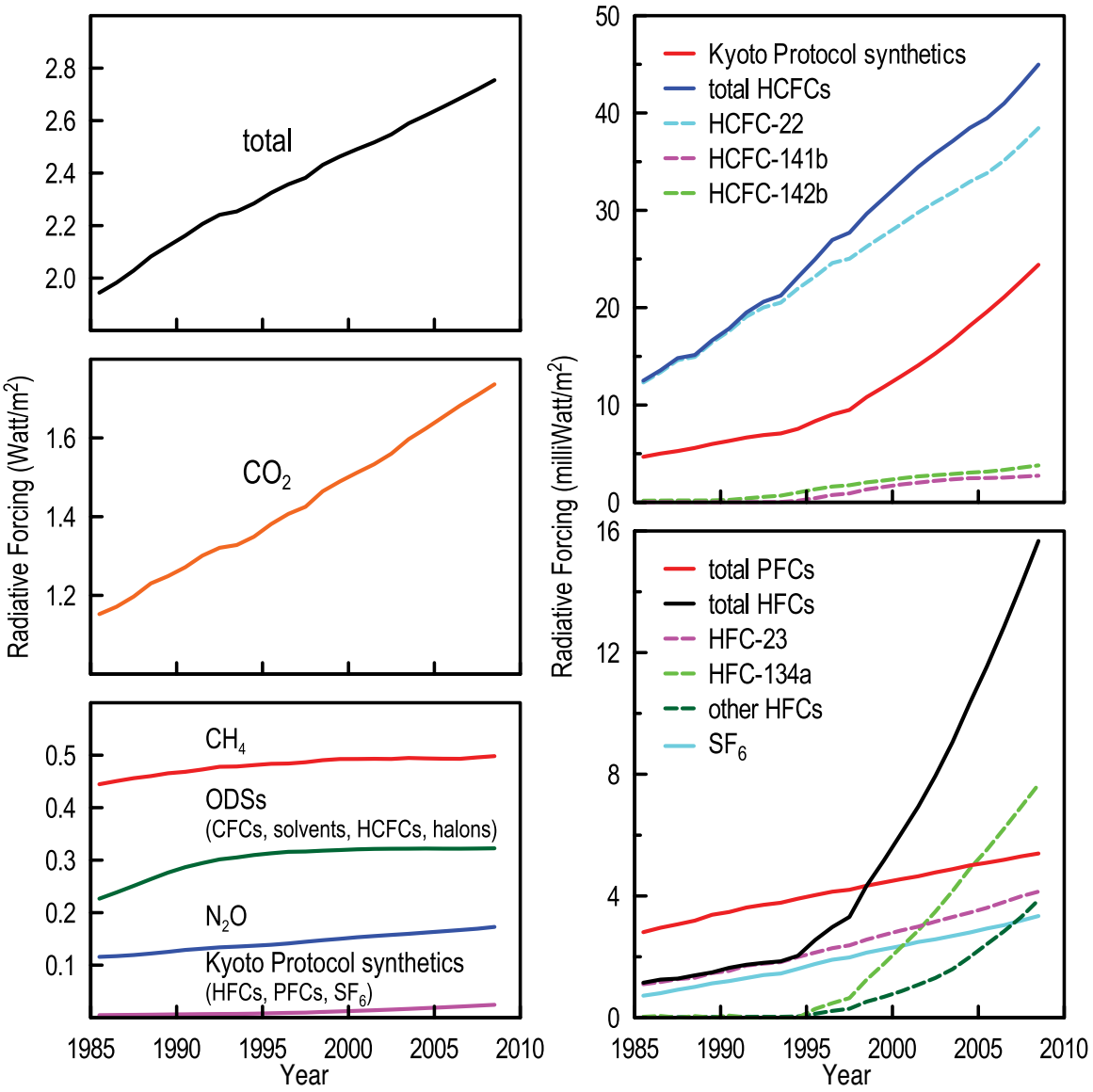

Figure 1-24. Left panels: The evolution of radiative forcings from the sum of the major greenhouse gases (CO_2, CH_4, N_2O), the ODSs (CFCs, HCFCs, halons, CH_3CCl_3, CCl_4), and the Kyoto Protocol synthetic gases (HFCs, PFCs, SF_6) in W/m^2. Right panels: The upper panel shows the evolution of radiative forcings (note change in scale) from individual HCFCs and their sum, and from the sum of Kyoto Protocol synthetic gases (HFCs, PFCs, and SF_6), which appear individually or grouped together in the lower right panel (in mW/m^2). Forcings are calculated from background mixing ratios in Table 1-1 and Table 1-15 and radiative efficiencies given in Chapter 5.

and Arctic isotopic signals by Dlugokencky et al. (2009) suggests primarily an increased wetland source in both the high latitudes and tropics for 2007, while the 2008 increase was predominantly seen at tropical latitudes. They argued for little influence from OH variations. Furthermore, an increase in interhemispheric exchange during the cool phase of the El Niño-Southern Oscillation (ENSO) (consistent with observed changes in the SF_6 mean interhemispheric difference), could have contributed, in part, to changes in Southern Hemisphere growth rates. Bousquet et al. (2006) suggested that the relatively stable period for CH_4 mixing ratios between 1999 and 2006 was a fortuitous combination of a decreasing wetland source masking an increasing anthropogenic energy-related source, with the chemical loss of CH_4 due to OH playing a potential role in the observed atmospheric variability. In compari-

son, Chen and Prinn (2006) evaluated growth rates and distributions of CH_4 during 1996–2001 relative to earlier years and found decreased energy-related emissions and increased emissions from rice, with the 1998 anomaly due to increased global wetland and wildfire emissions. Chen and Prinn (2006) note that their inferred increased rice emissions (about 25 Tg CH_4/yr) could also be attributed to surrounding non-rice wetland emissions.

While the possibility of very large methane emissions from plants (as proposed by Keppler et al., 2006) has been ruled out (Ferretti et al., 2007; Beerling et al., 2008; Bloom et al., 2010a), laboratory experiments have shown that UV-irradiated plant pectin produces CH_4 (Vigano et al., 2008). While not ascribed to aerobic methanogenesis, Carmo et al. (2006) presented evidence for a canopy source of CH_4 from upland forest and Rice et al. (2010) reported a "bottom-up" estimate of global CH_4 emissions of 60 ± 20 Tg/year from trees in flooded soils.

In the last decade, satellite observations have become available that fill an important gap in the global coverage of the temporal and spatial variations of CH_4 (e.g., Frankenberg et al., 2005; Frankenberg et al., 2008). Furthermore, satellite observations have also detected an increase in global mixing ratios in recent years (Bloom et al., 2010b) and identified increased wetland emissions as a potential cause, consistent with in situ measurements.

Future trends in atmospheric CH_4 are highly uncertain and depend to a large extent on the proportion of the carbon stored in Arctic permafrost that emanates as CH_4 following permafrost thaw and the extent of permafrost thawing. Tarnocai et al. (2009) estimate that frozen Arctic soils contain about 1670 petagrams (Pg) of carbon. While current observations do not imply a large role for thawing permafrost, this could change with large future Arctic warming. Additionally, large stores of CH_4 exist in the form of frozen CH_4 hydrates on the sea floor (Buffett, 2004). These potentially could be liberated either by warming induced by ocean circulation changes or via attempted extraction for fuel usage. Changes in wetland extent, agricultural practice, and fossil fuel extraction (excluding hydrates) could also affect future atmospheric CH_4 levels, but have much smaller potential for impact than the large frozen soil-carbon reservoirs mentioned above.

1.5.1.2 Nitrous Oxide (N_2O)

The photochemical degradation of nitrous oxide (N_2O) in the stratosphere leads to ozone-depleting nitric oxide (NO) and nitrogen dioxide (NO_2) and to important free radical reservoir species (e.g., HNO_3, $ClONO_2$). In addition, N_2O is an important greenhouse gas.

Forster et al. (2007) reported that the global average mole fraction of N_2O in 2005 was 319 ppb compared to a preindustrial value of 270 ppb. The growth rate has been approximately constant since 1980 with more than one-third of its emissions being anthropogenic (agriculture, etc.). In 2005–2008 the average growth rate of N_2O was 0.8 ppb/yr (NOAA and AGAGE), with an average global mixing ratio in 2008 of 321.5 ppb (NOAA) and 321.6 ppb (AGAGE) (Table 1-15). N_2O is an important ozone-depleting and greenhouse gas. For the A2 IPCC scenario, Portmann and Solomon (2007) compute 21st century ozone decreases up to 8% in the 20–40 km altitude region from changes in N_2O alone. By comparing the Ozone Depletion Potential-weighted anthropogenic emissions of N_2O with those of ozone-depleting substances, Ravishankara et al. (2009) show that N_2O emissions currently are the single most important emissions of a chemical that depletes ozone. Yet, N_2O is not controlled by the Montreal Protocol. The findings of Ravishankara et al. (2009) are discussed in more depth in Sections 5.2 and 5.4 of Chapter 5. Future anthropogenic emissions of N_2O may increase if nitrogen-containing fertilizer use is enhanced for the production of biofuels, as discussed by Crutzen et al. (2008). Limiting or reducing future N_2O emissions, one target of the Kyoto Protocol, would enhance the recovery of the ozone layer from its depleted state and would also reduce anthropogenic forcing of the climate system.

Recently, Huang et al. (2008) used AGAGE, NOAA/ESRL, and Commonwealth Scientific and Industrial Research Organisation (CSIRO) observations, the 3-D MATCH model (1.8° × 1.8°), and a Kalman filter to deduce regional N_2O emissions. The effects of model errors were assessed using a large ensemble of 2-D model inversions. They concluded that global N_2O emissions with 66% probability errors are $16.3^{+1.5}_{-1.2}$ and $15.4^{+1.7}_{-1.3}$ Tg N (N_2O)/yr, for 1997–2001 and 2001–2005, respectively. Emissions from the equator to 30°N increased significantly from the earlier Bouwman et al. (1995) estimates, while emissions from the southern oceans (30°S–90°S) decreased significantly. Relative to Bouwman et al. (1995), Huang et al. (2008) found that land emissions from South America, Africa, and China/Japan/South East Asia are larger, while land emissions from Australia/New Zealand are smaller. Their study also showed a shift of the oceanic sources from the extratropical to the tropical oceans relative to Bouwman et al. (1995). Between the periods 1996–2001 and 2002–2006, emissions increased in China/Japan/South East Asia, 0°–30°N oceans, and North West Asia; emissions decreased in Australia/New Zealand, 30°S–90°S oceans, 30°N–90°N oceans, and Africa. The lower tropical ocean emissions in 1997–2001 relative to 2002–2005 could result from the effects of the 1997–1998 El Niño in the earlier period.

The N_2O fluxes from the equator to 30°N region reported by Hirsch et al. (2006) and Huang et al. (2008) are significantly larger than estimated by Bouwman et al. (1995) and Prinn et al. (1990), while the emissions

from the southern oceans (30°S–90°S) are significantly smaller. The differences between the two recent and two earlier studies may be due to either real long-term variations or different modeling and methodological approaches. Huang et al. (2008) found that 23 ± 4% of the global total N_2O emissions come from the oceans, which is at the low range of the Hirsch et al. (2006) and Bouwman et al. (1995) estimates. Overall, the Hirsch et al. (2006) and Huang et al. (2008) studies show reasonably good agreement. Considering the fact that Hirsch et al. (2006) only used N_2O measurements from NOAA/ESRL for the 1998 to 2001 time period and the inversion techniques and transport models used in the two studies differ as well, these good agreements may indicate that the relative contributions of regional N_2O surface fluxes to the global total may indeed have changed significantly from the Bouwman et al. (1995) estimates for 1990 and the Prinn et al. (1990) estimates for 1978–1988. In comparison with Prinn et al. (1990), the Huang et al. (2008) study shows smaller surface emissions in the 30°S–90°S and 30°N–90°N regions, significantly higher fluxes in the 0°–30°N region, and similar fluxes in the 0°–30°S region. Huang et al. (2008) concluded that uncertainty in modeling troposphere and stratosphere exchange is the most significant source of uncertainty in deriving regional N_2O emissions.

High-precision measurements of atmospheric N_2O over the last decade reveal subtle signals of interannual variability (IAV) superimposed upon the more prominent growth trend. Nevison et al. (2007) explored the causes of both seasonal and interannual variability using comparisons of a 1993–2004 3-D model simulation to observations of N_2O at five AGAGE stations. The model does not include a stratospheric sink and thus isolates the effects of surface sources and tropospheric transport. Both model and observations yield correlations in seasonal and interannual variability among species, but only in a few cases are model and observed variability correlated to each other. The results suggest that tropospheric transport contributes significantly to observed variability, especially at the Samoa station. However, some features of observed variability (e.g., at Mace Head, Ireland) are not explained by the model simulation and appear more consistent with the effects of downward mixing of N_2O-poor stratospheric air.

Finally, Jiang et al. (2007) carried out a systematic study of the N_2O seasonal cycle and its latitudinal variation using AGAGE and NOAA/ESRL data. The seasonal cycles were statistically significant at Alert (82°N, 62°W), Barrow (71°N, 157°W), Mace Head (53°N, 10°W), Cape Kumukahi (19°N, 155°W), Cape Matatula (14°S, 171°W), Cape Grim (41°S, 145°E), and South Pole (90°S, 102°W). The amplitude (peak to peak) of the seasonal cycle varies from 0.29 ppb at the South Pole to 1.15 ppb at Alert. The month at which the seasonal cycle is at a minimum varies monotonically from April (South Pole) to September (Alert). The seasonal cycle in the Northern Hemisphere shows the influence of the stratosphere, owing to seasonal variations in exchange between the stratosphere and troposphere in the Arctic; the seasonal cycle in the Southern Hemisphere suggests greater influence from surface sources.

1.5.1.3 COS, SO_2, and Sulfate Aerosols

Carbonyl sulfide (COS) and other sulfur-containing gases such as sulfur dioxide (SO_2) are important precursors of sulfate aerosols in the stratosphere (Notholt et al., 2005; SPARC, 2006), which catalyze ozone depletion by ODSs (e.g., Newman and Pyle et al., 2003; Danilin and McConnell, 1995) and affect the radiative balance of the atmosphere (e.g., Forster et al., 2007). The relative contributions of the sulfate aerosol precursors are difficult to quantify because SO_2 has a short lifetime, and the nonvolcanic stratospheric sulfur (S) burden is not well determined.

COS is the most abundant sulfur-containing trace gas in the atmosphere. Long-term trends in COS mixing ratios suggest that global changes during the past decade have been fairly small (Aydin et al., 2008; Montzka et al., 2004; Montzka et al., 2007; Zander et al., 2005). Updated data show a mean global surface mixing ratio of 491 ppt in 2008 and a mean rate of increase of 1.8 ppt/yr during 2000–2008 (Table 1-15). The current background concentration is more than 60% higher than preindustrial values of ~300 ppt (Montzka et al., 2004; Aydin et al., 2008). Long-term COS trends from long-path infrared solar absorption measurements above Jungfraujoch (Switzerland) (updated from Zander et al., 2005) show an annual increase in the total vertical column of 0.79 ± 0.09% over 2000–2008 (relative to January 2000 values) and an increased growth rate of 1.26 ± 0.29%/yr over 2005–2008 (relative to January 2005 values). Over decadal-to-centennial periods, COS mixing ratios appear correlated to anthropogenic sulfur emissions (Montzka et al., 2004). The updated Jungfraujoch data also show this behavior, exhibiting decreases in total column COS during the late 1980s to early 1990s. Both ground-based flask sampling and Jungfraujoch remote sensing results then show a reversal, with increases since the mid-2000s, concurrent with 5%/yr increases in global coal combustion since then (BP, 2009).

Global flask measurements show large seasonal changes across broad geographic scales (Montzka et al., 2007). The observed variations suggest an important role for the oceans in determining the seasonality in the SH and uptake by the terrestrial biosphere during the growing season in the NH. The amplitude of observed seasonal changes in the NH suggests significantly larger vegetative

uptake of COS and, as a result, a shorter global lifetime of 2-4 yrs (Montzka et al., 2007; Suntharalingam et al., 2008) than derived in earlier studies.

COS mixing ratio distributions derived from satellites have provided an estimate of COS stratospheric loss. From correlations to measured CFC abundances, a stratospheric lifetime of 64 ± 21 years can be derived. This lifetime suggests that COS contributes 34–66 Gg S/yr to the stratosphere (Barkley et al., 2008). Given the wide range in estimates of sulfur emissions necessary to maintain the stratospheric sulfate aerosol layer, it is difficult to accurately estimate the contribution of sulfur from COS to this layer. Some estimates from midlatitude data suggest that COS could contribute ~50% of aerosol sulfur mass being transported to the midlatitude lower stratosphere (Martinsson et al., 2005). Other results implying 300–400 Gg S/yr to explain observed seasonal changes above some NH sites would suggest a much smaller relative contribution of COS to stratospheric sulfur (Hofmann et al., 2009). This latter study also provided evidence for large changes in stratospheric aerosol during recent years. Because COS mixing ratios in the background atmosphere have not increased by more than a few percent since 2000, the cause for this aerosol increase is not likely attributable entirely to the observed COS changes (Hofmann et al., 2009).

Sources of atmospheric SO_2 have been reviewed by Stern (2005) and Fisher et al. (2007). Anthropogenic emissions of SO_2 are mainly due to fossil fuel burning and metal smelting. Natural sources consist of the oxidation of COS, dimethyl sulfide (DMS), carbon disulfide (CS_2), and hydrogen sulfide (H_2S), as well as emissions from volcanic activities. Based on "bottom-up" estimates (see Box 1-1), anthropogenic sulfur emissions reached a maximum of ~75 Tg S/yr in the 1980s (Stern, 2005). Emissions subsequently decreased as a consequence of legislation addressing enhanced acidification (in industrialized countries) and because of reduced industrial activity in Eastern Europe (Stern, 2005). In 2000, global emissions were estimated to be 55–62 Tg S/yr (Fisher et al., 2007), of which ~17 Tg S/yr was emitted from Asia (Stern, 2005; Klimont et al., 2009). In some projections future emissions from Asia are expected to increase substantially (e.g., 40 Tg S/yr by 2030; Klimont et al., 2009), with the main increase expected to occur either in China (Fisher et al., 2007) or in India (Klimont et al., 2009). SO_2 mixing ratios decline rapidly with height and distance from the source regions to a few tens of ppt (SPARC, 2006), and therefore the same limitations for its transport into the stratosphere apply as for VSLS discussed in Section 1.3.

Natural sources of atmospheric SO_2, which consist of volcanic eruptions and the oxidation of primarily oceanic substances (COS, DMS, and H_2S), are estimated to account for 17–41 Tg S/yr (Haywood and Boucher, 2000). Infrequent explosive volcanic eruptions do temporarily enhance the sulfate aerosol burden of the stratosphere dramatically. For example, in 1991 the eruption of Mt. Pinatubo added ~10 Tg S into the atmosphere (Read et al., 1993; Guo et al., 2004), which partly reached the stratosphere and significantly affected the atmospheric radiative balance. Deliberately enhancing S in the stratosphere is being discussed as a geoengineering option for mitigating the heating influence from greenhouse gases (see Chapter 5).

1.5.2 Changes in Radiative Trace Gases that Indirectly Influence Ozone

Carbon dioxide and fluorinated compounds are greenhouse gases and have no direct effect on stratospheric ozone. Nevertheless, they are discussed in this section, as their impact on global warming can indirectly lead to changes in stratospheric ozone, as discussed in Chapter 4 of this Assessment.

1.5.2.1 Carbon Dioxide (CO_2)

Since 1750 CO_2 has been the most important anthropogenic greenhouse gas and it still continues to dominate atmospheric radiative forcing at 1.74 W/m^2 in 2008 (Hofmann et al., 2006) (Figure 1-24). The 2003.5–2008.5 increase in CO_2 radiative forcing (0.14 W/m^2) was six times greater than the total direct forcing increase from all other radiatively active, long-lived gases in this same period.

In 2008, the global average CO_2 mole fraction was 384.8 ppm (Table 1-15). The global growth rate of CO_2 averaged 2.1 ppm/yr between 2005 and 2008, when derived with results from all 37 marine boundary layer sites in the NOAA/ESRL surface air sampling network. This is similar to the average growth rate for the previous four-year period (2.0 ppm/yr), but significantly higher than the average growth rate in the 1990s (1.5 ppm/yr). The increase in atmospheric growth rate in the last 8 years corresponds closely with acceleration in the combustion of fossil fuels (Boden et al., 2009; BP, 2009). The increase in global fossil fuel-based CO_2 emissions averaged 0.8%/yr in the 1990s and 3.2%/yr between 2000 and 2008 (with estimated emissions of 8.7 Pg C/yr in 2008).

The fraction of fossil carbon remaining in the atmosphere (airborne fraction) shows no discernible trend over the past 20 years, with 5-year means stable at about 50% (Knorr et al., 2009). There is significant interannual variability in the atmospheric growth (and airborne fraction), of which about 50% can be explained by ENSO and volcanism (Bacastow, 1976; Reichenau and Esser, 2003) and their effect on carbon balance of the land biosphere.

Although the number of coupled climate carbon cycle models and their mechanistic sophistication has increased, there is still no consensus as to the centennial-

scale fate of the airborne fraction and the 50% radiative forcing discount that it has provided in recent decades. Most models predict a declining efficiency in the uptake of atmospheric carbon by the oceans by the middle of the century (Friedlingstein et al., 2006). Whether or not this decline can be observed already in the Southern Ocean is a matter of scientific debate and is discussed in detail in Chapter 4. The fate of the land biosphere sink of CO_2 is also uncertain, with some models predicting increased uptake due to boreal forest expansion and general CO_2 fertilization, while others predict drought-stress related die back of forests and losses in productivity (Friedlingstein et al., 2006). The coupling of the carbon cycle to climate variability remains a first-order uncertainty in the prediction of future climate. This is especially true considering the uncertain fate of an estimated 1000 Pg C of carbon frozen in the top 3 meters of Arctic soils (Tarnocai et al., 2009), which have not been considered in coupled climate carbon cycle models.

1.5.2.2 Fluorinated Greenhouse Gases

With the exception of carbon tetrafluoride (CF_4), the fluorinated compounds discussed in this section are virtually entirely of anthropogenic origin. Hydrofluorocarbons (HFCs) are replacement chemicals for the long-lived ODSs in various applications such as refrigeration, fire extinguishers, propellants, and foam blowing (IPCC/TEAP, 2005). The very long-lived perfluorocarbons (PFCs) and sulfur hexafluoride (SF_6) have been emitted over past decades from established industrial processes and, in the case of PFCs, recently from newer applications largely in the electronics sector. The newest compounds detected in the atmosphere are sulfuryl fluoride (SO_2F_2) (used as a replacement for CH_3Br) and nitrogen trifluoride (NF_3) used in the electronic sector.

By mid-2008, the contribution of the fluorinated substances (HFCs, PFCs, SF_6) to radiative forcing had increased to ~24 mW/m^2. Contributions were 16 mW/m^2 for HFCs (including HFC-23), 3.4 mW/m^2 for SF_6, and 5.4 mW/m^2 from the sum of CF_4, C_2F_6, and C_3F_8 (Mühle et al., 2010), assuming a natural background for CF_4 of 34.7 ppt (Figure 1-24). These contributions to total radiative forcing by 2008 are small compared to CO_2 (1740 mW/m^2), CH_4 (500 mW/m^2), CFCs (262 mW/m^2), and N_2O (170 mW/m^2), but amount to about half of the radiative forcing from HCFCs (45 mW/m^2) (Figure 1-24). However, these values are radiative forcings since preindustrial times. Considering changes only over the past 5 years (2003.5–2008.5), CO_2 direct radiative forcing increased by 139 mW/m^2, that from N_2O increased by 12 mW/m^2, and that from CH_4 increased by 4 mW/m^2. Radiative forcing from the sum of HFCs, PFCs, and SF_6 increased by 8 mW/m^2 over this same period, whereas the ODSs controlled under the Montreal Protocol have positive and negative contributions (CFCs, Cl-solvents, and halons: −8 mW/m^2; HCFCs: +8 mW/m^2). This means that during 2003.5–2008.5, the change in direct radiative forcing from the sum of HFCs, PFCs, and SF_6 was comparable to the change in direct radiative forcing from either CH_4 or N_2O. Further impacts of the potential large future increase of fluorinated greenhouse gases are discussed in Chapter 5 of this Assessment.

Summed emissions from HFCs used primarily as replacements for ODSs (i.e., not HFC-23) have increased since 2004. The sum of emissions (weighted by GWP) of HFCs used as ODS replacements increased by 8–9%/yr from 2004 to 2008, and by 2008 amounted to 0.39 ± 0.03 gigatonnes of CO_2 equivalents per year (Gt CO_2-eq/yr). Emissions of HFC-23, predominantly the result of HCFC-22 production, contributed an additional ~0.2 Gt CO_2-eq/yr emission during 2006–2008 (Montzka et al., 2010). Recently published data with higher time resolution suggest that the 2008 HFC-23 emission may be slightly less than this 3-year average (~0.17 Gt CO_2-eq/yr in 2008; Miller et al., 2010).

The following paragraphs are an update on the abundance and the sources of different types of fluorinated greenhouse gases (GHGs).

HFC-134a (CH_2FCF_3)

HFC-134a has replaced CFC-12 as the preferred refrigerant in refrigeration and mobile air conditioning (MAC), and it also has a minor usage in foam blowing applications. Observed global abundances and rates of change estimated by two independent global sampling networks (NOAA and AGAGE) are in good agreement. HFC-134a has been growing steadily and reached a global mean mole fraction of ~48 ppt in 2008 (Table 1-15), with an average trend of 4.6 ppt/yr (or ~10%/yr) in 2007–2008. HFC-134a contributed ~8 mW/m^2 to atmospheric radiative forcing in 2008.

A 12-box model analysis of measured changes in the global atmospheric abundance of HFC-134a was used to derive global emissions of 149 ± 27 Gg/yr during 2008 (approximately 125 ± 16 Gg/yr was derived for 2005–2006). Stohl et al. (2009) used regional-scale inversions with a global coverage to derive global HFC-134a emissions in 2005–2006 of 130–140 Gg/yr, similar to the 12-box model result for these years once uncertainties are considered. Analyses of pollution events observed by high-frequency measurements and other regional studies provide insights into regional contributions to these global emissions. In the Stohl et al. (2009) study for the period 2005–2006, about 40 Gg/yr was attributed to North America, 25 Gg/yr to Europe, 43 Gg/yr to Asia, and lesser amounts were derived for other regions of the globe. For the United States alone, Stohl et al. (2009) derived 28–35

Gg/yr of HFC-134a emission in 2005 and 2006, which is similar to the 27 (12–39) Gg/yr HFC-134a emissions from the United States estimated from aircraft measurement campaigns in 2004 and 2006 (Millet et al., 2009). In a separate study in which high-frequency data from three stations in Eastern Asia were considered, East Asian emissions of HFC-134a were estimated at 19.2 Gg/yr in 2008, of which 12.9 ± 1.7 Gg/yr was attributed to China (Stohl et al., 2010). This is only slightly higher than the HFC-134a emission estimate for China of 8.7 (6.5–12) Gg/yr in 2008 derived from high-frequency atmospheric measurements in South Korea (Kim et al., 2010).

Because of the long lifetime of HFC-134a (13.4 years, Table 1-3) and a relatively high GWP_{100} (1370, Chapter 5), the use of HFC-134a will eventually be phased out in Europe. This will lead to a very gradual phase-down of the use of HFC-134a in cars, which is expected to also take place outside Europe because of the global nature of the car industry. However, in developing countries the potential for growth of HFC-134a is potentially large (Velders et al., 2009).

HFC-23 (CHF_3)

HFC-23 is primarily emitted to the atmosphere from over-fluorination of chloroform during the production of HCFC-22. Other minor emissions of HFC-23 arise from the electronics industry, refrigeration, and fire extinguishers (Oram et al., 1998). Due to its long lifetime of 222 years (Table 1-3) and continued emissions, HFC-23 global mixing ratios reached 22 ppt in 2008, with a growth rate of 0.83 ppt/yr (Miller et al., 2010). At this global abundance, HFC-23 contributed ~4 mW/m^2 to the atmospheric radiative forcing in 2008 (Figure 1-24).

A study of Antarctic firn air suggested a 50% increase in global HFC-23 emissions from 8.7 ± 2 Gg/yr during the 1990s to a mean of 13.5 ± 2 Gg/yr during 2006–2008 (Montzka et al., 2010). HFC-23 emissions increased even though emissions reported by developed countries declined from 6–8 Gg/yr in the late 1990s to 2.8 Gg/yr in 2007 and despite the destruction by incineration of 5–7 Gg of HFC-23 in developing countries in 2007–2008 through United Nations Framework Convention on Climate Change (UNFCCC) Clean Development Mechanism (CDM) projects (Montzka et al., 2010). The increase inferred for global HFC-23 emissions is coincident with a substantial increase in HCFC-22 production in developing countries, which accounted for 60% of global HCFC-22 production in 2007. The mean yield of HFC-23 emission from global HCFC-22 production during 2006–2008 was estimated at 1.7 ± 0.3%, which is slightly lower than the mean of 2.3% derived for the early 1990s (Montzka et al., 2010).

These firn-air-derived global emission estimates for HFC-23 are largely consistent with a recent analysis of archived air (back to 1978) and ongoing remote atmospheric measurements at multiple sites since late 2007 (Miller et al., 2010). These ongoing data provide higher time resolution during 2006–2008 than the analysis of firn measurements, however, and suggest that global HFC-23 emissions declined after 2006 and were 12.0 (+0.6/−0.7) Gg/yr in 2008.

East Asian HFC-23 emission magnitudes and distributions have been derived using inversion modeling of in situ measurements at three locations (Stohl et al., 2010). Emissions from this region during 2008 were dominated by 6.2 ± 0.7 Gg/yr from China. This analysis yielded enhanced emissions from locations where HCFC-22 production facilities are known to be located, both in China and Japan (Stohl et al., 2010). The uncertainties (1 standard deviation) quoted in Stohl et al. (2010) do not include any systematic errors in their dispersion model or in the meteorological input data used in their inversion analysis. A higher HFC-23 emission of 12 (8.6–15 Gg/yr) was derived in 2008 for China recently from a combined inversion/ratio method based on data from the Korean Gosan station (Kim et al., 2010). This is similar to the 10 ± 5 Gg/yr inferred from China for 2004 and 2005 in an earlier study (Yokouchi et al., 2005). Substantial HFC-23 emissions from China are likely ongoing in 2008 because less than half of HCFC-22 production in developing countries during this time was associated with the UNFCCC CDM projects (Montzka et al., 2010).

HFC-152a (CH_3CHF_2)

HFC-152a is used as a foam-blowing agent and as an aerosol propellant (Greally et al., 2007). In 2008 its globally averaged mole fraction was 5.9 ppt and its radiative forcing 0.5 mW/m^2. It has a relatively short lifetime of 1.5 years (Table 1-3), due to efficient removal by OH oxidation. HFC-152a has the smallest GWP_{100} (133; Chapter 5) of all major HFCs. Given its short lifetime, the increase in background concentrations (0.6 ppt/yr (+11%/yr) in 2007–2008) implies a substantial increase of emissions in recent years. Emissions derived from the observed atmospheric change were 50 Gg/yr in 2008 (AGAGE data), compared to 28 Gg/yr in 2004 (Greally et al., 2007).

As was found for HFC-134a, an analysis of mixing ratio enhancements above background levels from high-frequency measurements suggest substantial emissions of HFC-152a from North America (12.3–15.1 Gg/yr), Asia (9.6–9.8 Gg/yr), and Europe (3.5–3.9 Gg/yr) during 2005–2006 (Stohl et al., 2009). The total global emissions derived from this regional study (29 Gg/yr in 2005 and 33 Gg/yr in 2006) are similar to the global emission totals derived from the 12-box analysis of mean global mixing ratio changes (34 ± 4 in 2005 and 41 ± 4 Gg in 2005 and 2006, respectively) once uncertainties are considered.

HFC-143a (CH_3CF_3)

Mixing ratios of HFC-143a, which is used mainly in refrigerant blends, of 1.8 ppt have been reported in 1997 by Culbertson et al. (2004), with a strong increase (25%/yr) in the second half of the 1990s. Recent independent measurements from the AGAGE network show that HFC-143a increased to 8.5 ppt in 2008, increasing by 1.0 ppt/yr (13%/yr) in 2007–2008 (updated from Greally et al., 2005), resulting in a radiative forcing of 1 mW/m^2 and global emissions of 17 Gg/yr in 2008.

HFC-32 (CH_2F_2)

Mixing ratios of HFC-32, which is mainly used in refrigerant blends, were reported by Greally et al. (2005) to be 0.7 ppt in 2004 at Mace Head (Ireland). Updated measurements from the AGAGE network show that mixing ratios have increased to 2.7 ppt in 2008 with a yearly increase of 0.6 ppt (26%) in 2007–2008. In 2008, emissions of 8.9 Gg/yr have been derived by applying the 12-box model to AGAGE measurements.

HFC-125 (CHF_2CF_3)

HFC-125 is used in refrigeration blends and for fire suppression (IPCC/TEAP, 2005). Background mixing ratios have grown to 6.1 ppt in 2008, which results in a direct radiative forcing contribution of 1.7 mW/m^2. The interhemispheric gradient (2008) and growth rate (2007–2008) were 1.4 ppt and 0.9 ppt/yr (16%/yr), respectively (O'Doherty et al., 2009; Table 1-15), from which global emissions increasing from 7.5 Gg in 2000 to 22 Gg in 2008 are derived. European emissions in 2007 have been estimated at 3.7–5.5 Gg/yr (O'Doherty et al., 2009).

HFC-365mfc ($CF_3CH_2CF_2CH_3$) and HFC-245fa ($CF_3CH_2CHF_2$)

HFC-365mfc and HFC-245fa are replacements for HCFC-141b in foam blowing applications (Vollmer et al., 2006). HFC-365mfc showed low mixing ratios of 0.05 ppt in early 2003 at Jungfraujoch (Switzerland) (Stemmler et al., 2007). An update, using AGAGE and SOGE measurements, shows a global mixing ratio of 0.44 ppt in 2008, with a mixing ratio increase of 0.05 ppt (11%/yr) in 2007–2008, and global emissions of 3 Gg/yr in 2008. Vollmer et al. (2006) reported HFC-245fa mixing ratios of 0.3 ppt at Jungfraujoch in 2004 and estimated global emissions of 5.1–5.9 Gg/yr during 2005. The remote-atmosphere mixing ratio of HFC-245fa (results from one site in each hemisphere) reached 1.0 ppt in 2008 and had increased by 0.4 ppt (32%) from 2007 to 2008 (Vollmer et al., 2006).

HFC-227ea (CF_3CHFCF_3)

HFC-227ea is mainly used for fire suppression and to a lesser extent in metered dose inhalers, refrigeration, and foam blowing. Laube et al. (2010) have recently reported the use of firn air measurements from Greenland to reconstruct the atmospheric history of HFC-227ea in the Northern Hemisphere. These results indicated the mixing ratio has grown from less that 0.1 ppt in the 1990s to 0.59 ppt in 2007. The rate of growth increased from 0.026 ppt/yr in 2000 to 0.057 ppt/yr in 2007. Global emissions were estimated to be ~1.8 Gg/yr in 2007.

Perfluorocarbons (PFCs)

Perfluorocarbons (PFCs) have very large radiative efficiencies and lifetimes in the range of 2,000 to 50,000 years (Table 1-3). PFC-14 (CF_4) is largely emitted as a by-product of aluminium production and to a smaller degree from the electronics industry (plasma etching), while for PFC-116 (C_2F_6) both sources are significant. PFC-218 (C_3F_8) is largely emitted by the electronics industry, with very small contributions from aluminium smelting and increasing contributions from refrigeration use. The origin of PFC-c-318 (c-C_4F_8) is uncertain but possibly due to a combination of electronics (plasma etching) and plastics (PTFE) thermal decomposition (Harnisch, 1999; Harnisch, 2000).

Recently developed gas chromatography-mass spectrometry (GC-MS) instrumentation has been deployed at AGAGE sites, achieving significantly improved precisions on annual means for CF_4 (~0.1%), C_2F_6 (~0.8%), and C_3F_8 (~3%) (Greally et al., 2005; Miller et al., 2008; Mühle et al., 2010). Global mixing ratios (2008) and annual growth rates (2007–2008) for CF_4, C_2F_6, and C_3F_8 of 77.1 ppt and 0.9%/yr, 3.9 ppt and 2.6%/yr, and 0.5 and 5.2%/yr, respectively, were measured in the AGAGE network. The radiative forcing contributions by 2008 for CF_4, C_2F_6, and C_3F_8 were 4, 1, and 0.1 mW/m^2, respectively.

The preindustrial CF_4 level has been re-estimated at 34.7 ± 0.2 ppt (Mühle et al., 2010), based on analysis of Greenland and Antarctic firn air samples, slightly less than the 39 ± 6 ppt estimated previously (Harnisch et al., 1996). Direct evidence of a natural source (crustal degassing) of CF_4 sufficient to maintain preindustrial CF_4 abundances (34 ppt) has been found in desert groundwaters (Deeds et al., 2008).

From the early 1970s to the late 1990s, Greenland and Antarctic firn data suggest a small decline in CF_4 emissions from 13 Gg/yr to 11–12 Gg/yr (Worton et al., 2007). Mühle et al. (2010) report that emissions were ~15 Gg/yr in 1975, rising to ~18 Gg/yr around 1980, generally declining to ~11 Gg/yr in 2000, and stabilizing at ~11 Gg/yr thereafter. They derive a growing difference between

emissions reported by the global aluminium industry and emissions derived from atmospheric measurements in the last years. They suggest that either nonmetallic CF_4 emissions (possibly from the electronics sector) are growing or that the "bottom-up" approach to estimating CF_4 emissions from the aluminium industry is under-estimating emissions, or a combination of both. The influence of the semiconductor industry on global C_2F_6 emissions can be seen in both "bottom-up" and "top-down" estimates of emissions, increasing from about 0.5 Gg/yr to 1.8 Gg/yr between 1990 and 2001 (Worton et al., 2007).

Sulfur Hexafluoride (SF_6)

Sulfur hexafluoride (SF_6) is an important greenhouse gas because it combines a high radiative efficiency with a very long lifetime and a considerable annual increase. Global average (NOAA, AGAGE) mixing ratios of SF_6 reached 6.4 ppt in 2008, with a yearly (2007–2008) increase of 0.2 ppt/yr (3%), resulting in a contribution to radiative forcing of 3.4 mW/m^2 by 2008. Levin et al. (2010) found a similar mixing ratio of 6.7 ppt in 2008 and inferred a global emission of 7.16 Gg/yr in 2008. Comparable global SF_6 growth rates (0.2–0.3 ppt/yr) have been derived from the MIPAS satellite data in 2002–2004 (Stiller et al., 2008), and solar spectroscopy at Jungfraujoch has been used to derive long-term trends in the total column of SF_6 (Zander et al., 2008).

Nitrogen Trifluoride (NF_3)

NF_3, which is used as a replacement for PFCs in plasma etching, in the semiconductor industry, and in the production of flat panel displays, has recently been discovered in the atmosphere by Weiss et al. (2008). Although NF_3 has a high GWP it is not currently included in the Kyoto Protocol (Prather and Hsu, 2008). In 2008 the mean global tropospheric concentration was 0.45 ppt, increasing at 0.05 ppt/yr, or 11%/yr (Weiss et al., 2008). "Bottom-up" emissions in 2006 were estimated at 0.14 Gg/yr (Robson et al., 2006). This emission figure was corrected to be 0.62 Gg/yr in 2008, based on the measured global background abundance and trend by Weiss et al. (2008).

The lifetime and GWP of NF_3 have been revised since the previous Assessment by Prather and Hsu (2008). As a result the NF_3 lifetime (740 years) and GWP_{100} (17,200) given in IPCC's 4th Assessment (Forster et al., 2007) have now been revised to 500 years and 17,500, respectively (see Section 1.2.2 and Chapter 5).

Sulfuryl Fluoride (SO_2F_2)

Sulfuryl fluoride (SO_2F_2) is used as a fumigant to replace methyl bromide (except for quarantine/pre-shipment uses). The global total atmospheric lifetime of SO_2F_2 has been recently assessed to be 36 ± 11 years (Mühle et al., 2009), which is significantly longer than previous estimates (<5 years) (Table 1-3). Oceanic hydrolysis is the major sink with the global oceanic uptake atmospheric lifetime being 40 ± 13 years. Compared to hydrolysis, gas-phase tropospheric and stratospheric loss processes are only marginally important (Papadimitriou et al., 2008b; Dillon et al., 2008). The global tropospheric background concentration of SO_2F_2 has increased from ~0.3 ppt in 1978 to 1.51 ppt in 2008, with a yearly increase (2007–2008) of 0.04 ppt (3%). Papadimitriou et al. (2008b) calculated that the GWP_{100} of SO_2F_2 is 4780, similar to that of CFC-11, using newly measured infrared absorption cross sections and the lifetime reported by Mühle et al. (2009). A slightly lower GWP_{100} of 4740 is reported for SO_2F_2 in Table 1-11 owing to a slightly different radiative efficiency being used in the calculations appearing in Chapter 5 (see note 19 to Table 1-11). Sulbaek-Anderson et al. (2009b) list a GWP_{100} range of 120–7600 for SO_2F_2 lifetimes from 1–100 years. The emissions calculated from atmospheric observations increased from ~0.6 Gg in 1978 to ~1.9 Gg in 2007. Global production magnitudes of SO_2F_2 are on average 1.5 times emissions deduced from global atmospheric measurements. This suggests that about one-third of SO_2F_2 may be destroyed during application (like CH_3Br) or the presence of additional losses.

1.5.3 Emissions of Rockets and Their Impact on Stratospheric Ozone

In this section the historic and actual emissions of rockets and their potential to impact stratospheric ozone are discussed. The future emissions and their impacts will be discussed in Section 5.4.2.5 of Chapter 5 of this Assessment.

A variety of propellant combinations contribute to the global emissions of rockets. All produce gases and particles that affect ozone chemistry in the stratosphere and mesosphere to varying degrees. The emissions from solid rocket motors (SRM) are much better understood than the emissions from the three liquid propellant types—liquid oxygen/kerosene (O_2/HC), cryogenic (O_2/H_2), hypergolic (N_2O_4/hydrazine), and hybrid (N_2O/HC).

It is thought that chlorine and aluminum oxide ("alumina") from SRMs account for most of the global ozone loss associated with worldwide rocket launches. Global, annually averaged ozone losses due to these emissions are estimated to be of the order of 0.1% or less (Ross et al., 2009), though this still has not been confirmed with observations or models.

Since the last Assessment of rocket impacts on stratospheric ozone (Newman and Pyle et al., 2003), there

have been some important developments that impact projections of ozone losses due to rockets. First, the decreasing trend in rocket launches at the start of the 21st century has reversed, with the global annual launch rate increasing by 20% since 2005 (http://planet4589.org/space/log/launchlog.txt). Second, recent studies of the mass fraction of SRM sub-micron alumina emissions call into question the assumptions that have gone into previous model estimates of the contribution of heterogeneous chlorine reactions on alumina to global ozone loss. Values for that sub-micron mass ranging from 2% (Danilin et al., 2001), 8% (Schmid et al., 2003), 12% (Brady and Martin, 1997), and 50% (Gossé et al., 2006) have now been reported. These sub-micron particles have a disproportionately large impact on ozone abundances, not only because of their high surface-to-mass ratios, but also because of their relatively long lifetimes above the tropopause compared to larger particles. In addition, the previously assumed heterogeneous reaction rates may be low compared to the actual reactivity in stratospheric plumes (Danilin et al., 2003). If the larger values of these parameters are confirmed, previous studies will have significantly underestimated ozone losses from SRMs by as much as a factor of ten. It will also be the case that rocket emissions of alumina will have a greater impact on ozone than rocket emissions of chlorine, in which case much larger impacts could be expected in cold, low-UV regions of the stratosphere (e.g., lowermost stratosphere and polar vortices in springtime). The geographic variations in ozone loss due to rockets have yet to be studied in detail.

There have been few studies of the role of rocket emissions of nitrogen oxides (NO_x). An estimate of global ozone loss from a hypergolic propellant (N_2O_4/hydrazine) rocket did show that it caused approximately 2% of the ozone loss from an SRM rocket of approximately the same payload (Ross et al., 2004). However, there are no measurements of NO_x emissions from these rockets to validate the NO_x emissions assumed in the model.

The impacts on ozone by rocket emissions other than alumina and chlorine remain unclear (e.g., water vapor, NO_x, HCs, and soot). Given the tendency for heterogeneous reactions to enhance ozone destruction, it is likely that all H_2O-containing particles produced by rockets, directly or as ice nucleation sources (e.g., alumina and soot), will be net-destroyers of ozone. Since rockets emit exhaust throughout the stratosphere, the net impact of NO_x emissions is most-likely ozone destruction via catalytic NO_x reactions and increased aerosol surface area with subsequent halogen activation. Rocket emissions of H_2O into the winter polar stratosphere and summer mesosphere can also increase occurrence frequencies of polar stratospheric and mesospheric clouds (Stevens et al., 2005; Meier, et al., 2010). At current launch rates, the impacts of non-SRM rocket emissions are thought to be less important than SRM emissions of alumina and chlorine (Ross et al., 2009).

REFERENCES

Abbatt, J.P.D., and J.G. Anderson, High-pressure discharge flow kinetics and frontier orbital mechanistic analysis for OH + CH_2CCl_2, *cis*-CHClCHCl, *trans*-CHClCHCl, $CFClCF_2$, and CF_2CCl_2 → products, *J. Phys. Chem.*, *95* (6), 2382-2390, doi: 10.1021/j100159a049, 1991.

Acerboni, G., J.A. Beukes, N.R. Jensen, J. Hjorth, G. Myhre, C.J. Nielsen, and J.K. Sundet, Atmospheric degradation and global warming potentials of three perfluoroalkenes, *Atmos. Environ.*, *35*, 4113-4123, 2001.

Aizawa, M., K. Asaoka, M. Atsumi, and T. Sakou, Seaweed bioethanol production in Japan – The Ocean Sunrise Project, *Oceans 2007*, 1-5, doi: 10.1109/OCEANS.2007.4449162, 2007.

Allen, N.D.C., P.F. Bernath, C.D. Boone, M.P. Chipperfield, D. Fu, G.L. Manney, D.E. Oram, G.C. Toon, and D.K. Weisenstein, Global carbon tetrachloride distributions obtained from the Atmospheric Chemistry Experiment (ACE), *Atmos. Chem. Phys.*, *9* (19), 7449-7459, doi: 10.5194/acp-9-7449-2009, 2009.

Andreae, M.O., and P. Merlet, Emission of trace gases and aerosols from biomass burning, *Global Biogeochem. Cycles*, *15* (4), 955-966, doi: 10.1029/2000GB001382, 2001.

Aschmann, J., B.-M. Sinnhuber, E.L. Atlas, and S.M. Schauffler, Modeling the transport of very short-lived substances into the tropical upper troposphere and lower stratosphere, *Atmos. Chem. Phys.*, 9 (23), 9237-9247, doi: 10.5194/acp-9-9237-2009, 2009.

Atkinson, R., D.L. Baulch, R.A. Cox, J.N. Crowley, R.F. Hampson, R.G. Hynes, M.E. Jenkin, M.J. Rossi, J. Troe, and T.J. Wallington, *Atmos. Chem. Phys.*, *8*, 4141-4496, 2008. Updates at: IUPAC Subcommittee for Gas Kinetic Data Evaluation: http://www.iupac-kinetic.ch.cam.ac.uk.

Aydin, M., M.B. Williams, C. Tatum, and E.S. Saltzman, Carbonyl sulfide in air extracted from a South Pole ice core: A 2000 year record, *Atmos. Chem. Phys.*, *8* (24), 7533-7542, doi: 10.5194/acp-8-7533-2008, 2008.

Bacastow, R.B., Modulation of atmospheric carbon dioxide by the Southern Oscillation, *Nature*, *261*, 116-118, doi: 10.1038/261116a0, 1976.

Barkley, M.P., P.I. Palmer, C.D. Boone, P.F. Bernath, and P. Suntharalingam, Global distributions of carbonyl sulfide in the upper troposphere and stratosphere, *Geophys. Res. Lett.*, *35*, L14810, doi:

10.1029/2008GL034270, 2008.

Beerling, D.J., T. Gardiner, G. Leggett, A. McLeod, and W.P. Quick, Missing methane emissions from leaves of terrestrial plants, *Global Change Biol.*, *14* (8), 1821-1826, doi: 10.1111/j.1365-2486.2008.01607.x, 2008.

Bell, N., L. Hsu, D.J. Jacob, M.G. Schultz, D.R. Blake, J.H. Butler, D.B. King, J.M. Lobert, and E. Maier-Reimer, Methyl iodide: Atmospheric budget and use as a tracer of marine convection in global models, *J. Geophys. Res.*, *107* (D17), 4340, doi: 10.1029/2001JD001151, 2002.

Bergamaschi, P., C. Frankenberg, J.F. Meirink, M. Krol, M.G. Villani, S. Houweling, F. Dentener, E.J. Dlugokencky, J.B. Miller, L.V. Gatti, A. Engel, and I. Levin, Inverse modeling of global and regional CH_4 emissions using SCIAMACHY satellite retrievals, *J. Geophys. Res.*, *114*, D22301, 28, doi: 10.1029/2009JD012287, 2009.

Berthet, G., J.G. Esler, and P.H. Haynes, A Lagrangian perspective of the tropopause and the ventilation of the lowermost stratosphere, *J. Geophys. Res.*, *112*, D18102, doi: 10.1029/2006JD008295, 2007.

Bhatia, A., H. Pathak, P.K. Aggarwal, and N. Jain, Trade-off between productivity enhancement and global warming potential of rice and wheat in India, *Nutr. Cycl. Agroecosyst.*, *86* (3), 413-424, doi: 10.1007/s10705-009-9304-5, 2010.

Bilde, M., T.J. Wallington, C. Ferronato, J.J. Orlando, G.S. Tyndall, E. Estupiñan, and S. Haberkorn, Atmospheric chemistry of CH_2BrCl, $CHBrCl_2$, $CHBr_2Cl$, $CF_3CHBrCl$, and CBr_2Cl_2, *J. Phys. Chem. A*, *102* (11), 1976-1986, doi: 10.1021/jp9733375, 1998.

Blei, E., C.J. Hardacre, G.P. Mills, K.V. Heal, and M.R. Heal, Identification and quantification of methyl halide sources in a lowland tropical rainforest, *Atmos. Environ.*, *44* (8), 1005-1010, doi: 10.1016/j.atmosenv.2009.12.023, 2010.

Bloom, A.A., J. Lee-Taylor, S. Madronich, D.J. Messenger, P.I. Palmer, D.S. Reay, and A.R. McLeod, Global methane emission estimates from ultraviolet irradiation of terrestrial plant foliage, *New Phytologist*, *187*, 417-425, doi: 10.1111/j.1469-8137.2010.03259.x, 2010a.

Bloom, A.A, P.I. Palmer, A. Fraser, D.S. Reay, and C. Frankenberg, Large-scale controls of methanogenesis inferred from methane and gravity spaceborne data, *Science*, *327* (5963), 322-325, doi: 10.1126/science.1175176, 2010b.

Boden, T.A., G. Marland, and R.J. Andres, Global, regional, and national fossil-fuel CO_2 emissions, Carbon Dioxide Information Analysis Center, Oak Ridge National Laboratory, U.S. Department of Energy, Oak Ridge, TN, U.S.A., doi: 10.3334/CDIAC/00001, 2009.

Bönisch, H., A. Engel, J. Curtius, Th. Birner, and P. Hoor, Quantifying transport into the lowermost stratosphere using simultaneous in-situ measurements of SF_6 and CO_2, *Atmos. Chem. Phys.*, *9* (16), 5905-5919, doi: 10.5194/acp-9-5905-2009, 2009.

Bousquet, P., P. Ciais, J.B. Miller, E.J. Dlugokencky, D.A. Hauglustaine, C. Prigent, G.R. Van der Werf, P. Peylin, E.-G. Brunke, C. Carouge, R.L. Langenfelds, J. Lathière, F. Papa, M. Ramonet, M. Schmidt, L.P. Steele, S.C. Tyler, and J. White, Contribution of anthropogenic and natural sources to atmospheric methane variability, *Nature*, *443*, 439-443, doi: 10.1038/nature05132, 2006.

Bouwman, A.F., K.W. Van der Hoek, and J.G.J. Olivier, Uncertainties in the global source distribution of nitrous oxide, *J. Geophys. Res.*, *100* (D2), 2785-2800, 1995.

BP (British Petroleum), *BP Statistical Review of World Energy 2009*, available: http://www.bp.com/liveassets/bp_internet/globalbp/globalbp_uk_english/reports_and_publications/statistical_energy_review_2008/STAGING/local_assets/2009_downloads/statistical_review_of_world_energy_full_report_2009.pdf, 2009.

Brady, B.B., and L.R. Martin, Modeling the multiphase atmospheric chemistry of launch clouds, *J. Space. Rockets*, *34* (6), 780-784, 1997.

Buffett, B., and D. Archer, Global inventory of methane clathrate: Sensitivity to changes in the deep ocean, *Earth Planet. Sci. Lett.*, *227* (3-4), 185-199, doi: 10.1016/j.espl.2004.09.005, 2004.

Butler, J.H., S.A. Montzka, A.D. Clarke, J.M. Lobert, and J.W. Elkins, Growth and distribution of halons in the atmosphere, *J. Geophys. Res.*, *103* (D1), 1503-1511, doi: 10.1029/97JD02853, 1998.

Butler, J.H., M. Battle, M.L. Bender, S.A. Montzka, A.D. Clarke, E.S. Saltzman, C.M. Sucher, J.P. Severinghaus, and J.W. Elkins, A record of atmospheric halocarbons during the twentieth century from polar firn air, *Nature*, *399* (6738), 749-755, doi: 10.1038/21586, 1999.

Butler, J.H., D.B. King, J.M. Lobert, S.A. Montzka, S.A. Yvon-Lewis, B.D. Hall, N.J. Warwick, D.J. Mondeel, M. Aydin, and J.W. Elkins, Oceanic distributions and emissions of short-lived halocarbons, *Global Biogeochem. Cycles*, *21*, GB1023, doi: 10.1029/2006GB002732, 2007.

Butler, J.H., T.G. Bell, B.D. Hall, B. Quack, L.J. Carpenter, and J. Williams, Technical Note: Ensuring consistent, global measurements of very short-lived halocarbon gases in the ocean and atmosphere, *Atmos. Chem. Phys.*, *10* (2), 327-330, doi: 10.5194/acp-10-327-2010, 2010.

Butz, A., H. Bösch, C. Camy-Peyret, M.P. Chipperfield,

M. Dorf, S. Kreycy, L. Kritten, C. Prados-Roman, J. Schwärzle, and K. Pfeilsticker, Constraints on inorganic gaseous iodine in the tropical upper troposphere and stratosphere inferred from balloon-borne solar occultation observations, *Atmos. Chem. Phys.*, *9* (18), 7229-7242, doi: 10.5194/acp-9-7229-2009, 2009.

Calvert, J.G., R.G. Derwent, J.J. Orlando, G.S. Tyndall, and T.J. Wallington, *Mechanisms of Atmospheric Oxidation of the Alkanes*, 1008 pp., Oxford University Press, New York, NY, 2008.

Carmo, J.B., M. Keller, J.D. Dias, P.B. Camargo, and P. Crill, A source of methane from upland forests in the Brazilian Amazon, *Geophys. Res. Lett.*, *33*, L04809, doi: 10.1029/2005GL025436, 2006.

Carpenter, L.J., C.E. Jones, R.M. Dunk, K.E. Hornsby, and J. Woeltjen, Air-sea fluxes of biogenic bromine from the tropical and North Atlantic Ocean, *Atmos. Chem. Phys.*, *9* (5), 1805-1816, doi: 10.5194/acp-9-1805-2009, 2009.

Chen, J., V. Young, H. Niki, and H. Magid, Kinetic and mechanistic studies for reactions of $CF_3CH_2CHF_2$ (HFC-245fa) initiated by H-atom abstraction using atomic chlorine, *J. Phys. Chem. A*, *101* (14), 2648-2653, doi: 10.1021/jp963735s, 1997.

Chen, L., S. Kutsuna, K. Tokuhashi, and A. Sekiya, Kinetics of the gas-phase reaction of $CF_3OC(O)H$ with OH radicals at 242-328 K, *Int. J. Chem. Kinet.*, *36* (6), 337-344, doi: 10.1002/kin.20004, 2004a.

Chen, L., S. Kutsuna, K. Tokuhashi, and A. Sekiya, Kinetics study of the gas-phase reactions of $C_2F_5OC(O)H$ and n-$C_3F_7OC(O)H$ with OH radicals at 253-328 K, *Chem. Phys. Lett.*, *400* (4-6), 563-568, 2004b.

Chen, L., S. Kutsuna, K. Tokuhashi, and A. Sekiya, Kinetics study of the gas-phase reactions of $CHF_2CF_2OCHF_2$ and $CF_3CHFCF_2OCH_2CF_2CF_3$ with OH radicals at 253-328 K, *Chem. Phys. Lett.*, *403* (1-3), 180-184, 2005a.

Chen, L., S. Kutsuna, K. Tokuhashi, A. Sekiya, R. Tamai, and Y. Hibino, Kinetics and mechanism of $(CF_3)_2CHOCH_3$ reaction with OH radicals in an environmental reaction chamber, *J. Phys. Chem. A*, *109* (21), 4766-4771, doi: 10.1021/jp050491f, 2005b.

Chen, Y.-H., and R.G. Prinn, Estimation of atmospheric methane emissions between 1996 and 2001 using a three-dimensional global chemical transport model, *J. Geophys. Res.*, *111*, D10307, 25, doi: 10.1029/2005JD006058, 2006.

Chipperfield, M.P., M. Burton, W. Bell, C.P. Walsh, T. Blumenstock, M.T. Coffey, J.W. Hannigan, W.G. Mankin, B. Galle, J. Mellqvist, E. Mahieu, R. Zander, J. Notholt, B. Sen, and G.C. Toon, On the use of HF as a reference for the comparison of stratospheric observations and models, *J. Geophys. Res.*, *102* (D11), 12901-12919, doi: 10.1029/96JD03964, 1997.

Christensen, L.K., J. Sehested, O.J. Nielsen, M. Bilde, T.J. Wallington, A. Guschin, L.T. Molina, and M.J. Molina, Atmospheric chemistry of HFE-7200 ($C_4F_9OC_2H_5$): Reaction with OH radicals and fate of $C_4F_9OCH_2CH_2O(\cdot)$ and $C_4F_9OCHO(\cdot)CH_3$ radicals, *J. Phys. Chem. A*, *102* (25), 4839-4845, doi: 10.1021/jp981128u, 1998.

Class, Th., and K. Ballschmiter, Global baseline pollution studies, X. Atmospheric halocarbons: Global budget estimations for tetrachloroethene, 1,2-dichloroethane, l,l,l,2-tetrachloroethane, hexachloroethane and hexachlorobutadiene. Estimation of the hydroxyl radical concentrations in the troposphere of the northern and southern hemisphere, *Fresenius' Z. Anal. Chem.*, *327* (2), 198-204, doi: 10.1007/BF00469817, 1987.

Clerbaux, C., and D.M. Cunnold (Lead Authors), J. Anderson, A. Engel, P.J. Fraser, E. Mahieu, A. Manning, J. Miller, S.A. Montzka, R. Nassar, R. Prinn, S. Reimann, C.P. Rinsland, P. Simmonds, D. Verdonik, R. Weiss, D. Wuebbles, and Y. Yokouchi, Long-lived compounds, Chapter 1 in *Scientific Assessment of Ozone Depletion: 2006*, Global Ozone Research and Monitoring Project—Report No. 50, 572 pp., World Meteorological Organization, Geneva, Switzerland, 2007.

Collins, W.J., R.G. Derwent, C.E. Johnson, and D.S. Stevenson, The oxidation of organic compounds in the troposphere and their global warming potentials, *Clim. Change*, *52* (4), 453-479, doi: 10.1023/A:1014221225434, 2002.

Conway, T.J., P.P. Tans, L.S. Waterman, K.W. Thoning, D.R. Kitzis, K.A. Masarie, and N. Zhang, Evidence for interannual variability of the carbon cycle from the National Oceanic and Atmospheric Administration/Climate Monitoring and Diagnostics Laboratory Global Air Sampling Network, *J. Geophys. Res.*, *99* (D11), 22831-22855, doi: 10.1029/94JD01951, 1994.

Cox, M.L., P.J. Fraser, G.A. Sturrock, S.T. Siems, and L.W. Porter, Terrestrial sources and sinks of halomethanes near Cape Grim, Tasmania, *Atmos. Environ.*, *38* (23), 3839-3852, doi: 10.1016/j.atmosenv.2004.03.050, 2004.

Crutzen, P.J., A.R. Mosier, K.A. Smith, and W. Winiwarter, N_2O release from agro-biofuel production negates global warming reduction by replacing fossil fuels, *Atmos. Chem. Phys.*, *8* (2), 389-395, doi: 10.5194/acp-8-389-2008, 2008.

Culbertson, J.A., J.M. Prins, E.P. Grimsrud, R.A. Rasmussen, M.A.K. Khalil, and M.J. Shearer, Observed trends for CF_3-containing compounds in background air at Cape Meares, Oregon, Point Barrow, Alaska, and Palmer Station, Antarctica, *Chemo-*

sphere, *55* (8), 1109-1119, doi: 10.1016/j.chemosphere.2003.11.002, 2004.

Daniel, J.S., and G.J.M Velders (Lead Authors), A.R. Douglass, P.M.D. Forster, D.A. Hauglustaine, I.S.A. Isaksen, L.J.M. Kuijpers, A. McCulloch, and T.J. Wallington, Halocarbon scenarios, ozone depletion potentials, and global warming potentials, Chapter 8 in *Scientific Assessment of Ozone Depletion: 2006*, Global Ozone Research and Monitoring Project—Report No. 50, 572 pp., World Meteorological Organization, Geneva, Switzerland, 2007.

Danilin, M.Y., and J.C. McConnell, Stratospheric effects of bromine activation on/in sulfate aerosol, *J. Geophys. Res*., *100* (D6), 11237-11243, doi: 10.1029/95JD00999, 1995.

Danilin, M.Y., R.-L. Shia, M.K.W. Ko, D.K. Weisenstein, N.D. Sze, J.J. Lamb, T.W. Smith, P.D. Lohn, and M.J. Prather, Global stratospheric effects of the alumina emissions by solid-fueled rocket motors, *J. Geophys. Res*., *106* (D12), 12727-12738, doi: 10.1029/2001JD900022, 2001.

Danilin, M.Y., P.J. Popp, R.L. Herman, M.K.W. Ko, M.N. Ross, C.E. Kolb, D.W. Fahey, L.M. Avallone, D.W. Toohey, B.A. Ridley, O. Schmid, J.C. Wilson, D.G. Baumgardner, R.R. Friedl, T.L. Thompson, and J.M. Reeves, Quantifying uptake of HNO_3 and H_2O by alumina particles in Athena-2 rocket plume, *J. Geophys. Res*., *108* (D4), 4141, doi: 10.1029/2002JD002601, 2003.

Deeds, D.A., M.K. Vollmer, J.T. Kulongoski, B.R. Miller, J. Mühle, C.M. Harth, J.A. Izbicki, D.R. Hilton, and R.F. Weiss, Evidence for crustal degassing of CF_4 and SF_6 in Mojave Desert groundwaters, *Geochim. Cosmochim. Acta*, *72* (4), 999-1013, doi: 10.1016/j.gca.2007.11.027, 2008.

Denman, K.L., G. Brasseur, A. Chidthaisong, P. Ciais, P.M. Cox, R.E. Dickinson, D. Hauglustaine, C. Heinze, E. Holland, D. Jacob, U. Lohmann, S. Ramachandran, P.L. da Silva Dias, S.C. Wofsy, and X. Zhang, Couplings between changes in the climate system and biogeochemistry, Chapter 7 in *Climate Change 2007: The Physical Science Basis. Contribution of Working Group I to the Fourth Assessment Report of the Intergovernmental Panel on Climate Change*, edited by S. Solomon, D. Qin, M. Manning, Z. Chen, M. Marquis, K.B. Averyt, M. Tignor, and H.L. Miller, 996 pp., Cambridge University Press, Cambridge, U.K., and New York, NY, U.S.A., 2007.

Derwent, R.G., M.E. Jenkin, S.M. Saunders, and M.J. Pilling, Photochemical ozone creation potentials for organic compounds in Northwest Europe calculated with a master chemical mechanism, *Atmos. Environ.*, *32* (14-15), 2429-2441, doi: 10.1016/S1352-2310(98)00053-3, 1998.

Derwent, R.G., M.E. Jenkin, N.R. Passant, and M.J. Pilling, Reactivity-based strategies for photochemical ozone control in Europe, *Environ. Sci. Policy*, *10* (5), 445-453, doi: 10.1016/j.envsci.2007.01.005, 2007.

Dessens, O., G. Zeng, N. Warwick, and J. Pyle, Short-lived bromine compounds in the lower stratosphere; impact of climate change on ozone, *Atmos. Sci. Lett.*, *10* (3), 201-206, doi: 10.1002/asl.236, 2009.

Dillon, T.J., A. Horowitz, and J.N. Crowley, The atmospheric chemistry of sulphuryl fluoride, SO_2F_2, *Atmos. Chem. Phys.*, *8* (6), 1547-1557, doi: 10.5194/acp-8-1547-2008, 2008.

Dimmer, C.H., P.G. Simmonds, G. Nickless, and M.R. Bassford, Biogenic fluxes of halomethanes from Irish peatland ecosystems, *Atmos. Environ.*, *35* (2), 321-330, doi: 10.1016/S1352-2310(00)00151-5, 2001.

Dlugokencky, E.J., L. Bruhwiler, J.W.C. White, L.K. Emmons, P.C. Novelli, S.A. Montzka, K.A. Masarie, P.M. Lang, A.M. Crotwell, J.B. Miller, and L.V. Gatti, Observational constraints on recent increases in the atmospheric CH_4 burden, *Geophys. Res. Lett.*, *36*, L18803, doi: 10.1029/2009GL039780, 2009.

Donner, L.J., L.W. Horowitz, A.M. Fiore, C.J. Seman, D.R. Blake, and N.J. Blake, Transport of radon-222 and methyl iodide by deep convection in the GFDL Global Atmospheric Model AM2, *J. Geophys. Res*., *112*, D17303, doi: 10.1029/2006JD007548, 2007.

Dorf, M., J.H. Butler, A. Butz, C. Camy-Peyret, M.P. Chipperfield, L. Kritten, S.A. Montzka, B. Simmes, F. Weidner, and K. Pfeilsticker, Long-term observations of stratospheric bromine reveal slow down in growth, *Geophys. Res. Lett.*, *33*, L24803, doi: 10.1029/2006GL027714, 2006.

Dorf, M., A. Butz, C. Camy-Peyret, M.P. Chipperfield, L. Kritten, and K. Pfeilsticker, Bromine in the tropical troposphere and stratosphere as derived from balloon-borne BrO observations, *Atmos. Chem. Phys.*, *8* (23), 7265-7271, doi: 10.5194/acp-8-7265-2008, 2008.

Douglass, A.R., R.S. Stolarski, M.R. Schoeberl, C.H. Jackman, M.L. Gupta, P.A. Newman, J.E. Nielsen, and E.L. Fleming, Relationship of loss, mean age of air and the distribution of CFCs to stratospheric circulation and implications for atmospheric lifetimes, *J. Geophys. Res.*, *113*, D14309, doi: 10.1029/2007JD009575, 2008.

Drewer, J., M.R. Heal, K.V. Heal, and K.A. Smith, Temporal and spatial variation in methyl bromide flux from a salt marsh, *Geophys. Res. Lett.*, *33*, L16808, doi: 10.1029/2006GL026814, 2006.

Drewer, J., K.V. Heal, K.A. Smith, and M.R. Heal, Methyl bromide emissions to the atmosphere from temperate woodland ecosystems, *Global Change*

Biol., *14* (11), 2539-2547, doi: 10.1111/j.1365-2486.2008.01676.x, 2008.

Duchatelet, P., E. Mahieu, R. Ruhnke, W. Feng, M. Chipperfield, P. Demoulin, P. Bernath, C.D. Boone, K.A. Walker, C. Servais, and O. Flock, An approach to retrieve information on the carbonyl fluoride (COF_2) vertical distributions above Jungfraujoch by FTIR multi-spectrum multi-window fitting, *Atmos. Chem. Phys.*, *9* (22), 9027-9042, doi: 10.5194/acp-9-9027-2009, 2009.

Dunse, B.L., L.P. Steele, S.R. Wilson, P.J. Fraser, and P.B. Krummel, Trace gas emissions from Melbourne, Australia, based on AGAGE observations at Cape Grim, Tasmania, 1995–2000, *Atmos. Environ.*, *39* (34), 6334-6344, doi: 10.1016/j.atmosenv.2005.07.014, 2005.

Engel, A., M. Strunk, M. Müller, H.-P. Haase, C. Poss, I. Levin, and U. Schmidt, Temporal development of total chlorine in the high-latitude stratosphere based on reference distributions of mean age derived from CO_2 and SF_6, *J. Geophys. Res.*, *107* (D12), 4136, doi: 10.1029/2001JD000584, 2002.

FAO (Food and Agriculture Organization of the United Nations), FAOSTAT database, available at: faostat.fao.org, 2009.

Feng, W., M.P. Chipperfield, M. Dorf, K. Pfeilsticker, and P. Ricaud, Mid-latitude ozone changes: Studies with a 3-D CTM forced by ERA-40 analyses, *Atmos. Chem. Phys*., *7* (9), 2357-2369, doi: 10.5194/acp-7-2357-2007, 2007.

Ferretti, D.F., J.B. Miller, J.W.C. White, K.R. Lassey, D.C. Lowe, and D.M. Etheridge, Stable isotopes provide revised global limits of aerobic methane emissions from plants, *Atmos. Chem. Phys.*, *7* (1), 237-241, doi: 10.5194/acp-7-237-2007, 2007.

Fisher, B., and N. Nakicenovic, (Co-ordinating Lead Authors), K. Alfsen, J. Corfee Morlot, F. de la Chesnaye, J.-Ch. Hourcade, K. Jiang, M. Kainuma, E. La Rovere, A. Matysek, A. Rana, K. Riahi, R. Richels, S. Rose, D. van Vuuren, and R. Warren, Issues related to mitigation in the long term context, Chapter 3 in *Climate Change 2007: Mitigation. Contribution of Working Group III to the Fourth Assessment Report of the Intergovernmental Panel on Climate Change*, edited by B. Metz, O.R. Davidson, P.R. Bosch, R. Dave, and L.A. Meyer, Cambridge University Press, Cambridge, U.K. and New York, NY, U.S.A., 2007.

Forster, P., V. Ramaswamy, (Coordinating Lead Authors), P. Artaxo, T. Berntsen, R. Betts, D.W. Fahey, J. Haywood, J. Lean, D.C. Lowe, G. Myhre, J. Nganga, R. Prinn, G. Raga, M. Schulz, and R. Van Dorland, Changes in atmospheric constituents and in radiative forcing, Chapter 2 in *Climate Change 2007: The Physical Science Basis. Contribution of Working Group I to the Fourth Assessment Report of the Intergovernmental Panel on Climate Change*, edited by S. Solomon, D. Qin, M. Manning, Z. Chen, M. Marquis, K.B. Averyt, M. Tignor, and H.L. Miller, 996 pp., Cambridge University Press, Cambridge, U.K., and New York, NY, U.S.A., 2007.

Frank, H., E.H. Christoph, O. Holm-Hansen, and J.L. Bullister, Trifluoroacetate in ocean waters, *Environ. Sci. Technol*., *36* (1), 12-15, doi: 10.1021/es0101532, 2002.

Frankenberg, C., J.F. Meirink, M. van Weele, U. Platt, and T. Wagner, Assessing methane emissions from global space-borne observations, *Science*, *308* (5724), 1010-1014, doi: 10.1126/science.1106644, 2005.

Frankenberg, C., P. Bergamaschi, A. Butz, S. Houweling, J.F. Meirink, J. Notholt, A.K. Petersen, H. Schrijver, T. Warneke, and I. Aben, Tropical methane emissions: A revised view from SCIAMACHY onboard ENVISAT, *Geophys. Res. Lett.*, *35*, L15811, doi: 10.1029/2008GL034300, 2008.

Fraser, P.J., D.E. Oram, C.E. Reeves, S.A. Penkett, and A. McCulloch, Southern Hemispheric halon trends (1978–1998) and global halon emissions, *J. Geophys. Res.*, *104* (D13), 15985-15999, doi: 10.1029/1999JD900113, 1999.

Friedlingstein, P., P. Cox, R. Betts, L. Bopp, W. von Bloh, V. Brovkin, P. Cadule, S. Doney, M. Eby, I. Fung, G. Bala, J. John, C. Jones, F. Joos, T. Kato, M. Kawamiya, W. Knorr, K. Lindsay, H.D. Matthews, T. Raddatz, P. Rayner, C. Reick, E. Roeckner, K.-G. Schnitzler, R. Schnur, K. Strassmann, A.J. Weaver, C. Yoshikawa, and N. Zeng, Climate–carbon cycle feedback analysis: Results from the (C^4MIP) model intercomparison, *J. Clim*., *19* (14), 3337-3353, doi: 10.1175/JCLI3800.1, 2006.

Frische, M., K. Garofalo, T.H. Hansteen, R. Borchers, and J. Harnisch, The origin of stable halogenated compounds in volcanic gases, *Environ. Sci. Pollut. Res.*, *13* (6), 406-413, doi: 10.1065/espr2006.01.291, 2006.

Froidevaux, L., J.W. Waters, W.G. Read, P.S. Connell, D.E. Kinnison, and J.M. Russell III, Variations in the free chlorine content of the stratosphere (1991–1997): Anthropogenic, volcanic, and methane influences, *J. Geophys. Res*., *105* (D4), 4471-4481, 2000.

Froidevaux, L., N.J. Livesey, W.G. Read, R.J. Salawitch, J.W. Waters, B. Drouin, I.A. MacKenzie, H.C. Pumphrey, P. Bernath, C. Boone, R. Nassar, S. Montzka, J. Elkins, D. Cunnold, and D. Waugh, Temporal decrease in upper atmospheric chlorine, *Geophys. Res. Lett*., *33*, L23812, doi: 10.1029/2006GL027600, 2006.

Froidevaux, L., Y.B. Jiang, A. Lambert, N.J. Livesey,

W.G. Read, J.W. Waters, R.A. Fuller, T.P. Marcy, P.J. Popp, R.S. Gao, D.W. Fahey, K.W. Jucks, R.A. Stachnik, G.C. Toon, L.E. Christensen, C.R. Webster, P.F. Bernath, C.D. Boone, K.A. Walker, H.C. Pumphrey, R.S. Harwood, G.L. Manney, M.J. Schwartz, W.H. Daffer, B.J. Drouin, R.E. Cofield, D.T. Cuddy, R.F. Jarnot, B.W. Knosp, V.S. Perun, W.V. Snyder, P.C. Stek, R.P. Thurstans, and P.A. Wagner, Validation of Aura Microwave Limb Sounder HCl measurements, *J. Geophys. Res*., *113*, D15S25, doi: 10.1029/2007JD009025, 2008.

Fromm, M., E.P. Shettle, K.H. Fricke, C. Ritter, T. Trickl, H. Giehl, M. Gerding, J.E. Barnes, M. O'Neill, S.T. Massie, U. Blum, I.S. McDermid, T. Leblanc, and T. Deshler, Stratospheric impact of the Chisholm pyrocumulonimbus eruption: 2. Vertical profile perspective, *J. Geophys. Res*., *113*, D08203, doi: 10.1029/2007JD009147, 2008.

Fu, D., C.D. Boone, P.F. Bernath, K.A. Walker, R. Nassar, G.L. Manney, and S.D. McLeod, Global phosgene observations from the Atmospheric Chemistry Experiment (ACE) mission, *Geophys. Res. Lett*., *34* (17), L17815, doi: 10.1029/2007GL029942, 2007.

Fu, D., C.D. Boone, P.F. Bernath, D.K. Weisenstein, C.P. Rinsland, G.L. Manney, and K.A. Walker, First global observations of atmospheric COClF from the Atmospheric Chemistry Experiment mission, *J. Quant. Spectrosc. Radiat. Transfer*, *110* (12), 974-985, doi: 10.1016/j.jqsrt.2009.02.018, 2009.

Fueglistaler, S., M. Bonazzola, P.H. Haynes, and T. Peter, Stratospheric water vapor predicted from the Lagrangian temperature history of air entering the stratosphere in the tropics, *J. Geophys. Res*., *110*, D08107, doi: 10.1029/2004JD005516, 2005.

Fueglistaler, S., A.E. Dessler, T.J. Dunkerton, I. Folkins, Q. Fu, and P.W. Mote, Tropical tropopause layer, *Rev. Geophys.*, *47*, RG1004, doi: 10.1029/2008RG000267, 2009a.

Fueglistaler, S., B. Legras, A. Beljaars, J.-J. Morcrette, A. Simmons, A.M. Tompkins, and S. Uppala, The diabatic heat budget of the upper troposphere and lower/mid stratosphere in ECMWF reanalyses, *Quart. J. Roy. Meteorol. Soc*., *135* (638), 21-37, doi: 10.1002/qj.361, 2009b.

Gan, J., S.R. Yates, H.D. Ohr, and J.J. Sims, Production of methyl bromide by terrestrial higher plants, *Geophys. Res. Lett.*, *25* (19), 3595-3598, doi: 10.1029/98GL52697, 1998.

Gardiner, T., A. Forbes, M. de Mazière, C. Vigouroux, E. Mahieu, P. Demoulin, V. Velazco, J. Notholt, T. Blumenstock, F. Hase, I. Kramer, R. Sussmann, W. Stremme, J. Mellqvist, A. Strandberg, K. Ellingsen, and M. Gauss, Trend analysis of greenhouse gases over Europe measured by a network of ground-based remote FTIR instruments, *Atmos. Chem. Phys.*, *8* (22), 6719-6727, doi: 10.5194/acp-8-6719-2008, 2008.

Gebhardt, S., A. Colomb, R. Hofmann, J. Williams, and J. Lelieveld, Halogenated organic species over the tropical South American rainforest, *Atmos. Chem. Phys.*, *8* (12), 3185-3197, doi: 10.5194/acp-8-3185-2008, 2008.

Geller, L.S., J.W. Elkins, J.M. Lobert, A.D. Clarke, D.F. Hurst, J.H. Butler, and R.C. Meyer, Troposheric SF_6: Observed latitudinal distribution and trends, derived emissions and interhemispheric exchange time, *Geophys. Res. Lett.*, *24* (6), 675-678, doi: 10.1029/97GL00523, 1997.

Gettelman, A., P.H. Lauritzen, M. Park, and J.E. Kay, Processes regulating short-lived species in the tropical tropopause layer, *J. Geophys. Res*., *114*, D13303, doi: 10.1029/2009JD011785, 2009.

Gossé, S., L. Hespel, P. Gossart, and A. Delfour, Morphological characterization and particle sizing of alumina particles in solid rocket motor, *J. Propul. Power*, *22* (1), 127-135, 2006.

Greally, B.R., P.G. Simmonds, S. O'Doherty, A. McCulloch, B.R. Miller, P.K. Salameh, J. Mühle, T. Tanhua, C. Harth, R.F. Weiss, P.J. Fraser, P.B. Krummel, B.L. Dunse, L.W. Porter, and R.G. Prinn, Improved continuous in situ measurements of C_1–C_3 PFCs, HFCs, HCFCs, CFCs and SF_6 in Europe and Australia, *J. Integr. Environ. Sci.*, *2* (2-3), 253-261, doi: 10.1080/15693430500402614, 2005.

Greally, B.R., A.J. Manning, S. Reimann, A. McCulloch, J. Huang, B.L. Dunse, P.G. Simmonds, R.G. Prinn, P.J. Fraser, D.M. Cunnold, S. O'Doherty, L.W. Porter, K. Stemmler, M.K. Vollmer, C.R. Lunder, N. Schmidbauer, O. Hermansen, J. Arduini, P.K. Salameh, P.B. Krummel, R.H.J. Wang, D. Folini, R.F. Weiss, M. Maione, G. Nickless, F. Stordal, and R.G. Derwent, Observations of 1,1-difluoroethane (HFC-152a) at AGAGE and SOGE monitoring stations in 1994–2004 and derived global and regional emission estimates, *J. Geophys. Res.*, *112*, D06308, doi: 10.1029/2006JD007527, 2007.

Guo, H., A.J. Ding, T. Wang, I.J. Simpson, D.R. Blake, B. Barletta, S. Meinardi, F.S. Rowland, S.M. Saunders, T.M. Fu, W.T. Hung, and Y.S. Li, Source origins, modeled profiles, and apportionments of halogenated hydrocarbons in the greater Pearl River Delta region, southern China, *J. Geophys. Res.*, *114*, D11302, doi: 10.1029/2008JD011448, 2009.

Guo, S., G.J.S. Bluth, W.I. Rose, I.M. Watson, and A.J. Prata, Re-evaluation of SO_2 release of the 15 June 1991 Pinatubo eruption using ultraviolet and infrared satellite sensors, *Geochem. Geophys. Geosyst.*, *5*, Q04001, doi: 10.1029/2003GC000654, 2004.

Hall, B.D., G.S. Dutton, and J.W. Elkins, The NOAA nitrous oxide standard scale for atmospheric observations, *J. Geophys. Res.*, *112*, D09305, doi: 10.1029/2006JD007954, 2007.

Hamilton, J.T.G., W.C. McRoberts, F. Keppler, R.M. Kalin, and D.B Harper, Chloride methylation by plant pectin: An efficient environmentally significant process, *Science*, *301* (5630), 206-209, doi: 10.1126/science.105036, 2003.

Happell, J.D., and D.W.R. Wallace, Removal of atmospheric CCl_4 under bulk aerobic conditions in groundwater and soils, *Environ. Sci. Technol.*, *32* (9), 1244-1252, doi: 10.1021/es970653o, 1998.

Happell, J.D., and M.P. Roche, Soils: A global sink of atmospheric carbon tetrachloride, *Geophys. Res. Lett.*, *30* (2), 1088, doi: 10.1029/2002GL015957, 2003.

Hardacre, C.J., E. Blei, and M.R. Heal, Growing season methyl bromide and methyl chloride fluxes at a sub-arctic wetland in Sweden, *Geophys. Res. Lett.*, *36*, L12401, doi: 10.1029/2009GL038277, 2009.

Harnisch, J., Reactive fluorine compounds, Chapter 3 in *The Handbook of Environmental Chemistry*, *Volume 4E: Reactive Halogen Compounds in the Atmosphere*, edited by P. Fabian, and O.N. Singh, 81-111, Springer-Verlag, Berlin Heidelberg, 1999.

Harnisch, J., Atmospheric perfluorocarbons: Sources and concentrations, in *Non-CO_2 Greenhouse Gases: Scientific Understanding*, *Control and Implementation*, edited by J. van Ham, A.P.M. Baede, L.A. Meyer, and R. Ybema, 205-210, Kluwer Academic Publishers, Dordrecht, Netherlands, 2000.

Harnisch, J., R. Borchers, P. Fabian, H.W. Gäggeler, and U. Schotterer, Effect of natural tetrafluoromethane, *Nature*, *384* (6604), 32, doi: 10.1038/384032a0, 1996.

Haywood, J., and O. Boucher, Estimates of the direct and indirect radiative forcing due to tropospheric aerosols: A review, *Rev. Geophys*., *38* (4), 513-543, 2000.

Hegglin, M.I., D. Brunner, H. Wernli, C. Schwierz, O. Martius, P. Hoor, H. Fischer, U. Parchatka, N. Spelten, C. Schiller, M. Krebsbach, U. Weers, J. Staehelin, and Th. Peter, Tracing troposphere-to-stratosphere transport above a mid-latitude deep convective system, *Atmos. Chem. Phys.*, *4* (3), 741-756, doi: 10.5194/acp-4-741-2004, 2004.

Hendrick, F., P.V. Johnston, M. De Mazière, C. Fayt, C. Hermans, K. Kreher, N. Theys, A. Thomas, and M. Van Roozendael, One-decade trend analysis of stratospheric BrO over Harestua (60°N) and Lauder (45°S) reveals a decline, *Geophys. Res. Lett.*, *35*, L14801, doi: 10.1029/2008GL034154, 2008.

Hense, I., and B. Quack, Modelling the vertical distribution of bromoform in the upper water column of the tropical Atlantic Ocean, *Biogeosciences*, *6* (4), 535-544, doi: 10.5194/bg-6-535-2009, 2009.

Hirsch, A.I., A.M. Michalak, L.M. Bruhwiler, W. Peters, E.J. Dlugokencky, and P.P. Tans, Inverse modeling estimates of the global nitrous oxide surface flux from 1998–2001, *Global Biogeochem. Cycles*, *20*, GB1008, doi: 10.1029/2004GB002443, 2006.

Hoffmann, L., M. Kaufmann, R. Spang, R. Müller, J.J. Remedios, D.P. Moore, C.M. Volk, T. von Clarmann, and M. Riese, Envisat MIPAS measurements of CFC-11: Retrieval, validation, and climatology, *Atmos. Chem. Phys.*, *8* (13), 3671-3688, doi: 10.5194/acp-8-3671-2008, 2008.

Hofmann, D.J., and S.A. Montzka, Recovery of the ozone layer: The Ozone Depleting Gas Index, *EOS Transactions*, *90* (1), 1-2, doi: 10.1029/2009EO010001, 2009.

Hofmann, D.J., J.H. Butler, E.J. Dlugokencky, J.W. Elkins, K. Masarie, S.A. Montzka, and P. Tans, The role of carbon dioxide in climate forcing from 1979 to 2004: Introduction of the Annual Greenhouse Gas Index, *Tellus*, *58B*, 614-619, doi: 10.1111/j.1600-0889.2006.00201.x, 2006.

Hofmann, D., J. Barnes, M. O'Neill, M. Trudeau, and R. Neely, Increase in background stratospheric aerosol observed with lidar at Mauna Loa Observatory and Boulder, Colorado, *Geophys. Res. Lett*., *36*, L15808, doi: 10.1029/2009GL039008, 2009.

Homan, C.D., C.M. Volk, A.C. Kuhn, A. Werner, J. Baehr, S. Viciani, A. Ulanovski, and F. Ravegnani, Tracer measurements in the tropical tropopause layer during the AMMA/SCOUT-O3 aircraft campaign, *Atmos. Chem. Phys*., *10* (8), 3615-3627, doi: 10.5194/acp-10-3615-2010, 2010.

Hoor, P., C. Gurk, D. Brunner, M.I. Hegglin, H. Wernli, and H. Fischer, Seasonality and extent of extratropical TST derived from in-situ CO measurements during SPURT, *Atmos. Chem. Phys*., *4* (5), 1427–1442, doi: 10.5194/acp-4-1427-2004, 2004.

Höpfner, M., J. Orphal, T. von Clarmann, G. Stiller, and H. Fischer, Stratospheric $BrONO_2$ observed by MIPAS, *Atmos. Chem. Phys.*, *9* (5), 1735-1746, doi: 10.5194/acp-9-1735-2009, 2009.

Hossaini, R., M.P. Chipperfield, B.M. Monge-Sanz, N.A.D. Richards, E. Atlas, and D.R. Blake, Bromoform and dibromomethane in the tropics: A 3-D model study of chemistry and transport, *Atmos. Chem. Phys*., *10* (2), 719-735, doi: 10.5194/acp-10-719-2010, 2010.

Hu, L., S.A. Yvon-Lewis, Y. Liu, J.E. Salisbury, and J.E. O'Hern, Coastal emissions of methyl bromide and methyl chloride along the eastern Gulf of Mexico and the east coast of the United States, *Global Biogeochem. Cycles*, *24*, GB1007, doi: 10.1029/2009GB003514, 2010.

Huang, J., A. Golombek, R. Prinn, R. Weiss, P. Fraser, P. Simmonds, E.J. Dlugokencky, B. Hall, J. Elkins,

P. Steele, R. Langenfelds, P. Krummel, G. Dutton, and L. Porter, Estimation of regional emissions of nitrous oxide from 1997 to 2005 using multinetwork measurements, a chemical transport model, and an inverse method, *J. Geophys. Res.*, *113*, D17313, doi: 10.1029/2007JD009381, 2008.

Huhn, O., W. Roether, P. Beining, and H. Rose, Validity limits of carbon tetrachloride as an ocean tracer, *Deep-Sea Res.*, *1*, *48* (9), 2025-2049, doi: 10.1016/S0967-0637(01)00004-8, 2001.

Hurley, M.D., J.C. Ball, T.J. Wallington, M.P. Sulbaek Andersen, O.J. Nielsen, D.A. Ellis, J.W. Martin, and S.A. Mabury, Atmospheric chemistry of *n*-$C_xF_{2x+1}CHO$ (x = 1, 2, 3, 4): Fate of *n*-$C_xF_{2x+1}C(O)$ radicals, *J. Phys. Chem. A*, *110* (45), 12443-12447, doi: 10.1021/jp064029m, 2006.

Hurley, M.D., T.J. Wallington, M.S. Javadi, and O.J. Nielsen, Atmospheric chemistry of $CF_3CF{=}CH_2$: Products and mechanisms of Cl atom and OH radical initiated oxidation, *Chem. Phys. Lett.*, *450* (4-6), 263-267, doi: 10.1016/j.cplett.2007.11.051, 2008.

Hurst, D.F., J.C. Lin, P.A. Romashkin, B.C. Daube, C. Gerbig, D.M. Matross, S.C. Wofsy, B.D. Hall, and J.W. Elkins, Continuing global significance of emissions of Montreal Protocol-restricted halocarbons in the United States and Canada, *J. Geophys. Res.*, *111*, D15302, doi: 10.1029/2005JD006785, 2006.

Inoue, Y., M. Kawasaki, T.J. Wallington, and M.D. Hurley, Atmospheric chemistry of $CF_3CH_2CF_2CH_3$ (HFC-365mfc): Kinetics and mechanism of chlorine atom initiated oxidation, infrared spectrum, and global warming potential, *Chem. Phys. Lett.*, *462*, 4-6, 164-168, doi: 10.1016/j.cplett.2008.07.054, 2008.

IPCC/TEAP (Intergovernmental Panel on Climate Change/Technology and Economic Assessment Panel), *IPCC/TEAP Special Report on Safeguarding the Ozone Layer and the Global Climate System: Issues Related to Hydrofluorocarbons and Perfluorocarbons*, prepared by Working Groups I and III of the Intergovernmental Panel on Climate Change, and the Technical and Economic Assessment Panel, Cambridge University Press, Cambridge, U.K. and New York, NY, U.S.A., 2005.

James, R., M. Bonazzola, B. Legras, K. Surbled, and S. Fueglistaler, Water vapor transport and dehydration above convective outflow during Asian monsoon, *Geophys. Res. Lett.*, *35*, L20810, doi: 10.1029/2008GL035441, 2008.

Javadi, M.S., R. Søndergaard, O.J. Nielsen, M.D. Hurley, and T.J. Wallington, Atmospheric chemistry of trans-$CF_3CH{=}CHF$: Products and mechanisms of hydroxyl radical and chlorine atom initiated oxidation, *Atmos. Chem. Phys.*, *8* (12), 3141-3147, doi: 10.5194/acp-8-3141-2008, 2008.

Jenkin, M.E., *Photochemical Ozone and PAN Creation Potentials: Rationalisation and Methods of Estimation*, AEA Technology plc, AEAT Report 4182/20150/003, Issue 1, National Environmental Technology Centre, U.K., 1998.

Jiang, X., W.L. Ku, R.-L. Shia, Q. Li, J.W. Elkins, R.G. Prinn, and Y.L. Yung, Seasonal cycle of N_2O: Analysis of data, *Global Biogeochem. Cycles*, *21*, GB1006, doi: 10.1029/2006GB002691, 2007.

Jourdain, J.L., G. Le Bras, and J. Combourieu, Kinetic study by electron paramagnetic resonance and mass spectrometry of the elementary reactions of phosphorus tribromide with H, O, and OH radicals, *J. Phys. Chem.*, *86* (21), 4170-4175, doi: 10.1021/j100218a016, 1982.

JPL 06-2: see Sander et al., 2006.

JPL 10-6: see Sander et al., 2010.

Kaminski, T., P.J. Rayner, M. Heimann, and I.G. Enting, On aggregation errors in atmospheric transport inversions, *J. Geophys. Res.*, *106* (D5), 4703-4715, doi: 10.1029/2000JD900581, 2001.

Keene, W.C., M.A.K. Khalil, D.J. Erickson, A. McCulloch, T.E. Graedel, J.M. Lobert, M.L. Aucott, S.L. Gong, D.B. Harper, G. Kleiman, P. Midgley, R.M. Moore, C. Seuzaret, W.T. Sturges, C.M. Benkovitz, V. Koropalov, L.A. Barrie, and Y.F. Li, Composite global emissions of reactive chlorine from anthropogenic and natural sources: Reactive Chlorine Emissions Inventory, *J. Geophys. Res.*, *104* (D7), 8429-8440, doi: 10.1029/1998JD100084, 1999.

Keppler, F., R. Eiden, V. Niedan, J. Pracht, and H.F. Schöler, Halocarbons produced by natural oxidation processes during degradation of organic matter, *Nature*, *403*, 298-301, doi: 10.1038/35002055, 2000.

Keppler, F., R.M. Kalin, D.B. Harper, W.C. McRoberts, and J.T.G. Hamilton, Carbon isotope anomaly in the major plant C_1 pool and its global biogeochemical implications, *Biogeosciences*, *1* (2), 123-131, doi: 10.5194/bg-1-123-2004, 2004.

Keppler, F., D.B. Harper, T. Röckmann, R.M. Moore, and J.T.G. Hamilton, New insight into the atmospheric chloromethane budget gained using stable carbon isotope ratios, *Atmos. Chem. Phys.*, *5* (9), 2403-2411, doi: 10.5194/acp-5-2403-2005, 2005.

Keppler, F., J.T.G. Hamilton, M. Braß, and T. Röckmann, Methane emissions from terrestrial plants under aerobic conditions, *Nature*, *439*, 187-191, doi: 10.1038/nature04420, 2006.

Kerkweg, A., P. Jöckel, N. Warwick, S. Gebhardt, C.A.M. Brenninkmeijer, and J. Lelieveld, Consistent simulation of bromine chemistry from the marine boundary layer to the stratosphere – Part 2: Bromocarbons, *Atmos. Chem. Phys.*, *8* (19), 5919-5939, doi: 10.5194/acp-8-5919-2008, 2008.

Kim, J., S. Li, K.-R. Kim, A. Stohl, J. Mühle, S.-K. Kim, M.-K. Park, D.-J. Kang, G. Lee, C.M. Harth, P.K. Salameh, and R.F. Weiss, Regional atmospheric emissions determined from measurements at Jeju Island, Korea: Halogenated compounds from China, *Geophys. Res. Lett.*, *37*, L12801, doi: 10.1029/2010GL043263, 2010.

Kindler, T.P., W.L. Chameides, P.H. Wine, D.M. Cunnold, F.N. Alyea, and J.A. Franklin, The fate of atmospheric phosgene and the stratospheric loadings of its parent compounds: CCl_4, C_2Cl_4, C_2HCl_3, CH_3CCl_3, and $CHCl_3$, *J. Geophys. Res.*, *100* (D1), 1235-1251, doi: 10.1029/94JD02518, 1995.

King, D.B., J.H. Butler, S.A. Yvon-Lewis, and S.A. Cotton, Predicting oceanic methyl bromide saturation from SST, *Geophys. Res. Lett.*, *29* (24), 2199, doi: 10.1029/2002GL016091, 2002.

Klimont, Z., J. Cofala, J. Xing, W. Wei, C. Zhang, S. Wang, J. Kejun, P. Bhandari, R. Mathur, P. Purohit, P. Rafaj, A. Chambers, M. Amann, and J. Hao, Projections of SO_2, NO_x and carbonaceous aerosols emissions in Asia, *Tellus*, *61B* (4), 602-617, doi: 10.1111/j.1600-0889.2009.00428.x, 2009.

Kloster, S., K.D. Six, J. Feichter, E. Maier-Reimer, E. Roeckner, P. Wetzel, P. Stier, and M. Esch, Response of dimethylsulfide (DMS) in the ocean and atmosphere to global warming, *J. Geophys. Res.*, *112*, G03005, doi: 10.1029/2006JG000224, 2007.

Knorr, W., Is the airborne fraction of anthropogenic CO_2 emissions increasing?, *Geophys. Res. Lett.*, *36*, L21710, doi: 10.1029/2009GL040613, 2009.

Ko, M.K.W., and G. Poulet (Lead Authors), D.R. Blake, O. Boucher, J.H. Burkholder, M. Chin, R.A. Cox, C. George, H.-F. Graf, J.R. Holton, D.J. Jacob, K.S. Law, M.G. Lawrence, P.M. Midgley, P.W. Seakins, D.E. Shallcross, S.E. Strahan, D.J. Wuebbles, and Y. Yokouchi, Very short-lived halogen and sulfur substances, Chapter 2 in *Scientific Assessment of Ozone Depletion: 2002*, Global Ozone Research and Monitoring Project–Report No. 47, World Meteorological Organization, Geneva, Switzerland, 2003.

Kovalenko, L.J., N.L. Livesey, R.J. Salawitch, C. Camy-Peyret, M.P. Chipperfield, R.E. Cofield, M. Dorf, B.J. Drouin, L. Froidevaux, R.A. Fuller, F. Goutail, R.F. Jarnot, K. Jucks, B.W. Knosp, A. Lambert, I.A. MacKenzie, K. Pfeilsticker, J.-P. Pommereau, W.G. Read, M.L. Santee, M.J. Schwartz, W.V. Snyder, R. Stachnik, P.C. Stek, P.A. Wagner, and J.W. Waters, Validation of Aura Microwave Limb Sounder BrO observations in the stratosphere, *J. Geophys. Res.*, *112*, D24S41, doi: 10.1029/2007JD008817, 2007.

Kremser, S., I. Wohltmann, M. Rex, U. Langematz, M. Dameris, and I. Wohltmann, Water vapour transport in the tropical tropopause region in coupled Chemistry-Climate Models and ERA-40 reanalysis data, *Atmos. Chem. Phys.*, *9* (8), 2679-2694, doi: 10.5194/acp-9-2679-2009, 2009.

Krüger, K., S. Tegtmeier, and M. Rex, Long-term climatology of air mass transport through the Tropical Tropopause Layer (TTL) during NH winter, *Atmos. Chem. Phys.*, *8* (4), 813-823, doi: 10.5194/acp-8-813-2008, 2008.

Krüger, K., S. Tegtmeier, and M. Rex, Variability of residence time in the Tropical Tropopause Layer during Northern Hemisphere winter, *Atmos. Chem. Phys.*, *9* (18), 6717-6725, doi: 10.5194/acp-9-6717-2009, 2009.

Kuell, V., D. Offermann, M. Jarisch, B. Schaeler, A. Engel, H. Claude, H.G.J. Smit, A. Ebel, and H. Feldmann, Tropopause region temperatures and CFC 11 mixing ratios from CRISTA 2, *J. Geophys. Res.*, *110*, D16104, doi: 10.1029/2004JD005592, 2005.

Kutsuna, S., L. Chen, T. Abe, J. Mizukado, T. Uchimaru, K. Tokuhashi, and A. Sekiya, Henry's law constants of 2,2,2-trifluoroethyl formate, ethyl trifluoroacetate, and non-fluorinated analogous esters, *Atmos. Environ.*, *39* (32), 5884-5892, doi: 10.1016/j.atmosenv.2005.06.021, 2005.

Langbein, T., H. Sonntag, D. Trapp, A. Hoffmann, W. Malms, E.P. Roth, V. Mors, and R. Zellner, Volatile anaesthetics and the atmosphere: Atmospheric lifetimes and atmospheric effects of halothane, enflurane, isoflurane, desflurane and sevoflurane, *British J. Anaesthesia*, *82* (1), 66-73, 1999.

Laube, J.C., A. Engel, H. Bönisch, T. Möbius, D.R. Worton, W.T. Sturges, K. Grunow, and U. Schmidt, Contribution of very short-lived organic substances to stratospheric chlorine and bromine in the tropics—a case study, *Atmos. Chem. Phys.*, *8* (23), 7325-7334, doi: 10.5194/acp-8-7325-2008, 2008.

Laube, J.C., P. Martinerie, E. Witrant, T. Blunier, J. Schwander, C.A.M Brenninkmeijer, T.J. Schuck, M. Bolder, T. Röckmann, C. van der Veen, H. Bönisch, A. Engel, G.P. Mills, M.J. Newland, D.E. Oram, C.E. Reeves, and W.T. Sturges, Accelerating growth of HFC-227ea (1,1,1,2,3,3,3-heptafluoropropane) in the atmosphere, *Atmos. Chem. Phys.*, *10* (13), 5903-5910, doi: 10.5194/acp-10-5903-2010, 2010.

Law, K.S., and W.T. Sturges (Lead Authors), D.R. Blake, N.J. Blake, J.B. Burkholder, J.H. Butler, R.A. Cox, P.H. Haynes, M.K.W. Ko, K. Kreher, C. Mari, K. Pfeilsticker, J.M.C. Plane, R.J. Salawitch, C. Schiller, B.-M. Sinnhuber, R. von Glasow, N.J. Warwick, D.J. Wuebbles, and S.A. Yvon-Lewis, Halogenated very short-lived substances, Chapter 2 in *Scientific Assessment of Ozone Depletion: 2006*, Global Ozone Research and Monitoring Project—

Report No.50, World Meteorological Organization, Geneva, Switzerland, 2007.

Le Calvé, S., G. Le Bras, and A. Mellouki, Temperature dependence for the rate coefficients of the reactions of the OH radical with a series of formates, *J. Phys. Chem. A*, *101* (30), 5489-5493, doi: 10.1021/jp970554x, 1997.

Lee, B.-S., J.L. Bullister, and F.A. Whitney, Chlorofluorocarbon CFC-11 and carbon tetrachloride removal in Saanich Inlet, an intermittently anoxic basin, *Mar. Chem.*, *66* (3-4), 171-185, doi: 10.1016/S0304-4203(99)00039-0, 1999.

Lee-Taylor, J.M., and E.A. Holland, Litter decomposition as a potential natural source of methyl bromide, *J. Geophys. Res.*, *105* (D7), 8857-8864, doi: 10.1029/1999JD901112, 2000.

Lee-Taylor, J., and K.R. Redeker, Reevaluation of global emissions from rice paddies of methyl iodide and other species, *Geophys. Res. Lett.*, *32*, L15801, doi: 10.1029/2005GL022918, 2005.

Leser, H., G. Hönninger, and U. Platt, MAX-DOAS measurements of BrO and NO_2 in the marine boundary layer, *Geophys. Res. Lett.*, *30* (10), 1537, doi: 10.1029/2002GL015811, 2003.

Levin, I., T. Naegler, R. Heinz, D. Osusko, E. Cuevas, A. Engel, J. Ilmberger, R.L. Langenfelds, B. Neininger, C. v. Rohden, L.P. Steele, R. Weller, D.E. Worthy, and S.A. Zimov, The global SF_6 source inferred from long-term high precision atmospheric measurements and its comparison with emission inventories, *Atmos. Chem. Phys.*, *10* (6), 2655-2662, doi: 10.5194/acp-10-2655-2010, 2010.

Levine, J.G., P. Braesicke, N.R.P. Harris, and J.A. Pyle, Seasonal and inter-annual variations in troposphere-to-stratosphere transport from the tropical tropopause layer, *Atmos. Chem. Phys.*, *8* (13), 3689-3703, doi: 10.5194/acp-8-3689-2008, 2008.

Li, Y., K.O. Patten, D. Youn, and D.J. Wuebbles, Potential impacts of CF_3I on ozone as a replacement for CF_3Br in aircraft applications, *Atmos. Chem. Phys.*, *6* (12), 4559-4568, doi: 10.5194/acp-6-4559-2006, 2006.

Liang, Q., R.S. Stolarski, S.R. Kawa, J.E. Nielsen, J.M. Rodriguez, A.R. Douglass, J.M. Rodriguez, D.R. Blake, E.L. Atlas, and L.E. Ott, Finding the missing stratospheric Br_y: A global modeling study of $CHBr_3$ and CH_2Br_2, *Atmos. Chem. Phys.*, *10* (5), 2269-2286, doi: 10.5194/acp-10-2269-2010, 2010.

Liu, A.Q., and G.W.K. Moore, Lake-effect snowstorms over southern Ontario, Canada, and their associated synoptic-scale environment, *Mon. Wea. Rev.*, *132* (11), 2595-2609, doi: 10.1175/MWR2796.1, 2004.

Liu, C., and E.J. Zipser, Global distribution of convection penetrating the tropical tropopause, *J. Geophys. Res.*, *110*, D23104, doi: 10.1029/2005JD006063, 2005.

Liu, C., E.J. Zipser, and S.W. Nesbitt, Global distribution of tropical deep convection: Different perspectives from TRMM infrared and radar data, *J. Clim.*, *20* (3), 489-503, doi: 10.1175/JCLI4023.1, 2007.

Liu, X.-F., Evidence of Biodegradation of Atmospheric Carbon Tetrachloride in Soils: Field and Microcosm Studies, Ph.D. thesis, 139 pp., Columbia University, New York, NY, U.S.A., 2006.

Livesey, N.J., L.J. Kovalenko, R.J. Salawitch, I.A. MacKenzie, M.P. Chipperfield, W.G. Read, R.F. Jarnot, and J.W. Waters, EOS Microwave Limb Sounder observations of upper stratospheric BrO: Implications for total bromine, *Geophys. Res. Lett.*, *33*, L20817, doi: 10.1029/2006GL026930, 2006.

Low, J.C., N.Y. Wang, J. Williams, and R.J. Cicerone, Measurements of ambient atmospheric C_2H_5Cl and other ethyl and methyl halides at coastal California sites and over the Pacific Ocean, *J. Geophys. Res.*, *108* (D19), 4608, doi: 10.1029/2003JD003620, 2003.

Lu, X.-L., G.-P. Yang, G.-S. Song, and L. Zhang, Distributions and fluxes of methyl chloride and methyl bromide in the East China Sea and the Southern Yellow Sea in autumn, *Mar. Chem.*, *118* (1-2), 75-84, doi: 10.1016/j.marchem.2009.11.002, 2010.

Luderer, G., J. Trentmann, K. Hungershöfer, M. Herzog, M. Fromm, and M.O. Andreae, Small-scale mixing processes enhancing troposphere-to-stratosphere transport by pyro-cumulonimbus storms, *Atmos. Chem. Phys.*, *7* (23), 5945-5957, doi: 10.5194/acp-7-5945-2007, 2007.

Luecken, D.J., R.L. Waterland, S. Papasavva, K.N. Taddonio, W.T. Hutzel, J.P. Rugh, and S.O. Andersen, Ozone and TFA impacts in North America from degradation of 2,3,3,3-tetrafluoropropene (HFO-1234yf), a potential greenhouse gas replacement, *Environ. Sci. Technol.*, *44* (1), 343-348, doi: 10.1021/es902481f, 2010.

Mahieu, E., P. Duchatelet, R. Zander, P. Demoulin, C. Servais, C.P. Rinsland, M.P. Chipperfield, and M. De Mazière, The evolution of inorganic chlorine above the Jungfraujoch station: An update, in *Ozone Vol. II*, *Proceedings of the XX Quadrennial Ozone Symposium*, 1-8 June 2004, Kos, Greece, edited by C.S. Zerefos, 997-998, Int. Ozone Comm., Athens, Greece, 2004.

Mahieu, E., P. Duchatelet, P. Demoulin, K.A. Walker, E. Dupuy, L. Froidevaux, C. Randall, V. Catoire, K. Strong, C.D. Boone, P.F. Bernath, J.-F. Blavier, T. Blumenstock, M. Coffey, M. De Mazière, D. Griffith, J. Hannigan, F. Hase, N. Jones, K.W. Jucks, A. Kagawa, Y. Kasai, Y. Mebarki, S. Mikuteit, R. Nassar, J. Notholt, C.P. Rinsland, C. Robert, O. Schrems, C. Senten, D. Smale, J. Taylor, C. Tétard, G.C. Toon, T. Warneke, S.W. Wood, R. Zan-

der, and C. Servais, Validation of ACE-FTS v2.2 measurements of HCl, HF, CCl_3F and CCl_2F_2 using space-, balloon- and ground-based instrument observations, *Atmos. Chem. Phys*., *8* (20), 6199-6221, doi: 10.5194/acp-8-6199-2008, 2008.

Maione, M., J. Arduini, G. Mangani, and A. Geniali, Evaluation of an automatic sampling gas chromatographic-mass spectrometric instrument for continuous monitoring of trace anthropogenic gases, *Int. J. Environ. Anal. Chem*., *84* (4), 241–253, doi: 10.1080/03067310310001626740, 2004.

Maione, M., U. Giostra, J. Arduini, L. Belfiore, F. Furlani, A. Geniali, G. Mangani, M.K. Vollmer, and S. Reimann, Localization of source regions of selected hydrofluorocarbons combining data collected at two European mountain stations, *Sci. Total Environ.*, *391* (2-3), 232-240, doi: 10.1016/j.scitotenv.2007.10.023, 2008.

Makide, Y., and F.S. Rowland, Tropospheric concentrations of methylchloroform, CH_3CCl_3, in January 1978 and estimates of the atmospheric residence times for hydrohalocarbons, *Proc. Natl. Acad. Sci.*, *78* (10), 5933-5937, 1981.

Manley, S.L., N.-Y. Wang, M.L. Walser, and R.J. Cicerone, Coastal salt marshes as global methyl halide sources from determinations of intrinsic production by marsh plants, *Global Biogeochem. Cycles*, *20*, GB3015, doi: 10.1029/2005GB002578, 2006.

Manley, S.L., N.-Y. Wang, M.L. Walser, and R.J. Cicerone, Methyl halide emissions from greenhouse-grown mangroves, *Geophys. Res. Lett.*, *34*, L01806, doi: 10.1029/2006GL027777, 2007.

Manning, A.J., D.B. Ryall, R.G. Derwent, P.G. Simmonds, and S. O'Doherty, Estimating European emissions of ozone-depleting and greenhouse gases using observations and a modeling back-attribution technique, *J. Geophys. Res.*, *108* (D14), 4405, doi: 10.1029/2002JD002312, 2003.

Marcy, T.P., P.J. Popp, R.S. Gao, D.W. Fahey, E.A. Ray, E.C. Richard, T.L. Thompson, E.L. Atlas, M. Loewenstein, S.C. Wofsy, S. Park, E.M. Weinstock, W.H. Swartz, and M.J. Mahoney, Measurements of trace gases in the tropical tropopause layer, *Atmos. Environ*., *41* (34), 7253-7261, doi: 10.1016/j.atmosenv.2007.05.032, 2007.

Martin, J.W., S.A. Mabury, C.S. Wong, F. Noventa, K.R. Solomon, M. Alaee, and D.C.G. Muir, Airborne haloacetic acids, *Environ. Sci. Technol*., *37* (13), 2889-2897, doi: 10.1021/es026345u, 2003.

Martin, M., D. Pöhler, K. Seitz, R. Sinreich, and U. Platt, BrO measurements over the Eastern North-Atlantic, *Atmos. Chem. Phys.*, *9* (24), 9545-9554, doi: 10.5194/acp-9-9545-2009, 2009.

Martinerie, P., E. Nourtier-Mazauric, J.-M. Barnola, W.T. Sturges, D.R. Worton, E. Atlas, L.K. Gohar, K.P. Shine, and G.P. Brasseur, Long-lived halocarbon trends and budgets from atmospheric chemistry modelling constrained with measurements in polar firn, *Atmos. Chem. Phys.*, *9* (12), 3911-3934, doi: 10.5194/acp-9-3911-2009, 2009.

Martinsson, B.G., H.N. Nguyen, C.A.M. Brenninkmeijer, A. Zahn, J. Heintzenberg, M. Hermann, and P.F.J. van Velthoven, Characteristics and origin of lowermost stratospheric aerosol at northern midlatitudes under volcanically quiescent conditions based on CARIBIC observations, *J. Geophys. Res*., *110*, D12201, doi: 10.1029/2004JD005644, 2005.

McCulloch, A., M.L. Aucott, T.E. Graedel, G. Kleiman, P.M. Midgley, and Y.-F. Li, Industrial emissions of trichloroethene, tetrachloroethene, and dichloromethane: Reactive Chlorine Emissions Inventory, *J. Geophys. Res.*, *104* (D7), 8417-8427, doi: 10.1029/1999JD900011, 1999.

McCulloch, A., Chloroform in the environment: Occurrence, sources, sinks and effects, *Chemosphere*, *50* (10), 1291-1308, doi: 10.1016/S0045-6535(02)00697-5, 2003.

McLinden, C.A., C.S. Haley, N.D. Lloyd, F. Hendrick, A. Rozanov, B.-M. Sinnhuber, F. Goutail, D.A. Degenstein, E.J. Llewellyn, C.E. Sioris, M. Van Roozendael, J.P. Pommereau, W. Lotz, and J.P. Burrows, Odin/OSIRIS observations of stratospheric BrO: Retrieval methodology, climatology, and inferred Br_y, *J. Geophys. Res.*, *115*, D15308, doi: 10.1029/2009JD012488, 2010.

Mead, M.I., I.R. White, G. Nickless, K.-Y. Wang, and D.E. Shallcross, An estimation of the global emission of methyl bromide from rapeseed (*Brassica napus*) from 1961 to 2003, *Atmos. Environ.*, *42* (2), 337-345, doi: 10.1016/j.atmosenv.2007.09.020, 2008a.

Mead, M.I., M.A.H. Khan, G. Nickless, B.R. Greally, D. Tainton, T. Pitman, and D.E. Shallcross, Leaf cutter ants: A possible missing source of biogenic halocarbons, *Environ. Chem.*, *5* (1), 5-10, doi: 10.1071/EN07068, 2008b.

Mead, M.I., M.A.H. Khan, I.R. White, G. Nickless, and D.E. Shallcross, Methyl halide emission estimates from domestic biomass burning in Africa, *Atmos. Environ.*, *42* (21), 5241-5250, doi: 10.1016/j.atmosenv.2008.02.066, 2008c.

Mébarki, Y., V. Catoire, N. Huret, G. Berthet, C. Robert, and G. Poulet, More evidence for very short-lived substance contribution to stratospheric chlorine inferred from HCl balloon-borne in situ measurements in the tropics, *Atmos. Chem. Phys*., *10* (2), 397-409, doi: 10.5194/acp-10-397-2010, 2010.

Meier, R.R., J.M.C. Plane, M.H. Stevens, L.J. Paxton, A.B. Christensen, and G. Crowley, Can mo-

lecular diffusion explain Space Shuttle plume spreading?, *Geophys. Res. Lett.*, 37, L08101, doi: 10.1029/2010GL042868, 2010.

Meirink, J.F., P. Bergamaschi, C. Frankenberg, M.T.S. d'Amelio, E.J. Dlugokencky, L.V. Gatti, S. Houweling, J.B. Miller, T. Röckmann, M.G. Villani, and M.C. Krol, Four-dimensional variational data assimilation for inverse modelling of atmospheric methane emissions: Analysis of SCIAMACHY observations, *J. Geophys. Res.*, *113*, D17301, doi: 10.1029/2007JD009740, 2008.

Mikuteit, S., Trendbestimmung stratosphärischer Spurengase mit Hilfebodengebundener FTIR-Messungen, dissertation, FZK Report No. 7385, Forschungszentrum Karlsruhe, Germany, available: http://www-imk.fzk.de/asf/ftir/refs.htm, 2008.

Miller, B.R., R.F. Weiss, P.K. Salameh, T. Tanhua, B.R. Greally, J. Mühle, and P.G. Simmonds, Medusa: A sample preconcentration and GC/MS detector system for in situ measurements of atmospheric trace halocarbons, hydrocarbons, and sulfur compounds, *Anal. Chem*., *80* (5), 1536-1545, doi: 10.1021/ac702084k, 2008.

Miller, B.R, M. Rigby, L.J.M. Kuijpers, P.B. Krummel, L.P. Steele, M. Leist, P.J. Fraser, A. McCulloch, C. Harth, P. Salameh, J. Mühle, R.F. Weiss, R.G. Prinn, R.H.J. Wang, S. O'Doherty, B.R. Greally, and P.G. Simmonds, HFC-23 (CHF_3) emission trend response to HCFC-22 ($CHClF_2$) production and recent HFC-23 emission abatement measures, *Atmos. Chem. Phys.*, *10* (16), 7875-7890, doi: 10.5194/acp-10-7875-2010, 2010.

Millet, D.B., E.L. Atlas, D.R. Blake, N.J. Blake, G.S. Diskin, J.S. Holloway, R.C. Hudman, S. Meinardi, T.B. Ryerson, and G.W. Sachse, Halocarbon emissions from the United States and Mexico and their global warming potential, *Environ. Sci. Technol.*, *43* (4), 1055-1060, doi: 10.1021/es802146j, 2009.

Møgelberg, T.E., J. Platz, O.J. Nielsen, J. Sehested, and T.J. Wallington, Atmospheric chemistry of HFC-236fa: Spectrokinetic investigation of the $CF_3CHO_2{\cdot}CF_3$ radical, its reactions with NO, and the fate of the $CF_3CHO{\cdot}CF_3$ radical, *J. Phys. Chem.*, *99* (15), 5373-5378, doi: 10.1021/j100015a021, 1995.

Molina, L.T., P.J. Wooldridge, and M.J. Molina, Atmospheric reactions and ultraviolet and infrared absorptivities of nitrogen trifluoride, *Geophys. Res. Lett.*, *22* (14), 1873-1876, doi: 10.1029/95GL01669, 1995.

Montzka, S.A., and P.J. Fraser (Lead Authors), J.H. Butler, P.S. Connell, D.M. Cunnold, J.S. Daniel, R.G. Derwent, S. Lal, A. McCulloch, D.E. Oram, C.E. Reeves, E. Sanhueza, L.P. Steele, G.J.M. Velders, R.F. Weiss, and R.J. Zander, Controlled substances and other source gases, Chapter 1 in *Scientific Assessment of Ozone Depletion: 2002*, Global Ozone Research and Monitoring Project—Report No. 47, Geneva, Switzerland, 2003.

Montzka, S.A., R.C. Myers, J.H. Butler, J.W. Elkins, L.T. Lock, A.D. Clarke, and A.H. Goldstein, Observations of HFC-134a in the remote troposphere, *Geophys. Res. Lett*., *23* (2), 169-172, doi: 10.1029/95GL03590, 1996.

Montzka, S.A., J.H. Butler, J.W. Elkins, T.M. Thompson, A.D. Clarke, and L.T. Lock, Present and future trends in the atmospheric burden of ozone-depleting halogens, *Nature*, *398*, 690-694, doi: 10.1038/19499, 1999.

Montzka, S.A., C.M. Spivakovsky, J.H. Butler, J.W. Elkins, L.T. Lock, and D.J. Mondeel, New observational constraints for atmospheric hydroxyl on global and hemispheric scales, *Science*, *288* (5465), 500-503, doi: 10.1126/science.288.5465.500, 2000.

Montzka, S.A., J.H. Butler, B.D. Hall, D.J. Mondeel, and J.W. Elkins, A decline in tropospheric organic bromine, *Geophys. Res. Lett.*, *30* (15), 1826, doi: 10.1029/2003GL017745, 2003.

Montzka, S.A., M. Aydin, M. Battle, J.H. Butler, E.S. Saltzman, B.D. Hall, A.D. Clarke, D. Mondeel, and J.W. Elkins, A 350-year atmospheric history for carbonyl sulfide inferred from Antarctic firn air and air trapped in ice, *J. Geophys. Res.*, *109*, D22302, doi: 10.1029/2004JD004686, 2004.

Montzka, S.A., P. Calvert, B.D. Hall, J.W. Elkins, T.J. Conway, P.P. Tans, and C. Sweeney, On the global distribution, seasonality, and budget of atmospheric carbonyl sulfide (COS) and some similarities to CO_2, *J. Geophys. Res.*, *112*, D09302, doi: 10.1029/2006JD007665, 2007.

Montzka, S.A., J.S. Daniel, J. Cohen, and K. Vick, Current trends, mixing ratios, and emissions of ozone-depleting substances and their substitutes, in *Trends in Emissions of Ozone-Depleting Substances*, *Ozone Layer Recovery*, *and Implications for Ultraviolet Radiation Exposure*, Synthesis and Assessment Product 2.4, report by the U.S. Climate Change Science Program and the Subcommittee on Global Change Research, edited by A.R. Ravishankara, M.J. Kurylo, and C.A. Ennis, 29-78, Department of Commerce, NOAA National Climatic Data Center, Asheville, NC, 2008.

Montzka, S.A., B.D. Hall, and J.W. Elkins, Accelerated increases observed for hydrochlorofluorocarbons since 2004 in the global atmosphere, *Geophys. Res. Lett.*, *36*, L03804, doi: 10.1029/2008GL036475, 2009.

Montzka, S.A., L. Kuijpers, M.O. Battle, M. Aydin, K.R. Verhulst, E.S. Saltzman, and D.W. Fahey, Recent increases in global HFC-23 emissions, *Geophys. Res. Lett.*, *37*, L02808, doi: 10.1029/

2009GL041195, 2010.

Moore, D.P., and J.J. Remedios, Growth rates of stratospheric HCFC-22, *Atmos. Chem. Phys*., *8* (1), 73-82, doi: 10.5194/acp-8-73-2008, 2008.

Moore, R.M., A photochemical source of methyl chloride in saline waters, *Environ. Sci. Technol.*, *42* (6), 1933-1937, doi: 10.1021/es0719201, 2008.

Moore, R.M., A. Gut, and M.O. Andreae, A pilot study of methyl chloride emissions from tropical woodrot fungi, *Chemosphere*, *58* (2), 221-225, doi: 10.1016/j.chemosphere.2004.03.011, 2005.

Mühle, J., J. Huang, R.F. Weiss, R.G. Prinn, B.R. Miller, P.K. Salameh, C.M. Harth, P.J. Fraser, L.W. Porter, B.R. Greally, S. O'Doherty, and P.G. Simmonds, Sulfuryl fluoride in the global atmosphere, *J. Geophys. Res.*, *114*, D05306, doi: 10.1029/2008JD011162, 2009.

Mühle, J., A.L. Ganesan, B.R. Miller, P.K. Salameh, C.M. Harth, B.R. Greally, M. Rigby, L.W. Porter, L.P. Steele, C.M. Trudinger, P.B. Krummel, S. O'Doherty, P.J. Fraser, P.G. Simmonds, R.G. Prinn, and R.F. Weiss, Perfluorocarbons in the global atmosphere: Tetrafluoromethane, hexafluoroethane, and octafluoropropane, *Atmos. Chem. Phys.*, *10* (11), 5145-5164, doi: 10.5194/acp-10-5145-2010, 2010.

Murphy, D.M., D.J. Cziczo, P.K. Hudson, and D.S. Thomson, Carbonaceous material in aerosol particles in the lower stratosphere and tropopause region, *J. Geophys. Res.*, *112*, D04203, doi: 10.1029/2006JD007297, 2007.

Naik, V., A.K. Jain, K.O. Patten, and D.J. Wuebbles, Consistent sets of atmospheric lifetimes and radiative forcings on climate for CFC replacements: HCFCs and HFCs, *J. Geophys. Res.*, *105* (D5), 6903-6914, doi: 10.1029/1999JD901128, 2000.

Neuman, J.A., J.B. Nowak, L.G. Huey, J.B. Burkholder, J.E. Dibb, J.S. Holloway, J. Liao, J. Peischl, J.M. Roberts, T.B. Ryerson, E. Scheuer, H. Stark, R.E. Stickel, D.J. Tanner, and A. Weinheimer, Bromine measurements in ozone depleted air over the Arctic Ocean, *Atmos. Chem. Phys.*, *10* (14), 6503-6514, doi: 10.5194/acp-10-6503-2010, 2010.

Nevison, C.D., N.M. Mahowald, R.F. Weiss, and R.G. Prinn, Interannual and seasonal variability in atmospheric N_2O, *Global Biogeochem. Cycles*, *21*, GB3017, doi: 10.1029/2006GB002755, 2007.

Newman, P.A. and J.A. Pyle (Lead Authors), J. Austin, G.O. Braathen, P.O. Canziani, K.S. Carslaw, P.M. de F. Forster, S. Godin-Beekmann, B.M. Knudsen, K. Kreher, H. Nakane, S. Pawson, V. Ramaswamy, M. Rex, R.J. Salawitch, D.T. Shindell, A. Tabazadeh, and D.W. Toohey, Polar stratospheric ozone: Past and future, Chapter 3 in *Scientific Assessment of Ozone Depletion: 2002*, Global Ozone Research and Monitoring Project—Report No. 47, Geneva, Switzerland, 2003.

Newman, P.A., J.S. Daniel, D.W. Waugh, and E.R. Nash, A new formulation of equivalent effective stratospheric chlorine (EESC), *Atmos. Chem. Phys.*, *7* (17), 4537-4522, doi: 10.5194/acp-7-4537-2007, 2007.

Nielsen, O.J., B.F. Scott, C. Spencer, T.J. Wallington, and J.C. Ball, Trifluoroacetic acid in ancient freshwater, *Atmos. Environ*., *35* (16), 2799-2801, doi: 10.1016/S1352-2310(01)00148-0, 2001.

Nielsen, O.J., M.S. Javadi, M.P. Sulbaek Andersen, M.D. Hurley, T.J. Wallington, and R. Singh, Atmospheric chemistry of $CF_3CF{=}CH_2$: Kinetics and mechanisms of gas-phase reactions with Cl atoms, OH radicals, and O_3, *Chem. Phys. Lett.*, *439* (1-3),18-22, doi: 10.1016/j.cplett.2007.03.053, 2007.

Notholt, J., B.P. Luo, S. Fueglistaler, D. Weisenstein, M. Rex, M.G. Lawrence, H. Bingemer, I. Wohltmann, T. Corti, T. Warneke, R. von Kuhlmann, and T. Peter, Influence of tropospheric SO_2 emissions on particle formation and the stratospheric humidity, *Geophys. Res. Lett*., *32*, L07810, doi: 10.1029/2004GL022159, 2005.

O'Brien, L.M., N.R.P. Harris, A.D. Robinson, B. Gostlow, N. Warwick, X. Yang, and J.A. Pyle, Bromocarbons in the tropical marine boundary layer at the Cape Verde Observatory – measurements and modelling, *Atmos. Chem. Phys*., *9* (22), 9083-9099, doi: 10.5194/acp-9-9083-2009, 2009.

O'Doherty, S., D.M. Cunnold, A. Manning, B.R. Miller, R.H.J. Wang, P.B. Krummel, P.J. Fraser, P.G. Simmonds, A. McCulloch, R.F. Weiss, P. Salameh, L.W. Porter, R.G. Prinn, J. Huang, G. Sturrock, D. Ryall, R.G. Derwent, and S.A. Montzka, Rapid growth of hydrofluorocarbon 134a and hydrochlorofluorocarbons 141b, 142b, and 22 from Advanced Global Atmospheric Gases Experiment (AGAGE) observations at Cape Grim, Tasmania, and Mace Head, Ireland, *J. Geophys. Res.*, *109*, D06310, doi: 10.1029/2003JD004277, 2004.

O'Doherty, S., D.M. Cunnold, B.R. Miller, J. Mühle, A. McCulloch, P.G. Simmonds, A.J. Manning, S. Reimann, M.K. Vollmer, B.R. Greally, R.G. Prinn, P.J. Fraser, L.P. Steele, P.B. Krummel, B.L. Dunse, L.W. Porter, C.R. Lunder, N. Schmidbauer, O. Hermansen, P.K. Salameh, C.M. Harth, R.H.J. Wang, and R.F. Weiss, Global and regional emissions of HFC-125 (CHF_2CF_3) from in situ and air archive atmospheric observations at AGAGE and SOGE observatories, *J. Geophys. Res.*, *114*, D23304, doi: 10.1029/2009JD012184, 2009.

Oram, D.E., Trends of Long-Lived Anthropogenic Halocarbons in the Southern Hemisphere and Model

Calculations of Global Emissions, Ph.D. thesis, Univ. of E. Anglia, Norwich, U.K., 249 pp., 1999.

Oram, D.E., W.T. Sturges, S.A. Penkett, A. McCulloch, and P.J. Fraser, Growth of fluoroform (CHF_3, HFC-23) in the background atmosphere, *Geophys. Res. Lett.*, *25* (1), 35-38, doi: 10.1029/97GL03483, 1998.

Orkin, V.L., F. Louis, R.E. Huie, and M.J. Kurylo, Photochemistry of bromine-containing fluorinated alkenes: Reactivity toward OH and UV spectra, *J. Phys. Chem. A*, *106* (43), 10195-10199, doi: 10.1021/jp014436s, 2002.

Orkin, V.L., L.E. Martynova, and A.N. Ilichev, High-accuracy measurements of OH reaction rate constants and IR absorption spectra: CH_2=CF-CF_3 and *trans*-CHF=CH-CF_3, *J. Phys. Chem. A.*, *114* (19), 5967-5979, doi: 10.1021/jp9092817, 2010.

Oyaro, N., S.R. Sellevåg, and C.J. Nielsen, Study of the OH and Cl-initiated oxidation, IR absorption cross-section, radiative forcing, and global warming potential of four C_4-hydrofluoroethers, *Environ. Sci. Technol.*, *38* (21), 5567-5576, doi: 10.1021/es0497330, 2004.

Oyaro, N., S.R. Sellevåg, and C.J. Nielsen, Atmospheric chemistry of hydrofluoroethers: Reaction of a series of hydrofluoroethers with OH radicals and Cl atoms, atmospheric lifetimes, and global warming potentials, *J. Phys. Chem. A*, *109* (2), 337-346, doi: 10.1021/jp047860c, 2005.

Packer, M., Algal capture of carbon dioxide; biomass generation as a tool for greenhouse gas mitigation with reference to New Zealand energy strategy and policy, *Energy Policy*, *37* (9), 3428-3437, doi: 10.1016/j.enpol.2008.12.025, 2009.

Palmer, C.J., and C.J. Reason, Relationships of surface bromoform concentrations with mixed layer depth and salinity in the tropical oceans, *Global Biogeochem. Cycles*, *23*, GB2014, doi: 10.1029/2008GB003338, 2009.

Papadimitriou, V.C., R.K. Talukdar, R.W. Portmann, A.R. Ravishankara, and J.B. Burkholder, CF_3CF=CH_2 and (*Z*)-CF_3CF=CHF: Temperature dependent OH rate coefficients and global warming potentials, *Phys. Chem. Chem. Phys.*, *10*, 808-820, doi: 10.1039/B714382F, 2008a.

Papadimitriou, V.C., R.W. Portmann, D.W. Fahey, J. Mühle, R.F. Weiss, and J.B. Burkholder, Experimental and theoretical study of the atmospheric chemistry and global warming potential of SO_2F_2, *J. Phys. Chem. A*, *112* (49), 12657-12666, doi: 10.1021/jp806368u, 2008b.

Park, M., W.J. Randel, L.K. Emmons, P.F. Bernath, K.A. Walker, and C.D. Boone, Chemical isolation in the Asian monsoon anticyclone observed in Atmospheric Chemistry Experiment (ACE-FTS) data, *Atmos. Chem. Phys.*, *8* (3), 757-764, doi: 10.5194/acp-8-757-2008, 2008.

Peters, W., A.R. Jacobson, C. Sweeney, A.E. Andrews, T.J. Conway, K. Masarie, J.B. Miller, L.M.P. Bruhwiler, G. Pétron, A.I. Hirsch, D.E.J. Worthy, G.R. van der Werf, J.T. Randerson, P.O. Wennberg, M.C. Krol, and P.P. Tans, An atmospheric perspective on North American carbon dioxide exchange: CarbonTracker, *Proc. Natl. Acad. Sci.*, *104* (48), 18925-18930, doi: 10.1073/pnas.0708986104, 2007.

Peylin, P., D. Baker, J. Sarmiento, P. Ciais, and P. Bousquet, Influence of transport uncertainty on annual mean and seasonal inversions of atmospheric CO_2 data, *J. Geophys. Res.*, *107* (D19), 4385, doi: 10.1029/2001JD000857, 2002.

Ploeger, F., P. Konopka, G. Günther, J.-U. Grooß, and R. Müller, Impact of the vertical velocity scheme on modeling transport in the tropical tropopause layer, *J. Geophys. Res.*, *115*, D03301, doi: 10.1029/2009JD012023, 2010.

Porter, E., J. Wenger, J. Treacy, H. Sidebottom, A. Mellouki, S. Téton, and G. LeBras, Kinetic studies on the reactions of hydroxyl radicals with diethers and hydroxyethers, *J. Phys. Chem. A*, *101* (32), 5770-5775, doi: 10.1021/jp971254i, 1997.

Portmann, R.W., and S. Solomon, Indirect radiative forcing of the ozone layer during the 21st century, *Geophys. Res. Lett.*, *34*, L02813, doi: 10.1029/2006GL028252, 2007.

Prather, M.J., Timescales in atmospheric chemistry: CH_3Br, the ocean, and ozone depletion potentials, *Global Biogeochem. Cycles*, *11* (3), 393-400, doi: 10.1029/97GB01055, 1997.

Prather, M., and D. Ehhalt (Co-ordinating Lead Authors), F. Dentener, R. Derwent, E. Dlugokencky, E. Holland, I. Isaksen, J. Katima, V. Kirchhoff, P. Matson, P. Midgley, and M. Wang (Lead Authors), Atmospheric chemistry and greenhouse gases, Chapter 4 in *Climate Change 2001: The Scientific Basis. Contribution of Working Group I to the Third Assessment Report of the Intergovernmental Panel on Climate Change*, edited by J.T. Houghton, Y. Ding, D.J. Griggs, M. Noguer, P.J. van der Linden, X. Dai, K. Maskell, and C.A. Johnson, 881 pp., Cambridge University Press, Cambridge, U.K., 2001.

Prather, M.J., and J. Hsu, NF_3, the greenhouse gas missing from Kyoto, *Geophys. Res. Lett.*, *35*, L12810, doi: 10.1029/2008GL034542, 2008.

Prather, M.J., and J. Hsu, Correction to "NF_3, the greenhouse gas missing from Kyoto," *Geophys. Res. Lett.*, *37*, L11807, doi: 10.1029/2010GL043831, 2010.

Prinn, R.G., and R. Zander (Lead Authors), D.M. Cunnold, J.W. Elkins, A. Engel, P.J. Fraser, M.R. Gunson, M.K.W. Ko, E. Mahieu, P.M. Midgley, J.M.

Russell III, C.M. Volk, and R.F. Weiss, Long-lived ozone-related compounds, Chapter 1 in *Scientific Assessment of Ozone Depletion: 1998*, Global Ozone Research and Monitoring Project–Report No. 44, World Meteorological Organization, Geneva, Switzerland, 1999.

Prinn, R., D. Cunnold, R. Rasmussen, P. Simmonds, F. Alyea, A. Crawford, P. Fraser, and R. Rosen, Atmospheric emissions and trends of nitrous oxide deduced from 10 years of ALE-GAGE data, *J. Geophys. Res*., *95* (D11), 18369-18385, doi: 10.1029/JD095iD11p18369, 1990.

Prinn, R.G., R.F. Weiss, P.J. Fraser, P.G. Simmonds, D.M. Cunnold, F.N. Alyea, S. O'Doherty, P. Salameh, B.R. Miller, J. Huang, R.H.J. Wang, D.E. Hartley, C. Harth, L.P. Steele, G. Sturrock, P.M. Midgley, and A. McCulloch, A history of chemically and radiatively important gases in air deduced from ALE/GAGE/AGAGE, *J. Geophys. Res.*, *105* (D14), 17751-17792, doi: 10.1029/2000JD900141, 2000.

Prinn, R.G., J. Huang, R.F. Weiss, D.M. Cunnold, P.J. Fraser, P.G. Simmonds, A. McCulloch, C. Harth, S. Reimann, P. Salameh, S. O'Doherty, R.H.J. Wang, L.W. Porter, B.R. Miller, and P.B. Krummel, Evidence for variability of atmospheric hydroxyl radicals over the past quarter century, *Geophys. Res. Lett.*, *32*, L07809, doi: 10.1029/2004GL022228, 2005.

Pyle, J.A., N. Warwick, X. Yang, P.J. Young, and G. Zeng, Climate/chemistry feedbacks and biogenic emissions, *Phil. Trans. R. Soc. A*, *365* (1856), 1727-1740, doi: 10.1098/rsta.2007.2041, 2007.

Quack, B., E. Atlas, G. Petrick, and D.W.R. Wallace, Bromoform and dibromomethane above the Mauritanian upwelling: Atmospheric distributions and oceanic emissions, *J. Geophys. Res*., *112*, D09312, doi: 10.1029/2006JD007614, 2007.

Ramaswamy, V. (Co-ordinating Lead Author), O. Boucher, J. Haigh, D. Hauglustaine, J. Haywood, G. Myhre, T. Nakajima, G.Y. Shi, and S. Solomon (Lead Authors), Radiative forcing of climate change, Chapter 6 in *Climate Change 2001: The Scientific Basis. Contribution of Working Group I to the Third Assessment Report of the Intergovernmental Panel on Climate Change*, edited by J.T. Houghton, Y. Ding, D.J. Griggs, M. Noguer, P.J. van der Linden, X. Dai, K. Maskell, and C.A. Johnson, 881 pp., Cambridge University Press, Cambridge, U.K., 2001.

Randel, W.J., M. Park, L. Emmons, D. Kinnison, P. Bernath, K.A. Walker, C. Boone, and H. Pumphrey, Asian monsoon transport of pollution to the stratosphere, *Science*, *328* (5978), 611-613, doi: 10.1126/science.1182274, 2010.

Ravishankara, A.R., S. Solomon, A.A. Turnipseed, and R.F. Warren, Atmospheric lifetimes of long-lived halogenated species, *Science*, *259* (5092), 194-199, doi: 10.1126/science.259.5092.194, 1993.

Ravishankara, A.R., J.S. Daniel, and R.W. Portmann, Nitrous oxide (N_2O): The dominant ozone-depleting substance emitted in the 21st century, *Science*, *326* (5949), 123-125, doi: 10.1126/science.1176985, 2009.

Read, K.A., A.S. Mahajan, L.J. Carpenter, M.J. Evans, B.V.E. Faria, D.E. Heard, J.R. Hopkins, J.D. Lee, S.J. Moller, A.C. Lewis, L. Mendes, J.B. McQuaid, H. Oetjen, A. Saiz-Lopez, M.J. Pilling, and J.M.C. Plane, Extensive halogen-mediated ozone destruction over the tropical Atlantic Ocean, *Nature*, *453*, 1232-1235, doi: 10.1038/nature07035, 2008.

Read, W.G., L. Froidevaux, and J.W. Waters, Microwave limb sounder measurement of stratospheric SO_2 from the Mt. Pinatubo Volcano, *Geophys. Res. Lett.*, *20* (12), 1299-1302, doi: 10.1029/93GL00831, 1993.

Redeker, K.R., and R.J. Cicerone, Environmental controls over methyl halide emissions from rice paddies, *Global Biogeochem. Cycles*, *18*, GB1027, doi: 10.1029/2003GB002092, 2004.

Reeves, C.E., W.T. Sturges, G.A. Sturrock, K. Preston, D.E. Oram, J. Schwander, R. Mulvaney, J.-M. Barnola, and J. Chappellaz, Trends of halon gases in polar firn air: Implications for their emission distributions, *Atmos. Chem. Phys.*, *5* (8), 2055-2064, doi: 10.5194/acp-5-2055-2005, 2005.

Reichenau, T.G., and G. Esser, Is interannual fluctuation of atmospheric CO_2 dominated by combined effects of ENSO and volcanic aerosols?, *Global Biogeochem. Cycles*, *17* (4), 1094, doi: 10.1029/2002GB002025, 2003.

Reimann, S., D. Schaub, K. Stemmler, D. Folini, M. Hill, P. Hofer, B. Buchmann, P.G. Simmonds, B.R. Greally, and S. O'Doherty, Halogenated greenhouse gases at the Swiss high alpine site of Jungfraujoch (3580 m asl): Continuous measurements and their use for regional European source allocation, *J. Geophys. Res.*, *109*, D05307, doi: 10.1029/2003JD003923, 2004.

Reimann, S., M.K. Vollmer, D. Folini, M. Steinbacher, M. Hill, B. Buchmann, R. Zander, and E. Mahieu, Observations of long-lived anthropogenic halocarbons at the high-Alpine site of Jungfraujoch (Switzerland) for assessment of trends and European sources, *Sci. Total Environ.*, *391* (2-3), 224-231, doi: 10.1016/j.scitotenv.2007.10.022, 2008.

Rhew, R.C., and T. Abel, Measuring simultaneous production and consumption fluxes of methyl chloride and methyl bromide in annual temperate grasslands, *Environ. Sci. Technol.*, *41* (22), 7837-7843, doi: 10.1021/es0711011, 2007.

Rhew, R.C., B.R. Miller, and R.F. Weiss, Natural methyl bromide and methyl chloride emissions from coastal salt marshes, *Nature*, *403*, 292-295, doi: 10.1038/35002043, 2000.

Rhew, R.C., B.R. Miller, M.K. Vollmer, and R.F. Weiss, Shrubland fluxes of methyl bromide and methyl chloride, *J. Geophys. Res.*, *106* (D18), 20875-20882, doi: 10.1029/2001JD000413, 2001.

Rhew, R.C., L. Østergaard, E.S. Saltzman, and M.F. Yanofsky, Genetic control of methyl halide production in Arabidopsis, *Current Biology*, *13* (20), 1809-1813, doi: 10.1016/j.cub.2003.09.055, 2003.

Rhew, R.C., Y.A. Teh, and T. Abel, Methyl halide and methane fluxes in the northern Alaskan coastal tundra, *J. Geophys. Res.*, *112*, G02009, doi: 10.1029/2006JG000314, 2007.

Rhew, R.C., B.R. Miller, and R.F. Weiss, Chloroform, carbon tetrachloride and methyl chloroform fluxes in southern California ecosystems, *Atmos. Environ.*, *42* (30), 7135-7140, doi: 10.1016/j.atmosenv.2008.05.038, 2008.

Rhew, R.C., C. Chen, Y.A. Teh, and D. Baldocchi, Gross fluxes of methyl chloride and methyl bromide in a California oak-savanna woodland, *Atmos. Environ.*, *44* (16), 2054-2061, doi: 10.1016/j.atmosenv.2009.12.014, 2010.

Ricaud, P., B. Barret, J.-L. Attié, E. Motte, E. Le Flochmoën, H. Teyssèdre, V.-H. Peuch, N. Livesey, A. Lambert, and J.-P. Pommereau, Impact of land convection on troposphere-stratosphere exchange in the tropics, *Atmos. Chem. Phys.*, *7* (21), 5639-5657, doi: 10.5194/acp-7-5639-2007, 2007.

Rice, A.L., C.L. Butenhoff, M.J. Shearer, D. Teama, T.N. Rosenstiel, and M.A.K. Khalil, Emissions of anaerobically produced methane by trees, *Geophys. Res. Lett.*, *37*, L03807, doi: 10.1029/2009GL041565, 2010.

Richter, A., F. Wittrock, A. Ladstätter-Weißenmayer, and J.P. Burrows, GOME measurements of stratospheric and tropospheric BrO, *Adv. Space Res.*, *29* (11), 1667-1672, doi: 10.1016/S0273-1177(02)00123-0, 2002.

Rigby, M., R.G. Prinn, P.J. Fraser, P.G. Simmonds, R.L. Langenfelds, J. Huang, D.M. Cunnold, L.P. Steele, P.B. Krummel, R.F. Weiss, S. O'Doherty, P.K. Salameh, H.J. Wang, C.M. Harth, J. Mühle, and L.W. Porter, Renewed growth of atmospheric methane, *Geophys. Res. Lett.*, *35*, L22805, doi: 10.1029/2008GL036037, 2008.

Rinsland, C.P., E. Mahieu, R. Zander, N.B. Jones, M.P. Chipperfield, A. Goldman, J. Anderson, J.M. Russell III, P. Demoulin, J. Notholt, G.C. Toon, J.-F. Blavier, B. Sen, R. Sussmann, S.W. Wood, A. Meier, D.W.T. Griffith, L.S. Chiou, F.J. Murcray, T.M. Stephen, F. Hase, S. Mikuteit, A. Schulz, and T. Blumenstock, Long-term trends of inorganic chlorine from ground-based infrared solar spectra: Past increases and evidence for stabilization, *J. Geophys. Res.*, *108* (D8), 4252, doi: 10.1029/2002JD003001, 2003.

Rinsland, C.P., C. Boone, R. Nassar, K. Walker, P. Bernath, E. Mahieu, R. Zander, J.C. McConnell, and L. Chiou, Trends of HF, HCl, CCl_2F_2, CCl_3F, $CHClF_2$ (HCFC-22), and SF_6 in the lower stratosphere from Atmospheric Chemistry Experiment (ACE) and Atmospheric Trace Molecule Spectroscopy (ATMOS) measurement near 30°N latitude, *Geophys. Res. Lett.*, *32* (16), L16S03, doi: 10.1029/2005GL022415, 2005.

Rinsland, C.P., R. Nassar, C.D. Boone, P. Bernath, L. Chiou, D.K. Weisenstein, E. Mahieu, and R. Zander, Spectroscopic detection of COClF in the tropical and mid-latitude lower stratosphere, *J. Quant. Spectrosc. Radiat. Transfer*, *105* (3), 467-475, doi: 10.1016/j.jqsrt.2006.11.013, 2007.

Rinsland, C.P., L. Chiou, C. Boone, P. Bernath, and E. Mahieu, First measurements of the HCFC-142b trend from atmospheric chemistry experiment (ACE) solar occultation spectra, *J. Quant. Spectrosc. Radiat. Transfer*, *110* (18), 2127-2134, doi: 10.1016/j.jqsrt.2009.05.011, 2009.

Robson, J.I., L.K. Gohar, M.D. Hurley, K.P. Shine, and T.J. Wallington, Revised IR spectrum, radiative efficiency and global warming potential of nitrogen trifluoride, *Geophys. Res. Lett.*, *33*, L10817, doi: 10.1029/2006GL026210, 2006.

Rödenbeck, C., S. Houweling, M. Gloor, and M. Heimann, CO_2 flux history 1982–2001 inferred from atmospheric data using a global inversion of atmospheric transport, *Atmos. Chem. Phys.*, *3* (6), 1919-1964, doi: 10.5194/acp-3-1919-2003, 2003.

Römpp, A., O. Klemm, W. Fricke, and H. Frank, Haloacetates in fog and rain, *Environ. Sci. Technol.*, *35* (7), 1294-1298, doi: 10.1021/es0012220, 2001.

Rontu Carlon, N., D.K. Papanastasiou, E.L. Fleming, C.H. Jackman, P.A. Newman, and J.B. Burkholder, UV absorption cross sections of nitrous oxide (N_2O) and carbon tetrachloride (CCl_4) between 210 and 350 K and the atmospheric implications, *Atmos. Chem. Phys.*, *10* (13), 6137-6149, doi: 10.5194/acp-10-6137-2010, 2010.

Ross, M.N., M.Y. Danilin, D.K. Weisenstein, and M.K.W. Ko, Ozone depletion caused by NO and H_2O emissions from hydrazine-fueled rockets, *J. Geophys. Res.*, *109*, D21305, doi: 10.1029/2003JD004370, 2004.

Ross, M., D. Toohey, M. Peinemann, and P. Ross, Limits on the space launch market related to stratospheric

ozone depletion, *Astropolitics*, *7* (1), 50-82, doi: 10.1080/14777620902768867, 2009.

Rowland, F.S., S.C. Tyler, D.C. Montague, and Y. Makide, Dichlorodifluoromethane, CCl_2F_2, in the Earth's atmosphere, *Geophys. Res. Lett.*, *9* (4), 481-484, doi: 10.1029/GL009i004p00481, 1982.

Rudolph, J., A. Khedim, R. Koppmann, and B. Bonsang, Field study of the emissions of methyl chloride and other halocarbons from biomass burning in Western Africa, *J. Atmos. Chem.*, *22* (1-2), 67-80, doi: 10.1007/BF00708182, 1995.

Rudolph, J., K. von Czapiewski, and R. Koppmann, Emissions of methyl chloroform (CH_3CCl_3) from biomass burning and the tropospheric methyl chloroform budget, *Geophys. Res. Lett*., *27* (13), 1887-1890, doi: 10.1029/1999GL011178, 2000.

Saito, T., and Y. Yokouchi, Diurnal variation in methyl halide emission rates from tropical ferns, *Atmos. Environ.*, *40* (16), 2806-2811, doi: 10.1016/j.atmosenv.2006.01.016, 2006.

Saito, T., and Y. Yokouchi, Stable carbon isotope ratio of methyl chloride emitted from glasshouse-grown tropical plants and its implication for the global methyl chloride budget, *Geophys. Res. Lett.*, *35*, L08807, doi: 10.1029/2007GL032736, 2008.

Saito, T., Y. Yokouchi, Y. Kosugi, M. Tani, E. Philip, and T. Okuda, Methyl chloride and isoprene emissions from tropical rain forest in Southeast Asia, *Geophys. Res. Lett.*, *35*, L19812, doi: 10.1029/2008GL035241, 2008.

Saiz-Lopez, A., J.M.C. Plane, and J.A. Shillito, Bromine oxide in the mid-latitude marine boundary layer, *Geophys. Res. Lett.*, *31*, L03111, doi: 10.1029/2003GL018956, 2004.

Salawitch, R.J., D.K. Weisenstein, L.J. Kovalenko, C.E. Sioris, P.O. Wennberg, K. Chance, M.K.W. Ko, and C.A. McLinden, Sensitivity of ozone to bromine in the lower stratosphere, *Geophys. Res. Lett.*, *32*, L05811, doi: 10.1029/2004GL021504, 2005.

Salawitch, R.J., T. Canty, T. Kurosu, K. Chance, Q. Liang, A. da Silva, S. Pawson, J.E. Nielsen, J.M. Rodriguez, P.K. Bhartia, X. Liu, L.G. Huey, J. Liao, R.E. Stickel, D.J. Tanner, J.E. Dibb, W.R. Simpson, D. Donohoue, A. Weinheimer, F. Flocke, D. Knapp, D. Montzka, J.A. Neuman, J.B. Nowak, T.B. Ryerson, S. Oltmans, D.R. Blake, E.L. Atlas, D.E. Kinnison, S. Tilmes, L.L. Pan, F. Hendrick, M. Van Roozendael, K. Kreher, P.V. Johnston, R.S. Gao, B. Johnson, T.P. Bui, G. Chen, R.B. Pierce, J.H. Crawford, and D.J. Jacob, A new interpretation of total column BrO during Arctic spring, *Geophys. Res. Lett.*, *37*, L21805, doi:10.1029/2010GL043798, 2010.

Saltzman, E.S., M. Aydin, W.J. De Bruyn, D.B. King, and S.A. Yvon-Lewis, Methyl bromide in preindustrial air: Measurements from an Antarctic ice core, *J. Geophys. Res.*, *109*, D05301, doi: 10.1029/2003JD004157, 2004.

Saltzman, E.S., M. Aydin, C. Tatum, and M.B. Williams, 2,000-year record of atmospheric methyl bromide from a South Pole ice core, *J. Geophys. Res.*, *113*, D05304, doi: 10.1029/2007JD008919, 2008.

Sander, S.P., R.R. Friedl, D.M. Golden, M.J. Kurylo, G.K. Moortgat, H. Keller-Rudek, P.H. Wine, A.R. Ravishankara, C.E. Kolb, M.J. Molina, B.J. Finlayson-Pitts, R.E. Huie, and V.L. Orkin, *Chemical Kinetics and Photochemical Data for Use in Atmospheric Studies*, Evaluation Number 15, JPL Publication 06-02, Jet Propulsion Laboratory, Pasadena, Calif., 2006.

Sander, S.P., J. Abbatt, J.R. Barker, J.B. Burkholder, R.R. Friedl, D.M. Golden, R.E. Huie, C.E. Kolb, M.J. Kurylo, G.K. Moortgat, V.L. Orkin, and P.H. Wine, *Chemical Kinetics and Photochemical Data for Use in Atmospheric Studies*, Evaluation Number 17, JPL Publication 10-6, Jet Propulsion Laboratory, Pasadena, Calif., available: http://jpldataeval.jpl.nasa.gov/, 2010.

Schauffler, S.M., E.L. Atlas, D.R. Blake, F. Flocke, R.A. Lueb, J.M. Lee-Taylor, V. Stroud, and W. Travnicek, Distributions of brominated organic compounds in the troposphere and lower stratosphere, *J. Geophys. Res.*, *104* (D17), 21513-21536, 1999.

Schauffler, S.M., E.L. Atlas, S.G. Donnelly, A. Andrews, S.A. Montzka, J.W. Elkins, D.F. Hurst, P.A. Romashkin, G.S. Dutton, and V. Stroud, Chlorine budget and partitioning during the Stratospheric Aerosol and Gas Experiment (SAGE) III Ozone Loss and Validation Experiment (SOLVE), *J. Geophys. Res.*, *108*, 4173, doi: 10.1029/2001JD002040, 2003.

Schiller, C., J.-U. Grooß, P. Konopka, F. Plöger, F.H. Silva dos Santos, and N. Spelten, Hydration and dehydration at the tropical tropopause, *Atmos. Chem. Phys.*, *9* (24), 9647-9660, doi: 10.5194/acp-9-9647-2009, 2009.

Schmid, O., J.M. Reeves, J.C. Wilson, C. Wiedinmyer, C.A. Brock, D.W. Toohey, L.M. Avallone, A.M. Gates, and M.N. Ross, Size-resolved particle emission indices in the stratospheric plume of an Athena II rocket, *J. Geophys. Res*., *108*, 4250, doi: 10.1029/2002JD002486, 2003.

Schmittner, A., A. Oschlies, H.D. Matthews, and E.D. Galbraith, Future changes in climate, ocean circulation, ecosystems, and biogeochemical cycling simulated for a business-as-usual CO_2 emission scenario until year 4000 AD, *Global Biogeochem. Cycles*, *22*, GB1013, doi: 10.1029/2007GB002953, 2008.

Schofield, R., K. Kreher, B.J. Connor, P.V. Johnston, A. Thomas, D. Shooter, M.P. Chipperfield, C.D.

Rodgers, and G.H. Mount, Retrieved tropospheric and stratospheric BrO columns over Lauder, New Zealand, *J. Geophys. Res.*, *109*, D14304, doi: 10.1029/2003JD004463, 2004.

Schofield, R., P.V. Johnston, A. Thomas, K. Kreher, B.J. Connor, S. Wood, D. Shooter, M.P. Chipperfield, A. Richter, R. von Glasow, and C.D. Rodgers, Tropospheric and stratospheric BrO columns over Arrival Heights, Antarctica, 2002, *J. Geophys. Res.*, *111*, D22310, doi: 10.1029/2005JD007022, 2006.

Shine, K.P., L.K. Gohar, M.D. Hurley, G. Marston, D. Martin, P.G. Simmonds, T.J. Wallington, and M. Watkins, Perfluorodecalin: Global warming potential and first detection in the atmosphere, *Atmos. Environ.*, *39* (9), 1759-1763, doi: 10.1016/j.atmosenv.2005.01.001, 2005.

Shorter, J.H., C.E. Kolb, P.M. Crill, R.A. Kerwin, R.W. Talbot, M.E. Hines, and R.C. Harriss, Rapid degradation of atmospheric methyl bromide in soils, *Nature*, *377*, 717-719, doi: 10.1038/377717ao, 1995.

Simmonds, P.G., R.G. Derwent, A.J. Manning, P.J. Fraser, P.B. Krummel, S. O'Doherty, R.G. Prinn, D.M. Cunnold, B.R. Miller, H.J. Wang, D.B. Ryall, L.W. Porter, R.F. Weiss, and P.K. Salameh, AGAGE Observations of methyl bromide and methyl chloride at Mace Head, Ireland, and Cape Grim, Tasmania, 1998–2001, *J. Atmos. Chem.*, *47* (3), 243-269, doi: 10.1023/B:JOCH.0000021136.52340.9c, 2004.

Simmonds, P.G., A.J. Manning, D.M. Cunnold, A. McCulloch, S. O'Doherty, R.G. Derwent, P.B. Krummel, P.J. Fraser, B. Dunse, L.W. Porter, R.H.J. Wang, B.R. Greally, B.R. Miller, P. Salameh, R.F. Weiss, and R.G. Prinn, Global trends, seasonal cycles, and European emissions of dichloromethane, trichloroethene, and tetrachloroethene from the AGAGE observations at Mace Head, Ireland, and Cape Grim, Tasmania, *J. Geophys. Res.*, *111*, D18304, doi: 10.1029/2006JD007082, 2006.

Simpson, I.J., S. Meinardi, N.J. Blake, F.S. Rowland, and D.R. Blake, Long-term decrease in the global atmospheric burden of tetrachloroethene (C_2Cl_4), *Geophys. Res. Lett.*, *31*, L08108, doi: 10.1029/2003GL019351, 2004.

Simpson, I.J., N.J. Blake, D.R. Blake, S. Meinardi, M.P.S. Andersen, and F.S. Rowland, Strong evidence for negligible methyl chloroform (CH_3CCl_3) emissions from biomass burning, *Geophys. Res. Lett.*, *34*, L10805, doi: 10.1029/2007GL029383, 2007.

Sinnhuber, B.-M., and I. Folkins, Estimating the contribution of bromoform to stratospheric bromine and its relation to dehydration in the tropical tropopause layer, *Atmos. Chem. Phys.*, *6* (12), 4755-4761, doi: 10.5194/acp-6-4755-2006, 2006.

Sinnhuber, B.-M., D.W. Arlander, H. Bovensmann, J.P. Burrows, M.P. Chipperfield, C.-F. Enell, U. Frieß, F. Hendrick, P.V. Johnston, R.L. Jones, K. Kreher, N. Mohamed-Tahrin, R. Müller, K. Pfeilsticker, U. Platt, J.-P. Pommereau, I. Pundt, A. Richter, A.M. South, K.K. Tørnkvist, M. Van Roozendael, T. Wagner, and F. Wittrock, Comparison of measurements and model calculations of stratospheric bromine monoxide, *J. Geophys. Res.*, *107*, 4398, doi: 10.1029/2001JD000940, 2002.

Sinnhuber, B.-M., A. Rozanov, N. Sheode, O.T. Afe, A. Richter, M. Sinnhuber, F. Wittrock, J.P. Burrows, G.P. Stiller, T. von Clarmann, and A. Linden, Global observations of stratospheric bromine monoxide from SCIAMACHY, *Geophys. Res. Lett.*, *32*, L20810, doi: 10.1029/2005GL023839, 2005.

Sinnhuber, B.-M., N. Sheode, M. Sinnhuber, M.P. Chipperfield, and W. Feng, The contribution of anthropogenic bromine emissions to past stratospheric ozone trends: A modelling study, *Atmos. Chem. Phys.*, *9* (8), 2863-2871, doi: 10.5194/acp-9-2863-2009, 2009.

Sioris, C.E., L.J. Kovalenko, C.A. McLinden, R.J. Salawitch, M. Van Roozendael, F. Goutail, M. Dorf, K. Pfeilsticker, K. Chance, C. von Savigny, X. Liu, T.P. Kurosu, J.-P. Pommereau, H. Bösch, and J. Frerick, Latitudinal and vertical distribution of bromine monoxide in the lower stratosphere from Scanning Imaging Absorption Spectrometer for Atmospheric Chartography limb scattering measurements, *J. Geophys. Res.*, *111*, D14301, doi: 10.1029/2005JD006479, 2006.

Siskind, D.E., L. Froidevaux, J.M. Russell, and J. Lean, Implications of upper stratospheric trace constituent changes observed by HALOE for O_3 and ClO from 1992 to 1995, *Geophys. Res. Lett*., *25* (18), 3513-3516, 1998.

Sive, B.C., R.K. Varner, H. Mao, D.R. Blake, O.W. Wingenter, and R. Talbot, A large terrestrial source of methyl iodide, *Geophys. Res. Lett.*, *34*, L17808, doi: 10.1029/2007GL030528, 2007.

Solomon, P., J. Barrett, T. Mooney, B. Connor, A. Parrish, and D.E. Siskind, Rise and decline of active chlorine in the stratosphere, *Geophys. Res. Lett*., *33*, L18807, doi: 10.1029/2006GL027029, 2006.

Søndergaard, R., O.J. Nielsen, M.D. Hurley, T.J. Wallington, and R. Singh, Atmospheric chemistry of *trans*-CF_3CH=CHF: Kinetics of the gas-phase reactions with Cl atoms, OH radicals, and O_3, *Chem. Phys. Lett*., *443* (4-6), 199-204, doi: 10.1016/j.cplett.2007.06.084, 2007.

Sorokin, V.I., N.P. Gritsan, and A.I. Chichinin, Collisions of $O(^1D)$ with HF, F_2, XeF_2, NF_3, and CF_4: Deactivation and reaction, *J. Chem. Phys.*, *108* (21), 8995-9003, doi: 10.1063/1.476346, 1998.

SPARC (Stratospheric Processes And their Role in Climate), *SPARC Assessment of Stratospheric Aerosol Properties*, edited by L. Thomason and Th. Peter, World Climate Research Program Report 124, SPARC Report 4, WMO/TD- No. 1295, 346 pp., Verrières le Buisson, France, 2006.

SPARC CCMVal (Stratospheric Processes And their Role in Climate), *SPARC Report on the Evaluation of Chemistry-Climate Models*, edited by V. Eyring, T.G. Shepherd, and D.W. Waugh, SPARC Report No. 5, WCRP-132, WMO/TD-No. 1526, 478 pp., available: http://www.atmosp.physics.utoronto.ca/SPARC/ccmval_final/index.php, 2010.

Spivakovsky, C.M., J.A. Logan, S.A. Montzka, Y.J. Balkanski, M. Foreman-Fowler, D.B.A. Jones, L.W. Horowitz, A.C. Fusco, C.A.M. Brenninkmeijer, M.J. Prather, S.C. Wofsy, and M.B. McElroy, Three-dimensional climatological distribution of tropospheric OH: Update and evaluation, *J. Geophys. Res.*, *105* (D7), 8931-8980, 2000.

Stemmler, K., D. Folini, S. Ubl, M.K. Vollmer, S. Reimann, S. O'Doherty, B.R. Greally, P.G. Simmonds, and A.J. Manning, European emissions of HFC-365mfc, a chlorine-free substitute for the foam blowing agents HCFC-141b and CFC-11, *Environ. Sci. Technol.*, *41* (4), 1145-1151, doi: 10.1021/es061298h, 2007.

Stephens, B.B., K.R. Gurney, P.P. Tans, C. Sweeney, W. Peters, L. Bruhwiler, P. Ciais, M. Ramonet, P. Bousquet, T. Nakazawa, S. Aoki, T. Machida, G. Inoue, N. Vinnichenko, J. Lloyd, A. Jordan, M. Heimann, O. Shibistova, R.L. Langenfelds, L.P. Steele, R.J. Francey, and A.S. Denning, Weak northern and strong tropical land carbon uptake from vertical profiles of atmospheric CO_2, *Science*, *316*, 1732-1735, doi: 10.1126/science.1137004, 2007.

Stern, D.I., Global sulfur emissions from 1850 to 2000, *Chemosphere*, *58* (2), 163-175, doi: 10.1016/j.chemosphere.2004.08.022, 2005.

Stevens, M.H., R.R. Meier, X. Chu, M.T. DeLand, and J.M.C. Plane, Antarctic mesospheric clouds formed from space shuttle exhaust, *Geophys. Res. Lett.*, *32*, L13810, doi: 10.1029/2005GL023054, 2005.

Stiller, G.P., T. von Clarmann, M. Höpfner, N. Glatthor, U. Grabowski, S. Kellmann, A. Kleinert, A. Linden, M. Milz, T. Reddmann, T. Steck, H. Fischer, B. Funke, M. López-Puertas, and A. Engel, Global distribution of mean age of stratospheric air from MIPAS SF_6 measurements, *Atmos. Chem. Phys.*, *8* (3), 677-695, doi: 10.5194/acp-8-677-2008, 2008.

Stohl, A., S. Eckhardt, C. Forster, P. James, and N. Spichtinger, On the pathways and timescales of intercontinental air pollution transport, *J. Geophys. Res.*, *107*, 4684, doi: 10.1029/2001JD001396, 2002.

Stohl, A., P. Seibert, J. Arduini, S. Eckhardt, P. Fraser, B.R. Greally, C. Lunder, M. Maione, J. Mühle, S. O'Doherty, R.G. Prinn, S. Reimann, T. Saito, N. Schmidbauer, P.G. Simmonds, M.K. Vollmer, R.F. Weiss, and Y. Yokouchi, An analytical inversion method for determining regional and global emissions of greenhouse gases: Sensitivity studies and application to halocarbons, *Atmos. Chem. Phys.*, *9* (5), 1597-1620, doi: 10.5194/acp-9-1597-2009, 2009.

Stohl, A., J. Kim, S. Li, S. O'Doherty, J. Mühle, P.K. Salameh T. Saito, M.K. Vollmer, D. Wan, R.F. Weiss, B. Yao, Y. Yokouchi, and L.X. Zhou, Hydrochlorofluorocarbon and hydrofluorocarbon emissions in East Asia determined by inverse modeling, *Atmos. Chem. Phys.*, *10* (8), 3545-3560, doi: 10.5194/acp-10-3545-2010, 2010.

Sturrock, G.A., L.W. Porter, P.J. Fraser, *In situ* measurement of CFC replacement chemicals and other halocarbons at Cape Grim: The AGAGE CG-MS program, in *Baseline.Atmospheric Program Australia 1997-98*, edited by N.W. Tindale, N. Derek, and R.J. Francey, Bureau of Meteorology and CSIRO Atmospheric Research, Melbourne, 2001.

Sturrock, G.A., D.M. Etheridge, C.M. Trudinger, P.J. Fraser, and A.M. Smith, Atmospheric histories of halocarbons from analysis of Antarctic firn air: Major Montreal Protocol species, *J. Geophys. Res.*, *107*, 4765, doi: 10.1029/2002JD002548, 2002.

Sulbaek Andersen, M.P., A. Toft, O.J. Nielsen, M.D. Hurley, T.J. Wallington, H. Chishima, K. Tonokura, S.A. Mabury, J.W. Martin, and D.A. Ellis, Atmospheric chemistry of perfluorinated aldehyde hydrates (n-$C_xF_{2x+1}CH(OH)_2$, x = 1, 3, 4): Hydration, dehydration, and kinetics and mechanism of Cl atom and OH radical initiated oxidation, *J. Phys. Chem. A*, *110* (32), 9854-9860, doi: 10.1021/jp060404z, 2006.

Sulbaek Andersen, M.P., E.J.K. Nilsson, O.J. Nielsen, M.S. Johnson, M.D. Hurley, and T.J. Wallington, Atmospheric chemistry of *trans*-CF_3CH=CHCl: Kinetics of the gas-phase reactions with Cl atoms, OH radicals, and O_3, *J. Photochem. Photobio. A: Chemistry*, *199* (1), 92-97, doi: 10.1016/j.jphotochem.2008.05.013, 2008.

Sulbaek Andersen, M.P., M.D. Hurley, and T.J. Wallington, Kinetics of the gas phase reactions of chlorine atoms and OH radicals with CF_3CBr=CH_2 and CF_3CF_2CBr=CH_2, *Chem. Phys. Lett.*, *482* (1-3), 20-23, doi: 10.1016/j.cplett.2009.09.056, 2009a.

Sulbaek Andersen, M.P., D.R. Blake, F.S. Rowland, M.D. Hurley, and T.J. Wallington, Atmospheric chemistry of sulfuryl fluoride: Reaction with OH radicals, Cl atoms and O_3, atmospheric lifetime, IR spectrum, and global warming potential, *Environ.*

Sci. Technol., *43* (4), 1067-1070, doi: 10.1021/es802439f, 2009b.

Suntharalingam, P., A.J. Kettle, S.M. Montzka, and D.J. Jacob, Global 3-D model analysis of the seasonal cycle of atmospheric carbonyl sulfide: Implications for terrestrial vegetation uptake, *Geophys. Res. Lett*., *35*, L19801, doi: 10.1029/2008GL034332, 2008.

Tanhua, T., and K.A. Olsson, Removal and bioaccumulation of anthropogenic, halogenated transient tracers in an anoxic fjord, *Mar. Chem.*, *94* (1-4), 27-41, doi: 10.1016/j.marchem.2004.07.009, 2005.

Taniguchi, N., T.J. Wallington, M.D. Hurley, A.G. Guschin, L.T. Molina, and M.J. Molina, Atmospheric chemistry of $C_2F_5C(O)CF(CF_3)_2$: Photolysis and reaction with Cl atoms, OH radicals, and ozone, *J. Phys. Chem. A*, *107* (15), 2674-2679, doi: 10.1021/jp0220332, 2003.

Tarnocai, C., J.G. Canadell, E.A.G. Schuur, P. Kuhry, G. Mazhitova, and S. Zimov, Soil organic carbon pools in the northern circumpolar permafrost region, *Global Biogeochem. Cycles*, *23*, GB2023, doi: 10.1029/2008GB003327, 2009.

Teh, Y.A., R.C. Rhew, A. Atwood, and T. Abel, Water, temperature, and vegetation regulation of methyl chloride and methyl bromide fluxes from a shortgrass steppe ecosystem, *Global Change Biol.*, *14* (1), 77-91, doi: 10.1111/j.1365-2486.2007.01480.x, 2008.

Teh, Y.A., O. Mazéas, A.R. Atwood, T. Abel, and R.C. Rhew, Hydrologic regulation of gross methyl chloride and methyl bromide uptake from Alaskan Arctic tundra, *Global Change Biol.*, *15* (2), 330-345, doi: 10.1111/j.1365-2486.2008.01749.x, 2009.

Theys, N., M. Van Roozendael, F. Hendrick, C. Fayt, C. Hermans, J.-L. Barray, F. Goutail, J.-P. Pommereau, and M. De Mazière, Retrieval of stratospheric and tropospheric BrO columns from multi-axis DOAS measurements at Reunion Island (21°S, 56°E), *Atmos. Chem. Phys.*, *7* (18), 4733-4749, doi: 10.5194/acp-7-4733-2007, 2007.

Thomas, V.M., J.A. Bedford, and R.J. Cicerone, Bromine emissions from leaded gasoline, *Geophys. Res. Lett*., *24* (11), 1371-1374, 1997.

Tokuhashi, K., A. Takahashi, M. Kaise, and S. Kondo, Rate constants for the reactions of OH radicals with CH_3OCF_2CHFCl, CHF_2OCF_2CHFCl, $CHF_2OCHClCF_3$, and $CH_3CH_2OCF_2CHF_2$, *J. Geophys. Res*., *104* (D15), 18681-18688, doi: 10.1029/1999JD900278, 1999.

Tokuhashi, K., L. Chen, S. Kutsuna, T. Uchimaru, M. Sugie, and A. Sekiya, Environmental assessment of CFC alternatives: Rate constants for the reactions of OH radicals with fluorinated compounds, *J. Fluor. Chem.*, *125* (11), 1801-1807, doi: 10.1016/j.jfluchem.2004.09.013, 2004.

Trentmann, J., G. Luderer, T. Winterrath, M.D. Fromm, R. Servranckx, C. Textor, M. Herzog, H.-F. Graf, and M.O. Andreae, Modeling of biomass smoke injection into the lower stratosphere by a large forest fire (Part I): Reference simulation, *Atmos. Chem. Phys.*, *6* (12), 5247-5260, doi: 10.5194/acp-6-5247-2006, 2006.

Trudinger, C.M., D.M. Etheridge, G.A. Sturrock, P.J. Fraser, P.B. Krummel, and A. McCulloch, Atmospheric histories of halocarbons from analysis of Antarctic firn air: Methyl bromide, methyl chloride, chloroform, and dichloromethane, *J. Geophys. Res.*, *109*, D22310, doi: 10.1029/2004JD004932, 2004.

UNEP (United Nations Environment Programme), *2006 Report of the Halons Technical Options Committee 2006 Assessment*, edited by D. Catchpole and D. Verdonik, Nariobi, Kenya, 2007a.

UNEP (United Nations Environment Programme), *2006 Report of the Methyl Bromide Technical Options Committee 2006 Assessment*, coordinated by M. Pizano, I. Porter, M. Marcotte, M. Besri, and J. Banks, Nariobi, Kenya, 2007b.

UNEP (United Nations Environment Programme), data reported to the ozone secretariat, available online at: http://ozone.unep.org/Data_Reporting/, 2010.

UNEP/TEAP (United Nations Environment Programme/Technology and Economic Assessment Panel), *1998 Assessment Report of the Technology and Economic Assessment Panel (TEAP)*, 286 pp., Nariobi, Kenya, available at: http://ozone.unep.org/teap/Reports/TEAP_Reports/TEAPAS98.pdf, 1998.

UNEP/TEAP (United Nations Environment Programme/Technology and Economic Assessment Panel), *Task Force on Emissions Discrepancies Report*, co-chaired by P. Ashford, L. Kuijpers, and S. Montzka, Nairobi, Kenya, 2006.

UNEP/TEAP (United Nations Environment Programme/Technology and Economic Assessment Panel), *Report of the Technology and Economic Assessment Panel (TEAP)*, *Progress report*, *Volume 2*, coordinated by L. Kuipers and M. Seki, Nairobi, Kenya, 2010.

van der Werf, G.R., J.T. Randerson, G.J. Collatz, L. Giglio, P.S. Kasibhatla, A.F. Arellano Jr., S.C. Olsen, and E.S. Kasischke, Continental-scale partitioning of fire emissions during the 1997 to 2001 El Niño/La Niña period, *Science*, *303* (5654), 73-76, doi: 10.1126/science.1090753, 2004.

Van Roozendael, M., T. Wagner, A. Richter, I. Pundt, D.W. Arlander, J.P. Burrows, M. Chipperfield, C. Fayt, P.V. Johnston, J.-C. Lambert, K. Kreher, K. Pfeilsticker, U. Platt, J.-P. Pommereau, B.-M. Sinnhuber, K.K. Tørnkvist, and F. Wittrock, In-

tercomparison of BrO measurements from ERS-2 GOME, ground-based and balloon platforms, *Adv. Space Res.*, *29* (11), 1661-1666, 2002.

Varner, R.K., P.M. Crill, and R.W. Talbot, Wetlands: A potentially significant source of atmospheric methyl bromide and methyl chloride, *Geophys. Res. Lett.*, *26* (16), 2433-2436, 1999a.

Varner, R.K., P.M. Crill, R.W. Talbot, and J.H. Shorter, An estimate of the uptake of atmospheric methyl bromide by agricultural soils, *Geophys. Res. Lett.*, *26* (6), 727-730, 1999b.

Varner, R.K., M.L. White, C.H. Mosedale, and P.M. Crill, Production of methyl bromide in a temperate forest soil, *Geophys. Res. Lett.*, *30*, 1521, doi: 10.1029/2002GL016592, 2003.

Vecchi, G.A., and B.J. Soden, Global warming and the weakening of the tropical circulation, *J. Climate*, *20* (17), 4316-4340, 2007.

Velders, G.J.M., D.W. Fahey, J.S. Daniel, M. McFarland, and S.O. Andersen, The large contribution of projected HFC emissions to future climate forcing, *Proc. Natl. Acad. Sci.*, *106* (27), 10949-10954, 2009.

Vigano, I., H. van Weelden, R. Holzinger, F. Keppler, A. McLeod, and T. Röckmann, Effect of UV radiation and temperature on the emission of methane from plant biomass and structural components, *Biogeosciences*, *5* (3), 937-947, doi: 10.5194/bg-5-937-2008, 2008.

Volk, C.M., J.W. Elkins, D.W. Fahey, G.S. Dutton, J.M. Gilligan, M. Loewenstein, J.R. Podolske, K.R. Chan, and M.R. Gunson, Evaluation of source gas lifetimes from stratospheric observations, *J. Geophys. Res.*, *102* (D21), 25543-25564, 1997.

Vollmer, M.K., S. Reimann, D. Folini, L.W. Porter, and L.P. Steele, First appearance and rapid growth of anthropogenic HFC-245fa ($CHF_2CH_2CF_3$) in the atmosphere, *Geophys. Res. Lett.*, *33*, L20806, doi: 10.1029/2006GL026763, 2006.

Vollmer, M.K., L.X. Zhou, B.R. Greally, S. Henne, B. Yao, S. Reimann, F. Stordal, D.M. Cunnold, X.C. Zhang, M. Maione, F. Zhang, J. Huang, and P.G. Simmonds, Emissions of ozone-depleting halocarbons from China, *Geophys. Res. Lett.*, *36*, L15823, doi: 10.1029/2009GL038659, 2009.

Wallace, D.W.R., P. Beining, and A. Putzka, Carbon tetrachloride and chlorofluorocarbons in the South Atlantic Ocean, 19°S, *J. Geophys. Res.*, *99* (C4), 7803-7819, 1994.

Wallington, T.J., W.F. Schneider, D.R. Worsnop, O.J. Nielsen, J. Sehested, W.J. DeBruyn, and J.A. Shorter, The environmental impact of CFC replacements – HFCs and HCFCs, *Environ. Sci. Technol.*, *28* (7), 320A-326A, doi: 10.1021/es00056a002, 1994.

Wallington, T.J., M.D. Hurley, J.M. Fracheboud, J.J. Orlando, G.S. Tyndall, J. Sehested, T.E. Møgelberg, and O.J. Nielsen, Role of excited CF_3CFHO radicals in the atmospheric chemistry of HFC-134a, *J. Phys. Chem.*, *100* (46), 18116-18121, doi: 10.1021/jp9624764, 1996.

Wallington, T.J., M.D. Hurley, J. Xia, D.J. Wuebbles, S. Sillman, A. Ito, J.E. Penner, D.A. Ellis, J. Martin, S.A. Mabury, O.J. Nielsen, and M.P. Sulbaek Andersen, Formation of $C_7F_{15}COOH$ (PFOA) and other perfluorocarboxylic acids during the atmospheric oxidation of 8:2 fluorotelomer alcohol, *Environ. Sci. Technol.*, *40* (3), 924-930, doi: 10.1021/es051858x, 2006.

Wallington, T.J., M.P. Sulbaek Andersen, and O.J. Nielsen, Estimated photochemical ozone creation potentials (POCPs) of $CF_3CF=CH_2$ (HFO-1234yf) and related hydrofluoroolefins (HFOs), *Atmos. Environ.*, *44* (11), 1478-1481, doi: 10.1016/j.atmosenv.2010.01.040, 2010.

Wan, D., J. Xu, J. Zhang, X. Tong, and J. Hu, Historical and projected emissions of major halocarbons in China, *Atmos. Environ.*, *43* (36), 5822-5829, doi: 10.1016/j.atmosenv.2009.07.052, 2009.

Wang, J., R. Li, Y. Guo, P. Qin, and S. Sun, The flux of methyl chloride along an elevational gradient of a coastal salt marsh, Eastern China, *Atmos. Environ.*, *40* (34), 6592-6605, doi: 10.1016/j.atmosenv.2006.05.065, 2006.

Wang, P.K., The thermodynamic structure atop a penetrating convective thunderstorm, *Atmos. Res.*, *83*, 254-262, doi: 10.1016/j.atmosres.2005.08.010, 2007.

Wang, P.K., M. Setvák, W. Lyons, W. Schmid, and H.-M. Lin, Further evidences of deep convective vertical transport of water vapor through the tropopause, *Atmos. Res.*, *94* (3), 400-408, doi: 10.1016/j.atmosres.2009.06.018, 2009.

Warwick, N.J., J.A. Pyle, G.D. Carver, X. Yang, N.H. Savage, F.M. O'Connor, and R.A. Cox, Global modeling of biogenic bromocarbons, *J. Geophys. Res.*, *111*, D24305, doi: 10.1029/2006JD007264, 2006.

Waugh, D., and T. Hall, Age of stratospheric air: Theory, observations, and models, *Rev. Geophys.*, *40*, 1010, doi: 10.1029/2000RG000101, 2002.

Weiss, R.F., J. Mühle, P.K. Salameh, and C.M. Harth, Nitrogen trifluoride in the global atmosphere, *Geophys. Res. Lett.*, *35*, L20821, doi: 10.1029/2008GL035913, 2008.

White, M.L., R.K. Varner, P.M. Crill, and C.H. Mosedale, Controls on the seasonal exchange of CH_3Br in temperate peatlands, *Global Biogeochem. Cycles*, *19*, GB4009, doi: 10.1029/2004GB002343, 2005.

Williams, J., V. Gros, E. Atlas, K. Maciejczyk, A. Batsaikhan, H.F. Schöler, C. Forster, B. Quack, N.

Yassaa, R. Sander, and R. Van Dingenen, Possible evidence for a connection between methyl iodide emissions and Saharan dust, *J. Geophys. Res.*, *112*, D07302, doi: 10.1029/2005JD0006702, 2007.

Wilson, E.W., Jr., W.A. Hamilton, and H.R. Mount, Rate constants for the reactions of hydroxyl radical with several fluoroethers by the relative rate method, *J. Phys. Chem. A*, *111* (9), 1610-1617, doi: 10.1021/jp068355d, 2007.

Wishkerman, A., S. Gebhardt, C.W. McRoberts, J.T.G. Hamilton, J. Williams, and F. Keppler, Abiotic methyl bromide formation from vegetation, and its strong dependence on temperature, *Environ. Sci. Tech.*, *42* (18), 6837-6842, doi: 10.1021/es800411j, 2008.

WMO (World Meteorological Organization), *Scientific Assessment of Ozone Depletion: 2006*, Global Ozone Research and Monitoring Project–Report No. 50, 572 pp., Geneva, Switzerland, 2007.

Worton, D.R., W.T. Sturges, J. Schwander, R. Mulvaney, J.-M. Barnola, and J. Chappellaz, 20th century trends and budget implications of chloroform and related tri- and dihalomethanes inferred from firn air, *Atmos. Chem. Phys.*, *6* (10), 2847-2863, doi: 10.5194/acp-6-2847-2006, 2006.

Worton, D.R., W.T. Sturges, L.K. Gohar, K.P. Shine, P. Martinerie, D.E. Oram, S.P. Humphrey, P. Begley, L. Gunn, J.-M. Barnola, J. Schwander, and R. Mulvaney, Atmospheric trends and radiative forcings of CF_4 and C_2F_6 inferred from firn air, *Environ. Sci. Technol.*, *41* (7), 2184-2189, doi: 10.1021/es061710t, 2007.

Wuebbles, D.J., D. Youn, K. Patten, D. Wang, and M. Martinez-Aviles, Metrics for ozone and climate: Three-dimensional modeling studies of ozone depletion potentials and indirect global warming potentials, in *Twenty Years of Ozone Decline*, *Proceedings of the Symposium for the 20th Anniversary of the Montreal Protocol*, edited by C. Zerefos, G. Contopoulos, and G. Skalkeas, 297-326, Springer, Netherlands, doi: 10.1007/978-90-481-2469-5_23, 2009.

Xiao, X., Optimal Estimation of the Surface Fluxes of Chloromethanes Using a 3-D Global Atmospheric Chemical Transport Model, Ph.D. thesis, Massachusetts Institute of Technology, Cambridge, MA, U.S.A., 210 pp., 2008.

Xiao, X., R.G. Prinn, P.J. Fraser, P.G. Simmonds, R.F. Weiss, S. O'Doherty, B.R. Miller, P.K. Salameh, C.M. Harth, P.B. Krummel, L.W. Porter, J. Mühle, B.R. Greally, D. Cunnold, R. Wang, S.A. Montzka, J.W. Elkins, G.S. Dutton, T.M. Thompson, J.H. Butler, B.D. Hall, S. Reimann, M.K. Vollmer, F. Stordal, C. Lunder, M. Maione, J. Arduini, and Y. Yokouchi, Optimal estimation of the surface fluxes of methyl chloride using a 3-D global chemical transport model, *Atmos. Chem. Phys.*, *10* (12), 5515-5533, doi: 10.5194/acp-10-5515-2010, 2010a.

Xiao, X., R.G. Prinn, P.J. Fraser, R.F. Weiss, P.G. Simmonds, S. O'Doherty, B.R. Miller, P.K. Salameh, C.M. Harth, P.B. Krummel, A. Golombek, L.W. Porter, J.W. Elkins, G.S. Dutton, B.D. Hall, L.P. Steele, R.H.J. Wang, and D.M. Cunnold, Atmospheric three-dimensional inverse modeling of regional industrial emissions and global oceanic uptake of carbon tetrachloride, *Atmos. Chem. Phys.*, *10* (21), 10421-10434, doi:10.5194/acp-10-10421-2010, 2010b.

Yang, E.-S., D.M. Cunnold, M.J. Newchurch, R.J. Salawitch, M.P. McCormick, J.M. Russell, J.M. Zawodny, and S.J. Oltmans, First stage of Antarctic ozone recovery, *J. Geophys. Res.*, *113*, D20308, doi: 10.1029/2007JD009675, 2008.

Yang, X., R.A. Cox, N.J. Warwick, J.A. Pyle, G.D. Carver, F.M. O'Connor, and N.H. Savage, Tropospheric bromine chemistry and its impacts on ozone: A model study, *J. Geophys. Res.*, *110*, D23311, doi: 10.1029/2005JD006244, 2005.

Yokouchi, Y., M. Ikeda, Y. Inuzuka, and T. Yukawa, Strong emission of methyl chloride from tropical plants, *Nature*, *416*, 163-165, doi: 10.1038/416163a, 2002.

Yokouchi, Y., F. Hasebe, M. Fujiwara, H. Takashima, M. Shiotani, N. Nishi, Y. Kanaya, S. Hashimoto, P. Fraser, D. Toom-Sauntry, H. Mukai, and Y. Nojiri, Correlations and emission ratios among bromoform, dibromochloromethane, and dibromomethane in the atmosphere, *J. Geophys. Res.*, *110*, D23309, doi: 10.1029/2005JD006303, 2005.

Yokouchi, Y., S. Taguchi, T. Saito, Y. Tohjima, H. Tanimoto, and H. Mukai, High frequency measurements of HFCs at a remote site in east Asia and their implications for Chinese emissions, *Geophys. Res. Lett.*, *33*, L21814, doi: 10.1029/2006GL026403, 2006.

Yokouchi, Y., T. Saito, C. Ishigaki, and M. Aramoto, Identification of methyl chloride-emitting plants and atmospheric measurements on a subtropical island, *Chemosphere*, *69* (4), 549-553, doi: 10.1016/j.chemosphere.2007.03.028, 2007.

Yokouchi, Y., K. Osada, M. Wada, F. Hasebe, M. Agama, R. Murakami, H. Mukai, Y. Nojiri, Y. Inuzuka, D. Toom-Sauntry, and P. Fraser, Global distribution and seasonal concentration change of methyl iodide in the atmosphere, *J. Geophys. Res.*, *113*, D18311, doi: 10.1029/2008JD009861, 2008.

Young, C.J., M.D. Hurley, T.J. Wallington, and S.A. Mabury, Atmospheric chemistry of CF_3CF_2H and $CF_3CF_2CF_2CF_2H$: Kinetics and products of gas-phase reactions with Cl atoms and OH radicals, infrared spectra, and formation of perfluorocar-

boxylic acids, *Chem. Phys. Lett.*, *473* (4-6), 251-256, doi: 10.1016/j.cplett.2009.04.001, 2009.

Yujing, M., and A. Mellouki, Rate constants for the reactions of OH with chlorinated propanes, *Phys. Chem. Chem. Phys.*, *3*, 2614-2617, doi: 10.1039/b102971c, 2001.

Yvon-Lewis, S.A., and J.H. Butler, Effect of oceanic uptake on atmospheric lifetimes of selected trace gases, *J. Geophys. Res.*, *107*, 4414, doi: 10.1029/2001JD001267, 2002.

Yvon-Lewis, S.A., E.S. Saltzman, and S.A. Montzka, Recent trends in atmospheric methyl bromide: Analysis of post-Montreal Protocol variability, *Atmos. Chem. Phys.*, *9* (16), 5963-5974, doi: 10.5194/acp-9-5963-2009, 2009.

Zander, R., E. Mahieu, P. Demoulin, P. Duchatelet, G. Roland, C. Servais, M. De Mazière, and C.P. Rinsland, Evolution of a dozen non-CO_2 greenhouse gases above central Europe since the mid-1980s, *Environ. Sci.*, *2* (2-3), 295-303, 2005.

Zander, R., E. Mahieu, P. Demoulin, P. Duchatelet, G. Roland, C. Servais, M. De Mazière, S. Reimann, and C.P. Rinsland, Our changing atmosphere: Evidence based on long-term infrared solar observations at the Jungfraujoch since 1950, *Sci. Tot. Environ.*, *391* (2-3), 184-195, doi: 10.1016/j.scitotenv.2007.10.018, 2008.

Zellner, R., G. Bednarek, A. Hoffmann, J.P. Kohlmann, V. Mörs, and H. Saathoff, Rate and mechanism of the atmospheric degradation of 2H-heptafluoropropane (HFC-227), *Ber. Bunsenges. Phys. Chem.*, *98* (2), 141-146, doi: 10.1002/bbpc.19940980202, 1994.

Zeng, G., J.A. Pyle, and P.J. Young, Impact of climate change on tropospheric ozone and its global budgets, *Atmos. Chem. Phys.*, *8* (2), 369-387, doi: 10.5194/acp-8-369-2008, 2008.

Zhao, Z., P.L. Laine, J.M. Nicovich, and P.H. Wine, Reactive and nonreactive quenching of $O(^1D)$ by the potent greenhouse gases SO_2F_2, NF_3, and SF_5CF_3, *Proc. Natl. Acad. Sci.*, *107* (15), 6610-6615, doi: 10.1073/pnas.0911228107, 2010.

Zhou, Y., H. Mao, R.S. Russo, D.R. Blake, O.W. Wingenter, K.B. Haase, J. Ambrose, R.K. Varner, R. Talbot, and B.C. Sive, Bromoform and dibromomethane measurements in the seacoast region of New Hampshire, 2002–2004, *J. Geophys. Res.*, *113*, D08305, doi: 10.1029/2007JD009103, 2008.